Lipopolyplexes containing bifunctional peptides for DNA and siRNA delivery

Cui, Lili

Awarding institution:
King's College London

Lipopolyplexes containing bifunctional peptides for DNA and siRNA delivery

Lili Cui

M.Sc

A thesis submitted in partial fulfilment of the requirements for the degree of

Doctor of Philosophy

In the

Doctor of Philosophy Programme

Faculty of Life Sciences & Medicine

King's College London

2015

Institute of Pharmaceutical Science

Faculty of Life Sciences & Medicine

King's College London

August 2015

Abstract

In order to improve DNA transfection/siRNA silencing, a series of novel bifunctional peptides had been designed in the present study. The bifunctional peptides had a complexing moiety (denoted B), and a targeting moiety (denote Y), connected by linker L. All the BLY peptides had the same sequence in region L and Y. Region B was composed of ether a single histidine (H), arginine (R) and lysine (K) residue, denoted Series I, or a combination of them, Series II. These peptides have been shown to be more efficient vectors for DNA/siRNA delivery, especially when assembled with cationic vesicles (DOTMA:DOPE 1:1 molar ratio) into a ternary **LPD** or **LPR** complex composing cationic **L**ipids/bifunctional **P**eptide/**D**NA or si**R**NA. The delivery of these LPDs/LPRs was assessed by luciferase transfection/silencing on lung carcinoma A549 cells.

Of a combination of preparation and transfection aqueous solutions, the LPDs/LPRs prepared in water and in NaCl solutions had the same level of transfection/silencing when diluted in Optimem to incubate with cells. However, only the LPDs/LPRs prepared in NaCl solutions showed effective transfection/silencing (proportional to NaCl concentration of up to 0.12 M) when diluted in RPMI-1640 Media containing 10% v/v fetal bovine serum. Of various combinations, the LPDs/LPRs containing Series II peptides appeared to be superior over those containing Series I. Agarose gel electrophoresis showed that the LPDs/LPRs prepared in NaCl solutions afforded more protection against enzyme than those prepared in water without difference in condensation and release. Picogreen fluorescence assay revealed that DNA/siRNA was weakly condensed in LPDs/LPRs when prepared in NaCl solutions due to charge screening effect of salt. Moreover, dynamic light scattering showed that the LPDs/LPRs prepared in NaCl solutions were larger than those prepared in water due to alleviated condensation as shown in picogreen fluorescence assay. Small angle neutron scattering exhibited that the LPDs/LPRs prepared in both water and NaCl solutions had the same single lipid bilayer structure with the same bilayer thickness.

The present study suggests that these novel LPDs/LPRs should be further studies *in vivo*. In particular, 0.12 M NaCl solution is close to isotonic NaCl solution (0.15 M) which can be injected directly into bodies, revealing that those LPDs/LPRs may have potential in clinical therapy of lung cancers.

Acknowledgements

My deepest gratitude goes to my supervisor Prof. Jayne Lawrence for her greatest guidance, support, help and encouragement throughout the research. I would never have gone so far without her supervision. I would like to acknowledge my co-supervisor Prof. Alethea Tabor (University College London) for her valuable guidance and help with peptide chemistry. I am very grateful to Dr. Laila Kudsiova who showed me practicals/calculations and gave me guidance and suggestions. I would like to express my gratitude to Dr. Ann Terry (ISIS, Rutherford Appleton Labs) for her great help with SANS and SAXS, and Dr. David Barlow for SANS analysis. Special thanks are given to Dr. Fred Campbell (University College London) for helping me with peptide synthesis.

I would love to acknowledge King's College London for providing financial support for my project. I thank all my colleagues and friends of the Biophysical group who have always been friendly, supportive and helpful. I would also like to extend my appreciation to all my friends for sharing a fantastic life together.

Finally, I own my gratitude to my family and my boyfriend for their selfless love, support and encouragement. Thank you all for being around.

Table of Contents

List of Figures

Chapter 1 Introduction

Chapter 2 Methodology

Chapter 3 Lipopolyplexes containing DNA

Chapter 4 Lipopolyplexes containing siRNA

List of Tables

Chapter 1 Introduction

Chapter 3 Lipopolyplexes containing DNA

Chapter 4 Lipopolyplexes containing siRNA

List of Appendices

Abbreviations and Symbols

ADA	adenosine deaminase
A	adenine
ATP	adenosine triphosphate
C	cytosine
DNA	deoxyribonucleic acid
DOPE	dioleoylphosphotidylethanolamine
DOTAP	N-[1-(2,3-Dioleoyloxy)propyl]-N,N,N-trimethylammonium methyl-sulfate
DOTMA	dioleylpropyltrimethylammonium chloride
DSPE	1,2-Distearoyl-sn-glycero-3-phosphoethanolamine
DLS	dynamic light scattering
dsRNA	double stranded ribonucleic acid
EGFR	epidermal growth factor receptor
EPC	1,2-dimyristoyl-sn-glycero-3-ethylphosphocholine
FBS	fetal bovine serum
G	guanine
i.v.	intravenous
KSP	kinesin spindle protein
LD	lipoplexes containing DNA
LPD	lipopolyplexes containing DNA
LPR	lipopolyplexes containing siRNA
LR	lipoplexes containing siRNA
L2K	Lipofectamine 2000 ®
mRNA	messenger ribonucleic acid
PD	polyplexes containing DNA
PDL	poly-D-lysine

PDI	polydispersity index
PEG	polyethylene glycol
PEI	polyethelyneimine
PLL	poly-L-lysine
PR	polyplexes containing siRNA
RGD	arginine-glycine-aspartic acid
RNA	ribonucleic acid
RRM2	M2 subunit of ribonucleotide reductase
RISC	RNA-induced silencing complex
RLU	relative light unit
SCID	severe combined immunodeficiency
SANS	small angle neutron scattering
STR-H8	stearyl octahistidine
STR-R8	stearyl octaarginine
siRNA	small silencing ribonucleic acid
T	thymine
U	uracil
VEGF	vascular epithelial growth factor

Chapter 1 Introduction

1.1 Nucleic acid

Nucleic acid, alongside with proteins and carbohydrate, are three major macromolecules essential for all known forms of life. Nucleic acid carries genetic information and is responsible for its transmission from generation to generation. Therefore, nucleic acid represents the most important and interesting molecules in life.

1.1.1 DNA and RNA

Nucleic acid can be sub-divided into deoxyribonucleic acid, denoted DNA, and ribonucleic acid, denoted RNA.

DNA

The basic unit of DNA molecule is composed of a nucleobase, a ribose sugar and a phosphate. A nucleobase and a ribose sugar make up a nucleoside. The ribose sugar of DNA is deoxylated, with a C-H bond on the 2'-position of pentose ring. The C-H bond is less reactive than C-OH bond and therefore improves its molecular stability. The nucleobase is attached to the 1'-position of ribose ring and the 5'-positon of the ribose ring is connected with phosphate via phosphodiester bonds. The connection of the ribose sugar and the phosphate forms a regular phosphate-ribose backbone chain with irregular nucleobases protruding outside. As the phosphates are negatively charged, the adjacent phosphates of the backbone chain repel each other, forming a helical 3-dimentional structure. While the molecular composition of the phosphate-ribose backbone chain is fixed, different nucleobases are incorporated into the two backbone chains, which interact with each other via strong hydrogen bonds.

DNA molecules contain four types of nucleobases: adenine (A), guanine (G), cytosine (C) and thymine (T). These nucleobases stick with strict pairing rule: adenine complementarily pairs with thymine via two hydrogen bonds (A=T) and cytosine with guanine via 3 hydrogen bonds (C≡G). The strong hydrogen bond interactions between the protruding nucleobases on two chains leads to the formation of a double helical structure as proposed by Watson and Crick (Watson J.D. et al, 1953). The space-filling model of DNA and siRNA helix is depicted in Figure 1.1.

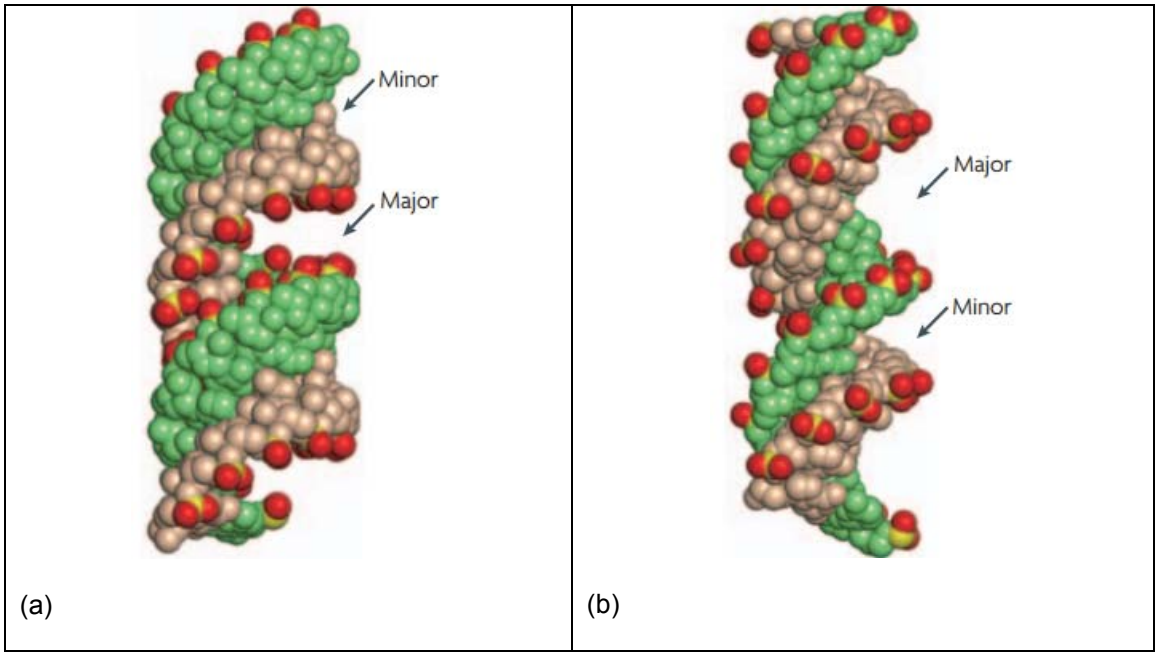

Figure 1.1 Space filling model of double helices (a) A form and (b) B form. The phosphorus, oxygen and heterocyclic nitrogen are shown in yellow, red and blue, respectively (Rana 2007).

Notably, the double helix can adopt different geometries such as A-form, B-form and Z-form. A-form and B-form DNA are right-handed in orientation while the Z-form DNA is left-handed. B-form DNA is the most common form found *in vivo*, as shown in Figure 1.1(b). The A-form, (Figure 1.1(a)), not found *in vivo*, resembles B-form DNA but is less hydrated. The helical structure of the DNA molecule is composed of alternating turns of nucleobase pairs attached to sugar-phosphate backbone. As the sugar-phosphate backbone is on the outside, the nucleobase pairs are protruding inwards. The nucleobase pairs occupy a much larger volume than the sugar-phosphate backbone. Therefore, as the sugar-phosphate backbone double chains are twisting and turning, the nucleobase pairs are exposed as two grooves not equal in size, forming a major groove and a minor groove. The major groove and the minor groove are a consequence of the geometry of the nucleobase pairs. The helical strands in the major grooves are further apart, while the strands in the minor groove are closer together. Therefore, the major groove is deep and wide, whereas the minor groove is narrow and shallow. These grooves, in particular major grooves, make the DNA molecule accessible to functional proteins. Each turn of the B-form DNA double helix has 10.5 nucleobase pairs with a diameter of 20 Å while that of A-form siRNA has 11-12 nucleobase pairs with a diameter of 23 Å.

In eukaryotes, most DNA is located in the nucleus with some found in mitochondria. The double helix of nuclear DNA can serve as a template to replicate exactly the same nucleobase pairs. This function makes it possible for genetic information to be passed on to daughter cells, which is critical for cell division. DNA is a large molecule, composed of millions of nucleobase pairs. For instance, human DNA consists of about 1.5 billion nucleobase pairs. The total length of DNA in a single somatic cell is approximately two meters, which is remarkable considering the size of an average cell is only several micro meters in diameter. In addition, the DNA molecule is very hydrophilic due to the presence of the negatively charged phosphates on the sugar-phosphate, behaving like a polyanion. Note, phosphodiester bonds connecting DNA backbones are prone to the 'attack' of DNA-degrading enzymes and therefore, DNA is not stable upon injection into human body.

RNA

Like DNA, RNA is assembled as a chain of nucleotides which contains a sugar-phosphate backbone chain and nucleobase pairs. However, the sugar for RNA is ribose and there is a C-OH bond on the 2'-position of pentose ring. The hydroxyl bond is more reactive than the hydrogen bond, making RNA less stable than DNA, especially in alkaline conditions. Another important difference is that there is a uracil base (U) in place of thymine (T). Therefore, pairing nucleobases are (A=U) and (C ≡ G) for RNA. Unlike DNA, RNA is more often found in nature as a short single-chain, rather than a paired double-chain. The single chain of RNA folds in on itself to link up its nucleobases. Therefore, not all nucleobases get partnered and RNA has a rough surface of sugar-phosphate backbone chain. RNA also has different resultant three-dimensional shapes, the most common being the hairpin loop. RNA is found in the nucleus, cytoplasm and ribosomes. Nuclear RNAs such as messenger RNA (mRNA) and transfer RNA (tRNA) are involved in protein translation, together with ribosomal RNA (rRNA). Cytoplasmic RNA includes micro RNA and small interfering RNA (siRNA) which act as down regulators of protein translation through RNA interference. Therefore, they play a complementary role with nuclear DNA.

siRNA is known to target a single gene while microRNA may target to 250-500 genes. Therefore, siRNA possesses a 100% perfect complementary match to target specific gene with minor off-target exception(Mack 2007). In addition, siRNA is a right-handed double-helix which

usually has 21-23 base pairs with two nucleotides overhanging at 3' ends. The space-filling model of the siRNA helix is shown in Figure 1.1(a). The helix of siRNA is usually found *in vivo* in the A form, which is more tightly packed than the B form. Therefore, the major groove of siRNA is narrower and deeper, making functional groups inaccessible for other molecules. However, the minor groove of siRNA is accessible for protein recognition. A siRNA comparison with DNA is described in Table 1.1.

Table 1.1 Comparison of DNA and siRNA

Properties	**DNA**	**siRNA**
Full name	Deoxyribonucleic acid	Ribonucleic acid
Backbone	Deoxyribose and phosphate	Ribose and phosphate
Bases	A, T, C, G	A, U, C, G
Base pairs	thousands	21-23
Helix geometry	B-form double-helix	A-form double-helix
Location	Nucleus	Cytosol
Role	Storage and transmission of genetic information, controlling protein synthesis	Transfer of genetic code from nucleus to cytosol, involved in protein synthesis

1.1.2 DNA expression and siRNA silencing

DNA and siRNA play an essential role in regulating the amount of cellular proteins through DNA expression and siRNA silencing.

DNA expression

The main function of DNA is to express proteins, namely gene expression. The functional sequence of DNA in a gene corresponds to a specific protein. The process of DNA expression is depicted in Figure 1.2. In the nucleus of a eukaryote, the double-helix of DNA is unwound. One strand of the double-helix is used as a template for the production of mRNA. The other strand is called the coding strand because it has the same sequence as newly formed mRNA

(but with uracil in place of thymine). The production of complementary RNA copies from DNA follows the Watson-Crick base-pairing rule. This process is called transcription.

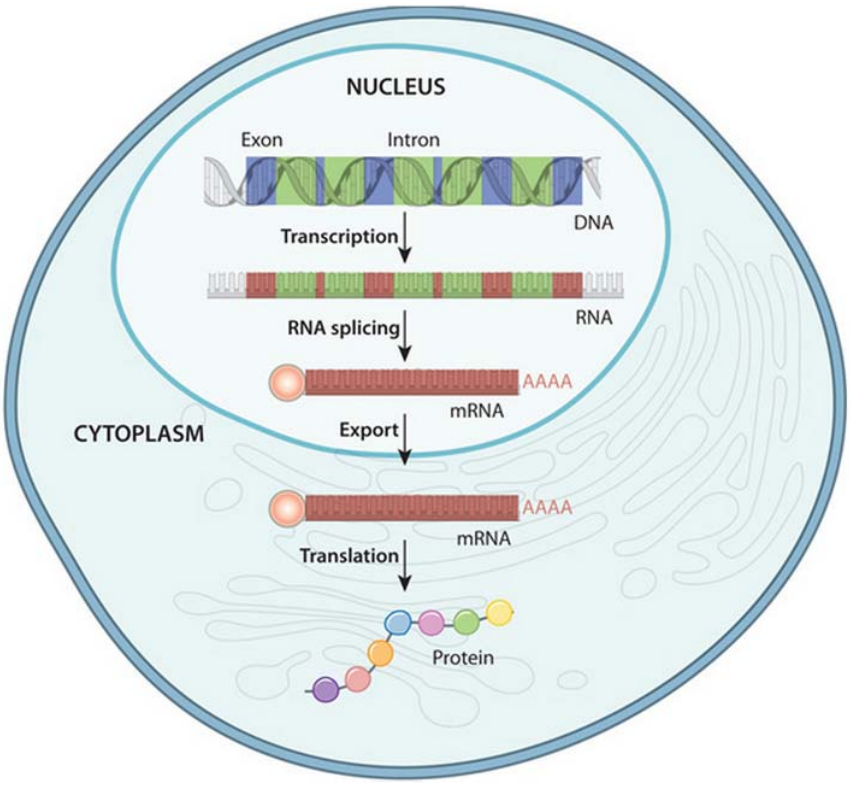

Figure 1.2 DNA expressions depicting the process of DNA-RNA transcription and RNA-protein translation in a eukaryotic cell.

During transcription, DNA is read by RNA polymerase from 3' end to 5' end and RNA is produced from 5' end to 3' end. In addition, only one RNA nucleotide is added to the growing RNA at a time. This ensures a strictly controlled process to limit error. The RNA copies formed are immature because of the intervening sequences, called introns. Therefore, the introns of immature RNA are removed leaving the remaining regions, which are called exons. The exons are spliced together to produce the mature messenger RNA (mRNA) including the protein-coding regions. Additionally, mRNA must be transported through nuclear pore into the cytosol in order for protein production to take place. This cytosolic process of protein production involves the translation of mRNA to protein. mRNA carriers encoding information for the protein is decoded by ribosomes during the translation process. As the mRNA passes through and is read by ribosomes, the specific amino acids are carried by tRNA and chained together in order to synthesise proteins.

Proteins are essential components of a single living cell. The combination of thousands of proteins that genes express determines what a single cell type can do. However, in human cells, if a piece of DNA encoding a protein is defective, the protein will not be produced or an abnormal protein is produced. The inadequate or defective protein can cause a disease.

siRNA silencing

Complementary with DNA, the main function of siRNA is to down regulate production of specific proteins, a process known as siRNA silencing. siRNA silencing was first discovered in a plant in 1997, and then demonstrated in nematodes (*Caenorhabditis elegans*) in 1998 (Ratcliff et al, 1997, Fire et al, 1998). It was founded that the gene expression of a myofilament protein in the nematode was effectively silenced by an exogenous double-stranded RNA (dsRNA) (Fire et al, 1998). The silencing was initialised by cleaving dsRNA to siRNA which then induced the degradation of the host mRNA coding for the myofilament protein (Montgomery et al, 1998).

As proteins are produced in the cytosol, this is the location where siRNA exerts its silencing effect, as depicted in Figure 1.3. siRNA is naturally cleaved from dsRNA by RNAse Dicer following cellular presentation (Bernstein et al, 2001). In the cytosol, siRNA is associated with a multi-protein complex, called RNA-induced silencing complex (RISC), which is activated through an Adenosine triphosphate (ATP)-dependent process. RISC contains several enzymatic activities including a helicase, dsRNA nuclease (possibly Dicer-like) and an RNA-dependent RNA polymerase activity. The siRNA molecules that are associated with RISC provide the sequence specificity to target a particular mRNA. Therefore, following the incorporation of siRNA into RISC, one strand of siRNA is cleaved by the enzyme components in the RISC, while the other strand remains incorporated in RISC. RISC is directed by the remaining strand to recognise a specific mRNA, followed by an ATP-independent cleavage of mRNA (Zamore et al, 2000) . The main components of the RISC complex are the Argonaute-2 protein, which is a member of the Argonaute family of proteins, responsible for mRNA degradation and single strand RNA formation (Hammond et al, 2000). As a consequence, the particular protein corresponding to the specific mRNA is silenced. Notably, the guiding strand of siRNA can be recycled to get involved in several rounds of mRNA degradation. Therefore, RNA silencing through siRNA can be long lasting.

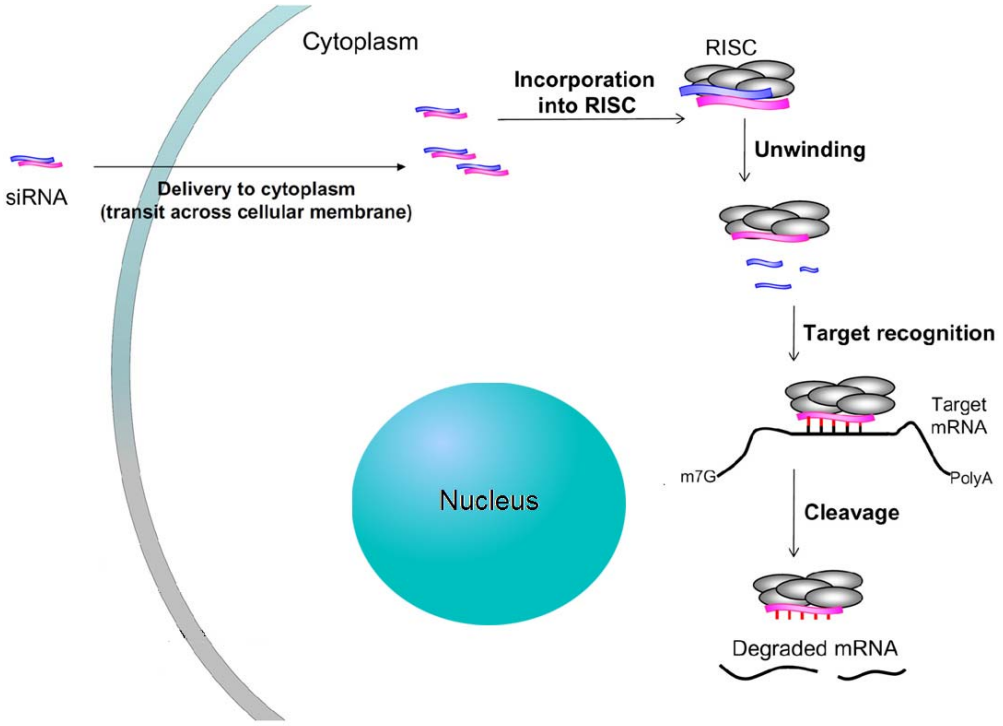

Figure 1.3 siRNA silencing process including siRNA associating with RNA-induced silencing complex (RISC) to directly target mRNA degradation in a eukaryotic cell (Takahashi et al, 2009).

1.1.3 Therapeutic effect

Most diseases are related to a failure in production of a particular protein or through the production of defective proteins. Therefore, DNA and siRNA can be used therapeutically to regulate the production of functional protein through DNA expression and siRNA silencing.

DNA

To correct failure or defective proteins, an exogenous DNA sequence can be introduced into cells by inserting it into a plasmid vector which can initiate DNA expression. Therefore, as a consequence, the amount of specific protein will be increased to normal and a disease is cured. Plasmid vector construction has been well established (Xu et al, 2004, Nguyen et al, 2005, Zhang et al, 2014), which is not the focus of the present study. However, it is worth noting that the resultant plasmid containing the therapeutic DNA sequence has all the functions of DNA molecules abovementioned in section 1.1.2.

The first clinical trial of DNA therapeutics was launched in 1990 (Blaese et al, 1995). In this treatment, DNA encoding adenosine deaminase (ADA) was introduced into T cells of patients

who had severe combined immunodeficiency (SCID). ADA is an enzyme that transforms adenosine (-OH) to deoxyladenosine (-H). Deoxyladenosine is DNA nucleoside A which pairs with deoxythymidine T in DNA double strands. In absence of ADA, adenosine accumulates in T lymphocytes and kills these cells, resulting in a genetic disorder known as ADA-SCID or ADA deficiency. Therefore, by introducing ADA-expressing DNA into T cells, the level of ADA and therefore the number of T cells are expected to be established to normal. Indeed, the number of T cells was normalized with the persistence of ADA expression, though DNA treatment ended after 2 years (Blaese 1995).

The first DNA therapeutic in market, trademarked as Gendicine, occurred in 2003 in China (Pearson et al, 2004, Wilson 2005). The DNA in Gendicine encodes a p53 protein, called p53-DNA. p53-DNA is a tumour suppressor gene, and is found to mutate or disappear in approximately 50% to 70% of human tumours. By injecting p53-DNA to patients, the exogenous p53-DNA can replace mutated endogenous p53-DNA which has been used for treating head and neck cancer. The introduction of p53-DNA has been shown to control or eliminate tumor cell growth by growth cycle arrest or apoptosis (Pearson 2004, Wilson 2005). In addition, p53-DNA therapy has a synergistic effect with radiotherapy and chemotherapy. Promisingly, in 2012, another DNA therapeutic, trademarked as Glybera, was recommended for approval for clinical use in the European Union (Bryant et al, 2013, Wirth et al, 2013). Glybera is used to treat a disease caused by a defect in DNA encoding lipoprotein lipase which can cause severe pancreatitis. Besides the above market products, numerous clinical trials using DNA as therapeutics are ongoing, involving various diseases such as cancer, monogenic disease, cardiovascular disease and infectious diseases (Sakurai et al, 2001, Sheridan 2011). Among these, cancer is the most common disease treated by DNA as demonstrated in Figure 1.4.

It has been suggested that cancer occurs due to DNA mutation. Mutations in two families of genes, namely oncongenes and tumour suppressor genes, are known to play a role in the pathogenesis of cancer. When an oncogene mutates, it becomes aggressive, protein-productive and eventually tumorous. In order to treat cancer, exogenous DNA that can suppress the ‘growing’ of the tumorous cells can be used. Oncogenes that have been evaluated to treat cancer include DNA-methyltransferase (Kanai et al, 2003). DNA-methyltransferase is a major enzyme that determines DNA methylation. The outcome of DNA methylation is that DNA cannot

start the process of making proteins which turns off the DNA. Tumour suppressor genes have the opposite function to tumour oncogenes, by slowing down cell division, repairing DNA mistakes, or by inducing apoptosis. When tumour suppressor genes do not work properly, cells can grow uncontrollably, which can also lead to cancer. The most famous tumour suppressor gene is p53 and abnormalities in p53 DNA have been found in more than half of human cancers. Therefore, by introducing exogenous p53-DNA, tumour cells can be killed in a variety of p53-inactivated tumour cells such as lung, colorectal, breast cancer and leukemia (Fang et al, 2003).

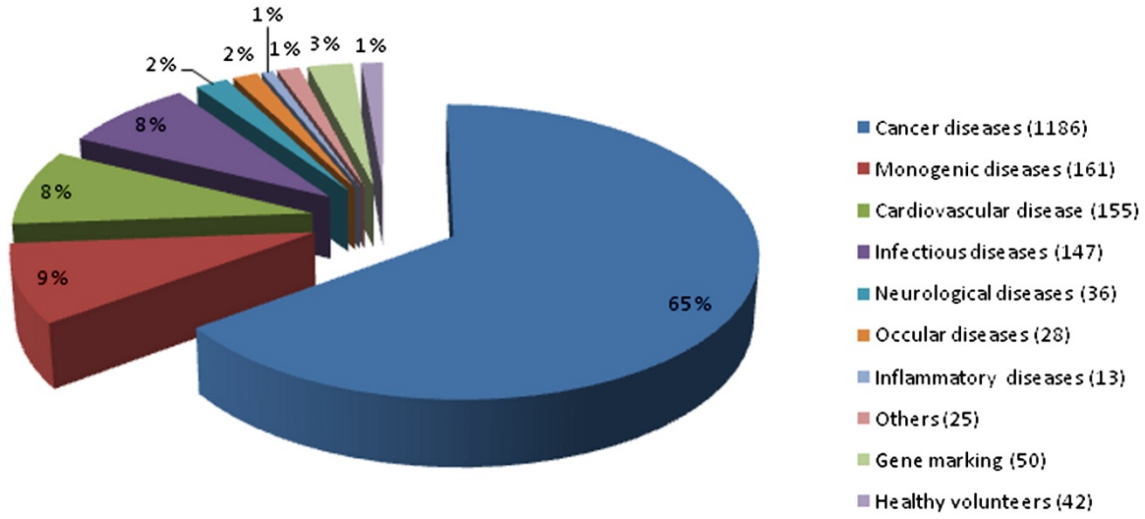

Figure 1.4 Diseases addressed by DNA therapy in clinical trials. Cancer became major interest (Wirth et al, 2013).

siRNA

The first successful siRNA study on human and animal cell lines was carried out as early as 2001 (Caplen et al, 2001). This lead to a rapid increase in the development of siRNA as a promising therapeutic platform (Timmons et al, 1998, Miyagishi et al, 2003, De Souza et al, 2006, Pushparaj et al, 2008). Over last 16 years, much progress has been made in research and development in both academia and the pharmaceutical industry (Pushparaj et al, 2008, Takahashi et al, 2009). The very recent study has reported a first clinical effect on the reduction in low density lipoprotein cholesterol levels using a siRNA silencing strategy (Fitzgerald et al, 2014). Other diseases that have been treated or that are undergoing clinical studies include

age-related macular degeneration, viral diseases, cystic fibrosis, metabolic diseases, ocular diseases and cancer (Devi 2006).

Of these diseases, much attention has been paid to the treatment of cancer. siRNA is generally used for oncogenes that encode protein kinases, e.g. epidermal growth factor receptor (EGFR) (Sharma et al, 2007) echinoderm microtubule-associated protein like lymphoma kinase (Kwak et al, 2010), and guanosine triphosphatease (Quaye et al, 2008). Increased levels of EGFR expression are observed in cancers of the head and neck, ovary, cervix, bladder, stomach, brain, breast, colon and lung, and frequently seem to confer an adverse prognosis (Nicholson et al, 2001, Hynes et al, 2005). EGFR has been explored to be silenced for the combinational treatment of non-small cell lung cancer with other inhibitors (Chen et al, 2012).

siRNA in clinical trial includes the targets of vascular epithelial growth factor (VEGF), kinesin spindle protein (KSP), protein kinase N3 (PKN3) and M2 subunit of ribonucleotide reductase (RRM2), as described below.

VEGF and KSP are over-expressed in numerous cancer cells, and are essential in tumour growth and survival. VEGF siRNA and KSP siRNA have been formulated in lipid nanoparticles used for intravenous administration. A decrease in microvessel density and vascular leakage due to VEGF knockdown, and in the formation of mitotic spindle due to KSP knockdown, was observed to cause tumour cell death in liver cancer mouse models (Tabernero et al, 2013). The following evaluation of activity and safety in patients with cancer suggests a target down regulation of VEGF and KSP, and complete regression of liver metastases in endometrial cancer. It becomes the first human trial of an RNA interference therapeutic targeting VEGF and KSP used for liver cancer (Tabernero 2013).

PKN3 is used as a therapeutic target, which when inhibited resulted in the reduction of lymph node metastases in orthotopic prostate cancer models (Leenders et al, 2004). Aleku et al showed that systemic administration of Atu027, a liposomal formulation containing protein kinase N3 siRNA, resulted in specific protein kinase N3 silencing and a significant inhibition of tumour growth and lymph node metastasis in various animal models (Aleku et al, 2008). RRM2 expression is involved in DNA replication. A transferrin receptor-targeted nanoparticle encapsulating a non-chemically modified RRM2 siRNA inhibits the expression of RRM2 and

thus prevents the proliferation of tumour cells (Davis et al, 2010). In addition, it clearly demonstrated that siRNA administered systemically to human patients was able to silence the cancer-associated gene in specifically-targeted tumour cells (Davis et al, 2010) .

1.2 Barriers for DNA/siRNA delivery

DNA and siRNA play their therapeutic role inside cells. It means that DNA/siRNA need to travel from their injection site to target cells. However, the physico-chemical environment of the human body makes it extremely difficult. DNA and siRNA are biological molecules which are large size and hydrophilic. Therefore, they will face many barriers upon administration.

The barriers that intravenous DNA/siRNA will experience can be categorized into extracellular and intracellular, as depicted in Figure 1.5. The preferred route of administration for DNA or siRNA is intravenously because this route avoids the danger of deactivation and degradation in the gastrointestinal tract in oral administration. Soon after intravenous injection, DNA/siRNA is distributed all over the body via blood circulation. However, DNA/siRNA is exposed to degrading enzymes present in serum, which 'attack' phosphodiester bonds in the phosphate-ribose backbone. This presents the first barrier for DNA/siRNA delivery (barrier I). Indeed, systematically delivered DNA/siRNA is readily degraded by serum endonucleases, resulting in a short plasma half-life of < 10min (van de Water et al, 2006, Liu et al, 2007). Moreover, in serum, the most abundant protein is albumin. Albumin is a globular protein with a molecular weight of 65,000 Daltons, and is ionised and negatively charged in a physiological environment. If negative DNA/siRNA is wrapped in a protective positively charged material, a non-specific interaction between the positive vector and the negative albumin would occur. As a consequence, the loaded DNA/siRNA, together with the positively charged carrier, will be recognised by the immune system and eliminated from blood circulation (Nel et al, 2009). This composes barrier II. Between blood vessels and tissue organs is the interstitium. To enter the interstitium, DNA/siRNA needs to cross the blood vessel via extravasation. To enter diseased tissues, such as tumours, DNA/siRNA needs to overcome physical barriers such as high pressure in the tumour site. Therefore, getting close to tumour cells represents the third barrier for DNA/siRNA delivery (barrier III). Barriers I, II, III are originated from outside of the cells and therefore denoted extracellular barriers.

Upon reaching target cells, wrapped DNA/siRNA may undergo cell internalisation via endocytosis. In the process of endocytosis, DNA/siRNA is initially coated by cell membrane which buds off as an endocytic vesicle. The endocytosis is an active molecule uptake process. It does not occur randomly but requires 'a driving force' to initialise such as ligand-receptor interaction (Nel et al, 2009). Therefore, DNA/siRNA needs to be somehow decorated by ligands specific to receptors present on cell surface, which represents the fourth barrier (barrier IV). Following endocytosis, the endocytic vesicles develop into endosomes. Endosomal pathways have been consistently observed for delivery (Lechardeur et al, 2005, Hama et al, 2006). The problem with endosomes is that the pH is only 4.5 in its compartment. Moreover, endosomes, behaving as the stomachs of cells, possess a lot of enzymes to digest foreign particles including DNA/siRNA molecules. Additionally, the large size of DNA/siRNA and their hydrophillicity do not support endosomal escape. Therefore, DNA/siRNA is easily swallowed into endosomes, unable to escape, and liable to complete degradation. For the above reasons, endosomes can be taken as the fifth barrier (barrier V). Generally, barrier V is the most challenging and endosomal escape is a rate-limiting step for DNA/siRNA delivery. Numerous strategies have been developed to facilitate DNA/siRNA to escape from endosomes, which will be discussed in the following section. Once DNA/siRNA has escaped from an endosome, it is released into the cytosol. In the cytosol, siRNA will induce a silencing effect by binding to RISC. In contrast, DNA takes effect in the nucleus which is surrounded by a thick wall of nuclear membrane. Therefore, DNA needs to be translocated from the cytosol to the nucleus, which forms an extra barrier for DNA delivery (barrier VI).

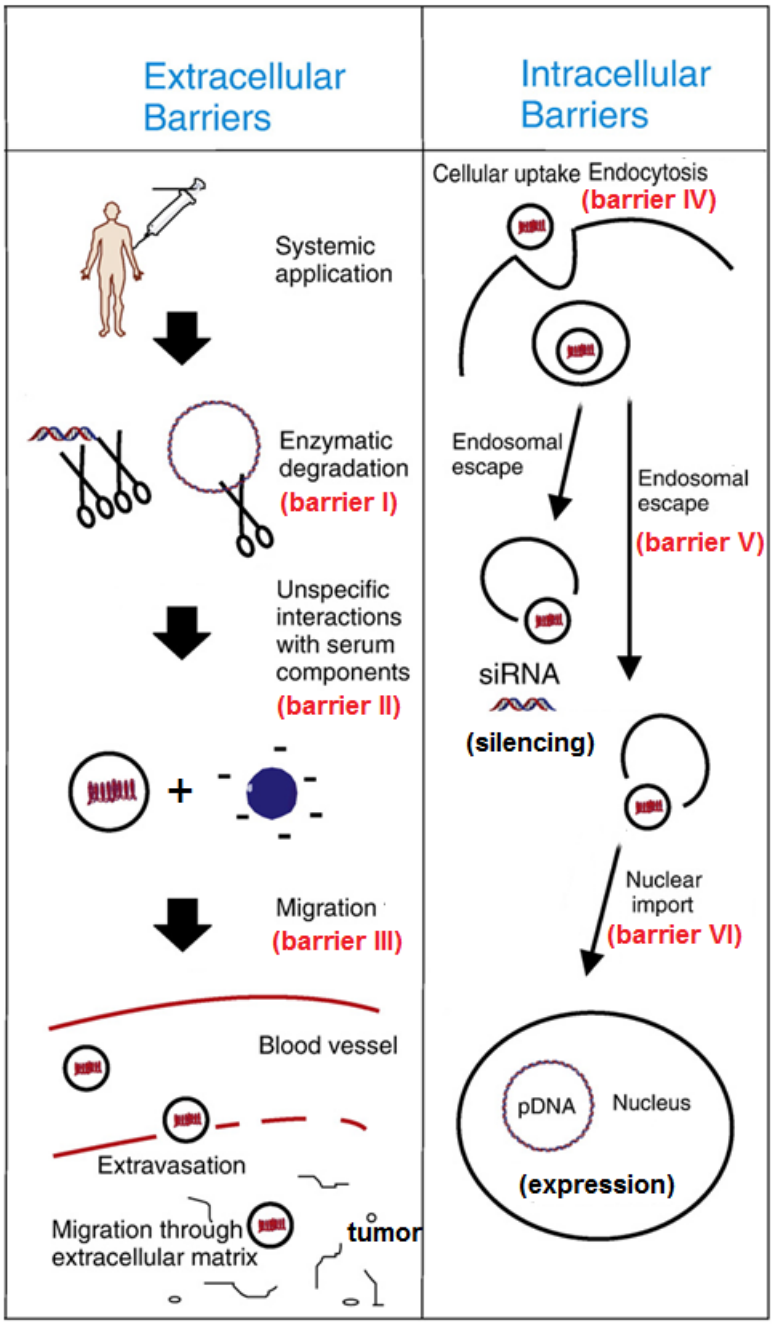

Figure 1.5 Extracellular barriers (I, II, II) and intracellular barriers (IV, V, VI) of DNA/siRNA delivery. Extra cellular barriers include enzyme degradation (barrier I), non-specific interaction (barrier II), crossing the blood vessel wall and migration to tumour cells (barrier III). Intracellular barriers are uptake via endocytosis (barrier IV), degradation in endosomes (barrier V), and the translocation of DNA into the nucleus (barrier VI) (Scholz et al, 2012). Barrier V and VI are the rate-limiting steps.

1.3 Strategies for DNA/siRNA delivery

In order to deliver DNA/siRNA, a vector that can overcome the above barriers is required. It is well known that viral vectors are highly efficient at DNA/siRNA delivery. However, the high risks arising from the characteristics of viral vectors seriously impede its clinical applications. It has been reported that a viral vector could integrate viral genes into the patient's gene regulatory areas or into transcriptionally active areas, which can adversely result in insertional mutagenesis and oncogenesis (Donsante et al, 2001, Cesana et al, 2014). In serious cases, using a viral vector can be fatal. For example, in 1999, 18 year-old Jesse Gelsinger died during a DNA therapy trial because of vector-associated toxicity (Sibbald 2001).

Compared with viral vectors, non-viral vectors including polymers, liposomes, nanoparticles/nanocapsules and carbon nanotubes are relatively safe, and could be further tailored according to the requirement for diverse bioactive delivery. Of non-viral vectors, lipid nanoparticles/nanocapsules have an advantage at loading lipophilic drugs (Huynh et al, 2009), while carbon nanotubes have problems associated with cytotoxicity (Varkouhi et al, 2011). As DNA and siRNA are highly hydrophilic and anionic, only cationic polymers, cationic lipids or a combination of both are focused on here.

Generally, polymers and lipids used for DNA/siRNA delivery are cationic. Therefore, anionic DNA/siRNA can be condensed and packaged via electrostatic interaction. Currently, there are three types of related complexes reported for DNA/siRNA delivery, which is shown in Figure 1.6. In complex A, cationic polymers/peptides are used to condense DNA/siRNA. The resultant complex forms a disordered structure, denoted polyplex. In complex B, cationic lipids are pre-prepared into liposomes that are vesicles with a single lipid bilayer. There is a strong electrostatic repulsion between cationic lipid molecules along the lipid bilayer. Therefore, upon mixing with anionic DNA/siRNA, vesicles break and rearrange into multiple bilayers to reduce electrostatic repulsion, resulting in DNA/siRNA being sandwiched between multilamellars. This complex is denoted lipoplex. Complex C is formulated from mixing a combination of cationic polymers and cationic lipids with DNA/siRNA. Correspondingly, the resulting complex is denoted lipopolyplex.

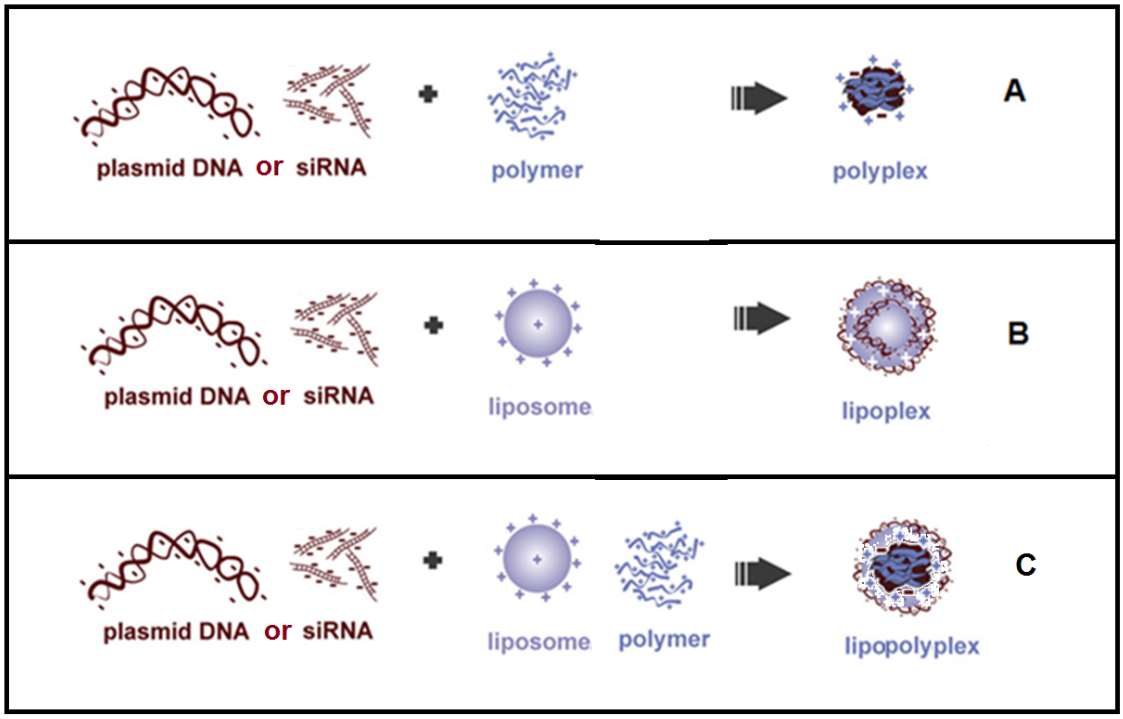

Figure 1.6 Non-viral vectors for DNA/siRNA delivery. Cationic polymers, cationic liposomes and a combination of them, used to complex DNA/siRNA via electrostatic interactions. The resultant complex is denoted (A) polyplex, (B) lipoplex and (C) lipopolyplex. Cationic polymers used are poly-L-lysine (PLL), polyethylenimine (PEI) and their derivatives. Typical cationic liposomes include cationic dioleylpropyltrimethylammonium chloride (DOTMA) and neutral dioleoylphosphotidylethanolamine (DOPE). This figure is modified from literature (Vercauteren et al, 2012).

It is worth noting that the abovementioned polymers, peptides and lipids can be further functionalised to achieve an efficient delivery for DNA/siRNA. The related strategies and examples are shown in Figure 1.7. Among these strategies, conjugating a poly(ethylene glycol) (PEG) motif onto polymers, peptides or lipids is the most popular. This is because a PEG motif modification could physically block the contact of serum protein with the delivery materials when circulating in the blood stream (Knop et al, 2010). In addition, water soluble PEG motifs cannot be recognised by the immune system and therefore could effectively avoid immune-related clearance. As a consequence, the resultant vector's plasma half-life can be significantly increased. Apart from PEGylation, tailoring the size, surface charge and composition of the delivery vector could also achieve a reduced affinity to serum proteins (Lundqvist et al, 2008).

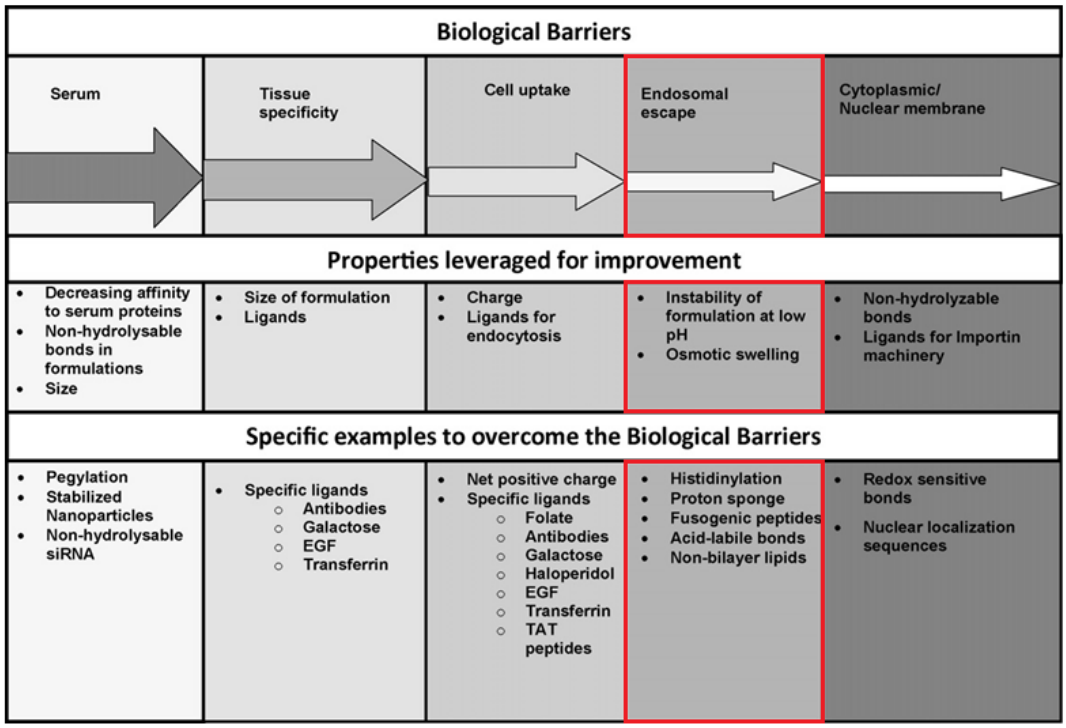

Figure 1.7 Biological barriers for DNA/siRNA delivery and the corresponding strategies/examples to overcome the barriers.

Along with PEGylation, conjugating specific ligands onto polymers, peptides or lipids is generally required to improve the tissue specificity of DNA/siRNA delivery. The improved specificity could not only avoid non-specific toxicity resulting from a wide distribution of vectors in the body, but also reduce the administration dose of DNA/siRNA. Commonly used ligands include antibodies, galactose, endothelial growth factor (EGF), and transferrin. By decorating with these ligands, the delivery vector carrying DNA/siRNA will be directed to specific cells and endocytosed. It is worth noting that ligand-receptor mediated endocytosis is indirectly affected by the surface charge property of the delivery vector. It is known that the cell surface is negatively charged due to cell surface elements, such asproteoglycan and sialic acids (Mounkes et al, 1998). Therefore, the positively charged vector is preferential for contact with cells, which is a prerequisite for endocytosis.

Among all strategies, endosomal escape is the key for both DNA and siRNA delivery. The escape from endosomes can be achieved by increasing interior osmotic pressure to swell the endosomal membrane using protonatable polymers/peptides. The disruptive effect of protonatable polymers/peptides is described as a ‘proton sponge’ effect, depicted in Figure 1.8.

Endosomes are the stomachs of cells and the interior is acidic (pH ~5). In such an acidic environment, the protonatable polymers/peptides can be heavily protonated and therefore distort the acidification of endosomes. As a result, more protons are actively pumped into the vesicles. To keep a neutral environment in endosomes, chloride ions passively diffuse into the endosomes, increasing ionic concentration. As a consequence, water is purged in, leading to a huge rise in osmotic pressure. Therefore, the endosome bursts and its contents are released.

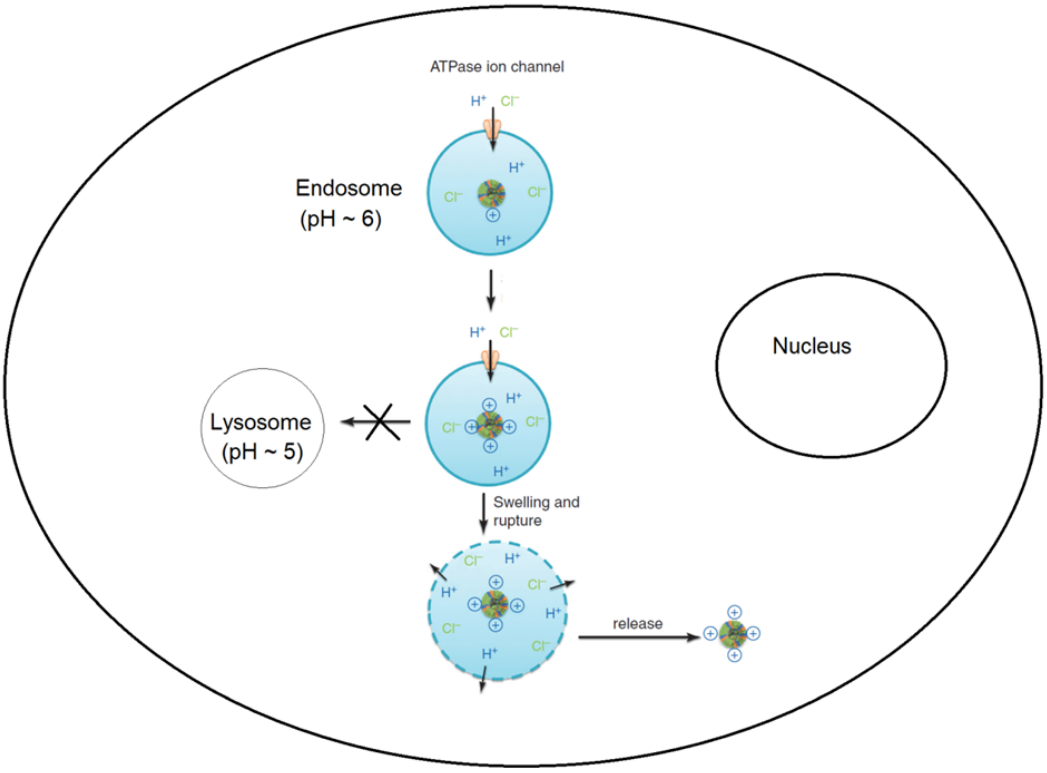

Figure 1.8 The proposed endosomal escape process of cationic polyplexes via the 'proton sponge' effect (Aied et al, 2013).

In the case of DNA delivery, it has to be transported into the nucleus to achieve therapeutic effect. Naturally, nuclear membrane, as a physical barrier, could block molecules with a MW above 40 kD or with a size larger than 10 nm (Shulga et al, 2000, Strasser et al, 2012). However, nuclear membrane has numerous nuclear pore complex (NPC) channels that transport proteins in and out. The mass flow of active translocation signal molecules through a single NPC was reported to be 100 mD at a flux rate of up to 1,000/s (Ribbeck et al, 2001). Therefore, NPC can be targeted to deliver DNA to the nucleus. It was reported that protamine-condensed DNA could be successfully delivered into the nucleus *in vitro* by the aid of NPC

targeting ligand-modified lipids (Masuda et al, 2008).Alternatively, active nuclear translocation signal peptides and their analogues could also be used to deliver DNA to the nucleus (Kalderon et al, 1984, Dingwall et al, 1991, Zanta et al, 1999).

1.3.1 Peptides

The peptides used to complex DNA/siRNA are generally made cationic by incorporating cationic amino acid residues such as, lysine, arginine and histidine. The following part mainly focuses on various cationic polypeptides and their application in gene delivery. The purpose is to gain an insight into the relationship between a vector's structure/properties and its improved transfection efficiency.

1.3.1.1 Linear polylysine and its derivatives

Polylysine is a synthetic repeat of the amino acid lysine. It is one of the earliest and well-known vectors for DNA/siRNA delivery. The advantages of using polylysine as a gene delivery vector include its degradability, low cytotoxicity and high modifiability. The progress in solid phase peptide synthesis technology also makes its large-scale production possible. It has been revealed that molecular weight, charge ratio and functional modification could tailor its potential in DNA/siRNA delivery.

The molecular weight of polylysine plays an important role in DNA/siRNA condensation and transfection. The most commonly used polylysines have a molecular weight in the range of 3 000-40 000 Daltons (Laemmli 1975, Mannisto et al, 2002). Poly-D-lysine (PDL) with a molecular weight of 40 000 Daltons was reported to condense DNA to a doughnut and rod-like mixed structure; 3 to 4 layers of DNA was estimated across the doughnut and rod particles as detected by transmission electron microscopy (Laemmli 1975). Doughnut particles were also observed in others' studies, such as poly-L-lysine (PLL, 27 000 Daltons)/DNA complexes (Tang et al, 1997) and PLL/DNA complexes (20 000 Daltons) (Mannisto et al, 2002). However, in another study, the DNA complexed by PLL was reported to be mainly spherical as revealed by atom force microscopy (Wolfert et al, 1996). The different structures of PLL/DNA complexes revealed by atom force microscopy and electron microscopy, may be a consequence of sample preparation for different techniques (Tang et al, 1997).

Besides molecular weight, the (+/-) charge ratio of positive polylysine to negative DNA is also important for the formulation of the PLL/DNA complex. It was found that PLL (2 900 Daltons) could not condense DNA efficiently at a (+/-) charge ratio of less than 2.5 while PLL (30 000 Daltons) condensed DNA at a (+/-) charge ratio of more than 0.6 (Mannisto et al, 2002). Interestingly, although at a (+/-) charge ratio of 1:1, the ζ-potential of the PLL/DNA complex was negative (-30 mV) and at least a 2:1 (+/-) charge ratio was required to get a positive ζ-potential (Zhu et al, 2014). The phenomenon is probably due to the large molecular nature of DNA and the relatively low condensation ability of polylysine (Mannisto et al, 2002, Zhu et al, 2014).

The above formulations have also been investigated in terms of transfection and their intra-cellular fates. Encouragingly, PLL with a molecular weight of 20 000 Daltons showed more effective transfection *in vitro* than that with a molecular weight of 2 900 Daltons at a 1:1 PLL:DNA weight ratio. However, PLL at both molecular weights were less efficient than positive controls, polyethelyneimine (PEI), N-[1-(2,3-Dioleoyloxy)propyl]-N,N,N-trimethylammonium methyl-sulfate (DOTAP) and DOTMA, respectively (Akinc et al, 2002). Further investigation showed that the PLL/DNA complex was taken by cells more than the positive controls. The high cellular uptake and low transfection of PLL was proposed to be related to intracellular events such as endosomal trapping. The reasonable assumption was confirmed by the low pH environment (4.0-4.5) of the PLL/DNA complex following cellular uptake (Akinc et al, 2002). The above studies indicate that PLL is not an ideal gene delivery carrier due to serious endosomal trapping, in spite of its excellent DNA condensation capacity and high cellular uptake (Lechardeur et al, 2005).

To improve the transfection efficiency of PLL/DNA, PLL decorated with histidine groups has been developed. Histidine has imidazol groups with a pKa ~6. It means upon incorporation into endosomes (pH ~5), histidine can be heavily protonated, which would exert a ‘proton sponge’ effect in endosomes (Behr 1997). The ‘proton sponge’ effect of histidine has shown a positive contribution to polylysine used for DNA/siRNA delivery (Midoux et al, 1999, Benns et al, 2000, Putnam et al, 2001). It was reported that PLL grafted with poly-L-histidine (PLH) (known as PLH-PLL) could condense DNA to 100-300 nm (Benns et al, 2000). Further studies revealed a strong buffering capability for PLH-PLL but none for PLL alone. Therefore, as a consequence, PLH-PLL demonstrated a higher transfection efficacy in 293T cells than PLL at all equivalent

weight ratios with DNA. In addition, it was found that chloroquine, an endosomolytic agent, could further enhance the transfection efficiency of both PLL and PLH-PLL (Benns et al, 2000). The above study showed that endosomal escape is the key step and that the presence of histidine residues is beneficial for efficient DNA transfection. The efficient gene transfer derived from histidylated polylysine/DNA complexes was also observed by others (Midoux et al, 1999). In addition, effective DNA delivery systems using conjugated imidazole groups to polylysine have also been studied (Putnam et al, 2001).

Another benefit from endosomal escape mediated by histidine residues is the resulting low cytotoxicity (Benns et al, 2000, Putnamet al, 2001). It was reported that the relative cell viability was still greater than 80% at a PLL:DNA 20:1 weight ratio (Benns et al, 2000). Further investigation revealed that the improved endosomal escape and the reduced cellular toxicity are due to the imidazole groups of histidine (Benns et al, 2000, Okuda et al, 2004). It was found that imidazole conjugated polylysine in varying mole ratios (73.5, 82.5, 86.5 mol % imidazole) condensed DNA into nanostructures <150 nm and possessed little cytotoxicity *in vitro* (Putnam et al, 2001). In addition, their transfection efficiency, as measured by luciferase protein expression, increased with increasing imidazole content of the polymers in a nonlinear relationship. The polymer with the highest imidazole content (86.5 mol %) mediated the highest protein expression, with levels equal to those mediated by polyethylenimine, but with little cytotoxicity.

For *in vivo* use, histidylated polylysine was also PEGylated and was used to carry and deliver siRNA for silencing endogenous vascular endothelial growth factor (VEGF) expression. The resultant polyplexes were reported to show distinct tumour suppression in terms of macroscopic tumour volume and molecular analysis in HepG2 tumour-bearing mice (Zhu et al, 2014).

The above studies suggested that linear polylysine with the appropriate molecular weight could efficiently complex DNA/siRNA at a certain charge ratio but exerts a limited transfection efficiency due to endosomal trapping. However, polylysine modified with histidine residues or imidazole groups could significantly improve DNA/siRNA transfection/silencing efficiency *in vivo* via ‘proton sponge’-mediated endosomal escape.

1.3.1.2 Dendritic polylysine

Besides chemically modified linear polylysine, dendritic polylysine was also explored as a DNA/siRNA delivery vector. Dendritic polylysine is a dendrimer consisting of L-lysine residues as a branch unit. Each branching is described as one generation.

Effect of generations of dendritic polylysine (PLL)

Ohsaki etc synthesized dendritic polylysine of the 1st to 7th generation (Ohsaki et al, 2002). They found that the 3rd generation and higher could form a complex with a plasmid DNA, and the degree of compaction of DNA was increased by increasing the number of generations. The dendritic polylysine of the 5th and 6th generation, which have 64 and 128 amine groups on the surface of the molecule respectively, showed efficient DNA transfection in several cultivated cell lines. In particular, the 6th generation shows a buffering effect in a weak acidic environment. It is likely that the escape of the DNA complex from the endocytotic vesicle to the cytosol was enhanced by the 'proton sponge' effect of the dendritic polylysine of the 6th generation itself (Boussif et al, 1995, Ohsaki et al, 2002). Encouragingly, the transfection efficiency of the 6th generation was not seriously reduced even in the presence of 50% serum. The superior stability of the complex in serum was attributed to a neutral or slightly positive ζ-potential even when the (±) charge ratio was increased to 8 (Ohsaki et al, 2002).

Dendritic PLL (5th/6th generation) and linear PLL

The 5th generation of polylysine/siRNA complexes were compared with linear PLL/siRNA counterparts. Significantly, the 5th generation of polylysine/siRNA complexes were reported to show a 300-fold increase in luciferase silencing *in vitro* compared with linear polylysine (Byrne et al, 2013). Moreover, the 5th generation of polylysine/siRNA complexes had a discrete spherical shape while the linear polylsine/siRNA complexes were elongated and irregular, as revealed by atom force microscopy. These differences in shape were consistent with the lower (+/-) charge ratio of the 5th generation of polylysine (<5) required to complex siRNA to nano size (<250 nm) in comparison with the linear polylysine (<300 nm).

In addition, Yamagata *et al* further compared dendritic PLL of the 6th generation and linear PLL (15 000 - 30 000 Daltons) in terms of their DNA condensation ability, cellular uptake, and transfection efficiency (Yamagata et al, 2007). Their studies showed that dendritic PLL of the 6th

generation formed a weaker DNA condensation than linear PLL, and that DNA binding and uptake into cells mediated by linear PLL was 4-fold higher. However, dendritic PLL-mediated DNA expression was 100-fold higher than that by linear PLL due to the 'proton sponge' effect mediated by amines of the dendritic PLL. In addition, weakly compacted DNA by dendritic PLL was advantageous in accessing transcription machinery in the nucleus. It is worth noting that dendritic PLL is suitable for *in vivo* application due to its low cytotoxicity. Indeed, little cytokine was produced by dendritic PLL after intravenous injection (Ohsaki 2002, Yamagata et al, 2007).

Derivatives of dendritic PLL (6th generation)

In another study, the terminal amino acids of the 6th generation dendritic polylysine were replaced by arginines and histidines, respectively (Okuda 2004). Interestingly, the arginine-replaced dendritic polylysines showed 3- to 12- fold higher transfection efficiency *in vitro*. In contrast, the DNA-binding ability of histidine-replaced dendritic polylysine was significantly lower than that of the unreplaced polylysine, and no transfection mediated by histidine-replaced dendritic polylysine was observed. However, once histidine-replaced dendritic polylysine was mixed with the DNA under acidic conditions, transfection was observed to be as effective as the unreplaced polylysine.

The above studies suggested that dendritic polylysine and its derivatives could be used as ideal DNA delivery vectors due to their excellent complexation, endosomal escape and release capacities. The terminal histidines, especially their imidazole groups, had a key role in the pH-dependent complex formation and transfection (Okuda 2004).

Besides DNA, the 6th generation of polylysines was also explored for siRNA delivery. Encouragingly, the 6th generation of polylysines was found to deliver fluorescein-labelled oligonucleotide into cells with high efficiency. However, a large amount of the fluorescence was localised and trapped in the endosomal compartment. In order to resolve this problem, the 6th generation of polylysines was combined with Endo-Porter which is a weak-base amphiphilic peptide that was expected to promote endosomal release (Summerton 2006). As expected, a combination of the 6th generation of polylysines and the Endo-Porter resulted in a widespread fluorescence in the cytosol as shown by confocal fluorescence microscopy. Moreover, the resulting polyplexes showed effective knockdown of several genes with low cytotoxicity, while

no knockdown was observed for the complex formed from either the 6th generation of polylysine and the Endo-Porter alone (Inoue et al, 2008). Used for siRNA delivery, the 6th generation of polylysines has also shown *in vivo* silencing promise. A significant reduction of serum low density lipoprotein cholesterol was observed after intravenous administration of the 6th generation of polylysines/siRNA complexes into diseased mice (Watanabe et al, 2009).

1.3.1.3 Branched histidine-lysine (HK) peptides

In an early report, highly branched histidine-lysine (HK) peptides were also explored in terms of DNA transfection by Mixson *et al* (Leng et al, 2005). It was shown that the histidine-rich tails of these peptides markedly improved DNA transfection efficiency in a variety of cell lines. Presumably, the improved transfection was attributed to the increased buffering capacity of the polymer. Significantly, one polymer with a histidine-rich tail was compared favourably with other commonly used transfection agents. The same branched HK peptides were also explored for siRNA delivery in the same group and it exhibited more than 80% knockdown *in vitro* (Leng et al, 2005). The histidine-rich domain and the length of the terminal arms of HK peptides were important for siRNA delivery.

Besides the siRNA silencing effect, the resulting complex was found to have minimal toxicity (Leng et al, 2005). In contrast, carriers of siRNA such as Oligofectamine and Lipofectamine 2000 were significantly more toxic. Notably, the HK peptides with a higher content of histidines induced the least cytokines *in vivo*. As the greater pH-buffering capacity of HK peptides helps the release of endosomal entrapped foreign particles, it may explain why cytokine levels were reduced (Leng et al, 2012).

Promisingly, these HK peptides have shown effective *in vivo* delivery of siRNA (Leng et al, 2008). The target Raf-1 protein within tumours was significantly decreased after treatment with the HK:Raf-1 siRNA polyplexes compared to the control treatment groups. Despite the striking effect of the HK peptides/siRNA complex on the tumour, there was little evidence of toxicity in normal tissues with this therapy. Following the above success, they sought to develop a more effective HK carrier of siRNA by modifying them with different ligand (cyclic arginine-glycine-aspartic acid, RGD)-pegylation patterns (Chou et al, 2011). Although the modified HK peptides by themselves did not form stable nanoplexes with siRNA, a combination of a highly charged unmodified HK peptide, H2K4b, with the modified HK peptides did form stable siRNA

nanoparticles. In contrast, the modified complex administered intravenously was more effective than the unmodified in silencing Luciferase in a tumour xenograft model. Moreover, the siRNA complex incorporating the highly modified peptide was the most effective at silencing its target *in vivo*. Their investigation reveals that through control of targeting ligand surface display in association with a steric PEG layer, modified HK peptides/siRNA complexes show promise to advance RNAi therapeutics in oncology and potentially other critical diseases (Chou et al, 2013).

1.3.1.4 Polyethylenimine (PEI)

Besides peptides, polymeric PEI is another highly investigated DNA/siRNA delivery vector. Like peptides, PEI contains amines in its repeating units. The idea of using PEI to deliver DNA was inspired by that of polycations such as lipopolyamines and polyamidoamine, which possess substantial buffering capacity below physiological pH, and are efficient transfection agents (Boussif 1995). Luciferase DNA delivery with PEI into a variety of cell lines and primary cells gave results comparable to, or even better than, lipopolyamines. Their hypothesis is that its efficiency relies on extensive endosomal buffering that protects DNA from nuclease degradation, and consequent lysosomal swelling and rupture that provides an escape mechanism for the PEI/DNA particles.

Following the above success, Behr proposed how PEI/DNA complexes can transfect cells and exert its ‘proton sponge’ effect (Behr 1997). Firstly, polycation/DNA complexes enter cells by spontaneous endocytosis. Secondly, a complex wholly covered with positive charges interacting with the cell membrane will produce a high local concentration of PEI in endosomes. During intracellular trafficking, PEI will not only tend to inhibit the action of the lysosomal nucleases, but will also alter the osmolarity of the vesicle, that is ‘proton sponge’ effect of PEI. Indeed, every third atom of each PEI unit is a protonable amino nitrogen atom, which makes it an effective ‘proton sponge’ at virtually any pH. As a consequence, DNA complexed with PEI will be rapidly released from the damaging endosomal environment. He concluded that this molecule constituted of PEI is a promising vector for gene therapy and an ideal structural base for constructing more sophisticated vectors.

The above hypothesis has been supported by measuring protonatability of PEI. At a pH 7, approximately 85% of the amines of PEI remain unprotonated compared to 52% at a pH of 5 (Suh J. et al, 1994). This buffering capacity allows PEI/DNA complexes to avoid lysosomal

trafficking and degradation once inside the cell. Sonawane et al. also showed reduced acidification and increased swelling and chloride concentration for PEI polyplexes as compared to those of polylysine, supporting the buffering capacity of polyethylenimine (Sonawane et al, 2003). Akinc et al. later showed that the removal of protonable amines reduced PEI transfection activity 50-fold, thus quantitatively verifying the 'proton sponge' hypothesis (Akinc et al, 2005). Therefore, the 'proton sponge' theory has gained widespread acceptance.

Transfection efficiency of PEI has been studied over a wide range of molecular weights. While Godbey et al. showed that transfection efficiency of PEI polyplexes increases with increased molecular weight ranging from 600 to 70 000 Daltons (Godbey et al, 1999). High molecular weight polymers also result in significantly higher cytotoxicity. In addition to the molecular weight, the degree of branching of PEI has been shown to affect DNA complex formation and stability. Dunlap et al. showed that linear PEI is less effective at condensing DNA compared to the branched form for similar molecular weights (Dunlap et al, 1997). Owing to high charge density, the branched polymers exhibit high transfection efficiency, and particularly PEI at a molecular weight of 25 000 Daltons is considered as a gold standard (Patnaik et al, 2013). However, a major drawback of the PEI polymers is the cytotoxicity which has limited its application in vivo and halted progress into clinical trials (Moghimi et al, 2005).

1.3.2 Lipids

Lipids are another class of synthetic materials which could be used for DNA/siRNA delivery, which are usually cationic. Generally, lipid needs to be prepared into liposome vesicles with/without other ingredients before formulating with DNA or siRNA via electrostatic interaction. The resultant complex is named as a lipoplex (Figure 1.6).

The cationic lipids used for DNA/siRNA delivery are summarised in these reviews (Zhang et al, 2004, Tros de Ilarduya et al, 2010, Balazs DA 2011). Among these lipids, DOTMA is one of the most famous cationic lipids, which is also the first synthetic cationic lipid that has shown successful DNA delivery (Felgner et al, 1987). The lipids that gives a higher *in vivo* transfection activity generally shares the following structural characteristics (Ren et al, 2000): (1) a cationic head group and its neighbouring aliphatic chain being in a 1,2-relationship on the backbone; (2) an ether bond for bridging the aliphatic chains to the backbone; and (3) paired oleyl chains as the hydrophobic anchor. Cationic lipids without these structural features were reported to have

lower *in vivo* transfection activity. A DOTMA/DOPE (1:1 w:w) liposome formulation, Lipofectin®, has been commercialised as a DNA/RNA transfection agent.

The role of neutral DOPE in this commercial formulation is to form a non-bilayer structure with endosomal membrane and aid in endosomal escape. DOPE adopts a reversed hexagonal H_{II} phase favourably and is widely used as a helper neutral lipid. DOPE has both a cationic amine and an anionic phosphate in the headgroup, described as a zwitterionic lipid. DOPE plays an important role in membrane fluidity and substance exchange. The endosomal membrane destabilisation mediated by DOPE in DNA/lipid complexes is depicted in Figure 1.9 (below). The cellular membrane and endosomal membrane are composed of both anionic and zwitterionic lipids, displaying a negatively charged surface. After forming electrostatic interactions with the negative cell membrane, cationic lipoplexes are endocytosed (Step 1). In the early endosomes, membrane destabilization results in anionic phospholipid flip-flop (Step 2). The anionic lipids diffuse into the complex and form a charge neutral ion pair. Eventually, the intermediate inverse micelles form between the opposed monolayers and assemble into an inverse hexagonal H_{II} phase (Step 3). The DNA/siRNA dissociates from the complex and is released into the cytoplasm (Step 4).

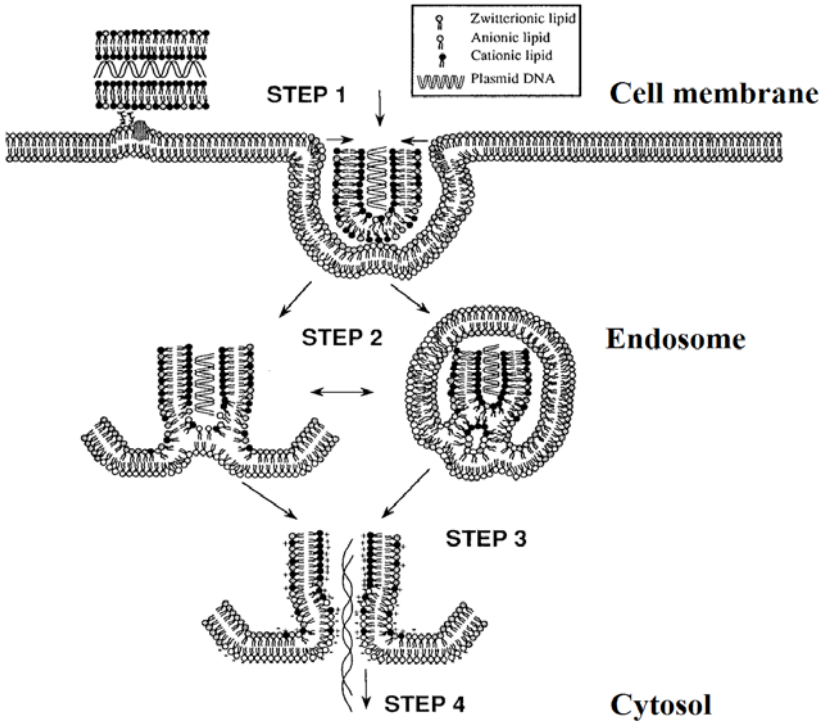

Figure 1.9 Mechanism of cellular uptake and endosomal escape of DNA/siRNA facilitated by non-bilayer lipid DOPE (Xu et al, 1996).

1.3.2.1 DOPE-containing lipoplexes

DOPE has been widely used for novel liposomal DNA/siRNA delivery (Hirsch-Lerner et al, 2005, Kazunori et al, 2005, Liu et al, 2011, Goldring et al, 2012, Opstad et al, 2013). For instance, DOPE was formulated with a cyclen-based cationic lipid to liposomes which then were complexed with DNA. The resultant lipoplexes (+/- 6:1) had a slightly higher transfection *in vitro* than that of Lipofectamine 2000 (Liu 2011). DOPE was also formulated with a novel lipid 1,2-dimyristoyl-sn-glycero-3-ethylphosphocholine (EPC) to make liposomes. The produced lipoplexes exhibited DNA binding and protection from DNase I degradation and concentration dependent cytotoxicity *in vitro* (Goldring et al, 2012). In addition, compared with cholesterol-containing liposomes, the DOPE-containing liposomes were less efficient at DNA transfection. In another study, protamine was introduced to the EPC-derivative/DOPE/DNA formulation. The resultant complex showed comparable *in vitro* transfection to EPC itself and performed equally to the standard reference Lipofectamine 2000 (Opstad et al, 2013).

1.3.2.2 DOTMA-containing lipoplexes

DOTMA has been formulated into liposomes with Tween 80 and used to complex DNA. The resultant lipolexes showed the best *in vivo* transfection in lungs among various organs (Liu et al, 1997). In addition, a higher (+/-) charge ratio resulted in a higher *in vivo* transfection in lungs which was correlated with cellular uptake and retention. It is worth noting that Tween 80 was used in the formulation because it was the best in preventing the formation of large DNA/lipid complexes and serum-induced inhibition of transfection activity among the surfactants they investigated so far (Liu et al, 1996). It was speculated that such inhibitory activity of the Tween 80 is related to the steric barrier formed by its four branched polyethylene oxide chains on its head group.

1.3.2.3 DOTMA/DOPE-containing lipoplexes

DOTMA/DOPE liposomes and DOTMA/Cholesterol liposomes have been compared in terms of DNA delivery *in vivo*. A higher DNA transfection efficiency was observed in the lung for DOTMA-cholesterol lipoplexes than that for DOTMA-DOPE lipoplexes (Sakurai et al, 2001a, Yoshioka et al, 2009). The higher transfection of DOTMA/Cholesterol/DNA complex compared with that of DOTMA/DOPE/DNA was also observed in ocular tissue after intravitreal injection on a rabbit model (Li et al, 1997). Further investigation showed that the low transfection activity of

DOTMA/DOPE complexes was due to their binding and fusion with erythrocytes. (Sakurai et al, 2001a). They also speculated that the DOTMA/DOPE complexes that fused with erythrocytes had a large size which could embolise lung capillaries and be washed away in the blood stream (Sakurai et al, 2001b). Consequently, they were no longer available for efficient internalization by the endothelial cells. In addition, DOTMA/Cholesterol and DOTMA complexes had a stable lamellar structure while DOTMA/DOPE complexes had a highly curved structure with high fluidity, which particularly absorbs serum proteins (Li et al, 1998). These results indicate that the interaction with erythrocytes and the resultant toxicity depends on the properties of the cationic lipid vectors, which is an important factor for intravenous DNA/siRNA delivery using cationic lipid vectors (Sakurai et al, 2001a).

1.3.2.4 Functionalisation of liposomes used for lipoplexes

PEG can be physically inserted into liposome bilayers or covalently bonded to the lipid component of liposomes (Immordino et al, 2006). The PEGylated liposome could be further formulated with DNA/siRNA to form PEGylated lipoplexes. It was reported that PEGylated lipoplexes yielded improved transfection efficiencies in the presence of serum as compared to the un-modified lipoplexes (Kim et al, 2003). In addition, targeting ligands can be attached to the lipid or the distal end of PEG and therefore giving the resultant lipoplexes a specific targeting function. Transferrin has been attached to the distal end of PEG-liposomes bearing approximately 25 Transferrin molecules per liposome and formulated with DNA. The resultant lipoplexes were administered to tumour-bearing mice. It was found that such Transferrin-PEG-liposomal formulation showed a prolonged residence time in the circulation and low reticuloendothelial system uptake, resulting in enhanced extravasation of DNA into the solid tumour tissue (Ishida et al, 2001). Moreover, the extravasated Transferrin-PEG-liposomal lipoplexes were internalized into tumour cells by receptor-mediated endocytosis (Ishida et al, 2001). Haloperidol is a ligand that associates with sigma receptors that are overexpressed in many types of cancer. Haloperidol-modified lipoplexes have been demonstrated to mediate efficient targeting of DNA to sigma receptor-overexpressing breast cancer cells (Mukherjee et al, 2005).

1.3.3 A combination of lipids and peptides

Lipopolyplexes are inspired by the advantage of lipoplexes and polyplexes in cellular transfection. Lipopolyplexes can be prepared by mixing **l**ipids, **p**eptide with **D**NA or si**R**NA. The resultant complexes are named **LPD** and **LPR** respectively. Upon mixing, the components can spontaneously rearrange to form a condensed DNA/siRNA core coated by lipid membranes (Li et al, 1998). It is worth noting that DNA and siRNA take effect in different sub-cellular sites and the delivery materials that are effective for DNA are not necessarily effective for siRNA. For example, Mixon et al has reported that branched HK peptides that were effective for DNA transfection were not effective for siRNA silencing (Leng et al, 2005). Therefore, lipopolyplexes used for DNA and siRNA delivery will be discussed separately.

1.3.3.1 Lipopolyplexes containing DNA (LPD)

Synergistic effect of lipids and peptides as a LPD

As previously mentioned, cationic liposomes can be used as promising vectors to complex and deliver DNA (lipoplexes). Numerous studies have proved its potential in DNA delivery (Xiong et al, 2011, Chen et al, 2012, Sugano et al, 2012). Unfortunately, it was found that cationic liposomes, alone, used for nucleic acid delivery had a dose-dependent cytotoxicity both *in vitro* and *in vivo* (Hofland et al, 1996, Scheule et al, 1997, Alton et al, 1999). In order to reduce the amount of cationic liposomes used to complex DNA, Gao et al incorporated polycations (PLL, protamine, spermine, decapeptide derived from SV40 T-antigen) into lipoplex formulations and investigated *in vitro* transfection efficiency of the resultant LPD complex. Surprisingly, up to a 28-fold increase in transfection was achieved in the presence of less liposomes (Gao et al, 1996). The above synergistic effect of PLL and liposomes on transfection was proposed to be due to reduced complex size, high cationic charges and therefore enhanced cellular uptake, and the protection of DNA from enzymatic degradation. In addition, PLL can possibly help with DNA release and nuclear transport which may contribute the synergistic effect (Gao et al, 1996).

The synergistic effect of peptides and lipids on LPD transfection has also been observed by other groups (Chen et al, 2010, Hart et al, 1998, Scott et al, 2001, Hyndman et al, 2004, Hyndman et al, 2004, Song et al, 2012). For example, in a LPD containing K16 targeting peptides and DOTMA/DOPE lipids, its transfection was observed to be more than 100-fold of the PD counterpart alone (Hart et al, 1998). The role of the DOTMA/DOPE lipids was proposed

to be a co-factor of enhancing transfection efficiency. The mechanism of the enhancement possibly involves a reduction in the extent of endosomal degradation of DNA (Hart et al, 1998). Yan etc. synthesized a polylysine derivative and the resultant DOTAP-containing LPD also exhibited higher transfection efficiency than the LD counterpart (Chen et al, 2010).

It was also found that molecular weights of polypeptides could significantly influence their performance on the aforementioned synergistic effect. For example, high molecular weight peptides, such as PLL and protamine, were found to significantly enhance DNA transfection while small peptides, such as spermine and a cationic decapeptide derived from SV40 T-antigen, were only moderately active *in vitro* (Gao et al, 1996). Considering increased DNA transfection, more attention was paid to PLL or protamine-containing lipopolyplexes (Kogure et al, 2004, Khalil et al, 2007, Yamauchi et al, 2010).

Functional modification of LPD

The purpose of functional modification of LPD is to improve its *in vivo* profiles, such as long-circulation and targeting delivery at cellular level or subcellular level. The modification of LPD can be achieved via: 1. lipid modification; 2. peptide modification; 3. modification of other ingredients. Generally, a long-circulation profile could be achieved through PEGylation of either lipids or peptides. However, the PEGylation covering on the surface of the LPD may hinder its contact with cells and therefore lead to a reduced cellular uptake. To solve this problem, a targeting ligand is generally required. The attachment of targeting ligand onto the LPD can be realized through conjugation modification of lipids and peptides, which is similar to that of PEGylation. Currently, a combination of PEGylation and targeting ligand is a very popular strategy to achieve high DNA transfection efficiency. However, both PEGylation and targeting ligands should be ideally exposed outside of the LPD particles in order to exert their desired effect.

The beneficial effect of PEGylation and targeting ligand modification of LPDs has been well investigated. Harvie et al compared a modified LPD with non-modified LPD composing of protamine and 1,2-Distearoyl-sn-glycero-3-phosphoethanolamine (DSPE) lipid in terms of cellular binding, uptake and transfection (Harvie et al, 2003). DSPE was modified by PEG and RGD ligand which could target integrin receptors present on tumour cells. The resulting DSPE-

PEG-RGD was then formulated into a LPD. Such a LPD-(DSPE-PEG-RGD) was shown to result in a 5-fold and 15-fold increase in cellular binding and uptake, respectively, compared with the unmodified LPD. Moreover, the increased cellular binding and uptake lead to a 100-fold enhancement of transfection efficiency *in vitro* (Harvie et al, 2003).

Besides at a cellular level, the targeting delivery potential of modified LPD at a subcellular level was also investigated. Masuda et al developed a nuclear pore complex-targeting DNA delivery carrier, which consisted of protamine, ligand-conjugated cholesterol, DOPE and stearylated octa-arginine. The subcellular (nuclear pore complex) targeting function of the carrier is derived from sugar (mannose, galactose, GlcNAc) modified cholesterol, while incorporating stearylated octa-arginine is to achieve an improved cellular uptake of this carrier. As expected, the resultant LPD showed a higher transfection efficiency than the unmodified in both non-dividing and dividing cells (Masuda et al, 2008). Moreover, their studies also suggested that destabilization of the lipid structure in the LPD on nuclear membrane was closely related to nuclear translocation and DNA transfection activity. The above study suggested that not only DNA binding but also DNA release inside cells should be considered when designing a novel DNA delivery system.

Apart from lipid and ingredient modification, peptide could also be functionally modified. For instance, the C-terminus of K16 peptide was modified with $\alpha_5\beta_1$ integrin targeting motif to target lung tumour cells. The resulting LPD (containing DOTMA/DOPE lipids) showed a higher transfection *in vitro* than that containing K16 peptide without the targeting motif (Hart et al, 1998), suggesting the importance of incorporating targeting ligands into LPDs. The K16 peptide with the $\alpha_5\beta_1$ targeting motif was further decorated with a PEG motif and the resultant LPDs were considerably more stable, and aggregated more slowly, than a complex formulated using a similar peptide lacking the short PEG spacer (Pilkington-Miksa et al, 2008).

Effect of cationic peptides on LPD transfection

For synthetic peptides, its components and sequence can significantly affect the transfection efficiency of the resultant LPD. Welser et al synthesised a series of peptides containing a cationic condensation moiety (lysine, arginine and histidine) and a targeting moiety, and then formulated these peptides with DNA in a combination of DOTMA/DOPE liposomes (Welser et al,

2013). The transfection efficiency of the resulting LPD was compared. They found that the LPDs containing R-rich branched peptide and K-rich linear peptides gave better transfection while those containing H-rich peptides were inefficient (Welser et al, 2013).

Besides condensational PLL and protamine, a functional protein, Tat, has also been explored in LPD delivery. Hyndman et al synthesized a PTD peptide (SYGRKKRRQRRRGPPCA), used for LPD formulation. In the presence of DOTAP lipid, the resulting LPD was taken up through endocytosis and showed effective transfection *in vitro* (Hyndman 2004). Moreover, the LPD possessed a higher transfection than the LD counterparts, suggesting that other processes such as nuclear entry and endosomal release are significant barriers to DNA transfection (Hyndman 2004). In the same studies, they also compared K16 peptide and K16 decorated with the PDT peptide (K16-PDT). Interestingly, when K16 was used in LPD, the transfection efficiency was less than for the K16-PDT formulation. Their results indicate that both the primary sequence of Tat or its derivatives, their net charge, and particle characteristics such as size and zeta potential, may all play a role in determining peptide enhanced transfection efficiency (Hyndman 2004).

The other small cationic peptides that bind to virus DNA are also identified and used for LPD formulation. Cationic μ peptide (MRRAHHRRRRASHRRMRGG), is known to be associated with the core complex of adenoviruses. The μ peptide-containing LPDs showed a comparable transfection efficiency in an undifferentiated neuronal ND7 cell line with PLL or protamine, which is five-fold more effective than a lipoplex counterpart (Murray et al, 2001). Cationic peptide Vp1 (MAPKRKSGVSKCETKCT) derived from the polyoma virus also enhanced LPD gene delivery in comparison with the corresponding lipoplexes (Wiseman et al, 2005). Vp1 possessed a DNA condensing region which overlapped with a classical nuclear localisation signal (NLS) region and was proposed to contribute to the enhancement.

1.3.3.2 Lipopolyplex containing siRNA (LPR)

Similar to DNA, siRNA has been attempted to be formulated in ternary lipopolyplexes, namely LPRs, to achieve effective silencing. As siRNA exerts its silencing effect in the cytosol, nuclear delivery is not necessary and endosomal escape represents the main barrier for siRNA delivery. Basically, fewer barriers mean simpler formulation. However, due to the small size and rigidity of siRNA, siRNA is usually more difficult to be condensed and delivered when compared with DNA.

This may explain why vectors working for DNA delivery are generally inefficient for siRNA delivery. Indeed, reports on LPR are not seen as much as that on LPD. However, theoretically, the cell targeting and endosomal escape strategies which work for DNA may be also suitable for siRNA delivery.

Effect of cationic peptides on LPR silencing

As mentioned above, endosomal trapping can lead to complete degradation of therapeutic siRNA. Therefore, functional vector is generally required to facilitate siRNA escape from endosomes after endocytosis. The escape from endosomes can be achieved by incorporating cell penetrating peptides into the siRNA formulation. Most of cell penetrating peptides are cationic peptides which contain arginine/lysine residues.

Stearyl octaarginine (STR-R8) peptide, together with cholesteryl hemisuccinate and DOPE lipids, has been explored to form LPR for siRNA delivery (Nakamura et al, 2007). The resultant LPR was less than 100 nm, exhibiting greater than 80% luciferase silencing *in vitro*. In another study, to achieve successful silencing, cholesterol was modified with Gala peptide (WEAALAEALAEALAEHLAEALAEALEALAA) (Hatakeyama et al, 2009). Gala is a pH sensitive fusogenic peptide which is designed to interact with lipid bilayers and induce leakage of its contents at pH 5.0 (Subbarao et al, 1987). The resulting LPR produced more efficient gene silencing compared with that containing unmodified cholesterol by *in vivo* topical administration. The improved gene silencing was proved to be due to Gala peptide-mediated endosomal escape of siRNA after internalization (Hatakeyama et al, 2009). To further trigger cytosolic release, stearyl octahistidine (STR-H8) was introduced to the above STR-R8/cholesterol-Gala/DOPE vector (Toriyabe et al, 2013). Significantly, the resulting complex showed increased *in vitro* luciferase silencing in contrast to the original vector, which was related with increased cytosolic release. Therefore, it would be beneficial to siRNA silencing by introducing functional peptide to the delivery vector.

Targeting modification of peptides used for LPR

Similar to DNA delivery, siRNA delivery requires disease site accumulation to maximise silencing and minimise cytotoxicity. The commonly used strategy is to decorate delivery vector with ligands that target specific receptors present on the surface of cancer cells. One of the

most employed receptors for siRNA delivery is integrins (Kim et al, 2009, Chen et al, 2013). Integrins mediate adhesion to the extracellular matrix and provide the traction necessary for cell motility and invasion. A wide variety of integrins contribute to tumour progression (Desgrosellier et al, 2010).

A ternary LPR, composed of K16 peptide linked with a $\alpha_5\beta_1$ integrin targeting motif (K16GACYGLPHKFCG) and the silencing effect of the resulting LPR was evaluated (Tagalakis et al, 2011). Significantly, such a targeting LPR showed a significant 80% silencing observed *in vitro*, similar in efficiency to the positive control Lipofectamine 2000. Furthermore, it was found that the LPR prepared from liposomes containing DOTMA, which has an 18-carbon alkyl tail, were significantly better in silencing than that containing cationic lipid with shorter alkyl tails. Moreover, the LPR can effectively package the siRNA to less than 100 nm in size, protect it from enzymatic cleavage, can be dissociated by heparin and is localised in cytoplasm following transfection of cells, suggesting the importance of the balance between condensation and release and the localisation in the cytoplasm. Therefore, the balance between siRNA condensation and release could be used as a factor to evaluate its efficiency as a delivery vector.

Branching peptides used for LPR

The branching of cationic peptides can affect their binding ability and therefore siRNA delivery and silencing. Tagalakis et al compared the LPR containing DOTMA/DOPE lipids and peptides with linear and branched structures regarding siRNA condensation and silencing (Tagalakis et al, 2013). Interestingly, they found that the LPR containing linear peptides were more condensed and stable than those containing branched peptide. However, the former possessed a lower silencing activity than the latter. Reassuringly, it suggests the importance of a balance between condensation and release within the cells (Tagalakis et al, 2013).

Other strategies used for LPR

To improve in vivo behaviour, novel strategies have been attempted. Based on the success of LPD containing protamine and lipids, anionic DNA was added to protamine and lipids to encapsulate siRNA. It was shown that the particle size of the resultant LPR was reduced by 10 - 30% while siRNA delivery efficiency increased by 20 - 80% (Li et al, 2008). The reduced size

was proposed to be due to improved core compaction provided by high molecular weight DNA. It is worth noting that the anionic DNA used is calf thymus DNA rather than plasmid DNA because calf thymus DNA contains limited amounts of immunostimulating CpG motifs. The resultant LPRs were also decorated with PEG and anisamide as a targeting ligand of a receptor overexpressed in many human tumour cells. It was found that the presence of the targeting ligand facilitated the internalization of siRNA by tumour cells and only siRNA formulated in the targeted complex showed significant gene silencing activity (Li et al, 2008). In addition, the results of *in vivo* animal experiments using Xenograft lung tumour models revealed that about 70 - 80% of siRNA formulated in the LPR accumulated in the tumour 4 hours after IV injection. Further investigation confirmed a 15% tumour cell apoptosis after three daily injections (1.2 mg/kg) (Li et al, 2008).

In their further studies, hyaluronic acid was used to replace calf thymus to work with liposomes and protamine to systemically deliver siRNA. The resultant LPR was also modified with PEG and anisamide to achieve a longer circulation and more efficient lung tumour cell targeting. The targeted LPR was found to show similar silencing activity compared to the calf thymus DNA containing LPR (Chono et al, 2008). However, the hyaluronic acid-containing LPR significantly improved the therapeutic window by at least 2.7-fold on metastatic tumour models. In addition, the hyaluronic acid-containing LPR possessed very little immunotoxicity in a wide dose range (0.15 - 11.2 mg/kg). They concluded that such a LPR without the presence of foreign DNA has a potential use in humans (Chono et al, 2008).

Similar to the above LPR, a novel ternary complex consisting of calcium phosphate/siRNA precipitates covered by cationic lipids was also reported (Li et al, 2010). Compared with conventional LPR, acid-sensitive calcium phosphate was used to replace peptide, making a LCR. However, similar endosomal escape could be achieved by a calcium phosphate-mediated ‘proton sponge’ effect. This replacement is also based on the hypothesis that after entering cells, LCR would disassemble in the acidic pH found in endosomes, which would increase the osmotic pressure, and as a consequence burst the endosome, releasing siRNA into the cytoplasm. In the LCRs, siRNA formed an amorphous nanoprecipitate with calcium phosphate coated with PEGylated lipids with or without anisamide, a sigma-1 receptor ligand for systemic administration. The anisamide modified LCP NP silenced about 70% and 50% of luciferase

activity for the tumour cells in culture and those grown in a xenograft model, respectively. The untargeted NP showed a very low silencing effect. It reveals that targeted delivery is important for *in vitro* and *in vivo* siRNA silencing (Li et al, 2010).

The success of the above novel LPR formulation suggested that effective siRNA silencing can be achieved *in vitro* and *in vivo* by adjusting delivery materials and making use of modification strategies.

1.4 Aim and objectives

The aim of the present project is to achieve efficient DNA/siRNA delivery through constructing multifunctional lipopolyplex carriers (LPDs and LPRs) containing novel bifunctional peptides. The bifunctional peptides are expected to have several key properties: condensation, protection, targeting, endosomal escape, and nuclear localisation for DNA.

The bifunctonal peptides have been designed shown in the upper panel in Figure 1.10. The bifunctional peptides are composed of complexing moieties and a targeting moiety, connected by a linker. The complexing moieties are branched, denoted B. B regions are designed to be cationic to complex DNA or siRNA. The targeting moiety, denoted Y, is designed to target integrin receptors on lung cancer cells. The linker, denoted L, is designed to be degradable in endosomes. So the bifunctional peptides are called BLY peptides. All the BLY peptides have the same amino acid sequence on regions L and Y, with differences only in region B. Region B is composed of either one amino acid, histidine, arginine or lysine (denoted Series I) or a combination of them (denoted Series II). A schematic representation of the bifunctional peptides, H12BLY from Series I peptides, is shown in the lower panel in Figure 1.10.

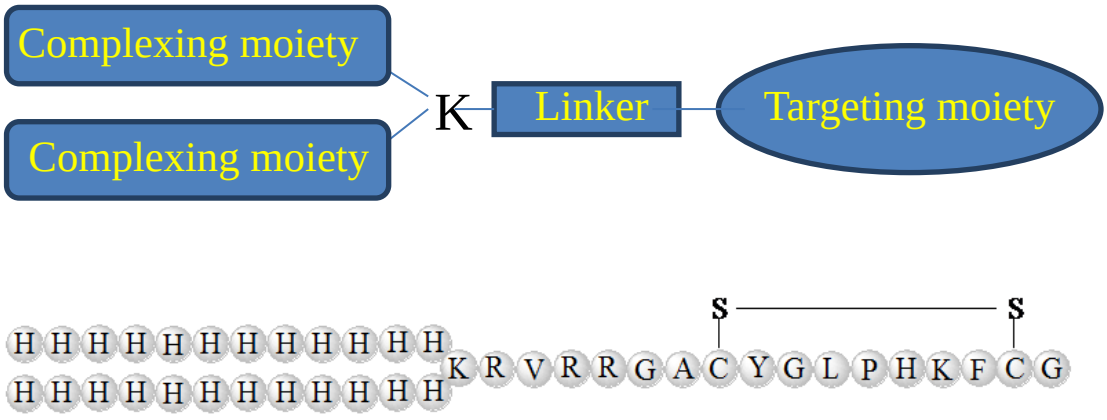

Figure 1.10 Structure depictions of bifunctional peptides and a representation, H12BLY in Series I peptides.

The peptide containing lipopolyplexes are constructed by mixing the peptide and liposomes followed by the addition of DNA or siRNA, producing LPDs or LPRs. The liposomes are used in the formulation because liposomes and peptide have been shown to exhibit a synergistic effect on the delivery of LPDs/LPRs (Chen 2010, Hart 1998, Scott 2001, Hyndman 2004, Song 2012).

The resultant LPDs/LPRs were proposed to have a core-shell structure as depicted in Figure 1.11 (Mustapa et al, 2007). DNA/siRNA is condensed by the peptide, forming an inner core. The DNA or siRNA/peptide inner core is coated by a lipid bilayer with the targeting moiety of the peptide protruding outside. This structure affords the dual protection of DNA/siRNA by peptide and lipid bilayer, and the effective targeting of the complex.

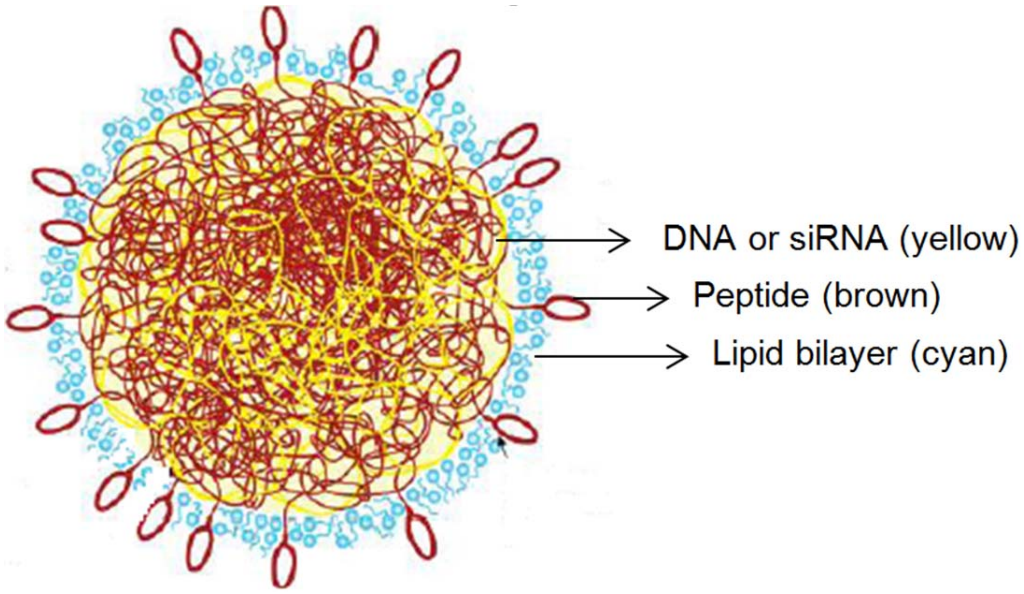

Figure 1.11 Proposed macromolecular structure of LPDs or LPRs. DNA/siRNA (yellow) interacts with peptide (brown) forming an inner core coated by lipid bilayer (cyan) with the targeting moiety of peptide protruding outside (Mustapa et al, 2007).

Thereafter, another aim of the present study is to investigate the delivery potential of the LPDs or LPRs to cancer cells. This will be performed by incubating LPDs or LPRs with lung carcinoma A549 cells *in vitro* and assessing their biological effect, that is DNA transfection and siRNA silencing. The DNA transfection and siRNA silencing will be conducted in either reduced serum Optimem or Media containing 10% fetal bovine serum (FBS). A reporter of luciferase-expressing DNA and a luciferase-silencing siRNA will be used as the methodology of luciferase quantification which has been well established *in vitro* and *in vivo*.

The third aim is to study the physico-chemical properties of the LPDs/LPRs and investigate their contributions to their transfection/silencing effect. For this reason, the condensation, release and protection properties of the LPDs/LPRs will be assessed by agarose gel electrophoresis. Particularly, the condensation will be quantified using a picogreen fluorescence assay. The size and the macromolecular structure of the LPDs/LPRs will also be measured using dynamic light

scattering (DLS) and small angle neutron scattering (SANS). For all the above studies, the LPDs/LPRs will be prepared in both water and NaCl solution to see the effect of salt, due to the presence of electrolytes in biological environments. Therefore, the physic-chemical properties of the LPDs or LPRs will be correlated with their *in vitro* biological behaviour.

Chapter 2 Methodology

2.1 Materials

2.1.1 Peptide synthesis

Fmoc-Gly-NovaSyn TGT resin (0.21 mmol·g^{-1}, 150 mg, 31.5 μmol) was purchased from Merck Chemicals Ltd (Nottingham, UK). Novabiochem® Fmoc-protected amino acids were obtained from Merck Millipore (Darmstadt, Germany). Peptide coupling reagent O-benzotriazole-*N*,*N*,*N*',*N*'-tetramethyl-uronium-hexafluoro-phosphate (HBTU) and reaction catalyst, *N*,*N*-diisopropylethylamine (DIPEA) were supplied by Sigma-Aldrich (Pool, UK) as where piperidine, HPLC-grade dimethylformamide (DMF), trifluoroacetic acid (TFA), triisopropylsilane (TIPS), 1, 2-ethanedithiol (EDT), water (HPLC- grade) and diethyl ether.

2.1.2 Vesicle preparation

Trimethyl [2,3-dioleyloxy-propyl] ammonium chloride (DOTMA) was obtained from Tokyo Chemical Industry (Tokyo, Japan). Dioleoylphosphotidylethanolamine (DOPE) was purchased from Avanti Polar Lipids (Alabama, US). Chloroform was supplied by Fisher Scientific (Loughborough, UK).

2.1.3 DNA Transfection and siRNA knockdown

A549 cells (adenocarcinomic human alveolar basal epithelial) were obtained from ATCC (Manassas, USA). A549 cells, stably transduced with the luciferase gene (Type I), were kindly donated by Dr Maya Thanou (King's College London, London, UK). gWiz-luciferase plasmid DNA (pDNA) was purchased from Aldevron (Frago, USA). Ambion® Silencer® firefly luciferase (GL2+GL3) siRNA® (+siRNA) and negative control siRNA (-siRNA), Invitrogen™, Lipofectamine and Lipofectamine 2000, Invitrogen™, 4% w/v of Trypan blue in phosphate buffer saline (PBS) and Gibco® reduced serum medium OPTI-MEM® I were all supplied by Life Technologies (Paisley, UK). Luciferase assay kit was obtained from Promega (Southampton, UK). Bicinchoninic acid (BCA) protein assay kit was purchased from Fisher Scientific (Loughborough, UK). RPMI-1640 cell culture medium, 0.25% w/v trypsin/ethylenediaminetetraacetic acid (EDTA) solution, foetal bovine serum (FBS), 1% v/v of 100x strength non-essential amino acids, 1% v/v of penicillin/streptomycin antibiotic solution (10 000 U·mL^{-1}/10 mg·mL^{-1}), L-glutamine were

purchased from Sigma-Aldrich (Pool, UK). CELLSTAR® 96 well clear or white polystyrene flat bottom plates and CELLSTAR® T75 filter cap tissue culture flasks were supplied by Greiner Bio-One (Stonehouse, UK).

2.1.4 Agarose gel electrophoresis

Gelred nucleic acid gel stain (10 000x in water) was purchased from Biotium (Heyward, USA). Ribonuclease A from bovine pancreas, ribonuclease inhibitor from human placenta, deoxyribonuclease I (DNAse I) Type II from bovine pancreas, poly-L-aspartic acid sodium salt (pAsp), tris(hydroxymethyl)aminomethane hydrochloride (trizma base), agarose, ethylenediaminetetraacetic acid disodium salt dehydrate (EDTA), boric acid, glacial acetic acid, bromophenol blue sodium salt, sucrose, magnesium chloride were all obtained from Sigma-Aldrich (Pool, UK). Glacial acetic acid was purchased from VWR International Ltd (West Sussex, UK). EDTA (0.5 M, pH 8.0) solution was supplied by Promega (Southampton, UK). Tris-acetic-EDTA (TAE, pH 7.4) buffer and tris-borate-EDTA (TBE, pH 8.3) buffer were prepared from the above ingredients. Picogreen fluorescence assay Quant-iT™ PicoGreen® dsDNA reagent was purchased from Life Technologies (Paisley, UK). Greiner CELLSTAR® 96 well black polystyrene flat bottom plates were obtained from Sigma-Aldrich (Pool, UK).

2.1.5 Small angle neutron scattering

Calf thymus DNA (ctDNA), custom-made siRNA (CUU ACG CUG AGU ACU UCG dTdT), described as Sigma siRNA, and D_2O (>99.9% purity) were obtained from Sigma-Aldrich (Pool, UK).

2.2 Methods

2.2.1 Peptide design

The bifunctional peptides developed in the present study consisted of a DNA/siRNA complexing moiety (denoted B), and a cellular targeting moiety (denoted Y), joined by a linker (denoted L) as shown before in Figure 1.10.

Region B is either composed totally of histidine (H), arginine (R) or lysine (K) residues (Series 1) or a combination thereof (Series 2), as shown in Figure 2.1. The use of two series of peptides, namely Series I and II, allow the effect of single and mixed amino acid residues on transfection or knockdown to be compared. Moiety Y was designed to target human airway lung epithelial

cells and was developed after screening by phage display (unknown epithelial cell receptor) (Writer et al, 2004). Moiety Y is cyclic in nature due to the presence of a disulfide bond formed from the two cystine residues. Interpeptide disulfide bonds between two cystine residues have been demonstrated to stabilise peptide/DNA complexes, leading to greater transfection efficiency (Lo et al, 2008). Linker L has a degradable sequence -RVRR-, which has been shown *in vitro* to be cleaved by the furin enzyme in 4 h under conditions approximating those found in the endosome. The introduction of the enzyme cleavable -RVRR- sequence in other bifunctional peptides has been found to significantly increase transfection efficiency in mouse neuroblastoma (Neuro 2A) cells, mouse endothelial (bEND.3) cells, mouse embryonic fibroblast (AJ3.1) cells, human bronchial epithelial (16HBE14o-) cells, and primary porcine vascular smooth muscle (PVSMCs) cells of lipopolyplexes (Mustapa et al, 2009).

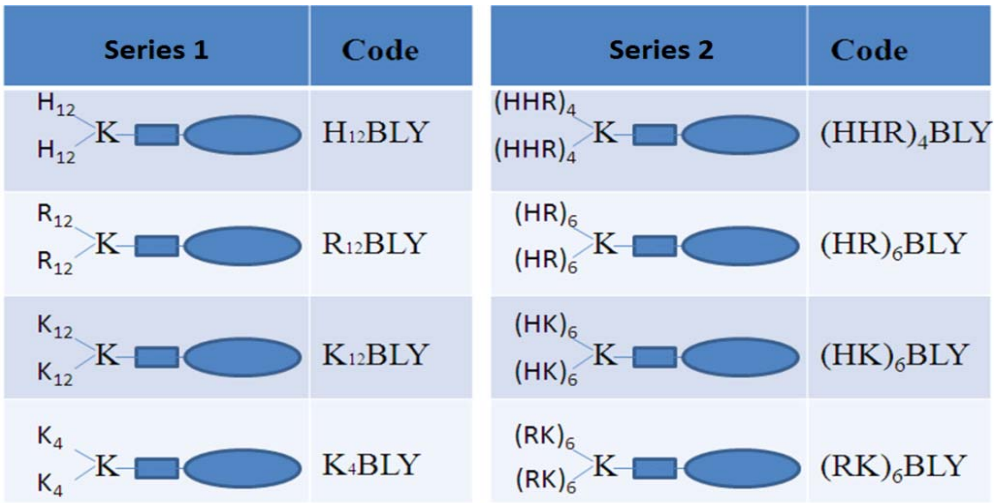

Figure 2.1 Two series of the bifunctional branched peptides investigated.

2.2.2 Peptide Synthesis

All peptides were synthesised by Standard Fmoc Solid Phase Peptide Synthesis (SPPS) methodology. SPPS synthesis was performed in reaction syringes housed in a MultiSynTech Syro I automated system (Witten, Germany). Fmoc-Gly-NovaSyn TGT resin (0.21 mmol·g^{-1}, 150 mg, 31.5 µmol) was loaded into the reaction syringes and the resin pre-swelled in 3 mL DMF (HPLC-grade) for at least 30 min prior to the start of the synthesis. The total volume of all reagents in the reaction syringe was maintained as 1.5 mL. All reagents used for the peptide synthesis were dissolved in DMF (HPLC-grade). The MultiSynTech Syro I automated system was programmed with the following automatic deprotection/coupling cycle:

Cycle one: deprotection

The resin-loaded reaction syringe was filled with 1.5 mL of 40% v/v piperidine in DMF. The mixture contained in the reaction syringe was then automatically agitated for 20 s every minute for a total of 3 min after which the reagent was removed by filtration under vacuum and the resin was washed with DMF (4 × 1.5 mL). 0.75 mL of 40% v/v piperidine in DMF was then added to the reaction syringe followed by a further 0.75 mL of DMF to make a 20% v/v solution of piperidine in DMF. The mixture in the reaction syringe was agitated for 20 s every minute for a total of 10 min after which time the reagents were removed by filtration under vacuum and the resin was washed with 6 aliquots of 1.5 mL DMF.

Cycle two: coupling

The reaction syringe was next filled with the required Fmoc-protected amino acid (0.600 mL, 0.084 M, 4 eq.), HBTU (0.600 mL, 0.084 M, 4eq.) and DIPEA (0.300 mL, 0.168 M, 8 eq.) using the automatic dispenser contained in the synthesizer. The resulting mixture was then agitated for 20 s every 3 min for a total of 40 min. The reagents were removed by filtration under vacuum and the resin was washed with 4 aliquots of 1.5 mL DMF.

To achieve peptide synthesis, the above deprotection/coupling cycle was repeated until all the amino acids were coupled to the resin. Upon the completion of this stage of the synthesis, 3 mL of a cleavage solution comprising of TFA/TIPS/EDT/H_2O (94:2.5:2.5:1 volume ratio) was added to the resin-loaded reaction syringe and the syringe was agitated for 3 h at room temperature. The cleavage solution was then removed from the syringe under vacuum and diethyl ether (10-15 mL) was added to precipitate the peptide. The resultant precipitate in diethyl ether was spun at 4°C and 4 000 rpm for 10 min to ensure pelleting the crude peptide. The diethyl ether supernatant was then decanted off and the peptide pellet was washed a further twice with diethyl ether. The crude peptide pellet was then re-dissolved in the minimum amount of water and freeze-dried using a Thermo Scientific Heto PowerDry LL1500 freeze-drier (Loughborough, UK) to remove any solvents. In order to form the disulfide bonds via aerial oxidation, the crude peptide was re-dissolved in water (1 mg 10 mL^{-1}) and stirred at room temperature for 7-10 days. The peptide solution was then concentrated and freeze-dried for storage prior to purification by HPLC.

2.2.3 Purification and characterisation of the peptides

Peptides were purified and analysed via reverse phase HPLC using a Varian Prostar system equipped with a Model 210 solvent delivery module and a Model 320 UV detector (West Sussex, UK). Preparative HPLC purification was performed using a Phenomenex@ Onyx Monolithic Semi-Pre C18 column (100 x 10 mm, 2 µm macropore size, 13 nm mesopore size, Macclesfield, UK). The column was loaded with 200-400 µL aliquots of 10-20 mg mL^{-1} of peptide dissolved in water containing 0.1% v/v of TFA. The mobile phase consisted of a decreasing gradient of water in acetonitrile (CH_3CN), both solvents contained 0.1% v/v of TFA. The precise experimental conditions, including mobile phase gradients, used are given below as Methods A and B.

Preparative high performance liquid chromatography:

Method A: Flow rate 9.5 mL/min; UV detection at 215 and 254 nm. Linear gradient: 5-25% B over 15 min. A = H_2O, 0.1% v/v of TFA, B = CH_3CN, 0.1% v/v of TFA.

Method B: Flow rate 9.5 mL/min; UV detection at 215 and 254 nm. Linear gradient: 5-30% B over 20 min. A = H_2O, 0.1% v/v of TFA, B = CH_3CN, 0.1% v/v of TFA.

The HLPC fractions containing the required peptide product were pooled and concentrated under reduced pressure to yield approximately 2 mL of solution prior to freeze-drying. The freeze-dried peptides were subsequently analysed by analytical HPLC using a Phenomenex@ Onyx Monolithic C18 column (100 x 3.0 µm, 2 µm micropore size, 13 nm mesopore size, Macclesfield, UK). The precise experimental conditions, including mobile phase gradients, used are given below as Methods C and D.

Analytical high performance liquid chromatography:

Method C: Flow rate 0.85 mL/min; UV detection at 215 and 254 nm. Linear gradient: 5-90% B over 20 min. A = H_2O, 0.1% v/v of TFA, B = CH_3CN, 0.1% v/v of TFA.

Method D: Flow rate 0.85 mL/min; UV detection at 215 and 254 nm. Linear gradient: 5-90% B over 30 min. A = H_2O, 0.1% v/v of TFA, B = CH_3CN, 0.1% v/v of TFA.

The analysis of the chromatograms was conducted using Star Chromatography Workstation software Version 1.9.3.2. ESI-MS analysis of the purified peptides was performed on a Waters

Acquity Ultra Performance LC/MS machine (Elstree, UK). The HPLC and ESI-MS spectra of the peptides are shown in Appendix I.

2.2.4 Vesicle preparation

Vesicles composed of cationic DOTMA and the neutral helper DOPE at a 1:1 molar ratio were prepared using a modification of the thin film method. Specifically the required amount of DOTMA and DOPE were weighed out into small glass vials, followed by the addition of chloroform (3 mL) to dissolve the lipids (total quantity ~ 2 mg). The chloroform was then removed from the clear lipid solution to leave a thin lipid film by storing the lipidic solution under vacuum overnight. The resulting thin lipid film was then hydrated by agitation with the required amount of ultrapure, double distilled water (resistivity >18 Ω·cm) from Thermo Scientific Barnstead water purification system EASYpure® UV/UF (Loughborough, UK) with or without NaCl (up to 0.12 M) to make a crude lipidic suspension, of concentration with respect to DOTMA of 1 mg mL^{-1}. The resulting crude suspension of vesicles in water was probe sonicated at room temperature for 10 min using a SKL-950WT ultrasonic cell crusher (Ningbo Haishu Sklon Electronic Instrument Co. Ltd., Ningbo, China) fitted with a microtip operating at 30% of maximum output to produce a more homogeneous vesicle suspension. In the case of vesicles made in NaCl solution, the crude vesicle suspension was water bath sonicated at 80% of maximum output and 40° for 10 min using a Fisherbrand precision general-purpose water bath (Loughborough, UK). Note that the use of bath sonication rather than the probe sonication for the vesicles made in 0.12 M NaCl solution used due to their tendency to aggregate/grow when probe sonicated.

2.2.5 Lipopolyplex preparation

Lipopolyplexes consisting of lipids, peptide and either DNA or siRNA (LPDs and LPRs, respectively) were prepared via a self-assembly process, in which the order of addition of the various components was controlled. It has previously found that the order of addition of the various components in a ternary complex had an impact on the biophysical property and biological activity of the resulting complex (Gao et al, 1996, Garcia et al, 2007, Zeng et al, 2007). Consequently, unless otherwise stated, the method described below was used for preparation of both LPDs and LPRs.

In brief, peptide solution was first added to an equal volume of vesicle suspension. Next an equal volume of DNA/siRNA solution was added, and the mixture was gently mixed. All LPDs/LPRs were prepared by diluting a stock suspension of vesicles composed of a 1:1 molar ratio of DOTMA:DOPE (containing 1 mg mL^{-1} of DOTMA) in water or an aqueous NaCl solution (containing up to 0.15 M NaCl). In addition 1 mg mL^{-1} stock solutions of either peptide, DNA or siRNA in water were also used. Note, that the reason that the stock solutions of peptide, DNA and siRNA were prepared in water is that so they could be diluted with NaCl solution to give the required final NaCl concentration. Unless otherwise stated, LPDs were prepared at lipid:peptide:DNA charge ratios of 0.5:6:1 while LPRs were made at lipid:peptide:siRNA charge ratios of 0.5:12:1. In all cases, a minimum of 15 min standing time of the lipid:peptide:nucleic acid mixture at room temperature was allowed to ensure complexation before use.

Binary lipoplexes (LDs/LRs) and polyplexes (PDs/PRs) were also prepared to compare their ability to tranfect/silence protein production, respectively using the corresponding ternary lipopolyplex. The lipoplexes and polyplexes were prepared by adding the aqueous DNA/siRNA stock solution to an equal volume of vesicle suspension or peptide solution, respectively followed by a gentle mixing and a minimum of 15 min standing time at room temperature before use of the complex. LDs/LRs and PDs/PRs were made at the same L:D/R charge ratio as in the corresponding LPDs/LPRs.

2.2.6 Cell culture

A549 cells and luciferase-transduced A549 cells were maintained in T75 tissue culture flasks in RPMI-1640 media supplemented with 10% v/v of FBS, 1% v/v of 100 x strength non-essential amino acids (NEAA), 1% v/v of 200 mM L-glutamine solution, and 1% of v/v penicillin/streptomycin solution (10 000 $IU \cdot mL^{-1}$/10 $mg \cdot mL^{-1}$). The cells were kept at 37°C in a CO_2 incubator (Nuaire Autoflow CO_2 Air-Jacketed Incubator, Plymouth, USA) with an atmosphere of 90% humidified air and 5% carbon dioxide. The cells were passaged twice a week when ~70% confluent in a Howorth Airtech Safety cabinet (Model SC II, Class 2, Farnworth, UK). Briefly, the spent RPMI-1640 media was removed under reduced pressure and the single layer of cells remaining washed using a 1 mL aliquot of 0.25% w/v of trypsin-EDTA solution. After removal of the preliminary trypsin-EDTA wash, a further 2 mL of trypsin-EDTA solution was added to detach the cells from the flask with the aid of an orbital incubator (Stuart

Orbital Incubator Model SI 50, Stafford, UK) at 120 rpm, 37°C for ~2 min. 3 mL of warm RPMI-1640 media was then added to dilute the trypsined cell suspension and the resulting suspension centrifuged at 1 500 rpm and 20°C for 5 min (Beckman Counter™ Allegra™ X-22R Centrifuge, London, UK). The resultant supernatant was decanted and the remaining pellet of cells gently re-suspended in 10 mL of warm RPMI-1640 media until uniform suspension of cells was obtained. An aliquot of the cell suspension was then mixed with an equal volume of 0.4 %v/v trypan blue in water and the density of cells counted using a cell counter (Countess™ Automated Cell Counter, Life Technologies, Paisley, UK) while the shape of the A549 cells was observed under an inverted microscope (Hund Wetzlar Wilovert S Inverted Phase-Contrast Microscope, Welzlar, Germany). 1 mL of A549 cell suspension or 1.5 mL of luciferase-transduced A549 cell suspension (both at an ~ density of 1 x 10^6/mL) was then transferred to a new flask containing 13 mL of warm, fresh RPMI-1640 media and the cells (~ density of 1 x 10^5/mL) incubated in a CO_2 incubator with 90% humidified air and 5% CO_2 atmosphere at 37°C.

2.2.7 Transfection/knockdown of lipopolyplexes

25 µL of lipopolyplex (LPD/LPR) suspension containing 0.25 µg DNA or 0.07 µg siRNA, respectively were prepared as described above, except that each component was diluted in different preparation media including water, NaCl solutions (up to 0.15 M), PBS (pH7.0), and OptiMEM. The above LPD/LPR suspension was 4-fold diluted with transfection media, e.g. OptiMEM or RPMI-1640 media before use for the below transfection. A549 cells or luciferase-transduced A549 cells were seeded in 96-well transparent plates at a density of 1.2×10^4 cells per well for 24 h prior to transfection with LPDs or knockdown with LPRs, respectively. After removal of the spent media, a 50 µL of OptiMEM or RPMI-1640 media was added to each well followed by the addition of 50 µL of the LPDs/LPRs (25 µL of LPDs/LPRs diluted with 25 µL of OptiMEM or RPMI-1640 media). All lipopolyplexes were seeded at 0.25 µg/well of pDNA or 50 nM/well of siRNA, in triplicate, and unless otherwise stated, incubated at 37°C in an atmosphere of 90% humidified air and 5% CO_2 for 4 h for LPDs and 24 h for LPRs. After removal of the LPD/LPR suspension from the cells, 100µL of growth media was added to the cells which were maintained at 37°C in an atmosphere of 90% humidified air and 5% CO_2 for a further 44 h for LPDs or 24 h for LPRs. After which time, the cells were rinsed with 50 µL of PBS (pH 7.0) and lysed with 50 µL of lysis buffer containing 200 nM Tris-HCl (pH 7.8), 2 mM EDTA and 0.05% v/v Triton X-100 using orbital shaking at 150 rpm for 1 h at room temperature. In order to further aid

the lysis process, the cells were frozen at -80 °C for 30 min before being defrosted and agitated in orbital incubator for a further 1 h at room temperature and used for determination of luciferase activity and protein assay.

Luciferase activity, expressed as relative light units (RLU) per milligram of protein (RLU/mg protein), was measured using a Promega luciferase assay kit and a Fisher Scientific BCA protein assay kit in accordance with the manufacturers protocol.

In brief for the luciferase assay, 30 µL of cell lysate was transferred to 96-well white plates and luminescence measured at a gain value of 2000 using an a FLUOstar Omega luminometer (BMG LABTECH GmbH, Ortenberg, Germany) with an autofeeding system delivering 100 µL of the reconstituted luciferase assay reagent into each well containing cell lysate. Measurements were made in triplicate and the mean and SD calculated.

Protein content was measured using placing a 20 µL aliquot of the remaining cell lysate in a 96-well transparent plate and mixing with 200 µL of protein assay reagent (Promega luciferase assay kit) and incubating at 150 rpm, 37°C for 30 min before reading absorbance at 562 nm using a SpectraMax 190 plate reader (Molecular Device, USA). Measurements were performed in triplicate allowing the mean and SD to be calculated.

The biological activity of LPDs was evaluated by determining the expression of the luciferase gene, expressed as RLU/mg protein. By contrast, the biological activity of LPRs was evaluated by determining the silencing (or knockdown) of the luciferase gene, expressed as the RLU/mg protein in comparison to a negative siRNA control, designated as 100% luciferase gene expression. Lipofactamine and Lipofectamine 2000 were used as positive control for the transfection/knockdown of the LPDs/LPRs.

2.2.8 Agarose gel electrophoresis of LPDs/LPRs

The biophysical properties of the LPDs/LPRs were assessed by agarose gel electrophoresis. LPDs and LPRs were prepared as described above. The lipopolyplexes tested contained either 0.25 µg of pDNA or 0.1 µg of siRNA and were dispersed in 10 µL of ultrapure double distilled water or aqueous NaCl solution (up to 0.12 M). LPDs were run in 0.8 % w/v of agarose gel in tris-acetic-EDTA (TAE, pH 7.4) buffer containing 40 mM of tris, 20 mM of glacial acetic acid and 1 mM of EDTA. In comparison, LPRs were run in 2.0% w/v of agarose gel in tris-borate-EDTA

(TBE, pH 8.3) buffer containing 89 mM of tris, 89 mM of boric acid and 2 mM of EDTA. The LPDs/LPRs were treated as described below.

Extent of DNA/siRNA complexation in LPDs/LPRs After standing at room temperature for 15 min after preparation, 10 μL of the LPDs or LPRs were mixed with 2 μL of gel loading buffer containing 40% w/v of sucrose and 0.25% w/v of bromophenol blue.

Release of DNA from LPDs Release of DNA from the ternary complexes was assessed by first adding 0.625 μL of a 10 mg mL^{-1} aqueous polyaspartic acid (pAsp) sodium salt solution to 10 μL of a LPD suspension. 2 μL of gel loading buffer was then added to the resultant mixture and the whole same added to the gel.

Release of siRNA from LPRs Release of siRNA from the ternary complexes was assessed by first adding 1.25 μL of a 1 mg mL^{-1} aqueous pAsp sodium salt solution to 10 μL of a LPR suspension, respectively. 2 μL of gel loading buffer was then added to the resultant mixture and the whole same added to the gel.

Protection of DNA in LPDs The extent of protection afforded to DNA by incorporation into a ternary complex was determined by pre-treating 10 μL of a LPD suspension with 0.5 μL of a 0.1 M solution of $MgCl_2$ in water and then mixing with 0.5 μL of a 500 U mL^{-1} aqueous solution of DNAse I followed by incubation at 37°C for 10 min. 1.25 μL of a 0.5 M aqueous solution of EDTA was added and the resulting mixture incubated for 10 min at room temperature to ensure complete deactivation of the DNAase I enzyme, after which time 0.625 μL of a 10 mg mL^{-1} pAsp aqueous solution was added to release any DNA remaining associated with the LPDs for detection on the agarose gel. The LPD suspension was then mixed with 3 μL of gel loading buffer.

Protection of siRNA in LPRs The extent of protection afforded to siRNA by incorporation in a complex was determined by incubating 10 μL of a LPR suspension with 0.4 μL of a 0.1 mg mL^{-1} aqueous solution of RNAse A at 37°C for 30 min. 0.4 μL of an aqueous solution of RNAse inhibitor (45 units μL^{-1}) was then added and the resulting mixture incubated at room temperature for 10 min to ensure complete deactivation of the RNAse A enzyme. 1.25 μL of a 1 mg mL^{-1} aqueous solution of pAsp was then added to the mixture to release any siRNA remaining

associated with the LPRs for detection on the agarose gel. The LPR suspension was then mixed with 3 µL of gel loading buffer.

Finally, both the treated LPDs and LPRs were loaded on to the agarose gel containing 3 µL gel red. The electrophoresis was performed at 80 mV (Fisher Brand Model HU12 electrophoreses chamber, Loughborough, UK) for 40 min and the gel visualized under UV light illumination using an Alphalmage EP MultiImage Light Cabinet (Randpark Ridge, South Africa). Uncomplexed, free DNA/siRNA and the enzyme-treated uncomplexed, free DNA/siRNA were used as controls. Each gel was repeated on more than one occasion to ensure reproducibility.

2.2.9 Picogreen fluorescence assay of LPDs/LPRs

A picogreen fluorescence assay was performed to determine the extent of condensation/complexation of DNA/siRNA in the LPDs/LPRs. When the LPDs were made in water, 0.2 µg of pDNA was used per well in 96-well black plates, while when the LPDs were prepared in a 0.12 M NaCl aqueous solution, only 0.1 µg/well of DNA was used due to the enhancing effect of salt on picogreen fluorescence (Georgiou et al, 2006). However, as there was no fluorescence enhancement due to NaCl, for the LPRs 0.2 µg of sigma siRNA was used in both water and 0.12 M NaCl conditions. This could be due to the small size of siRNA in comparison with DNA, supported by the enhanced picogreen fluorescence observed for the whole DNA molecules rather than its fragments (Georgiou 2006). Two protocols were used to assess the extent of picogreen-binding to the LPDs/LPRs.

Protocol 1, 100 µL of LPDs/LPRs were prepared as described in Section 2.2.5. After preparation, 50 µL of picogreen reagent (namely 1:150 v:v picogreen in 3 x tris-EDTA (TE) buffer) was added to the LPD/LPR suspension and incubated at room temperature for 5 min before its fluorescence was determined as described below.

Protocol 2, 50 µL of DNA/siRNA solution was mixed with 50 µL of picogreen reagent (1:150 v:v picogreen in 3 x TE buffer) and the resulting solution used to prepare 150 µL of LPD/LPR suspension as described in Section 2.2.5. After preparation the suspension was incubated for 5 min at room temperature before its fluorescence was measured as described below.

For the picogreen complexation experiments, the lipid:DNA/RNA charge ratio was fixed at 0.5:1 while the peptide:DNA/RNA charge ratio varied in the range of 18-1:1 (i.e. 1:1, 2:1, 4:1, 6:1, 9:1, 12:1, 18:1).

The fluorescence associated with the ternary complexes was measured at an excitation wavelength of 485 nm and an emission wavelength of 520 nm with a gain of 1000 using a FLUOstar Omega fluorimeter (BMG LABTECH GmbH, Ortenberg, Germany) equipped with a plate reader. Any DNA/siRNA not incorporated in the lipopolyplexes was quantified and expressed as relative fluorescence units (RFU) compared to the free DNA/siRNA control, which was denoted as 100% RFU in order to normalise the fluorescence signal. All experiments were performed in triplicate and the mean and SD calculated.

2.2.10 Apparent hydrodynamic size and ζ-potential of LPDs/LPRs

50 µL of LPD/LPR suspension containing 0.5 µg of pDNA/1.25 µg of Sigma siRNA, respectively was prepared as described above. The apparent hydrodynamic size of the LPDs/LPRs in suspension was measured without dilution using a Malvern low-volume quartz cuvette, while the determination of ζ-potential was performed by diluting 50 µL of the LPD/LPR suspension with either 900 µL of ultrapure double distilled water or an aqueous NaCl solution, as appropriate, and measuring using disposable Malvern capillary cells using a Malvern Nano ZS Zetasizer (Worcestershire, UK) at a back scattering angle of 173° at 25 ± 0.1 °C. At these concentrations the number of particles was sufficiently low to ensure the absence of any inter-particle interactions interfering with the measurement by dynamic light scattering. All samples were measured in triplicate and the mean and SD value of the apparent hydrodynamic size and the ζ-potential calculated.

2.2.11 Small angle neutron scattering

SANS (small angle neutron scattering) studies were performed on the instruments LoQ and SANS2D with pulsed neutron source at ISIS (Rutherford-Appleton Laboratories, Didcot, UK). LOQ uses neutrons of wavelengths 2.2 to 10 Å, which are separated by time-of-flight and recorded at a 64 cm^2, two-dimensional detector at a fixed distance of 4.1 m from the sample. This setup gives a scattering vector $(4\pi/\lambda)\sin(\theta/2)$ in the range of 0.008 $Å^{-1}$ to 0.22 $Å^{-1}$. SANS 2D uses neutrons of wavelengths 2 to 14 Å, which are separated by time of flight and recorded by a 96.5 cm square, two-dimensional detector at 4 m from the sample. The instrument set up gives a scattering vector in the range $0.0045 \leq Q \leq 0.8$ $Å^{-1}$. The SANS and the transmissions (TRANS) of the samples were measured separately on LoQ while they were simultaneously on SANS2D. In the present study, a 12 mm circular beam was used for the static neutron scattering measurements and an 8 mm circular beam for the stopped flow measurements.

2.2.11.1 Experimental and data collection

Before any sample was measured, the instrument was first calibrated with a substance TK49 whose scattering was known. For the SANS measurements, the LPDs/LPRs were freshly prepared as described in Section 2.2.5. Irrespective of the method of preparation, unless otherwise stated, the final concentration of the DNA/siRNA in the LPD/LPR suspension was 0.1 mg mL^{-1} while the DNA/siRNA concentration in the LD/LR suspension was 0.05 mg mL^{-1}. The parent vesicle suspension, comprising of a 1:1 molar ratio of DOTMA/DOPE, was prepared using either 1 or 2 mg mL^{-1} DOTMA in D_2O or NaCl in D_2O solution (at NaCl concentrations of up to 0.12 M). The aqueous solutions of peptide and ctDNA/Sigma siRNA were prepared in D_2O at concentrations of 4 and 1 mg mL^{-1}, respectively.

The SANS of the various samples and their corresponding solvents were measured in disk-shaped fused silica banjo cells of 2 or 1 mm path length depending upon the D_2O content of the sample being measured, with samples containing greater than 50 vol% D_2O being measured in 2 mm path length cells. On LoQ, the SANS of vesicles and the LPDs/LPRs were counted for 30 and 40 μA, respectively, while the TRANS were counted for 10 μA. On SANS2D, the SANS and TRANS of all samples and their corresponding solvents were counted for 20 μA. All samples and their corresponding solvents were measured at 25 ± 0.1°C. After the SANS measurements, the LPDs/LPRs were recovered, diluted with an equal volume of either OptiMEM or media

containing 10% v/v FBS and the SANS measured in 1 mm path length banjo cells due to the presence of a high concentration of H_2O. Appropriate solvents were measured.

The scattering intensity, I(Q), of the samples as a function of the scattering vector, $Q = (4\pi/\lambda)\sin(\theta/2)$ where $\sin(\theta/2)$ is the scattering angle, was determined by normalising the scattering to the appropriate sample transmission after subtraction of the scattering from the relevant solvent also normalised to its corresponding transmission.

2.2.11.2 Data analysis and model fitting

The fitting of the SANS data always included flat background corrections to allow for any mismatch in the incoherent and inelastic scattering between the sample and the solvent, with the levels of the fitted background being checked to ensure that they were physically reasonable. The SANS data for the DOTMA:DOPE vesicles and LPD/LPR complexes dispersed in D_2O were routinely modelled either assuming a mixture of (isolated/single) infinite planar (lamellar) sheets with or without one-dimensional paracrystals (stacks) to account for the presence in the sample of any multilamellar vesicles. When modelling the vesicles and LPD/LPR complexes dispersed in D_2O as (single) lamellar sheets, the fits to the SANS data were obtained by the least-squares refinement of three parameters, namely L, $R\sigma$, and the absolute scale factor (together with the background, as described above), where $R\sigma$ is the Lorentz correction factor which provides information about the extent of rigidity/curvature of the lamellar sheets. Unless otherwise stated a $R\sigma$ of 300 Å was used. In this study the polydispersity on the thickness of the bilayer ($\sigma(L)/L$) was fixed at 0.1. When stacks were added to the (single) lamellar sheet model, the fit to the SANS data was obtained by least-squares refinement of seven parameters, namely, the mean bilayer thickness (L), the Lorentz factor ($R\sigma$), the number of bilayers in the stack (M), their mean separation or d-spacing (D), the width of the Gaussian distribution in the plane, ($\sigma(D)/D$), and the absolute scale factors for the unilamellar and multilamellar vesicles. In the present study, $\sigma(L)/L$ was again fixed as 0.1 and $\sigma(D)/D$ at 0.05, with a $R\sigma$ of 300 Å was used. In addition, when modeling the SANS data using a mixed population of sheets and stacks, L, $\sigma(L)/L$, and $R\sigma$ were constrained to be the same for the isolated/single and stacked lamellae, a not unreasonable assumption. If no Bragg peak was seen in the SANS data, it was fitted using a stack with a maximum of 2 bilayers. In such cases the data was fitted using a higher number of bilayers comprising the stacks to ensure that it did

not improve the quality of the fit obtained. For all models, the least-squares refinements were performed using the model-fitting routines provided in the FISH software.

2.2.12 Small angle neutron scattering with stopped flow mode

2.2.12.1 Experimental

The kinetics of the interaction of the formation of the LD/PD and lipopolyplexes were studied on SANS2D using stopped flow experiments employing a Bio-Logic SFM-400 (Claix, France) fitted with a neutron-scattering observation head and Bio-Kine software (Figure 2.2).

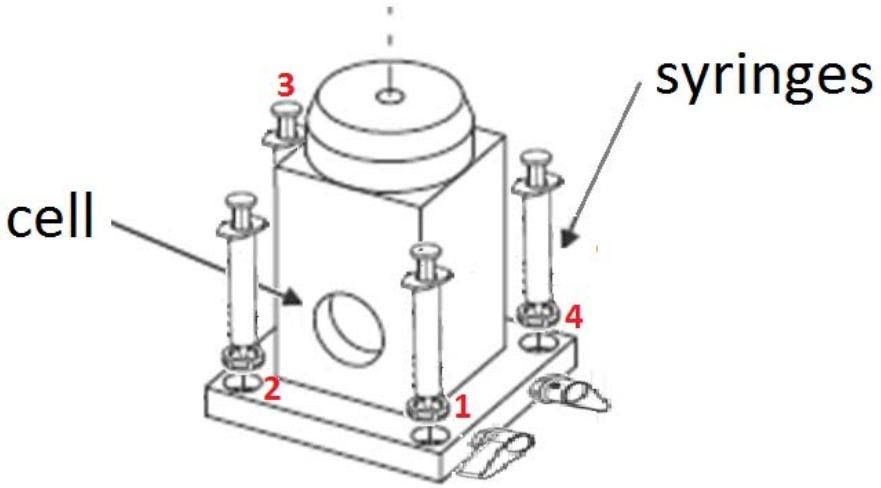

Figure 2.2 SANS stopped flow apparatus consisting of an observation/measurement cell and four x 10 mL injection syringes.

SANS measurements were performed at 298 ± 0.1 K, using an 8 mm diameter neutron beam and in event mode. Equal volumes (300 µL) of any two of the following systems either (a) DNA/RNA solution (0.1 mg/mL for LDs/Rs and 0.2 mg/mL for LPDs/Rs) in D_2O, (b) vesicle suspension (for LDs/LRs), (c) a mixture of vesicle suspension and peptide (for LPDs/LPRs) or (d) D_2O were injected into a 1 mm path length measuring cell (Hellma, Essex, UK) at a flow rate of less than 2 mL/s to produce the required sample and the SANS measured for a total of 10 min with the last acquisition being measured for 30 minutes. (For the LPDs/LPRs the charge ratio of L:P:DNA/RNA was fixed at 0.5:6:1 while for the LDs/Rs, the charge ratio of L:DNA/RNA was fixed at 2:1.) Note that the total volume injected was more than the volume of the measuring cell to ensure complete removal of the previous sample. A D_2O background was

subsequently subtracted from all data sets. Each experiment was repeated at least 15 times, and the corresponding (retrospectively) time-sliced data summed to give SANS profiles with acceptable statistics. A series of long time course experiments were performed to model static measurements. Each individual kinetic SANS run was time-sliced at the desired interval and each time-slice summed (n = 15) using the MantidPlot software.

Chapter 3 Lipopolyplexes containing DNA

3.1 Results

3.1.1 *In vitro* transfection of lipopolyplexes

To evaluate the biological effect of the constructed lipopolyplex vector (LPDs), the *in vitro* transfection efficiency is assessed by measuring the luciferase unit produced by lung carcinoma A549 cells. The effect of the preparation (mixing protocols) and formulation (+/- charge ratio) of the LPDs is evaluated, followed by the transfection factors (incubation time). More importantly, the effect of the preparation aqueous solutions for the LPD preparation and the transfection medium for cell incubation have been thoroughly investigated, in view of the presence of electrolytes and serum in the body. Therefore, the present study is more likely to be related with the *in vivo* transfection.

3.1.1.1 Preparation of lipopolyplexes

The effect on transfection in A549 cells and lipopolyplex structure on the order of mixing of each component of the LPD was investigated. Series I and II peptides, H12BLY and (HR)6BLY, respectively were selected for this study. Mixing protocols 1 and 2 looked at first adding either peptide or DNA solution to the vesicle suspension. In protocol 1 (denoted **LPD**) an equal volume of peptide solution and vesicle suspension were mixed (peptide solution added to vesicle suspension) followed by the addition of an equal volume of DNA solution, (this is the order of mixing has been routinely used by other researchers to prepare LPDs). In contrast in protocol 2 (**LDP**), DNA solution was added to the equal volume of vesicle suspension followed by the addition of an equal volume of peptide solution. Mixing protocols 3 and 4 investigated first adding either vesicle suspension or DNA solution to peptide solution. In protocol 3 (**PLD**), vesicle suspension was added to an equal volume of peptide solution, followed by the addition of DNA solution while in protocol 4 (**PDL**) DNA solution was added to the equal volume of the peptide solution followed by the addition of an equal volume of vesicle suspension. Mixing protocols 5 and 6 examined first adding peptide solution and DNA solution to the suspension of vesicles. In protocol 5 (**DLP**), vesicle suspension was first added to an equal volume of DNA solution and the resulting solution add to vesicle suspension. In protocol 6 (**DPL**) peptide solution was added to an equal volume of DNA solution which was then mixed with an equal volume of vesicle suspension.

For this part of the study, both the vesicle suspension and the resulting LPDs were prepared in water. In order to indicate the use of water in preparation of the vesicles and resulting LPDs, the following nomenclature was used, VwLPDw. In addition, the LPDs studied here were prepared at a lipid:peptide:DNA charge ratio of 0.5:6:1 and the transfection of the LPDs was performed in the presence of OptiMEM (LPDs mixed with OptiMEM such that the final composition contained 25% v/v of the LPD suspension. OptiMEM is a commercially available, reduced eagle serum used to maintain normal cell growth and is commonly used for gene transfection. As can be seen in Figure 3.1(a), the A549 cells incubated with the negative control of naked DNA exhibited no luciferase expression and therefore no transfection efficiency. In contrast, A549 cells incubated with the commercially available, positive control, Lipofectamine 2000, expected exhibited a high level of luciferase expression and therefore transfection efficiency. All of the binary complexes (i.e. LPs and PDs) investigated, with the exception of the PD containing (HR)6BLY, resulted in a poor level of luciferase expression in the A549 cells. In contrast, some of the LPDs resulted in the production of good levels of luciferase expression in the A549 cells, albeit not as great as that achieved after incubation with Lipofectamine 2000. Interestingly, regardless of the protocol used to prepare the LPDs, LPDs prepared using the Series II peptide, (HR)6BLY, exhibited a greater level of transfection efficiency than those prepared using the Series 1 peptide, H12BLY. Furthermore, when comparing data from A549 cells incubated with LPDs prepared using (HR)6BLY but using different mixing protocols, differences in luciferase expression were observed. Note that corresponding differences between LPDs containing H12BLY but prepared using the different protocols was not clear due to the very low levels of luciferase production obtained. When examining the levels of transfection resulting from incubation with the LPDs containing (HR)6BLY, it was clear that those LPDs made following protocols 1, 3, 4 and 6 demonstrated a much higher level of transfection efficiency than those prepared using protocols 2 and 5. As a consequence mixing protocol 1 was used in the following study, unless otherwise stated. Consideration of the order of mixing shows that the LPDs that result in the lowest levels of transfection both involve mixing the DNA and vesicle suspension prior to mixing with the peptide solution, suggesting possibly that LD complexes as opposed to LPDs prepared using this methodology.

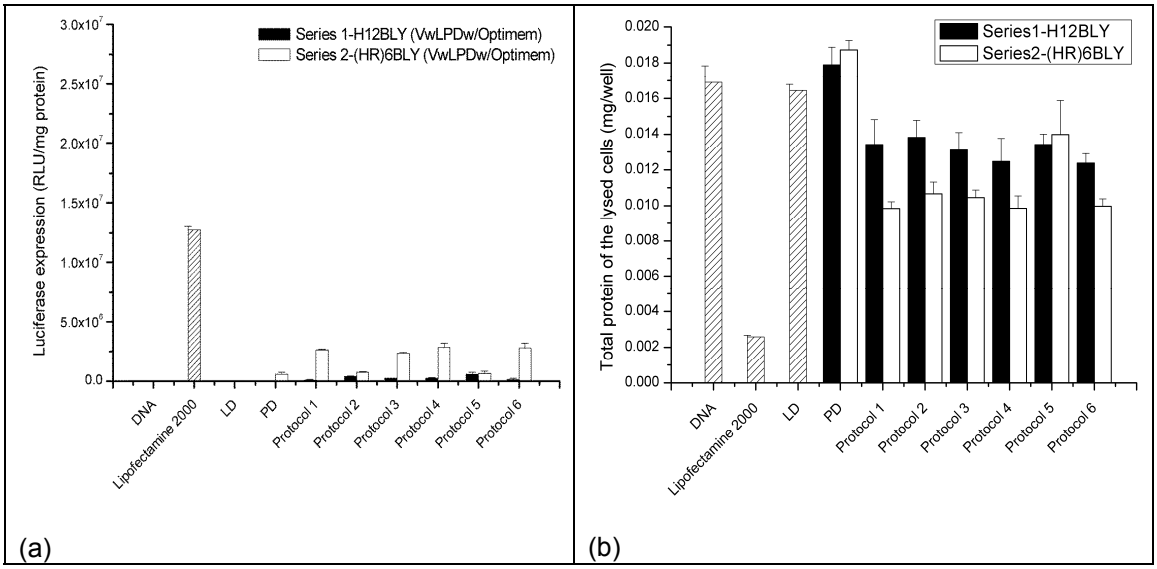

Figure 3.1 (a) levels of luciferase transfection and (b) protein assay after 24+24h incubation of A549 cells with LPDs prepared using different protocols to examine the effect of order of mixing: 1 = LPD; 2 = LDP; 3 = PLD; 4 = PDL; 5 = DLP; 6 = DPL. LPDs were prepared fully in water at a L:P:D charge ratio of 0.5:6:1, and mixed in a 1:3 volume ratio of LPDs in water and OptiMEM (VwLPDw/OptiMEM), final DNA concentration was 0.25 μg/well. Vesicles used to prepare the LPDs composed of DOTMA:DOPE at 1:1 molar ratio. Error bars are the SD of three measurements of a single formulation (n=3). Only one experiment was performed.

Significantly for the present study, the protein assay shown in Figure 3.1(b) indicated that Lipofectamine 2000 was far more toxic towards the A459 cells than the PDs and LPDs prepared with peptides from Series I and II. Although both the Series I and II peptides exhibited some toxicity towards the A549 cells, this toxicity was much less than that seen with Lipofectamine 2000, indicating that, as a whole, the LPDs prepared in the present study were much less toxic. Furthermore, the LPDs prepared using Series I peptide, H12BLY was less toxic than those prepared using the Series II peptide, (HR)6BLY. Interestingly, the order of mixing appeared to have no influence on the toxicity of the LPDs suggesting that it was the components of the LPDs that exerted toxicity rather than the delivery system.

Small angle neutron scattering (SANS) studies were performed in an attempt to detect any difference in the macromolecular structure of the LPDs prepared using the different protocols. In order to reduce the breadth of the study, only protocols 1 (LPD), 2 (LDP) and 6 (DPL) were studied. Protocol 1 (LPD) was selected for study as the LPDs with the maximum transfection have been prepared using this methodology (Kudsiova et al, 2011). Preparation of LPDs using

protocol 3 was not selected for SANS studies as preliminary SANS data (not shown) indicated that there was no detectable difference between the cationic vesicles and the cationic peptide, hence protocols 1 and 3 were deemed to be equivalent because the DNA was added last. Similarly, because protocols 2 and 5 involved mixing vesicle suspension and DNA solution first, they were also deemed equivalent and thus only protocol 2 was tested. Finally, protocols 1, 3, 4 and 6 yielded similar levels of luciferase transfection, suggesting that protocols 4 (**PDL**) and 6 (**DPL**) were similar in structure, a not unreasonable assumption because in both cases the vesicle suspension was added last and hence only protocol 6 was studied. In addition because preliminary SANS studies (data not shown) indicated no difference in the internal structure of LPDs composed of the different peptides, it was decided to study LPDs prepared using the Series II peptide, (HHR)4BLY.

Figure 3.2(a) gives the intensity of the small angle neutron scattering (I) in cm^{-1} as a function of momentum transfer (q) in $Å^{-1}$ for cationic DOPE:DOTMA vesicles (scaled to the lipid concentration present in the final LPDs tested using SANS) and LPDs prepared using protocols 1, 2 and 6 and containing peptide (HHR)4BLY. Figure 3.2(b) gives the variation in intensity of the SANS obtained for LDs and PDs containing (HHR)4BLY, and for the purposes of comparison LPDs prepared using protocol 2 and containing (HHR)4BLY. In all cases the vesicles, PDs, LDs and LPDs were prepared in D_2O as opposed to H_2O in order to provide the necessary contrast for the SANS measurements. The background, attained at a scattering intensity of I of ~ 0.01 is a result of the mismatch in the incoherent and inelastic scattering between the LPDs and the solvents.

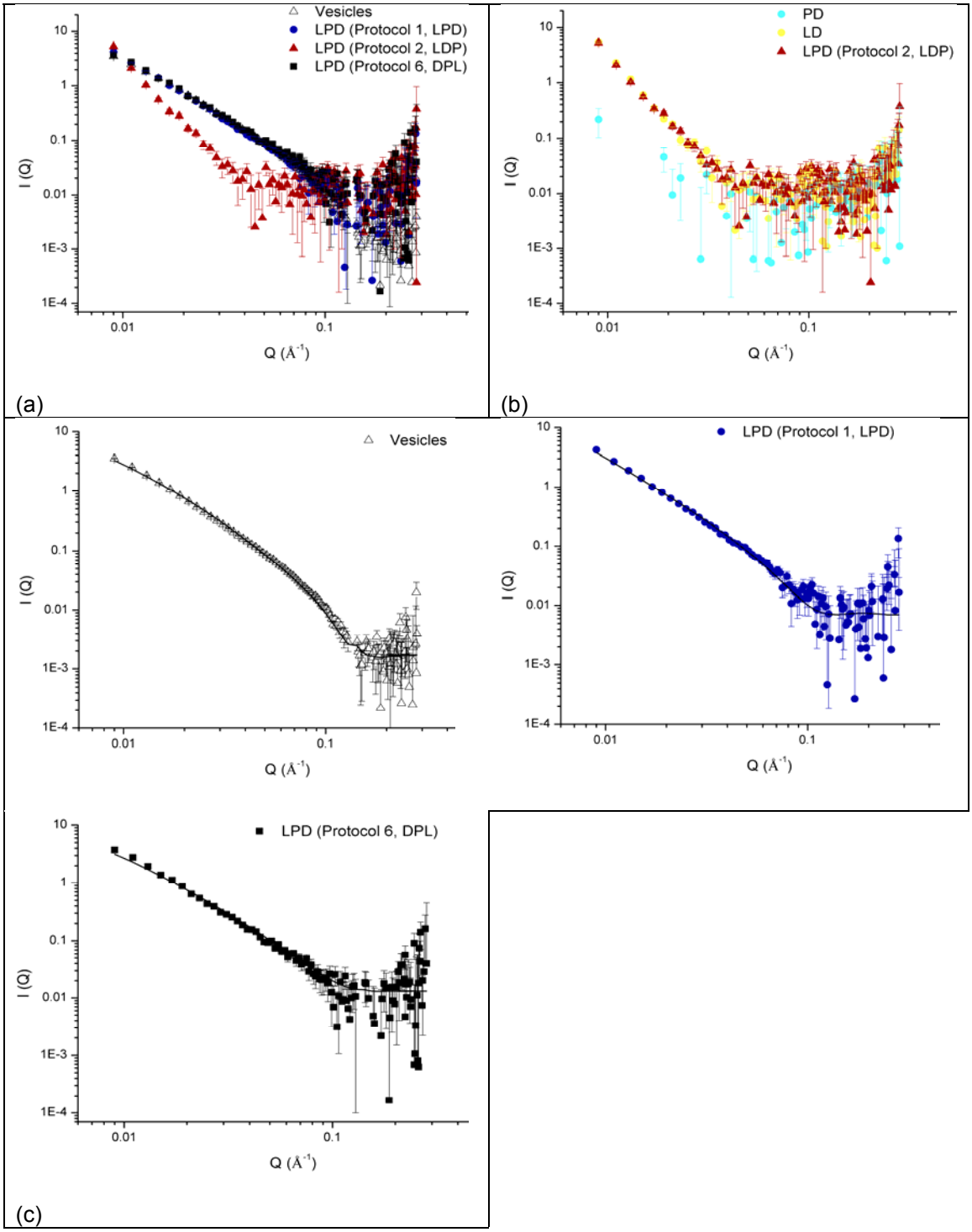

Figure 3.2 Small angle neutron scattering data (dots) for (a) LPD containing (HHR)4BLY and prepared by different protocols (i.e. protocols 1, 2 and 6) and cationic vesicles, (b) PD, LD and LPD containing (HHR)4BLY (prepared using protocol 2) and (c) the best fit (solid line) to the data in (a). All samples prepared in D_2O. LPDs were made at lipid:peptide:DNA charge ratio of 0.5:6:1 (0.1 mg/mL ctDNA). LD prepared at a L:D charge ratio of 0.5:1 (0.1 mg/mL ctDNA) and PD at a P:D charge ratio of 6:1 (0.1 mg/mL ctDNA). Vesicles used to prepare the LPDs composed of DOTMA:DOPE at 1:1 molar ratio (1 mg/mL of DOTMA) and were aged ~48 h. SANS was measured at 25 ± 0.1°C on LoQ at ISIS.

The SANS data obtained for LPD prepared using protocol 1 (LPD) and 6 (DPL) and their parent vesicles, shown in Figure 3.2(a) was well fitted assuming the presence of single sheets – the vesicles and LPDs being too large to be analysed as hollow spherical structures (Table 3.1). In contrast, however, it was not possible to analyse the SANS data obtained for the LPDs prepared using protocol 2 using single sheets even with the presence of some multilamellar structure suggesting that the LPDs prepared using this methodology possessed a different structure. This observation is consistent with the fact that LPDs prepared by protocol 1 (LPD) and 6 (DPL) exhibited a similar level of transfection efficiency to each other and which was higher than that obtained using LPDs prepared using protocol 2 (LDP).

Table 3.1 Structural parameters obtained for cationic vesicles, LPD-(HHR)4BLY (0.5:6:1 charge ratio) and LD (2:1 lipid:DNA charge ratio) at 0.1 mg/mL ctDNA (derived from FISH modelling of their SANA data). All samples prepared using D_2O as solvent. Vesicles used to prepare the LPDs and LD composed of DOTMA:DOPE at 1:1 molar ratio.

Samples	*L* (Å)	No. of layers	*d*-spacing (Å)	R sigma (Å)	Ratio of stack:sheet	SWSE
Vesicles	39.7 (±0.9)	2.0	60.0 (±7.6)	300	0.058	727
LPD (protocol 1)	39.7 (±2.5)	-	-	300	-	436
LPD (protocol 6)	39.7 (±2.3)	-	-	300	-	133
LD	34.5 (±4.2)	4.0	57.8 (±2.4)	800	1.05	9631

Figures in brackets indicate the standard errors on the fitted parameter values. SWSE is sum of weighted square error. Ratio of stack to sheet represents the ratio of multilamellar surface area to unilamellar surface area. SANS was measured at 25 ± 0.1°C on LoQ at ISIS for the LPDs and SANS2D for the LD.

The model used for analysis of the SANS data obtained for the vesicles and LPDs consisted of single lipid bilayer sheets, together with stacks (multilayers) of the same. The *d*-spacing being the sum of the thickness of the vesicle's lipid bilayer (*L*) and the thickness of the aqueous layer that separates the bilayers (d_w) as illustrated in Figure 3.3. The parameters used for the best fit to the SANS data are given in Table 3.1 and indicate that for the DOTMA:DOPE vesicles, the bilayer thickness and *d*-spacing were 39.7 ± 0.9 Å and 60.0 ± 7.6 Å, respectively. These values are reassuringly consistent with the values of ~41 Å and ~65 Å obtained for vesicles of the same composition in a previous study (Welser et al, 2013).

As mentioned above in the present study, the LPD prepared from protocol 1 (LPD) and 6 (DPL) had the same bilayer thickness as their parent DOTMA:DOPE vesicles. In addition, the LPDs prepared using protocol 1 (LPD) and 6 (DPL) have the same bilayer rigidity as their parent

vesicles as indicated by a R_{sigma} of 300 Å. It is worth noting that the significant difference between LPDs prepared using protocols 1 (LPD) & 6 (LDP) with those prepared using protocol 2 (DPL), was that the DNA solution was mixed with the vesicular suspensions, prior to being added to the peptide solution. In this case, it might be anticipated that the LPDs prepared using protocol 2 (LDP) would possess a structure more like that of the corresponding LD, which did not show high level of transfection efficiency (Figure 3.1(a)).

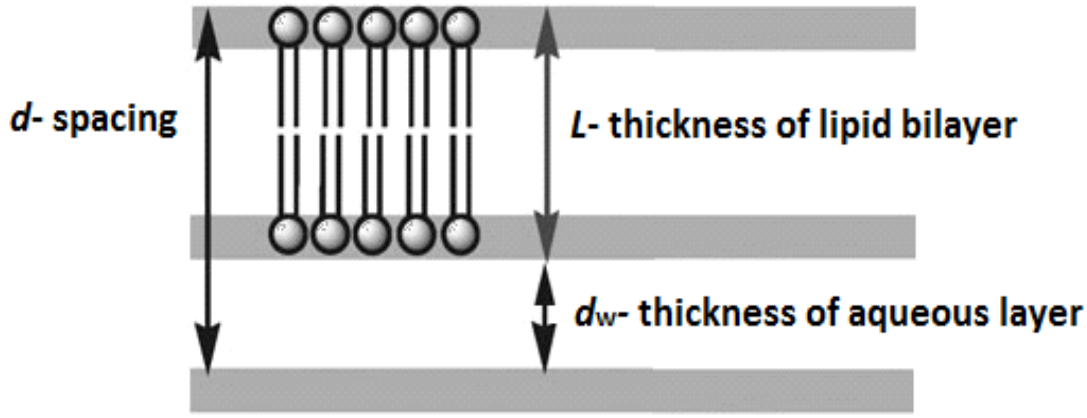

Figure 3.3 Schematic representation of a lipid bilayer (*L*) and *d*-spacing in multilamellar vesicles. The *d*-spacing is the sum of the thickness of the lipid bilayer (*L*) and the aqueous layer (*d*w) between bilayers (Kudsiova et al, 2011b).

In order to prove this hypothesis, the structure of the LD formed from the DOTMA:DOPE vesicles and DNA at the same charge ratio as was present in the LPDs, namely 0.5:1, was determined (Figure 3.2(b)). Also included in Figure 3.2(b) for the purposes of comparison is the SANS data obtained for (HHR)4BLY-containing LPDs prepared using protocol 2 (LDP). It can be seen that the SANS data for the LPDs prepared at a L:P:D charge ratio of 0.5:6:1 protocol 2 (LDP) and the corresponding LDs at a L:D charge ratio of 0.5:1 overlapped, suggesting that the structure of the two types of complex were similar, supporting the hypothesis that LPDs prepared in this way possessed a structure comparable to that of the corresponding LDs, thereby accounting for their low level of transfection efficiency.

Note that the scattering pattern obtained for the PD was very weak. This is probably a consequence of their large size and 'fluffy' (unstructured) nature as the calculated SLD of the

6:1 PDs is sufficiently different from the SLD of the D_2O solvent ($6.35x10^{-6}$ $Å^{-2}$) used for the experiments to enable their 'visualisation'.

The scattering profile of LDs prepared at a 2:1 ratio is also shown in Figure 3.4. It is striking that the LDs produce a very different SANS curve compared to the vesicles. The SANS data of the LDs exhibited a distinct 'Bragg peak' at a q value ~0.1 $Å^{-1}$, suggesting that the LDs contained a regular repeating structure. As a consequence, therefore, the SANS data obtained for the LDs were fitted with a model with a large portion of multilamellar stacks, rather than a large portion of unilamellar sheets for the LPD and vesicles. The parameters used for fitting the SANS curves are shown in Table 3.1. Interestingly it appears that the thickness of the lipid bilayer and the *d*-spacing present in the LD were lower than those of its parent vesicles, although the thickness of d_w in the LDs was 23.3 Å, comparable to that present in the vesicles. However, it should be noted that it was necessary to increase the value of R_{sigma} from 300 to 800 to obtain good fits to the SANS data, suggesting that the bilayer has become more rigid in the presence of DNA. The slightly higher number of layers used to model the SANS data is not significant other than to indicate that the number of repeat structures is higher in the LD complexes (the ratio of stack to sheet was 1.05) compared to the vesicles. LDs containing a large number of repeat structures were observed in previous studies using electron microscopy (Kudsiova et al, 2011b).

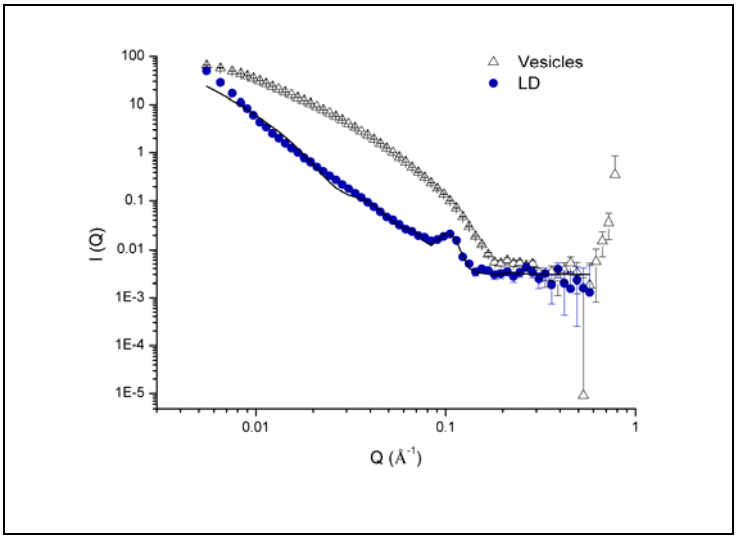

Figure 3.4 Small angle neutron scattering data (dots) and the best fit to the data (solid line) for LD prepared at a L:D charge ratio of 2:1 (0.05 mg/mL ctDNA). Vesicles used to prepare the LD composed of DOTMA:DOPE at 1:1 molar ratio (2.0 mg/mL DOTMA) and were aged ~48 h. SANS was measured at 25 ± 0.1°C on SANS2D at ISIS.

3.1.1.2 Effect of charge ratio and incubation time

During preliminary studies, investigations of LPDs prepared at lipid:peptide:DNA charge ratios of 0.5:6:1 and 0.5:12:1 indicated that the optimal transfection occurred within this range (Welser 2013). Figure 3.4(a) shows the transfection obtained after incubation of A549 cells with LPDs for 24+24 h and 4+44 h. Figure 2.4(b) shows the quantification of the protein in the cell lysates obtained from the same incubation study.

As can be seen in Figure 3.4(a) for an incubation of 24+24 h, the LPDs tended to exhibit a lower level of transfection efficiency upon increasing the charge ratio from 0.5:6:1 to 0.5:12:1. As a consequence therefore, a lipid:peptide:DNA charge ratio of 0.5:6:1 was used to prepare the LPDs, except otherwise stated. In agreement with the results shown in Figure 3.1, LPDs prepared using Series II peptides, especially (HK)6BLY, exhibited a higher level of transfection efficiency, than the LPDs prepared using Series I peptides. The only exception being the LPDs prepared with K4BLY where the level of transfection varied greatly from experiment to experiment. At present no reason for this variability has been determined. It is worth noting that while A549 cells exposed to the positive control, Lipofectamine 2000, exhibited a high level of transfection, this result was considered to be largely as consequence of the high toxicity of the delivery vehicle towards the cells as evidenced by the low amount of protein present in the cell lysates (Figure 3.5(b)). In contrast, the other positive control, Lipofectamine (also commercially available) while not as effective at delivering DNA as Lipofectamine 2000 (and indeed many of the LPDs prepared in the present study), was much less toxic.

Interestingly however, irrespective of the charge ratio used to prepare the LPDs, the LPDs demonstrated a higher level of transfection efficiency than Lipofectamine at both incubation times and Lipofectamine 2000 at the 4+44 h incubation. When examining the effect of LPD incubation time on the transfection obtained with the A549 cells, it is clear that at both charge ratios, the 24+24 h protocol tended to exhibit the lower level of transfection efficiency. As a consequence, unless otherwise stated the 4+44 h incubation protocol was used throughout the study.

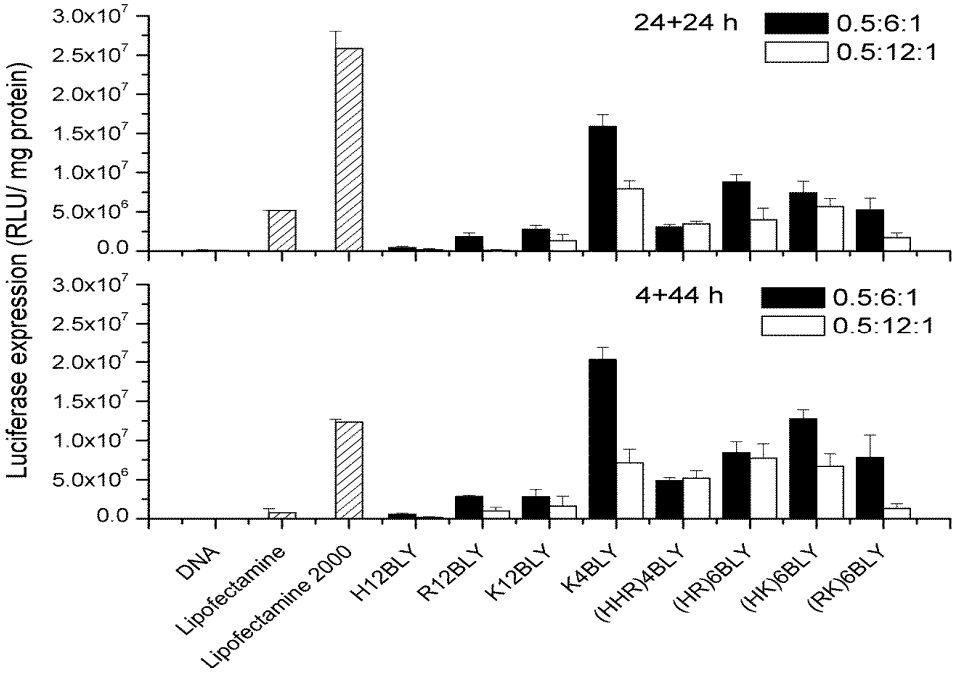

(a)

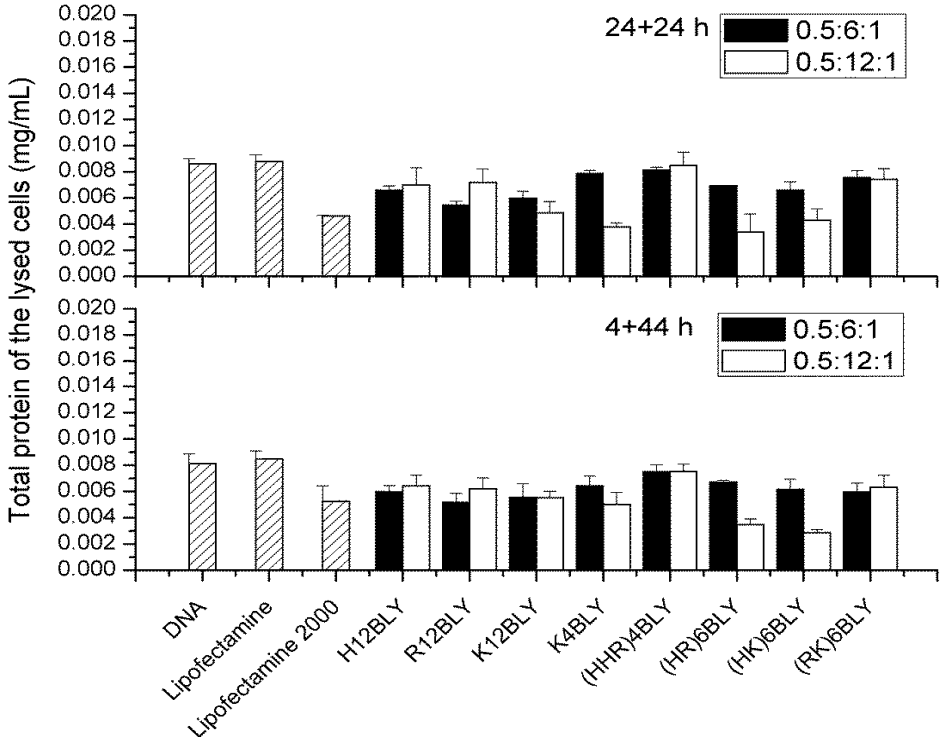

(b)

Figure 3.5 Levels of luciferase transfection (a) and protein assay (b) after 24+24h (upper panel) and 4+44h (lower panel) incubation of A549 cells with LPDs. LPDs were prepared fully in water at a L:P:D charge ratio of 0.5:6:1, and mixed in a 1:3 volume ratio of LPDs in water and OptiMEM (VwLPDw/OptiMEM). The final DNA concentration was 0.0025 mg/mL. Vesicles used to prepare the LPDs composed of DOTMA:DOPE at 1:1 molar ratio. Error bars are the SD of triplicate measurements of a single (n = 3). Replicate experiment contained in Appendix II.

3.2.1.3 Effect of solvent

In the preliminary studies described above, both the vesicles used to prepare the LPDs and the LPDs themselves were prepared in water (described as VwLPDw). The ability of the VwLPDw to transfect A549 cells were studied after a 4 fold dilution of the LPDs in OptiMEM (denoted as VwLPDw/OptiMEM). In order to prepare LPDs suitable for parenteral administration to humans, it is necessary to make the LPD suspension isotonic with the body fluids. In addition, transfection *in vitro* using OptiMEM cannot be readily correlated with transfection *in vivo* because of the serum present in the body. As a consequence, it was necessary, therefore to examine the effect of varying the nature of the continuous phase in which the LPDs were made on their transfection efficiency. In order to do this, the addition of NaCl to the water used to prepare the LPDs was studied as was the replacement of OptiMEM by RPMI-1640 media containing 10% v/v of fetal bovine serum (FBS).

The effect of replacing OptiMEM with serum-containing RPMI-1640 media can be seen in Figure 3.6. Disappointingly, there was no luciferase expression (i.e. transfection) recorded when the LPDs and their constituent vesicles were prepared in water (VwLPDw). Interestingly, however, when the LPDs were prepared in OptiMEM in place of water, vesicles still made in water (VwLPDo) and transfection performed in the presence of serum-containing RPMI-1640 media, a high level of transfection was observed.

This observation is significant, as it is often extremely difficult to experimentally observe any DNA transfection *in vitro* in the presence of serum (Turek et al, 2000). Indeed many researchers do not report the ability of their delivery systems to transfect in the presence of serum, preferring instead to use OptiMEM for their transfection studies as better levels of transfection are generally recorded when using this media (Lo et al, 2008, Tagalakis et al, 2011). OptiMEM is a modification of eagle's minimum essential media, buffered with HEPES and sodium bicarbonate and supplemented with hypoxanthine, thymidine, sodium pyruvate, L-glutamine, trace elements and growth factors as described on the product information sheet. A consideration of the composition of OptiMEM lead us to consider using electrolyte solution instead of water for the preparation of the LPDs to see if it was possible to retain the activity of the LPDs when diluted in serum-containing RPMI-1640 media. The electrolyte selected for the

present study was NaCl as it is widely used in a range of clinical applications and is already used to produce isotonic medicinal preparations.

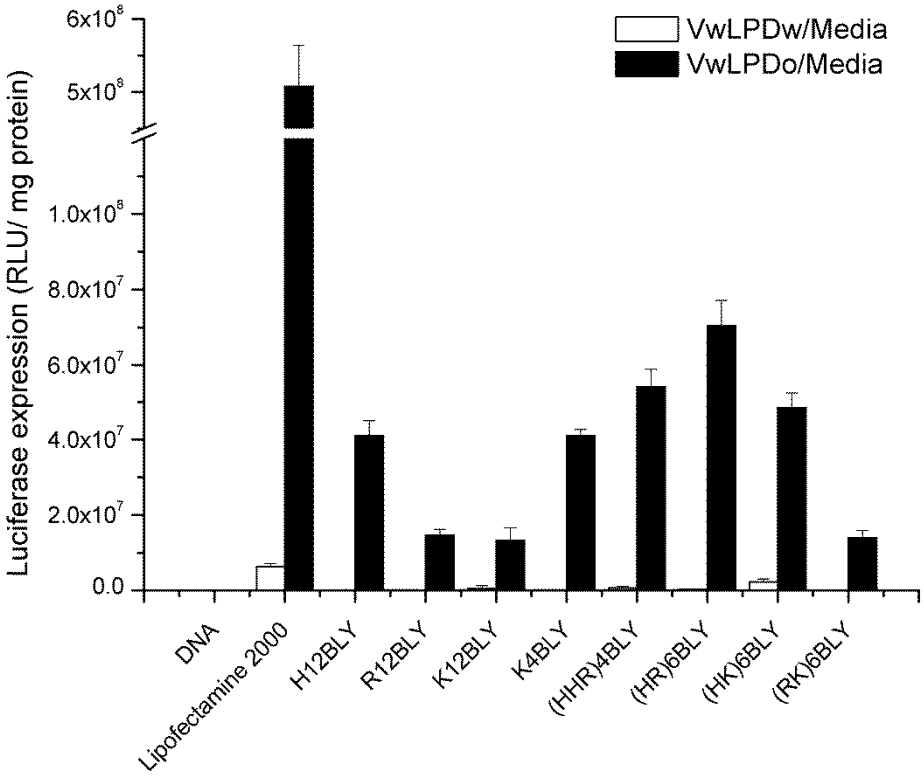

Figure 3.6 Luciferase expression in A549 cells after a 4+44 h incubation with LPDs containing various peptides. LPDs were prepared fully in water (VwLPDw) or partly in OptiMEM (VwLPDo) at a L:P:D charge ratio of 0.5:6:1 and transfected in 75% v/v RPMI-1640 media containing 10% v/v FBS. Cationic vesicles were composed of DOTMA/DOPE lipids at 1:1 molar ratio. Error bars are the SD of 3 measurements of a single formulation (n = 3).

Figure 3.7(a) shows the transfection obtained in A549 cells after incubation with LPDs prepared in water (VwLPDw) and in saline solution, i.e. 0.12 M NaCl (VsLPDs) and diluted with OptiMEM. As can be observed, a high level of transfection efficiency was obtained for both types of the LPDs, with no difference being observed with peptide structure, with the exception of the LPDs containing K4BLY, where the LPD prepared in water exhibited a much greater level of transfection. In contrast with these results, Figure 3.7(b) shows that the levels of transfection obtained in the A549 cells after exposure to LPDs prepared in water (VwLPDw) and LPDs prepared in saline (VsLPDs) but diluted with serum-containing media exhibited very different levels of transfection, with little/no transfection being observed in the systems containing LPDs prepared in water (VwLPDw) and a high level of transfection being seen when LPDs prepared

in 0.12 M NaCl solution (VsLPDs) was used, supporting the hypothesis that preparing the LPDs using electrolyte solution instead of water lead to a retention of activity of the LPDs when diluted in serum-containing RPMI-1640 media, albeit not to quite the same levels as obtained using diluting in Optimem. Once again, with the exception of K4BLY, the LPDs containing the Series I peptides exhibited a higher level of transfection than those containing the Series II peptides.

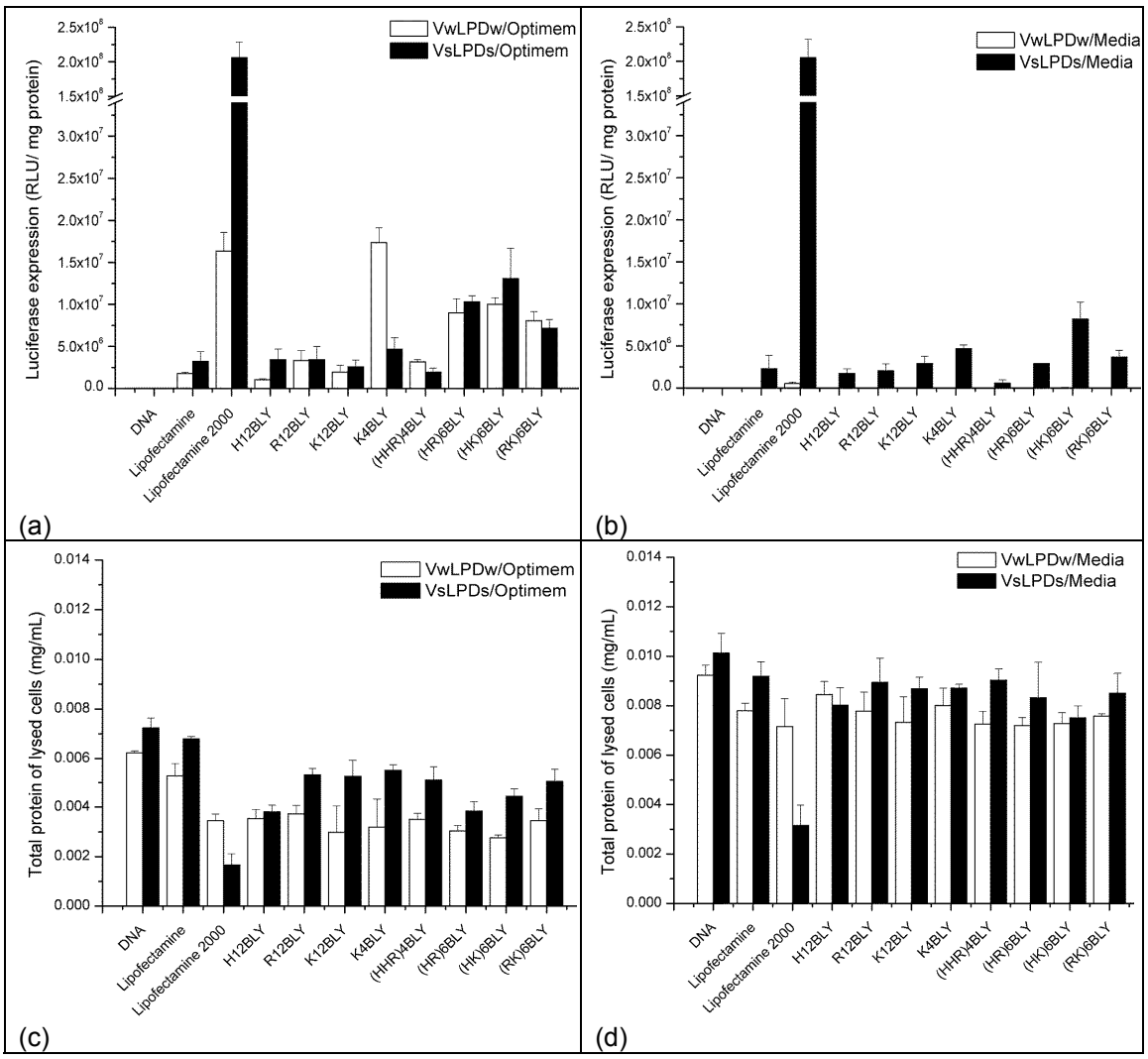

Figure 3.7 Luciferase expression in A549 cells after exposure to LPDs using a 4+44 h incubation protocol. (a) LPDs were prepared fully in water or 0.12 M NaCl solution and diluted with 75 %v/v OptiMEM (VwLPDw/OptiMEM or VsLPDs/OptiMEM), (b) LPDs were prepared fully in water or 0.12 M NaCl solution and diluted with 75% v/v RPMI-1640 media containing 10% v/v FBS (VwLPDw/Media or VsLPDs/Media), (c) level of protein assay of (a), and (d) level of protein assay of (b). LPDs were prepared at a L:P:D charge ratio of 0.5:6:1. Cationic vesicles used to prepare the LPDs were composed of DOTMA/DOPE lipids at 1:1 molar ratio. Error bars are the SD of 3 measurements of a single formulation (n = 3). Experiments repeat 4 times; replicate experiment contained in Appendix II.

Figure 3.7(c) and 3.7(d) shows the protein assay for the cells exposed to the VwLPDw and VsLPDs diluted in Optimem and Media, respectively. Reassuringly, Lipofectamine 2000 was far more toxic towards the A549 cells than the LPDs. Moreover, the VsLPDs and those diluted in the Media exhibited little toxicity towards the A549 cells. This toxicity was much less than that seen with Lipofectamine 2000, indicating that the LPDs prepared in the present study were much less toxic.

A study was performed determine whether it was important for prepare LPDs using vesicles made in saline or water. This study was of interest because the vesicles made in saline were less stable and therefore less amenable to formulation. As can be seen in Figure 3.8, significantly higher levels of transfection were obtained in A549 cells after incubation with LPDs prepared from vesicles made in 0.12 M NaCl solution (VsLPDs) when compared to those made in water (VwLPDs). Figure 3.8 also shows that LPDs prepared fully in (VsLPDs) when incubated with A549 cells for 24 h yielded a higher level of transfection than those incubated for 4 h, although for the reasons outlined above and because most researchers incubate the cells with the delivery vehicles for 4 h, it was this incubation time that was used for all studies, unless otherwise stated.

To further explore the influence of NaCl on the ability of the LPDs to transfect A549 cells *in vitro* in the presence of serum-containing media, a study was performed in which LPDs were prepared using vesicles in water or in varying concentrations of NaCl in water. As can be seen from Figure 3.9(a), the amount of NaCl present had a profound effect on the level of transfection achieved, with the highest level of transfection being obtained with the LPDs were fully made in saline, confirming earlier studies that the presence of NaCl was important in achieving transfection in the presence of serum. Figure 3.9(b) shows that the presence of saline when preparing the LPDs had no detrimental effect on toxicity of the A549 cells as evidenced by the high amount of protein present in the cell lysates.

On the basis of these preliminary studies, it is possible to conclude that LPDs prepared totally in NaCl saline give the highest level of transfection under conditions that were most applicable to *in vivo* use. In order to explore the factors that influence transfection efficiency, the physico-chemical properties of the LPDs prepared in water and saline are investigated.

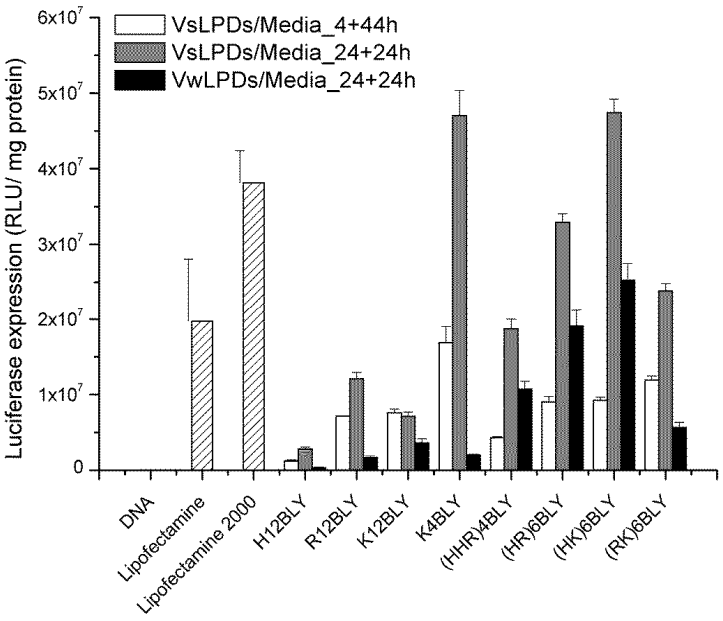

(a)

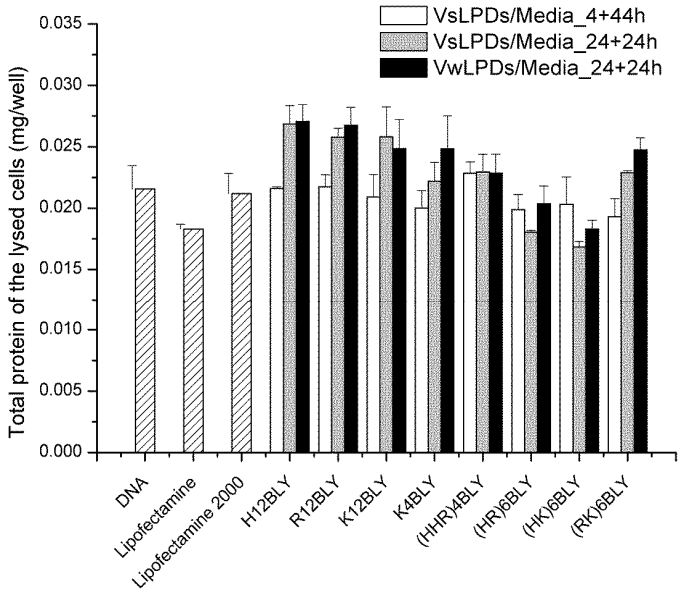

(b)

Figure 3.8 Luciferase transfection efficiency of LPDs on A549 cells using either a 4+44 h or 24 + 24 h incubation. (a) the level of luciferase transfection and (b) the level of protein assay. LPDs were prepared either fully (VsLPDs) or partly (VwLPDs) in 0.12 M NaCl solution and transfected in 75% v/v RPMI-1640 media containing 10% v/v FBS. LPDs were prepared at a L:P:D charge ratio of 0.5:6:1. Cationic vesicles were composed of DOTMA/DOPE lipids at 1:1 molar ratio. Error bars are the SD of three measurements of a single formulation (n = 3).

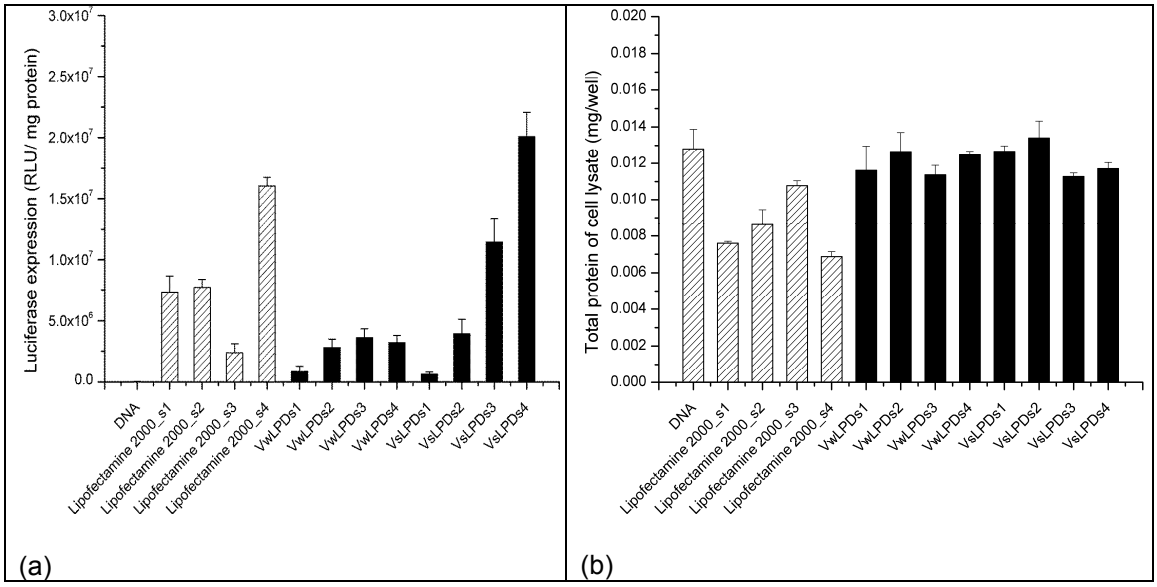

Figure 3.9 Luciferase transfection efficiency of LPD-(HHR)4BLY on A549 cells using a 24+24 h incubation. LPD-(HHR)4BLY were prepared partly (VwLPDs) or fully (VsLPDs) in various NaCl solution (s1 = 0.008 M; s2 = 0.04 M; s3 = 0.08 M; s4 = 0.12 M) and transfected in 75% v/v RPMI-1640 media containing 10% v/v FBS. (a) the level of luciferase transfection and (b) the level of protein assay. LPDs were prepared at a L:P:D charge ratio of 0.5:6:1. Cationic vesicles were composed of DOTMA/DOPE lipids at 1:1 molar ratio. Error bar means SD of three measurements of a single formulation (n =3).

3.1.2 Condensation, release and protection properties of lipopolyplexes

In order to ensure the successful delivery of the anionic DNA macromolecule into the target cells, it is essential for it to be packed inside a delivery vehicle that condenses it and reduces its size, neutralises its charge thereby removing/reducing negative charge, protects it from degradation by enzymes and at the same time facilitates its entry into the cell. In order for DNA to exert its effect, it needs to be in the free form and not associated with its carrier vehicle (Schaffer et al, 2000). Once inside the target cell it is necessary, therefore, for the delivery system to release its DNA payload into cytoplasm from where it can travel to the nuclei. The next section will therefore focus on the DNA condensation, release and protection properties of the LPDs as measured via electrophoresis on an agarose gel.

3.1.2.1 LPDs prepared in water

The results of the electrophoresis experiments performed on the various LPDs prepared fully in water (VwLPDw) at charge ratios of 0.5:2.4:1 and 0.5:6:1 are given in Figure 3.10. For each LPD, the results are shown in three lanes, with Lane A giving the results of the complexation experiment, Lane B, the release studies and Lane C the degradation studies. As expected the

naked DNA exhibited two bands, an intense 'lower' band and a faint 'upper' band, attributable to the DNA's open circular and supercoiled forms, respectively. When DNAse I was added to the naked/free DNA no bands attributable to the parent DNA were seen in Lane B due to the complete degradation by DNAse I of the naked DNA, into much smaller molecular weight fragments which were seen as a diffuse bands towards the bottom of the gel.

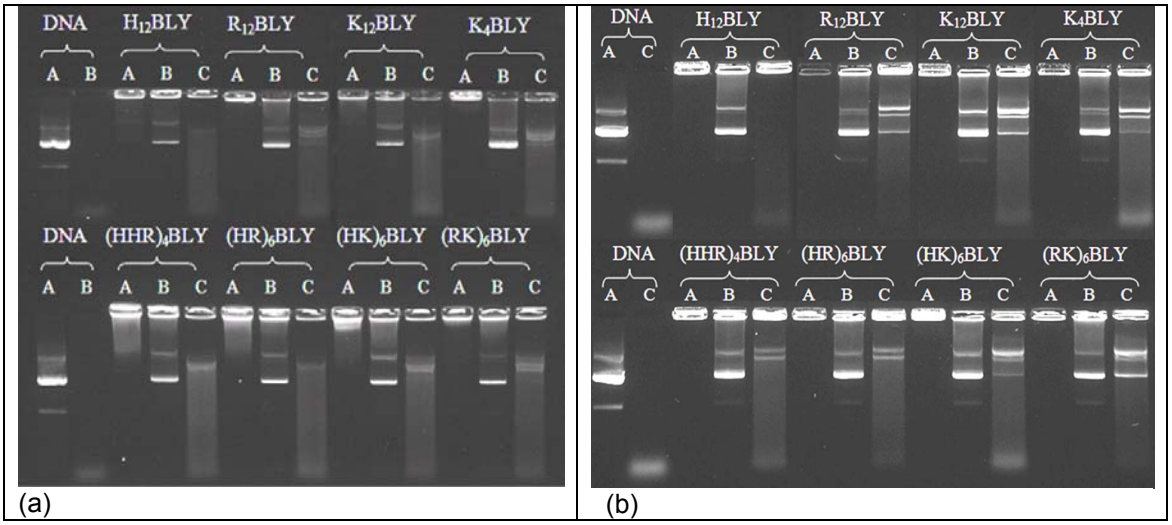

Figure 3.10 Condensation, release and protection properties of the LPDs (VwLPDw) containing Series I and II peptides using agarose gel electrophoresis (0.025 mg/mL of pDNA per well). LPDs were prepared at lipid:peptide:DNA charge ratio of (a) 0.5:2.4:1 (b) 0.5:6:1. Lane A: DNA or LPD. Lane B: DNA or LPD treated with pAsp. Lane C: LPD treated with DNAse I at 37 ± 0.1°C followed by pAsp. Experiment (b) was repeated 2 times, repeat experiment shown in Appendix II.

When considering the results of the gel electrophoresis studies on LPDs prepared at a charge ratio of 0.5:2.4:1 (Figure 3.10(a)), it can be seen that LPDs prepared using the Series I peptides yielded no bands in Lane A that were attributable to free DNA. In contrast, the LPDs prepared using Series II peptides, with the exception of (RK)6BLY, all produced some smearing, suggesting that the DNA was not fully complexed. These results imply that the Series I peptides were generally more effective at condensing DNA than Series II peptides. The lower condensation efficiency seen with the Series II peptides was especially noticeable when one of the peptide residues contained, in the DNA condensing region, histidine (H) residues. This lower condensation seen with these peptides are due to the low pka (6.10) and therefore low percent ionisation of H. Interestingly, in this context, the Series I peptide, H12BLY did appear to fully condense DNA. The reason for this observation is not currently known. When the LPDs were prepared at the higher charge ratio of 0.5:6:1 (Figure 3.10(b)), DNA appeared to be fully

complexed, regardless of the peptide used to prepare the complex, giving further justification to the use of LPDs prepared at this mixing ratio for detailed study.

The results of the release study, shown in Lane B, suggest that it is possible to release DNA from the all the LPDs (regardless of the peptide that was used to prepare them) via displacement with the anionic polymer, pAsp. Moreover, the extent of release did not appear to change with the charge ratio used to prepare the complex, suggesting that the interaction between the DNA and the peptides/lipid was not very strong.

Encouragingly, while not offering total protection, the LPDs did to some extent protect the DNA from enzymatic degradation as can be seen from Lane C. The protection offered by the LPDs was in sharp contrast to the degradation seen when the naked/free DNA was exposed to DNAse I where a far greater amount of DNA was degraded to smaller molecular weight fragments. The LPDs prepared using the higher charge ratio of 0.5:6:1 exhibited the greatest level of protection as indicated by the greater prominence of the (upper) bands of DNA, attributable to its open circular form. To note, supercoiled DNA is relaxed to the open circular and then linear form after which the endonuclease, DNAse I, cleaves DNA preferentially at the phosphodiester linkages adjacent to a pyrimidine nucleotide (Weintraub et al, 1986, Cherng et al, 1999, Koichiro Kishia 2001). The biological activity of DNA in open circular form was reported to be comparable to that in supercoiled form (Weintraub 1986, Xie et al, 1993, Niven et al, 1998).

3.1.2.2 Lipopolyplexes prepared in NaCl solution

The protection of DNA in LPDs prepared at a 0.5:6:1 charge ratio and made in a 0.12 M aqueous NaCl solution (VsLPDs) was also examined (Figure 3.11). For comparison purposes LPDs prepared in water (VwLPDw) were also examined at the same time. In agreement with the results obtained for LPDs prepared in water (VwLPDw) shown in Figure 3.10, DNA was totally complexed in the LPDs (Lane A) and was well released from the LPDs in the presence of pAsp (Lane B). Excitingly, and in contrast to the results obtained with the LPDs prepared in water, those prepared in NaCl solution appeared to totally protect the DNA from DNAse I degradation as the bands in Lane C were identical to that in Lane B and for the naked DNA in Lane A. This protection of DNA could be one of the reasons for high level of transfection efficiency observed with the VsLPDs, although interestingly no difference was observed between the two series of

LPDs. Indeed it has been reported that incubation of plasmid DNA with serum showed that sodium phosphate protected the DNA from degradation and sodium phosphate enhanced plasmid DNA expression *in vivo*, although the mechanism was unclear (Hartikka et al, 2000).

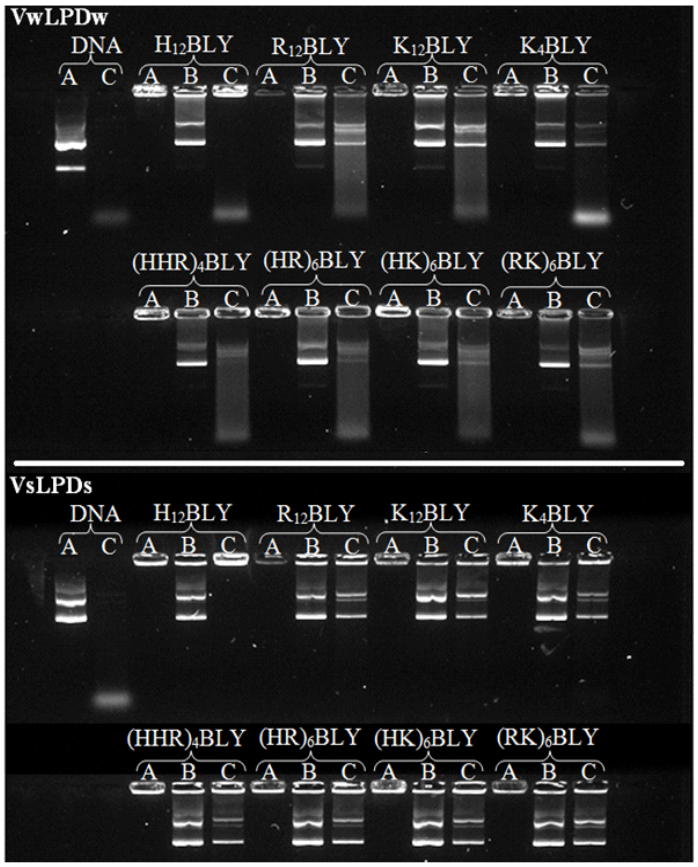

Figure 3.11 Condensation, release and protection properties of LPDs (VwLPDw and VsLPDs) using agarose gel electrophoresis (0.025 mg/mL of pDNA). LPDs were prepared at lipid:peptide:DNA charge ratio of 0.5:6:1. The effect of the peptide component on DNA condensation (Lane A), DNA release (Lane B), and protection from DNAse I (Lane C) was studied. Lane A: DNA or LPD. Lane B: DNA and LPDs treated with pAsp. Lane C: LPDs treated with DNAse I at 37 ± 0.1°C °C followed by pAsp. Experiment repeated 2 times, repeat experiments shown in Appendix II.

3.1.2.3 Lipopolyplexes prepared in NaCl solution of varying concentrations

In order to further study the effect of NaCl on the protection of DNA afforded by the LPDs, LPDs with the vesicles made in water and the LPDs prepared in aqueous NaCl solutions of differing strength, namely 0.008, 0.04, 0.08 and 0.12 M NaCl (i.e. VwLPDs) and LPDs made fully in aqueous NaCl solutions of differing strength (i.e. VsLPDs) were studied using gel electrophoresis. For this study a Series I peptide, K12BLY and a Series II peptide (HHR)4BLY were examined, the results are shown in Figure 3.12. Firstly, in line with the electrophoresis studies reported above, the DNA was fully complexed (Lane A) and fully released (Lane B)

irrespective of the amount of NaCl present in the complex. It was clear, however, from the results in Lane C that, as the concentration of NaCl solution used to prepare the complex increased, the protection afforded by the complex increased. Moreover, there was no difference in the DNA protection afforded by VsLPDs and VwLPDs.

Figure 3.12 Condensation, release and protection properties of LPDs (VwLPDs and VsLPDs) using agarose gel electrophoresis (0.025 mg/mL of pDNA). LPDs were prepared at lipid:peptide:DNA charge ratio of 0.5:6:1. The effect of NaCl concentration on DNA condensation (Lane A), DNA release (Lane B), and protection from DNAse I (Lane C) was studied. Lane A: DNA or LPD. Lane B: DNA or LPDs treated with pAsp. Lane C: LPDs treated with DNAse I at 37 ± 0.1°C °C followed by pAsp. W = water; S1 = 0.008 M NaCl; S2 = 0.04 M NaCl; S3 = 0.08 NaCl; S4 = 0.12 M NaCl.

3.1.2.4 Effect of enzyme incubation time

A further protection experiment was carried out using gel electrophoresis. Figure 3.13(a) shows the effect of the incubation time with DNAse I on the protection provided by the LPDs containing H12BLY. The LPDs were prepared in either in water (VwLPDw) or saline solution (VwLPDs). Note, there was no difference in gel electrophoresis seen between VwLPDs and VsLPDs (Figure 3.12). The incubation time of the LPDs with DNAse I was either 0, 1, 3, 5, 10 or 20 minutes. As can be seen in Lane C of the lower panel in Figure 3.13, the strength of the lower bands arising from the degradation of DNA increased as the incubation time increased from 1 to 20 minutes, regardless of whether the LPDs are prepared in water or 0.12 M NaCl saline solution. Interestingly, it can be seen that amount of supercoiled DNA (middle band) decreased and the amount of linear DNA (upper band) increased as the incubation time increased. The change from the supercoiled form of DNA to its linear form over time in contact with DNAse I has also be observed by other researchers (Cherng et al, 1999). For DNA complexed in LPDs prepared using H12BLY in water (VwLPDw), only faint degradation bands were observed while in band due to degradation of DNA was seen in when the LPDs were made in 0.12 M NaCl solution (VwLPDs). These results suggest that DNA complexed in LPDs prepared using 0.12 M NaCl solution (VwLPDs) were both well protected and indeed better protected than DNA complexed inside LPDs prepared fully in water (VwLPDw).

Significantly, the protection of DNA in the VwLPDs lasted at least 20 mins (longer time points not measured). It is worth noting that the well-protected DNA in the VwLPDs remained in the wells rather than moved down the gel. This could be due to the weak electrostatic interaction between H12BLY and DNA. Furthermore, this weak electrostatic interaction is further reduced in saline solution due to charge screening effect of salt. Unlike other peptides, histidine residues on H12BLY have a pKa value ~6 and therefore H12BLY are more neutral-like. Therefore, negative pAsp molecule is not able to interact with H12BLY and is thus not able to replace DNA from the LPDs.

Figure 3.13(b) depicts the condensation, release and protection properties of the LPDs containing the peptide (HHR)4BLY diluted 1 in 4 by volume in either in Optimem (o) or Media containing 10% v/v FBS (m) (upper panel). The lower panel shows the undiluted LPDs as controls. For naked DNA diluted in either Optimem (DNAw/o and DNAs/o) or Media (DNAs/m

and DNAs/m), in Lane C there were no bands attributable to DNA, rather strong bands due to degradation of DNA, suggesting the complete degradation of DNA in both media.

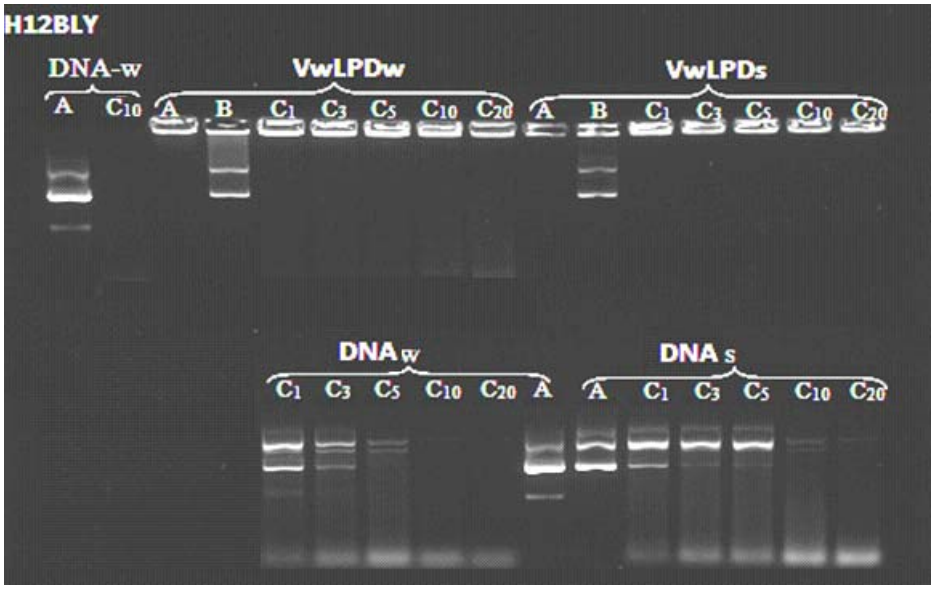

(a)

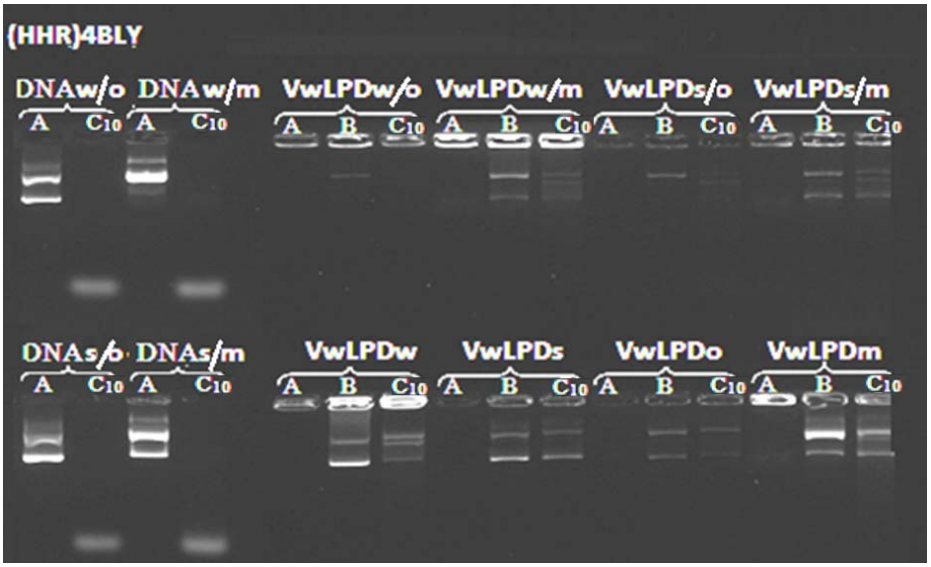

(b)

Figure 3.13 Condensation, release and protection properties of LPDs containing (a) H12BLY (VwLPDw and VwLPDs) using agarose gel electrophoresis (0.025 mg/mL of pDNA) and (b) LPD containing (HHR)4BLY diluted 1 in 4 by volume in Optimem (o) or media containing 10% v/v FBS (m). LPDs were prepared at lipid:peptide:DNA charge ratio of 0.5:6:1. The effect of DNAse I incubation time on DNA condensation (Lane A), DNA release (Lane B), and protection from DNAse I (Lane C) was studied. Lane A: DNA or LPD. Lane B: DNA or LPDs treated with pAsp. Lane C: LPDs treated with DNAse I followed by pAsp. S = 0.12 M NaCl. Incubation time = 1, 2, 3, 5, 10, 20 minutes at 37 ± 0.1°C.

In contrast, when the LPDs were diluted in either Optimem (VwLPDs/o and VsLPDs/o) or Media (VwLPDs/m and VsLPDs/m), there were no degradation fragments bands in Lane C, rather just

bands attributable to DNA, suggesting that DNA complexed in these LPDs was protected from enzymatic degradation due to DNAse I. This observation is supported by the fact that only faint DNA bands were observable for the LPDs treated with pAsp in Lane B suggesting that DNA was not readily released from these LPDs. In addition, there was no free DNA, attributable to uncomplexed DNA, present in Lane A for the LPDs diluted in Optimem (VwLPDs/o and VsLPDs/o) and Media (VwLPDs/m and VsLPDs/m), suggesting that the lipopolyplexes was efficient at complexing.

3.1.3 Quantification of DNA condensation in lipopolyplexes

Picogreen is an ultra-sensitive, fluorescent stain used for DNA quantification. Once bound to DNA, picogreen exhibits a greater than 1000 times increase in fluorescence than its unbound state. As a consequence, it is possible to determine the amount of DNA free in LPD formulations by quantifying the fluorescence of picogreen. A series of LPDs were therefore prepared at different P:D charge ratios whilst keeping the L:D charge ratio constant at 0.5:1. As picogreen competes with the peptides to bind to the DNA, two preparation protocols were explored. In protocol 1, pre-formed LPDs were mixed with picogreen while in protocol 2, DNA was mixed with picogreen and then formulated as LPDs. The two protocols were studied as previous studies had indicated that the method of addition of the picogreen may influence the results obtained.

3.1.3.1 Lipopolyplexes prepared in water

The results obtained for the two series of peptides using protocol 1 and 2 are shown in Figures 3.14(a) and 3.14(b), respectively. As can be seen at a P:D charge ratio of 1:1, ~20 and ~40% of naked/free DNA was detected in LPDs prepared with Series I and Series II peptides, respectively. The only exception being the Series I peptide, H12BLY, where ~45% naked/free DNA was seen. This amount of naked/free DNA corresponds to ~80 and ~60% of the DNA being condensed in the LPDs prepared using Series I and Series II, respectively. As can be seen, Series I containing LPDs condensed more DNA than those prepared using Series II peptides, which was interesting because in theory, all DNA should be condensed at a P:D charge ratio of 1:1 (assuming all charges are freely accessible for complexation). This observation may help understand the detailed molecular structure of the LPDs. At a charge ratio

greater than 1:1, the extent of condensation was seen to slowly increase for the LPDs, regardless of whether they were prepared using either a Series I or Series II peptide.

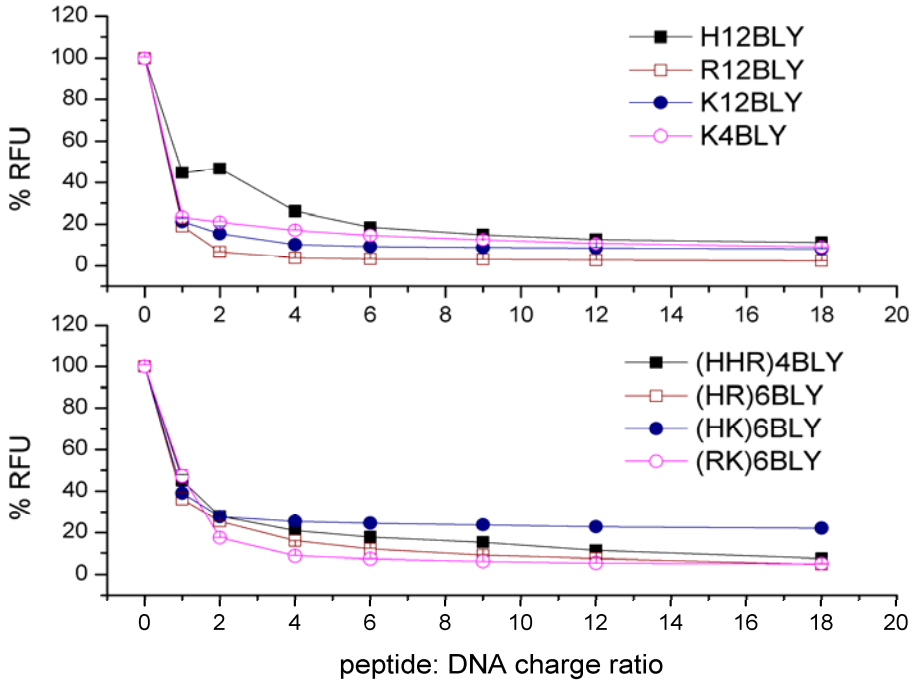

(a)

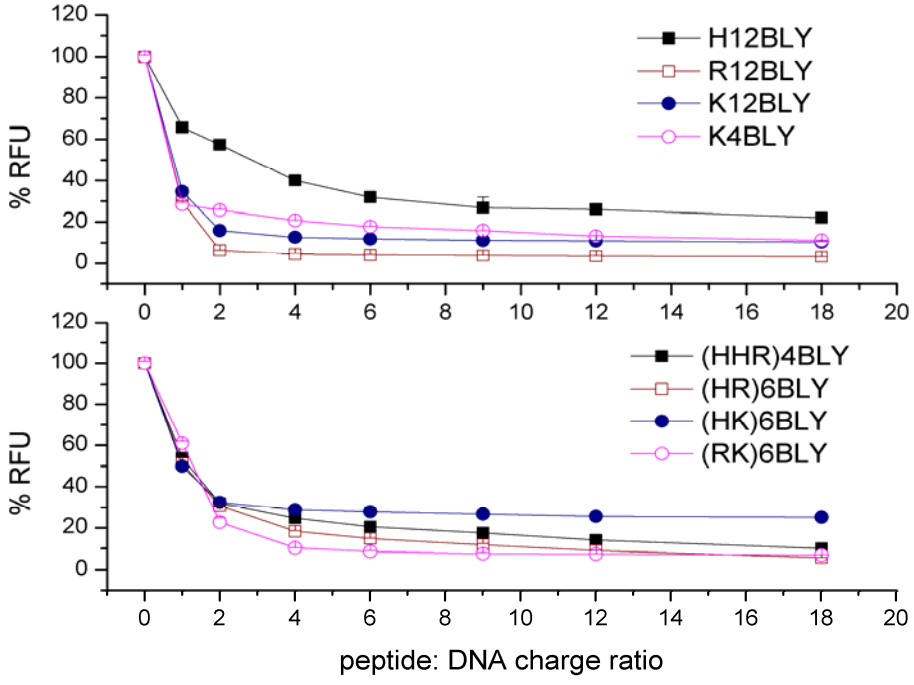

(b)

Figure 3.14 Quantification of DNA complexed in LPDs (VwLPDw) as determined using a picogreen fluorescence assay. LPDs were prepared by (a) protocol 1 and (b) protocol 2 (0.02 mg/mL pDNA). Protocol 1 = LPD+picogreen. Protocol 2 = LP+(D+picogreen). Error bar are the SD of three measurements of a single formulation (n = 3) at 25 ± 0.1°C.

At a P:D charge ratio of 6:1, ~75% of DNA was condensed in LPDs prepared using the Series II peptides, although little change was seen in the extent of complexation observed with the LPDs prepared using the Series I peptides. At P:D charge ratios greater than 6:1, no further increase in the extent of complexation was noted. Not surprisingly from a consideration of its pKa, the extent of incorporation of LPDs incorporating H-containing peptides tended to be less under the conditions of the experiment.

When protocol 2 was used, the extent of condensation was lower than that observed using protocol 1, the only exception being the LPDs prepared using the Series I peptide R12BLY, where there was no difference in the extent of condensation between the two protocols. The difference between the extents of the condensation achieved with both protocols was particularly noticeable for LPDs containing the Series I peptide H12BLY, most probably due to its weak interaction with DNA.

3.1.3.2 Lipopolyplexes prepared in NaCl solutions

Interestingly, the LPDs prepared in 0.12 M NaCl saline (VsLPDs) exhibited a much lower ability to condense DNA when compared to those prepared in water (VwLPDw) as seen in Figure 3.15. When studied LPDs prepared using protocol 1, those LPDs made in 0.12 M NaCl saline solution (VsLPDs) exhibited a lower propensity to condense DNA than the LPDs prepared in water as seen in Figure 3.15(a) and 3.15(b), with the extent of DNA condensation gradually increasing over the whole range of P:D charge ratios studied. For example, out of the Series 1 peptides, the LPDs containing H12BLY and K4BLY prepared at a P:D charge ratio of 6:1 condensed only ~50 and ~70% of DNA, respectively. Furthermore, with the exception of (RK)6BLY, the LPDs prepared with Series 2 peptides condensed DNA even less well. When using protocol 2, LPDs prepared with either series of peptide condensed even less DNA - this was especially true of LPDs containing H12BLY, K4BLY, (HHR)4BLY and (HK)6BLY. Clearly, these differences were due to the presence of NaCl saline reducing the interaction between DNA and peptides.

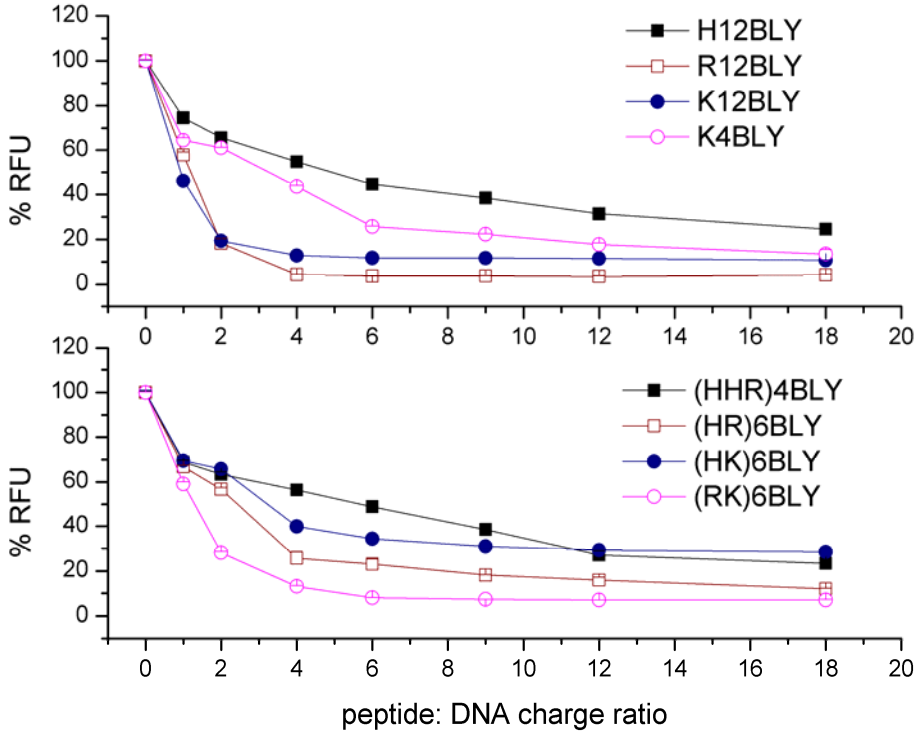

(a)

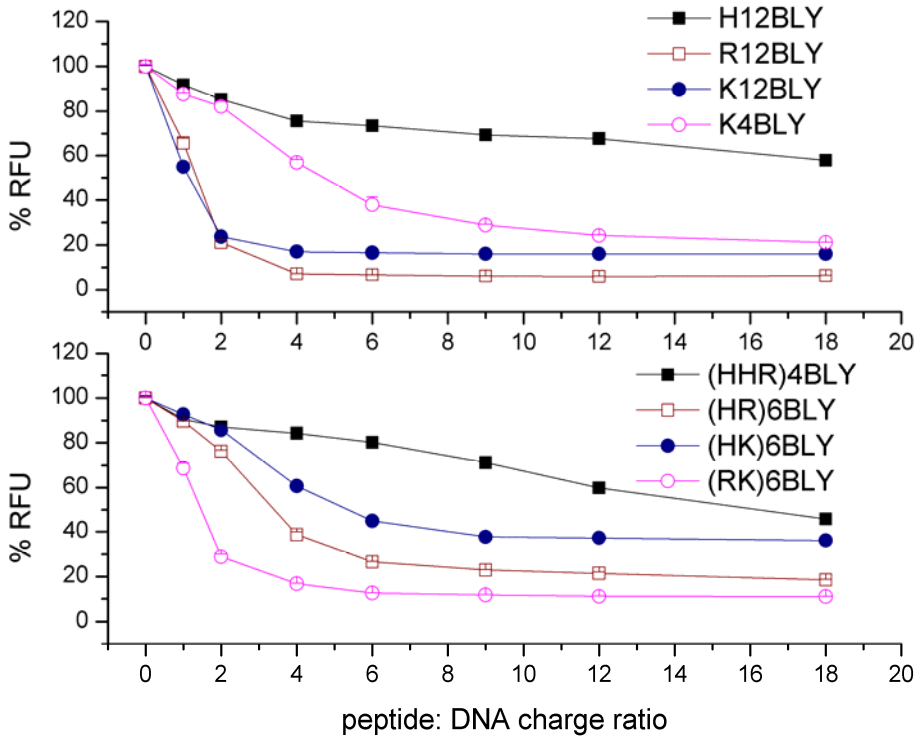

(b)

Figure 3.15 Quantification of DNA complexed in LPDs (VsLPDs) as determined using a picogreen fluorescence assay. LPDs were prepared by (a) Protocol 1 and (b) Protocol 2 (0.01 mg/mL pDNA). Protocol 1 = LPD+picogreen. Protocol 2 = LP+(D+picogreen). Error bar means SD of three measurements of a single formulation (n = 3) at 25 ± 0.1°C.

3.1.4 Size and ζ- potential measurement of lipopolyplexes

From the gel electrophoresis and picogreen fluorescence studies, there is a suggestion that the extent and strength of DNA condensation in the LPDs varies with both the peptides used to prepare the LPDs and the presence of NaCl. The effect of peptide structure and the method of preparation on other of the biophysical properties of the complexes is not known. In this section, dynamic light scattering will therefore be used to determine the apparent hydrodynamic size of the LPDs. Moreover, as the surface properties of nanoparticles are known to affect their behaviour *in vivo,* the ζ-potential of the LPDs prepared in water and NaCl solutions will be investigated.

3.1.4.1 Lipopolyplexes prepared in water

Figure 3.16(a) shows the apparent hydrodynamic size and ζ-potential of DOTMA:DOPE vesicles, the binary LD complexes they form, together with a range of binary PD and ternary LPDs containing K4BLY, when prepared in water. Figure 3.16(b) shows the polydispersity index (PDI) of the LPDs shown in Figure 3.16(a). As can be seen the cationic vesicles were of ~65 nm in diameter with a ζ-potential of ~50 mV. Their small apparent hydrodynamic size indicates that the vesicles were predominately small unilamellar in nature. Their high ζ-potential suggests that the vesicles will be stable in water. Upon the addition of DNA to the vesicular suspension at a range of L:D charge ratios (i.e. 1:1, 2:1 and 4:1), LDs in the size range of 100 - 140 nm, were formed. Unlike the LDs, PDs formed by mixing DNA with the peptide K4BLY were small and of the order of ~60 nm in size. Interestingly, the ζ-potential of both LDs and PDs were slightly negative when the charge ratio was 1:1 or 2:1 and 6:1 for LDs and PDs respectively, possibly indicating that a high L/P:D charge ratio is required to completely condense the DNA. This observation is supported by the condensation results seen using gel electrophoresis (Figure 3.10). Furthermore, even at the highest L/P:D charge ratios of 4:1 and 18:1, the ζ-potential of LDs and PDs formed exhibited ζ-potentials of no more than 20 mV. Usually, a ζ-potential of no less than 25 - 30 mV is required to maintain charge-charge repulsion and therefore size stability (Freitas et al, 1998), suggesting that the LDs and PDs may not exhibit long term stability.

In contrast, the LPDs prepared using K4BLY tended to be small at less than 100 nm and highly reproducible in size (size measured on at least 4 separate occasions). While the apparent hydrodynamic size of the LPDs decreased upon increasing the amount of peptide present with

the LPDs prepared at a L:P:D charge ratio 0.5:18:1 exhibiting the smallest size, their ζ-potential increased from a value of ~ 25 to ~ 35 mV as the P:D charge ratio increased from 6:1 through 12:1 to 18:1. The small size of the LPDs, combined with their relatively high ζ-potential suggests that the LPDs will exhibit a high degree of stability. The size stability over time of the LPDs prepared in water will be discussed later.

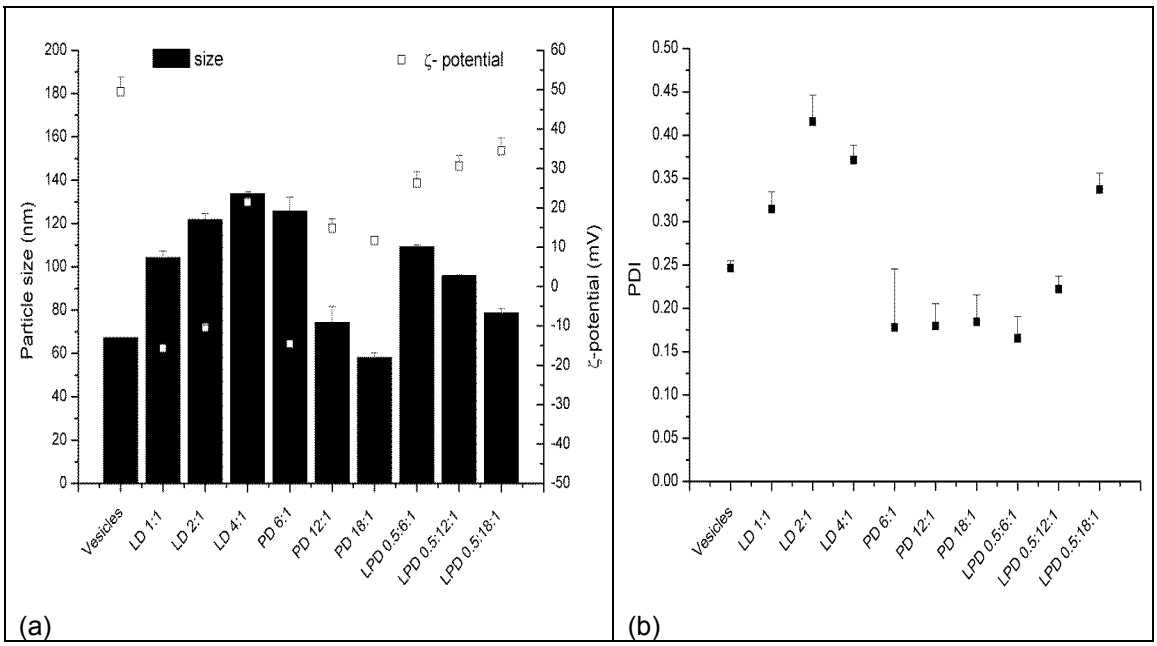

Figure 3.16 Mean hydrodynamic particle size and ζ-potential of LDs, PDs and LPDs (K4BLY) using dynamic light scattering (DLS). Both binary and ternary complex prepared at lipid:peptide:DNA charge ratio of 0.5:6:1 in water (0.005 mg/mL of ctDNA). Cationic vesicles composed of DOTMA:DOPE at 1:1 molar ratio. (a) mean apparent hydrodynamic size and ζ-potential. (b) polydispersity index (PDI) of mean apparent hydrodynamic size. Error from SD of three measurements of one formulation (n = 3) at 25 ± 0.1°C.

A more detailed study of the apparent hydrodynamic size and ζ-potential of the LPDs prepared totally in water using the various peptides (VwLPDw) was performed and the results of the study shown in Figure 3.17(a). In line with the previous results obtained for LPDs containing the peptide K4BLY, the LPDs containing K4BLY and prepared at L:P:D charge ratios of either 0.5:6:1 or 0.5:12:1 exhibited an apparent hydrodynamic size in the range of ~80-100 nm and possessed a ζ-potential of ~35 mV. When considering the LPDs as a group, apparent hydrodynamic sizes in the range of 80-140 nm were seen, with the exception of the LPDs containing (HHR)4BLY where a large apparent hydrodynamic size of 170 nm was obtained. The LPDs prepared at the higher L:P:D charge ratio of 0.5:12:1 tended to be smaller. Furthermore,

the LPDs containing the Series II peptides exhibited a larger size than those containing Series I peptides. This is consistent with the fact that the LPDs containing the Series II peptides tended to condense DNA to a less extent than those containing Series I peptides (Figure 3.14).

The polydispersity index (PDI) determined for particle size is another indicator of the size quality of the preparation as reported in Figure 3.17(b). A particulate system such as an LPD would be considered to be homogeneous if the LPDs exhibited PDIs of less than 0.15 (or ideally 0.10). For comparison with a PDI of 0.2 obtained for the cationic vesicles is also reported. As shown in Figure 3.17(b), all LPDs were heterogeneous in nature. With the exception of the LPDs containing (HHR)4BLY, the PDI of the LPDs fluctuated around 0.25. The LPDs containing (HHR)4BLY and prepared at a L:P:D charge ratio of 0.5:6:1 exhibited a higher PDI of ~0.35 which maybe a consequence of there being insufficient peptide present to fully complex the DNA. In accordance with the sizing results, the PDI of the LPDs prepared at 0.5:12:1 charge ratio tended to be very slightly lower than that of the LPDs prepared at 0.5:6:1 charge ratio. There was no obvious difference in PDI obtained for the LPDs containing the various peptides.

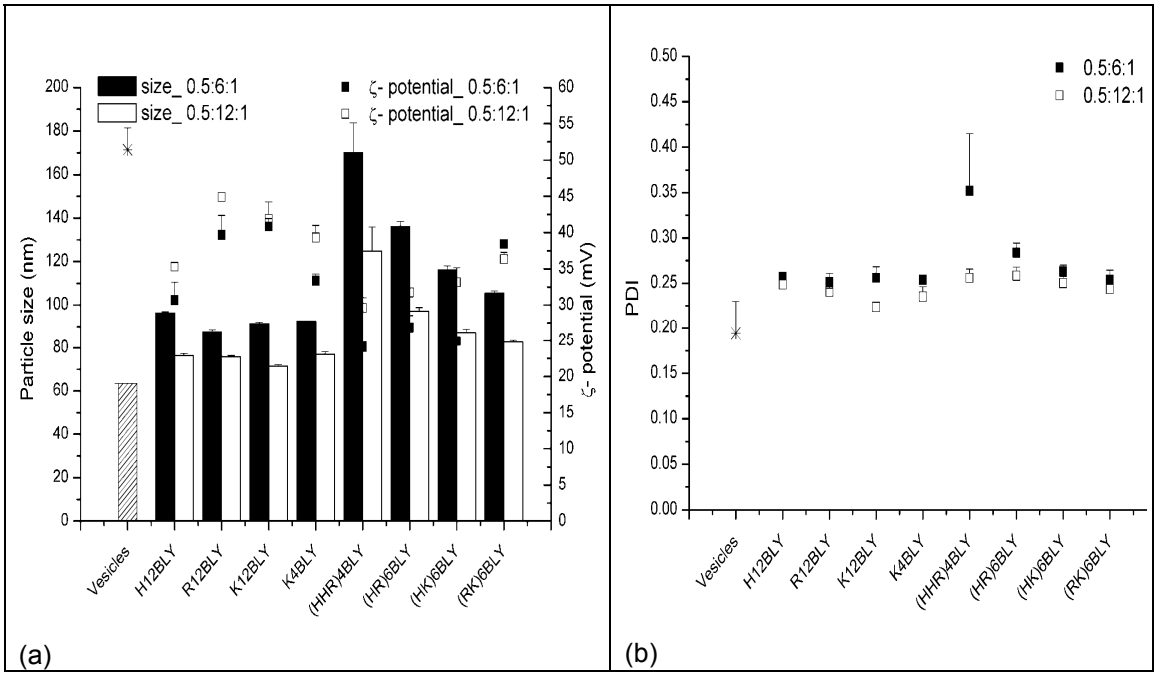

Figure 3.17 Mean apparent hydrodynamic particle size and ζ-potential of LPDs made in water (VwLPDw). Samples prepared at a lipid:peptide:DNA charge ratios of 0.5:6:1 and 0.5:12:1 (final DNA concentration of 0.01 mg/mL). Vesicle suspension composed of DOTMA/DOPE at 1:1 molar ratio. (a) mean apparent hydrodynamic size and ζ-potential, (b) polydispersity index (PDI) of mean apparent hydrodynamic size (n=3). Error from SD of three measurements of a single formulation at 25 ± 0.1°C. 1 repeat in Appendix II.

The surface properties of the LPDs were evaluated by determining their surface ζ-potential. As can be seen from Figure 3.17(a), the LPDs possessed ζ-potentials in the range of 25 - 40 mV, with the LPDs prepared at the higher L:P:D charge ratio of 0.5:12:1 tending to possess the higher ζ-potential. Furthermore, the LPDs containing the Series II peptides tended to exhibit a lower ζ-potential than those containing Series I peptides. When comparing the results of the gel electrophoresis studies (Figure 3.10(a) and 3.10(b)), it is clear that the LPDs that exhibited a stronger condensation of DNA possessed a higher ζ-potential and smaller particle size.

The surface ζ-potential can also be used as an indicator of the LPD size stability, with the greater the surface ζ-potential, the more stable the LPD. Figure 3.18(a) shows the variation of the apparent hydrodynamic size of LPDs prepared in water (i.e. VwLPDw) at an L:P:D charge ratio of 0.5:6:1 over a period of 10 days.

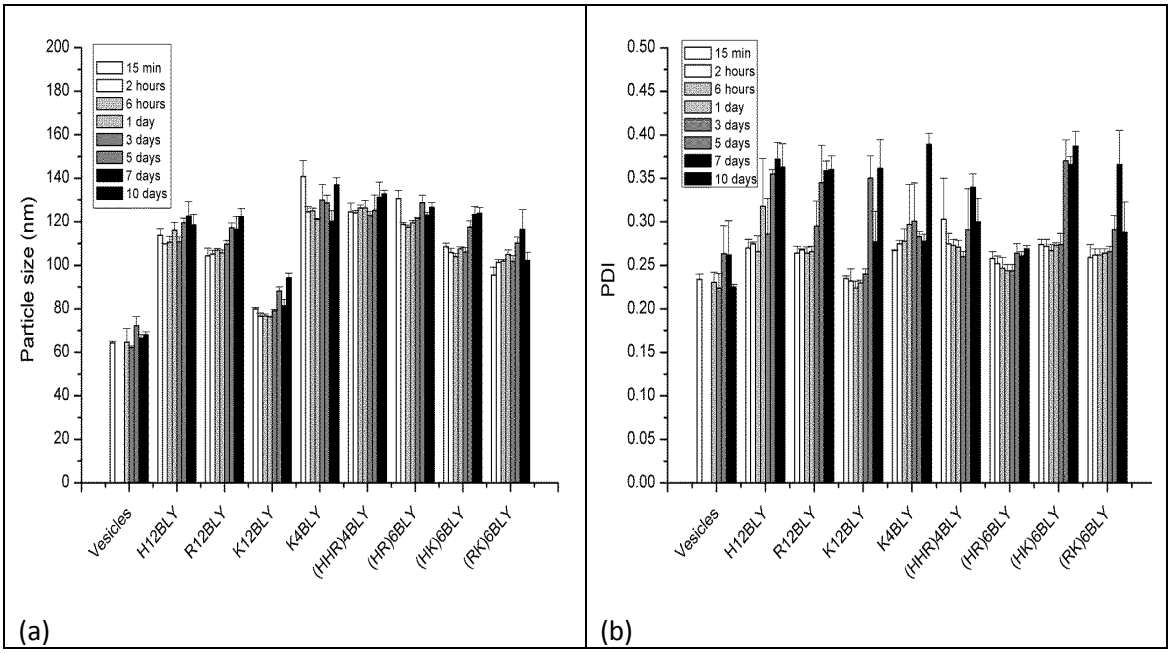

Figure 3.18 Mean hydrodynamic particle size stability and ζ-potential of LPDs made in water (VwLPDw). All samples prepared at lipid:peptide:DNA charge ratio of 0.5:6:1 (0.01 mg/mL of pDNA). Vesicle suspension composed of DOTMA/DOPE at 1:1 molar ratio. (a) mean apparent hydrodynamic size, (b) polydispersity index (PDI) of mean apparent hydrodynamic size. Error from SD of three measurements of a single formulation (n = 3) at 25 ± 0.1°C.

As can be seen the LPDs were very stable, with respect to apparent hydrodynamic size, over the time course tested (longer time periods were not tested). The high size stability of the LPDs is believed to be a consequence of their possession of a high ζ-potential. Interestingly, however,

despite their high size stability, the PDIs recorded increased over the same period, particularly at 7 and 10 days suggesting either the formation of a few very large particles and/or contamination of the cuvettes in which the samples were standing. Note, the change is not shown in the size measurement which might be because of the change in count rate.

3.1.4.2 Lipopolyplexes prepared in NaCl solutions

In order to understand the effect of NaCl on transfection of LPDs, the above studies were repeated replacing the water with NaCl solution during the preparation of both the vesicles and LPDs (VsLPDs). The apparent hydrodynamic size and ζ-potential of the vesicles and LPDs made in 0.12 M NaCl solution at a L:P:D charge ratio of either 0.5:6:1 or 0.5:12:1 are shown in Figure 3.19(a).

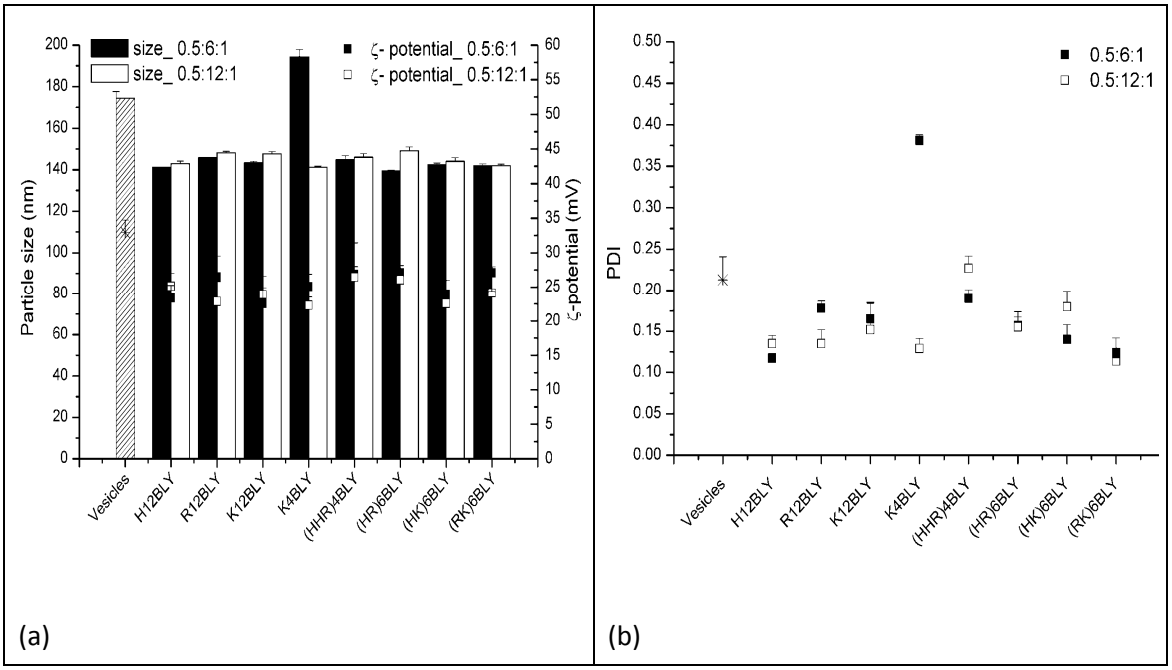

Figure 3.19 Mean hydrodynamic particle size and ζ-potential of LPDs made in 0.12 M NaCl solution (VsLPDs) using dynamic light scattering. All samples prepared at lipid:peptide:DNA charge ratio of 0.5:6:1 (0.01 mg/mL of pDNA). Lipidic suspension composed of DOTMA/DOPE at 1:1 molar ratio. (a) mean apparent hydrodynamic size, (b) polydispersity index (PDI) of mean apparent hydrodynamic size. Error from SD of three measurements of a single formulation (n = 3) at 25 ± 0.1°C.

It is particularly noteworthy that the apparent hydrodynamic size of the cationic vesicles, prepared in 0.12 M NaCl (saline) solution, at 175 nm, are ~ 3 times larger than those prepared in water. The large size of the vesicles in saline would suggest that they are multilamellar in nature. In addition, the cationic vesicles, when dispersed in 0.12 M NaCl solution, possessed a

lower ζ-potential of ~35 mV as opposed to ~50 mV when the vesicles were dispersed in water. This lower ζ-potential is likely to be a consequence of the charge screening effect of the electrolyte.

Interestingly, the apparent hydrodynamic size and ζ-potential of the LPDs prepared in 0.12 M NaCl solution (VsLPDs) were all very similar at ~150 nm and ~25 mV, respectively. The only exception being the LPDs prepared containing K4BLY and made at a charge ratio of 0.5:6:1 which were larger at ~200 nm. It is worth noting that the LPDs prepared in 0.12 M NaCl solution were smaller than the cationic vesicles from which they were prepared.

Inspection of the PDIs of the LPDs (Figure 3.19(b)) indicated that, with the exception of the LPDs prepared using K4BLY, the PDI of the various LPDs was only ~0.15, suggesting that the particles are fairly monodisperse. Indeed, the VsLPDs appeared to be more monodisperse than their VwLPDw counterparts.

In order to investigate the effect of NaCl concentration on transfection of LPDs, the effect of the various strength NaCl solutions on the size and the ζ-potential of the resulting LPDs was also studied. The LPDs containing (HHR)4BLY were selected for study. Figure 3.20(a) shows the apparent hydrodynamic size stability and the ζ-potential of LPDs containing (HHR)4BLY prepared in 0.008, 0.04, 0.08 and 0.12 M NaCl solutions. In this study the parent cationic vesicles were either made in water or NaCl solution. In the case of the LPD that were prepared in varying strength NaCl solution but using vesicles which had been prepared in water, these LPDs were denoted as VwLPDs. Figure 3.20(b) shows the polydispersity index (PDI) obtained for the various systems shown in Figure 3.20(a).

As seen in Figure 3.20(a), the apparent hydrodynamic size of the cationic vesicles prepared in the various NaCl solutions was larger than the vesicles made in water (~60 nm) and increased with increasing sodium chloride solution from ~120 nm to ~300 nm. In addition, the apparent hydrodynamic size of the LPDs prepared fully in the various strength NaCl solutions, were larger than those prepared using vesicles made in water. This size increase was particularly noticeable at the higher NaCl concentrations of 0.08 and 0.12 M. This observation shows that the apparent hydrodynamic size of the LPDs was affected the apparent hydrodynamic size of the vesicles from which the LPDs were prepared.

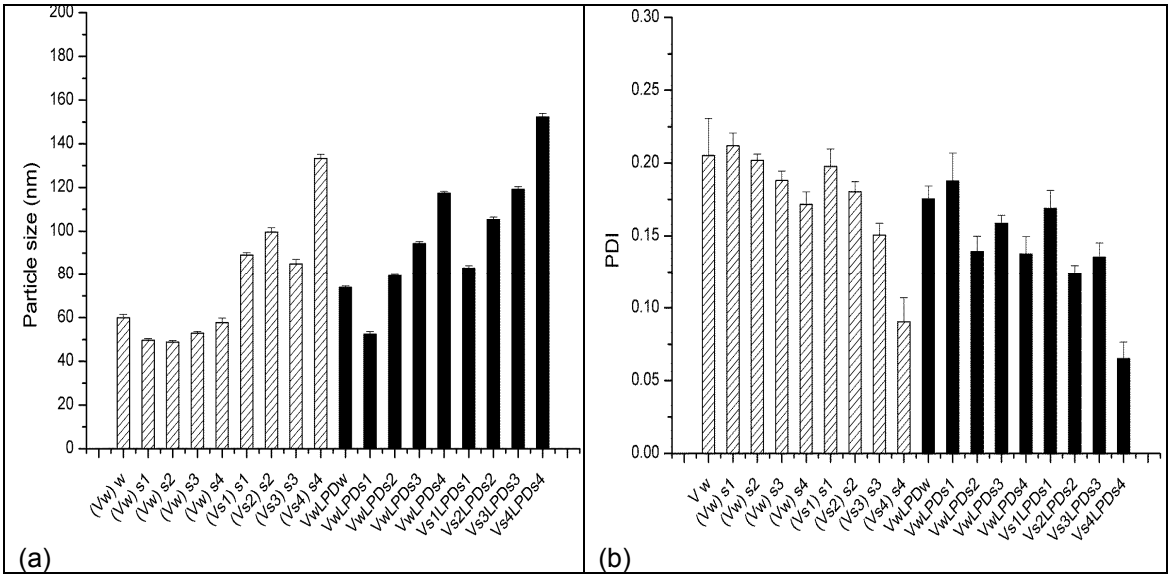

Figure 3.20 Mean hydrodynamic particle size and ζ-potential of LPDs containing-(HHR)4BLY and made in various NaCl solution (i.e. S1 = 0.008; S2 = 0.04; S3=0.08; S4=0.12 M NaCl). (a) mean apparent hydrodynamic size, (b) polydispersity index (PDI) of mean apparent hydrodynamic size. VwLPDs: LPD prepared in NaCl solutions and its parent vesicles in water. VsLPDs: both LPD and its parent vesicles prepared in NaCl solutions. All samples prepared at a lipid:peptide:DNA charge ratio of 0.5:6:1 (0.01 mg/mL pDNA). Vesicle suspension (V) composed of DOTMA/DOPE at 1:1 molar ratio. (Vw)s: vesicles prepared in water and diluted in NaCl solution. (Vs)s: vesicles prepared and diluted in NaCl solutions. Error bars are the SD of three measurements of a single formulation (n = 3) at 25 ± 0.1°C.

Figure 3.21(a) describes the stability of the LPDs containing (HHR)4BLY and vesicles (insert) prepared in various NaCl solutions over time in terms of apparent hydrodynamic sizes and ζ-potentials. The hydrodynamic sizes of the Lipofectamine 2000/DNA particles (denoted L2K/DNA) were also measured as they were used as a positive control in the transfection studies. Consistent with the results shown in Figure 3.20(a), the size of the LPDs was larger as the NaCl concentration increased. Moreover, the ζ-potential of the LPDs decreased as the NaCl concentration increased becoming 20 - 25 mV when 0.08 and 0.12 M NaCl solutions, respectively due to the charge screening effect of the NaCl. To note, the LPDs prepared in various NaCl solutions possessed the same trend in apparent hydrodynamic size and ζ-potential as the corresponding vesicles (Vs). In addition, the apparent hydrodynamic size of the LPDs prepared fully in the various NaCl solutions (VsLPDs), were larger than those prepared using vesicles made in water (VwLPDs). The exception is that when prepared in 0.12 M NaCl solution (S4), the LPDs were larger in this occasion (VsLPDs) which might be due to contamination present in the measuring cuvettes.

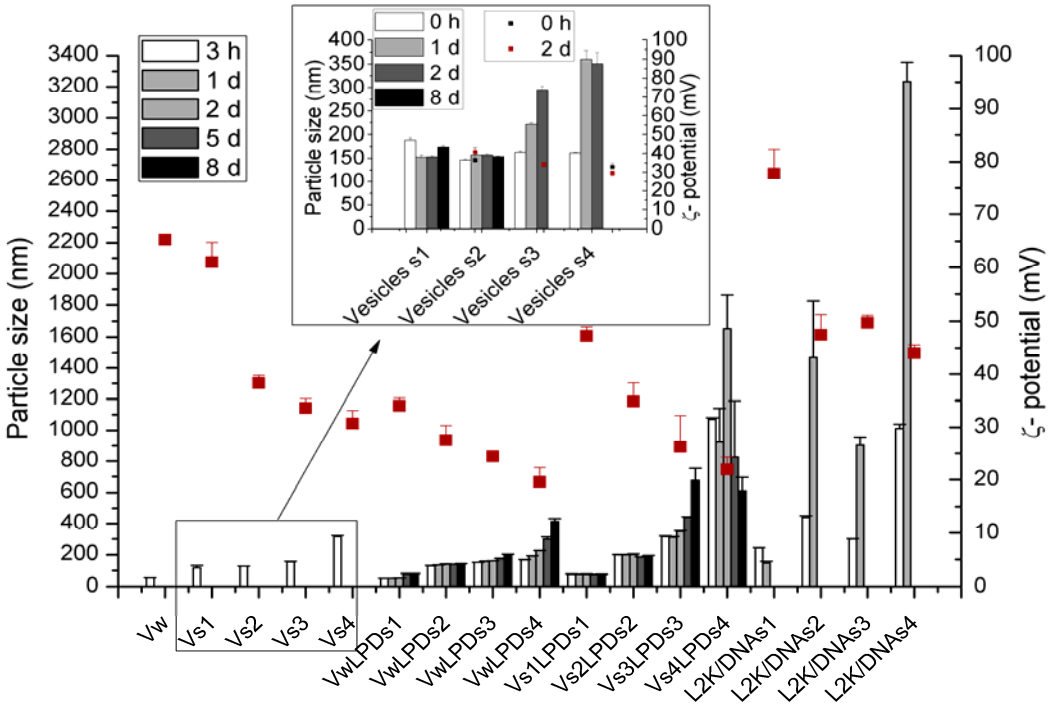

(a)

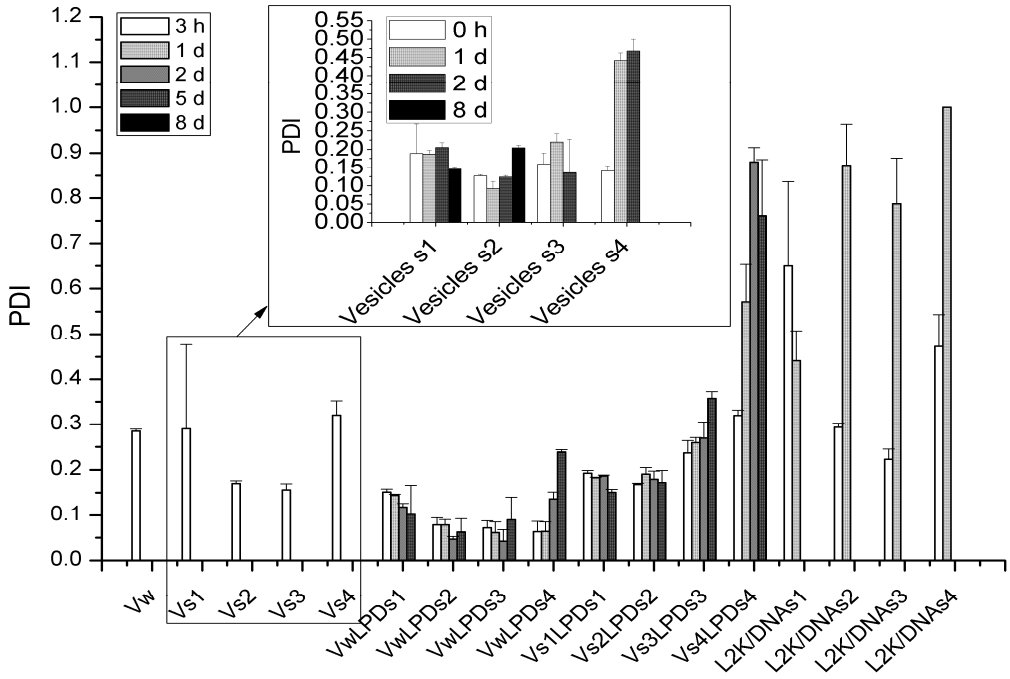

(b)

Figure 3.21 Mean hydrodynamic particle size stability and ζ-potential of vesicles, LPDs containing (HHR)4BLY, Lipofectamine 2000 (L2K)/DNA complexes and made in various NaCl solution (i.e. S1 = 0.008; S2 = 0.04; S3=0.08; S4=0.12 M NaCl). (a) mean apparent hydrodynamic size, (b) polydispersity index (PDI) of mean apparent hydrodynamic size. VwLPDs: LPD prepared in NaCl solutions and its parent vesicles in water. VsLPDs: both LPD and its parent vesicles prepared in NaCl solutions. All samples prepared at a lipid:peptide:DNA charge ratio of 0.5:6:1 (0.01 mg/mL pDNA). Vesicle suspension (V) composed of DOTMA/DOPE at 1:1 molar ratio (1.0 mg/mL DOTMA). Error bars are the SD of three measurements of a single formulation (n = 3) at 25 ± 0.1°C.

Regarding the size stability, the LPDs prepared in both fully and partly NaCl solutions (VsLPDs and VwLPDs) were relatively stable in five days. However, the particle size of the LPDs was noticeably increased over eight days, in particular those prepared fully in NaCl solutions with high NaCl concentrations (i.e. 0.08 and 0.12 M). The increased size of the LPDs prepared using 0.08 and 0.12 M NaCl solutions may be due to their relatively low ζ-potential (20 - 25 mV). In comparison, the commercial vehicle Lipofectamine 2000 (L2K) formed L2K/DNA particles with larger size than the VsLPDs prepared using the same NaCl solution. Note that the apparent hydrodynamic size of the L2K/DNA complex prepared in 0.12 M NaCl increased to ~3200 nm within 1 day, despite the complex exhibiting a higher ζ-potential than the corresponding LPDs.

Figure 3.21(b) displays the polydispersity indexes (PDI) of the apparent hydrodynamic sizes of the LPDs over time. The PDI of both the LPDs prepared fully and partially in NaCl solutions (VsLPDs and VwLPDs) remained stable in 5 days, although increased on day 8 for the LPDs prepared in 0.08 and 0.12 M NaCl solutions. As well, the vesicles from which the LPDs were prepared had a rising PDI, especially those prepared in 0.12 M NaCl solution. Furthermore, the PDI of the L2K/DNA particles was much higher and increased more quickly than those of the corresponding LPDs.

A size stability study of the various VsLPDs prepared in 0.12 M NaCl solution is shown in Figure 3.22. Consistent with the results shown in Figure 3.19(a), the LPDs containing the various peptides showed a narrow size distribution at ~180 nm as shown in Figure 3.22(a). The PDI of the LPDs was again in the range 0.15 - 0.20, suggesting that the LPDs were fairly monodisperse as described in Figure 3.22(b). Promisingly, the LPDs containing the various peptides all remained stable with respect to the apparent hydrodynamic size and the PDI, for periods of up to 20 days, longer than was seen with the LPDs prepared in water (Figure 3.18(b)).

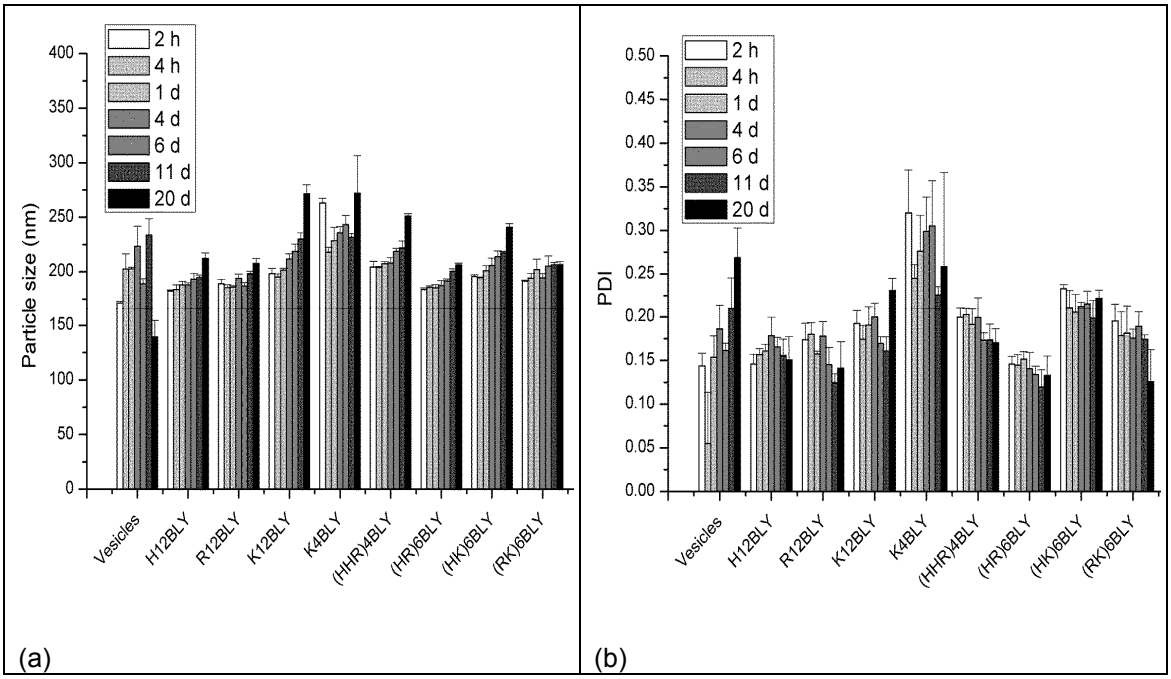

Figure 3.22 Mean hydrodynamic particle size stability of LPDs made in 0.12 M NaCl solution (VsLPDs). All samples prepared at a lipid:peptide:DNA charge ratio of 0.5:6:1 (final DNA concentration of 0.01 mg/mL). Vesicle suspension composed of DOTMA/DOPE at 1:1 molar ratio. (a) mean apparent hydrodynamic size, (b) polydispersity index (PDI) of mean apparent hydrodanamic size. Error bars are SD of three measurements of a single formulation (n = 3) at 25 ± 0.1°C.

3.1.5 Small angle neutron scattering

The self-assembly structure of the LPDs was investigated using small angle neutron scattering (SANS). The structure information of DOTMA:DOPE vesicles from which the LPDs were prepared was also investigated. The SANS data of the preparations, the neutron scattering intensity (I) as a function of momentum transfer, *Q*, was plotted against *Q*. In the present model of the single lipid bilayer sheets and stacks, the space between sheet repeats (*d*-spacing) is the sum of the thickness of the vesicle's lipid bilayer (*L*) and that of the aqueous layer (d_w) as illustrated in Figure 3.3 (page 80).

3.1.5.1 Lipopolyplexes prepared in D_2O

Figure 3.23 and 3.24 exhibits the SANS data for the LPDs containing peptides, R12BLY, K12BLY, (HHR)4BLY and (HK)6BLY prepared in D_2O (at 0.5:6:1 and 0.5:12:1 lipid:peptide:DNA charge ratios, respectively). The scattering patterns recorded for the LPDs are very similar to one another and to the parent vesicles. The modelling of their SANS data was performed

assuming the presence of single sheets. The fitted parameters including bilayer thickness are given in Table 3.2.

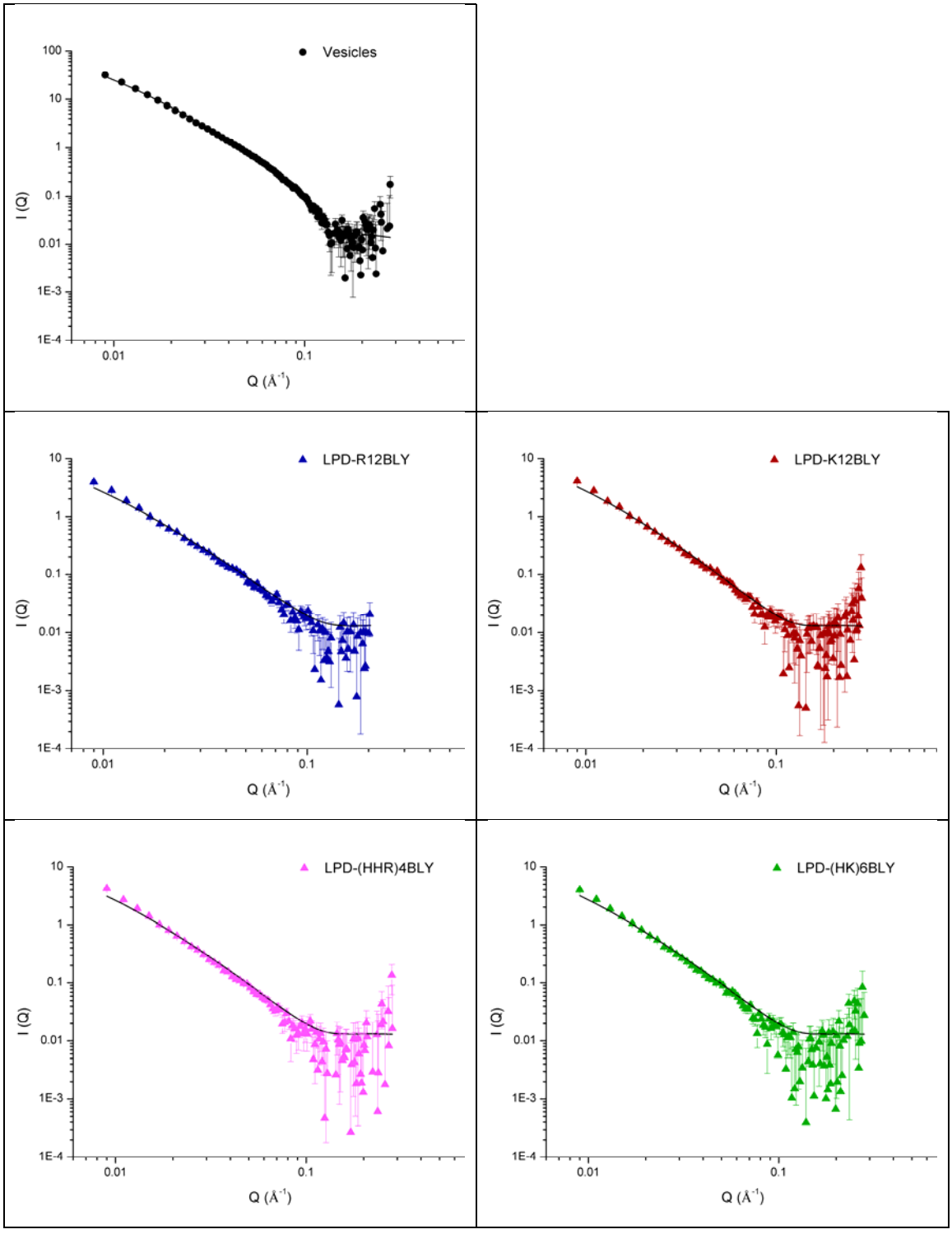

Figure 3.23 Small angle neutron scattering (SANS) data (dots) for vesicles and the LPD containing various peptides and prepared at 0.5:6:1 lipid:peptide:DNA charge ratio and the best fit (solid line) to the data. All the LPDs prepared in D_2O (0.1 mg/mL ctDNA). Vesicles used to prepare the LPDs composed of DOTMA:DOPE at 1:1 molar ratio (1.0 mg/mL DOTMA) and were aged for ~48 h. SANS was measured at 25 ± 0.1°C on LoQ at ISIS.

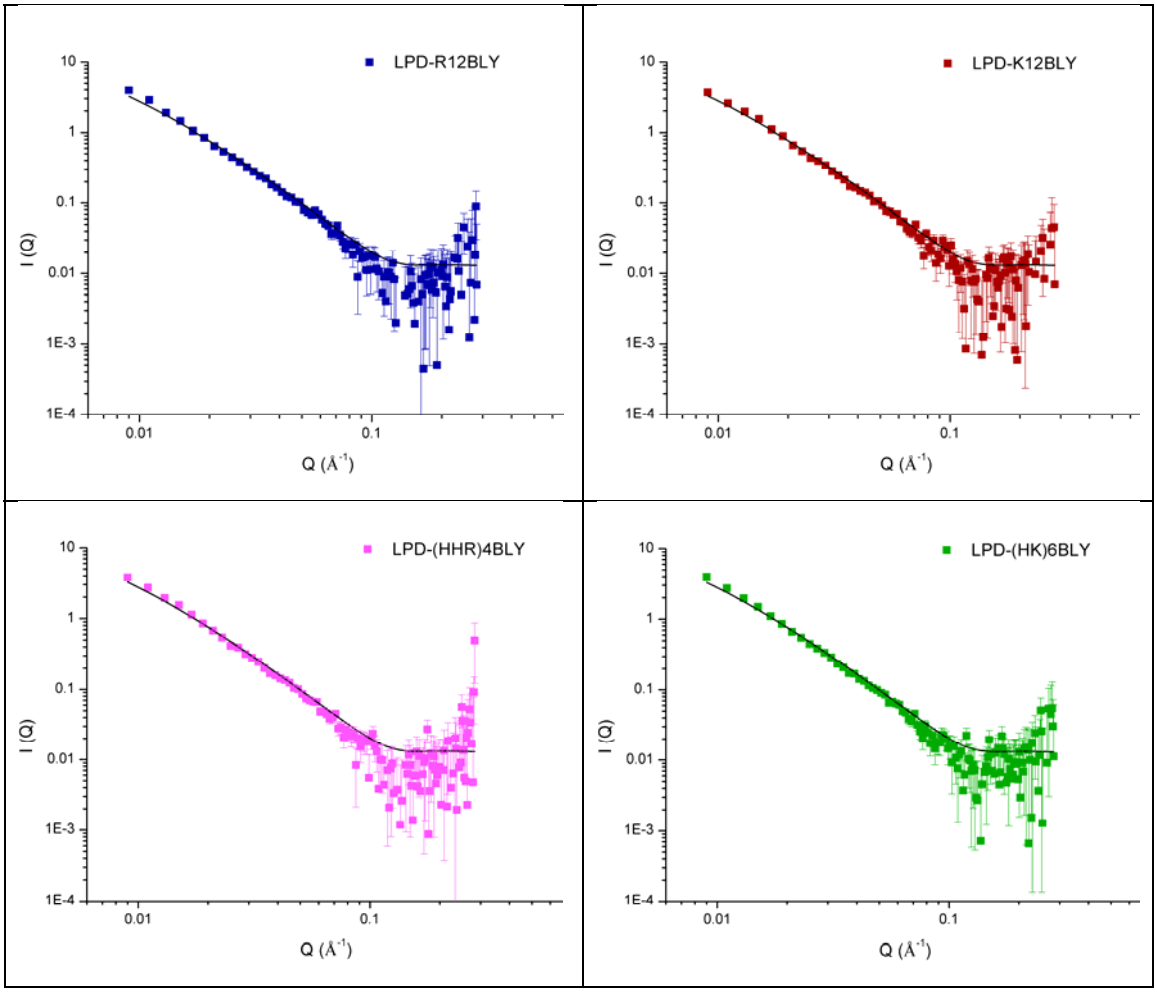

Figure 3.24 Small angle neutron scattering (SANS) data (dots) for vesicles and the LPD containing various peptides and prepared at 0.5:12:1 lipid:peptide:DNA charge ratio and the best fit (solid line) to the data. All the LPDs prepared in D_2O (0.1 mg/mL ctDNA). Vesicles used to prepare the LPDs composed of DOTMA:DOPE at 1:1 molar ratio (1.0 mg/mL DOTMA) and were aged for ~48 h. SANS was measured at 25 ± 0.1°C on LoQ at ISIS.

Unexpectedly, there was no difference in the bilayer thickness/structure for the LPDs containing various peptides at the same charge ratio and between charge ratios. This result suggests that the LPDs have the same bilayer structure as the vesicles.

Table 3.2 Structural parameters obtained for the vesicles, LPDs containing the peptide R12BLY, K12BLY, (HHR)4BLY, and (HK)6BLY derived from FISH modelling of their SANS data. LPDs was prepared at a DNA concentration of 0.1 mg/mL and a lipid:peptide:DNA charge ratio of 0.5:6:1 and 0.5:12:1. Vesicles used to prepare the LPDs composed of DOTMA:DOPE at 1:1 molar ratio (1.0 mg/mL DOTMA) and were aged for ~48 h. SANS was measured at 25 ± 0.1°C on SANS2D.

Samples and mixing ratio	*L* (Å)	No. of layers	*d*-spacing (Å)	R_{sigma} (Å)	Ratio of stack: sheet	SWSE
Vesicles	39.7 (±0.9)	2	60.0 (±7.6)	300	0.058	727
LPD-R12BLY (0.5:6:1)	39.7 (±2.5)	2	-	300	-	492
LPD-K12BLY (0.5:6:1)	39.7 (±1.8)	2	-	300	-	334
LPD-(HHR)4BLY (0.5:6:1)	39.7 (±2.5)	2	-	300	-	436
LPD-(HK)6BLY (0.5:6:1)	39.7 (±2.2)	2	-	300	-	492
LPD-R12BLY (0.5:12:1)	39.7 (±2.0)	2	-	300	-	347
LPD-K12BLY (0.5:12:1)	39.7 (±1.7)	2	-	300	-	286
LPD-(HHR)4BLY (0.5:12:1)	39.7 (±2.0)	2	-	300	-	387
LPD-(HK)6BLY (0.5:12:1)	39.7 (±1.8)	2	-	300	-	382

Figures in brackets indicate the standard errors on the fitted parameter values. Ratio of stack to sheet represents the ratio of multilamellar surface area to unilamellar surface area. SWSE is sum of weighted square error.

3.1.5.2 Lipopolyplexes prepared D_2O and diluted in Optimem or Media

In order to clarify the effect of transfection solvents on self-assembly structure, the LPDs containing (HHR)4BLY and prepared in D_2O is 1:1 (v/v) diluted either in Optimem or Media containing 10% v/v FBS. The SANS data of the LPD dilutions is shown in Figure 3.25. The fitting of the LPD dilutions assuming the presence of single sheets is given in Table 3.3. There was no difference in the scattering pattern for the LPDs diluted either in Optimem or Media, revealing the same internal structure. Interestingly, the intensity of the LPD dilutions was only 0.07-fold of that of the original LPDs. It suggests that the LPDs precipitate when diluted in Optimem or Media. The LPDs precipitation may be resulted from absorption of serum protein present in Optimem or Media, which requires further investigation. In addition, the *d*-spacing of the LPD dilutions had a much higher error than that of the original, revealing a significant change on the structure upon contact with Optimem or Media.

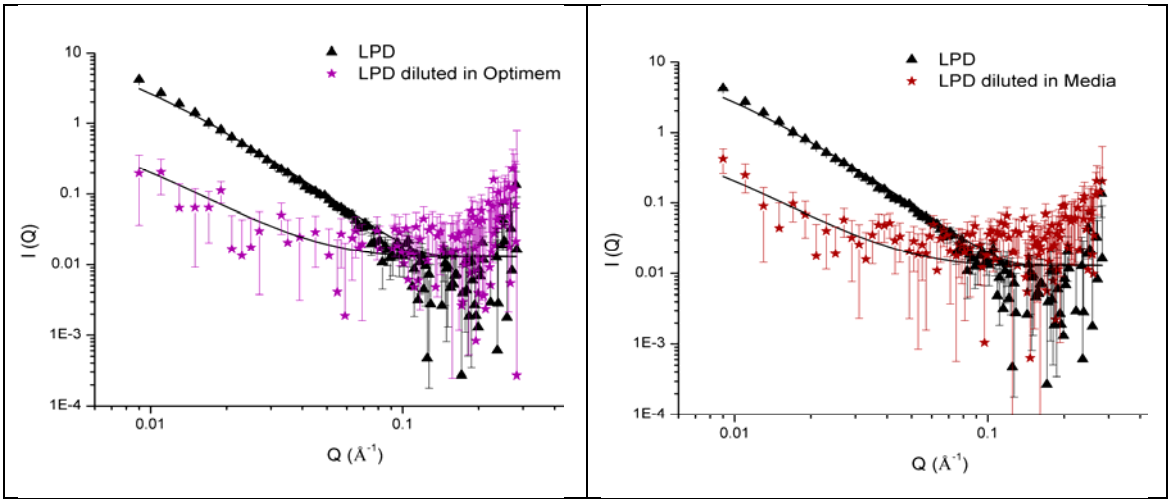

Figure 3.25 Small neutron scattering data (dots) and the best fit (solid line) to the data obtained for LPDs prepared using (HHR)4BLY in D2O and 1:1 diluted in Optimem and Media containing 10% FBS. The LPDs were made at lipid:peptide:DNA charge ratio of 0.5:6:1 (0.1 mg/mL ctDNA). Vesicles composed of DOTMA:DOPE at 1:1 molar ratio (1.0 mg/mL DOTMA) and were aged for ~48 h. SANS measured at 25 ± 0.1°C on LoQ.

Table 3.3 Structural parameters obtained from FISH modelling of the SANS data for LPDs containing (HHR)4BLY in D2O and 1:1 diluted in Optimem and Media containing 10% FBS. LPDs were made at lipid:peptide:DNA charge ratio of 0.5:6:1 (0.1 mg/mL ctDNA). Vesicles composed of DOTMA:DOPE at 1:1 molar ratio (1.0 mg/mL DOTMA) and were aged for ~48 h. SANS was measured at 25 ± 0.1°C on LoQ.

Samples	***L* (Å)**	**No. of layers**	***d*-spacing (Å)**	**R $_{sigma}$ (Å)**	**Ratio of stack:sheet**	**Ratio of (I)**	**SWSE**
LPD	39.7 (±5.4)	2	60.0 (±45.4)	300	0.047	-	346
LPD diluted in Optimem	39.7 (±37.5)	-	-	300	-	0.07	52
LPD diluted in Media	39.7 (±39.5)	-	-	300	-	0.07	109

Figures in brackets indicate the standard errors on the fitted parameter values. Ratio of stack to sheet represents the ratio of multilamellar surface area to unilamellar surface area. Ratio of (I) reveals the ratio of diluted LPD's scattering intensity to the original LPD's scattering intensity. SWSE is sum of weighted square error.

3.1.5.3 Lipopolyplexes prepared in various strength NaCl solutions

The SANS data obtained for the (HHR)4BLY-containing LPDs prepared in the various NaCl solutions and the parent are shown in Figure 3.26, together with the best fits obtained for the data using mixed lipid bilayer sheet and stack model. The SANS data for the parent vesicles are shown in Figure 3.26(a), upper left, and the corresponding LPDs, upper left, are shown in Figure 3.26(b), and the parameters used to obtain the best fit in Table 3.3. For the vesicles, a

bilayer thickness and *d*-spacing of 39.4 ±1.1 Å and 60.0 ±8.2 Å, respectively were obtained. These values are reassuringly consistent with the values of 39.7 ±0.9 Å and 60.0 ±7.6 Å obtained from an earlier experiment (see Table 3.1). The above results suggest that the vesicles prepared for different experiments were highly reproducible.

For the vesicles prepared using 0.04, 0.08, 0.12 M aqueous NaCl solutions, the SANS curves (with the exception of the low Q region) overlapped the data obtained for the vesicles prepared in D_2O. The high similarity suggests that the vesicles prepared in various NaCl solutions have the same bilayer thickness as those prepared in D_2O, as evidenced by the modelling of the SANS data. For instance, the vesicles prepared in D_2O had a bilayer thickness of 39.7 ±1.1 Å while the vesicles prepared using 0.04, 0.08, 0.12 M NaCl solution were 39.7 ±2.5 Å, 39.7 ±4.5 Å, 39.7 ±6.3 Å, respectively, as shown in Appendix II Table 1. The parameters used to fit the SANS data obtained for the LPDs prepared in D_2O using mixed lipid bilayer sheet and stack model are shown in Table 3.3. The bilayer thickness of the LPD prepared in D_2O was 39.4 ±4.8 Å and 39.4 ±6.4 Å, respectively, which is very similar to those obtained for the parent vesicles (39.7 ±1.1 Å and 40.2 ±0.8 Å).

As mentioned above, the low Q portion of the SANS curves of the vesicles prepared in 0.04, 0.08, 0.12 M NaCl solutions are different from those of the vesicles prepared in D_2O and was possibly a consequence of the Porod scattering due to the presence of vesicles of large size. This also means that there are probably two populations of particles present in the vesicle suspensions prepared using the various NaCl solutions.

Figure 3.26(a), lower left, shows the SANS profiles of the vesicles produced from bath sonication. Interestingly these SANS curves did not show significant difference from those prepared using probe sonication - despite the fact that the sizes obtained for the vesicles using dynamic light scattering did (the size of the probe-sonicated vesicles in 0.15 M NaCl solution was larger than that of the bath-sonicated (sonication time ≥ 5 min), as depicted in Appendix II Figure 6). The above results indicate that the greater in-put in energy due to the probe sonication did not cause a difference in the bilayer thickness of the vesicles. Figure 3.26(a), lower right, shows the SANS curves of the vesicles prepared from bath sonication and aged for 48 h before measurement using SANS. The vesicle aging was investigated because it may

affect the physicochemical properties of the LPDs and therefore their transfection efficiency. The SANS of the vesicles was measured right away after their preparation. It was also compared with that of the vesicles aged for 48 h. As can be seen, there was a big difference observed for the vesicles prepared in the aqueous NaCl solution over time, this was particularly noticeable in NaCl solution with higher ionic strength and is possibly due to the growth in the size of the vesicles as shown in Figure 3.21.

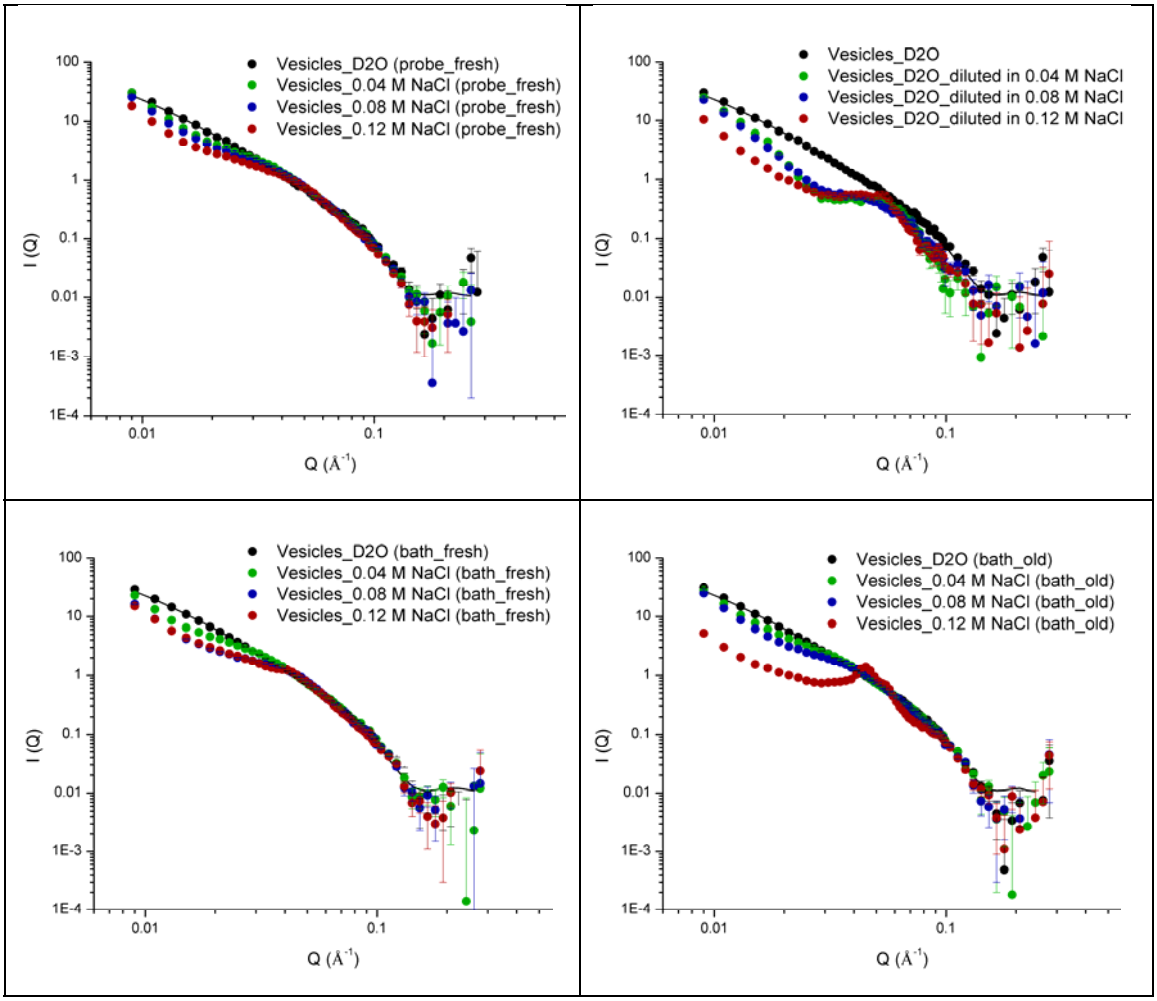

(a)

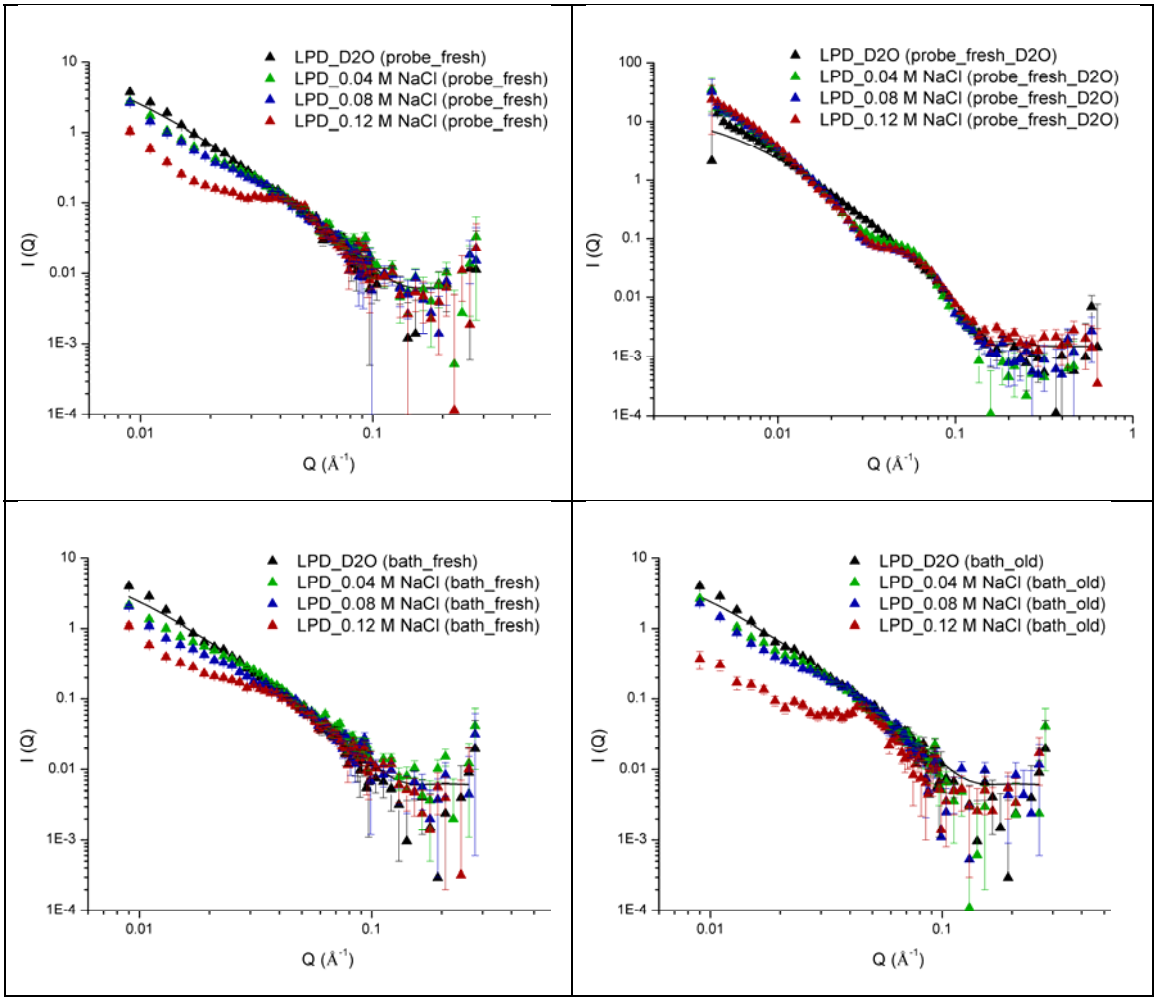

(b)

Figure 3.26 Small neutron scattering data obtained for (a) DOTMA:DOPE vesicles (1:1 molar ratio) prepared in various strengths of aqueous NaCl solution at 1 mg/mL of DOTMA. The vesicles were prepared using probe sonication (upper left panel), probe sonication and diluted with various strengths of NaCl solution (upper right panel), bath sonication (lower left panel), and bath sonication and aged for 48 h (lower right panel) and (b) LPDs prepared using (HHR)4BLY in various strength NaCl solutions using vesicles from (a). The LPDs were made at lipid:peptide:DNA charge ratio of 0.5:6:1 (0.1 mg/mL ctDNA). SANS measured at 25 ± 0.1°C on LoQ.

Table 3.4 Structural parameters obtained from FISH modelling of the SANS data for LPDs containing (HHR)4BLY and prepared in D_2O and their parent vesicles. LPDs were made at lipid:peptide:DNA charge ratio of 0.5:6:1 (0.1 mg/mL ctDNA). Vesicles composed of DOTMA:DOPE at 1:1 molar ratio (1.0 mg/mL DOTMA). SANS was measured at 25 ± 0.1°C on LoQ and SANS2D.

Samples_D_2O	*L* (Å)	No. of layers	*d*-spacing (Å)	R_{sigma} (Å)	Ratio of stack:sheet	SWSE
Vesicles_probe_fresh	39.7 (±1.1)	2.0	60.0 (±8.1)	300	0.068	183
Vesicles_probe_old	39.4 (±1.1)	2.0	60.0 (±8.2)	300	0.068	650
Vesicles_bath_fresh	40.2 (±0.8)	2.0	60.0 (±7.8)	300	0.052	323
Vesicles_bath_old	39.3 (±1.1)	2.0	60.0 (±9.1)	300	0.057	560
LPD (probe_fresh)-1	39.4 (±4.8)	2.0	-	300	-	189
LPD (probe_fresh)-2	39.0 (±3.3)	2.0	-	300	-	1777
LPD (bath_fresh)	39.4 (±6.4)	2.0	-	300	-	322

Figures in brackets indicate the standard errors on the fitted parameter values. SWSE is sum of weighted square error. Ratio of stack to sheet represents the ratio of multilamellar surface area to unilamellar surface area.

The SANS data obtained for the LPDs prepared from the above vesicles is given in Figure 3.26(b). Interestingly, the shape of the SANS curves of the LPDs prepared in various NaCl solutions were generally close to those obtained for their parent vesicles (Figure 3.26(a)). This observation suggests that the internal structure of the LPDs is closely related to those of the parent vesicles. The parameters used to fit the SANS data obtained for the LPDs prepared in D_2O using mixed lipid bilayer sheet and stack model are shown in Table 3.3. The bilayer thickness of the LPD prepared in D_2O was 39.4 ±4.8 Å and 39.4 ±6.4 Å, respectively, similar to that obtained for the parent vesicles (39.7 ±1.1 Å and 40.2 ±0.8 Å). The above results reveal that the presence of DNA does not influence the structure of the bilayers. Similarly, the *d*-spacing of the LPDs were 60.0 ±29.0 Å and 60.0 ±34.7 Å, respectively, the same as those of their parent vesicles (60.0±8.1 Å and 60.0 ±7.8 Å). This observation is in line with the hypothesis that the structure of the LPDs is related to those of the parent vesicles. It reveals that the water layer between the lipid bilayers is sufficient to accommodate DNA molecules without any re-arrangement. Furthermore, the observation is consistent with the results of the earlier study shown in Table 3.1 and suggests that the LPDs prepared from different experiments are reproducible. It is notable that the LPDs had stronger SANS scattering at the

first 3 points in the low Q region than their parent vesicles, which is probably a consequence of the scattering due to the presence of particles of large size.

3.1.6 Small angle neutron scattering with stopped flow mode

In an attempt to probe the formation of the lipopolyplexes (LPDs) and lipoplexes (LDs), a stopped flow small angle neutron scattering (SANS) experiment was performed. Figure 3.27(a) shows the SANS curve obtained for the LPDs containing peptide K16 (0.5:6:1 lipid:peptide:DNA charge ratio) using the usual 'static' measurement and the kinetic measurements at equilibration. For comparison, the scattering curve for the parent DOTMA:DOPE vesicles is also included (scaled to the lipid concentration contained in the LPDs). It is of note that the SANS curves obtained for the vesicles and the LPDs using the static method were virtually identical except for the background levels, which is probably a result of the scaling of the SANS data. When comparing the SANS data obtained for the LPDs prepared using the two different methods, although the LPDs were overlapped well in the intermediate Q range of $0.01 < Q < 0.05$ $Å^{-1}$, they did not overlap at high and low Q. The origin of the high background for the SANS curve obtained using stopped flow is believed to be due to the gas detectors fitted at the time of the stopped flow experiments. The origin of the deviation at low Q is still not known. The data does, however, suggest that at long time courses the various LPDs possessed the same structure.

Figure 3.27(b) depicts the evolution of the SANS curves for the LPDs using stopped flow measured every 60 sec for a total of 10 minutes. As can be seen, the neutron scattering does not show any change over this time period, suggesting that any structural change probably occur more quickly than 60 seconds. The faster evolution (every 10 sec for a total of 1 minute) of the SANS curve for the LPDs is shown in Figure 3.27(c). No change was observed over this time period, suggesting that any structural change maybe occurs more quickly than 10 seconds.

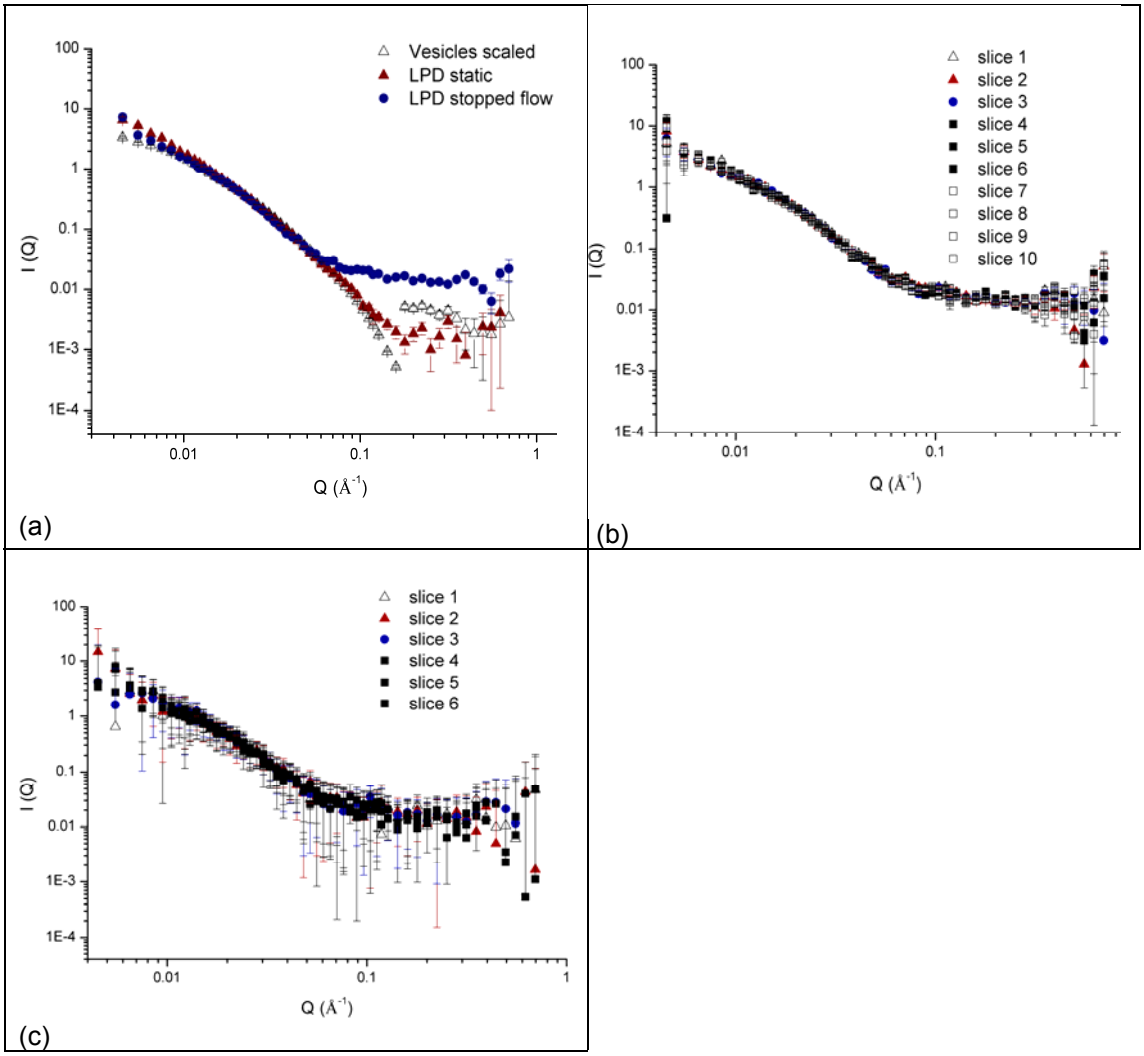

Figure 3.27 Small neutron scattering data for LPDs prepared using K16 in D_2O. (a) static; (b) kinetic measurements (time-sliced every 60 seconds for 600 seconds, n = 14): slice 1 = 0-60 seconds; slice 2 = 61-120 seconds; slice 3 = 121-180 seconds; slice 4 = 181-240 seconds; slice 5 = 241-300 seconds; slice 6 = 301-360 seconds; slice 7 = 361-420; slice 8 = 421-480 seconds; slice 9 = 481-540 seconds; slice 10 = 541-600 seconds; (c) kinetic measurements (time-sliced every 10 seconds for 60 seconds, n = 14): slice 1 = 0-10 seconds; slice 2 = 11-20 seconds; slice 3 = 21-30 seconds; slice 4 = 31-40 seconds; slice 5 = 41-50 seconds; slice 6 = 51-60 seconds. LPDs were made at lipid:peptide:DNA charge ratio of 0.5:6:1 (0.1 mg/mL ctDNA). Vesicles composed of DOTMA:DOPE at 1:1 molar ratio (1 mg/mL DOTMA) and were aged for ~48 h. SANS measured at 25 ± 0.1°C on SANS2D.

Figure 3.28(a) shows the SANS curves obtained for the parent vesicles, the LDs measured using the usual 'static' methodology and by stopped flow at equilibration. While the SANS curve obtained using the normal static method exhibits a distinct Bragg peak, the corresponding data obtained from the stopped flow methodology did not. The SANS curve obtained for the LD is clearly the same to that seen for the parent vesicles while its intensity is 2-fold that of the parent vesicles. As the mixing volume ratio is 1:1, it suggests that the parent vesicle suspension was not mixed with DNA solution and therefore only vesicles were 'seen' by neutrons.

Figure 3.28(b) depicts the evolution of the SANS curves for the LDs obtained using stopped flow measured every 60 sec for a total of 10 minutes. As can be seen, the neutron scattering does not change over this time period, suggesting that any structural change must occur more quickly than 60 seconds. The 10 sec evolution for a total of 1 minute of the SNAS curve for the LPDs is displayed in Figure 3.28(c). There is no change observed over this time period, suggesting that any structural change occurs more quickly than 10 seconds.

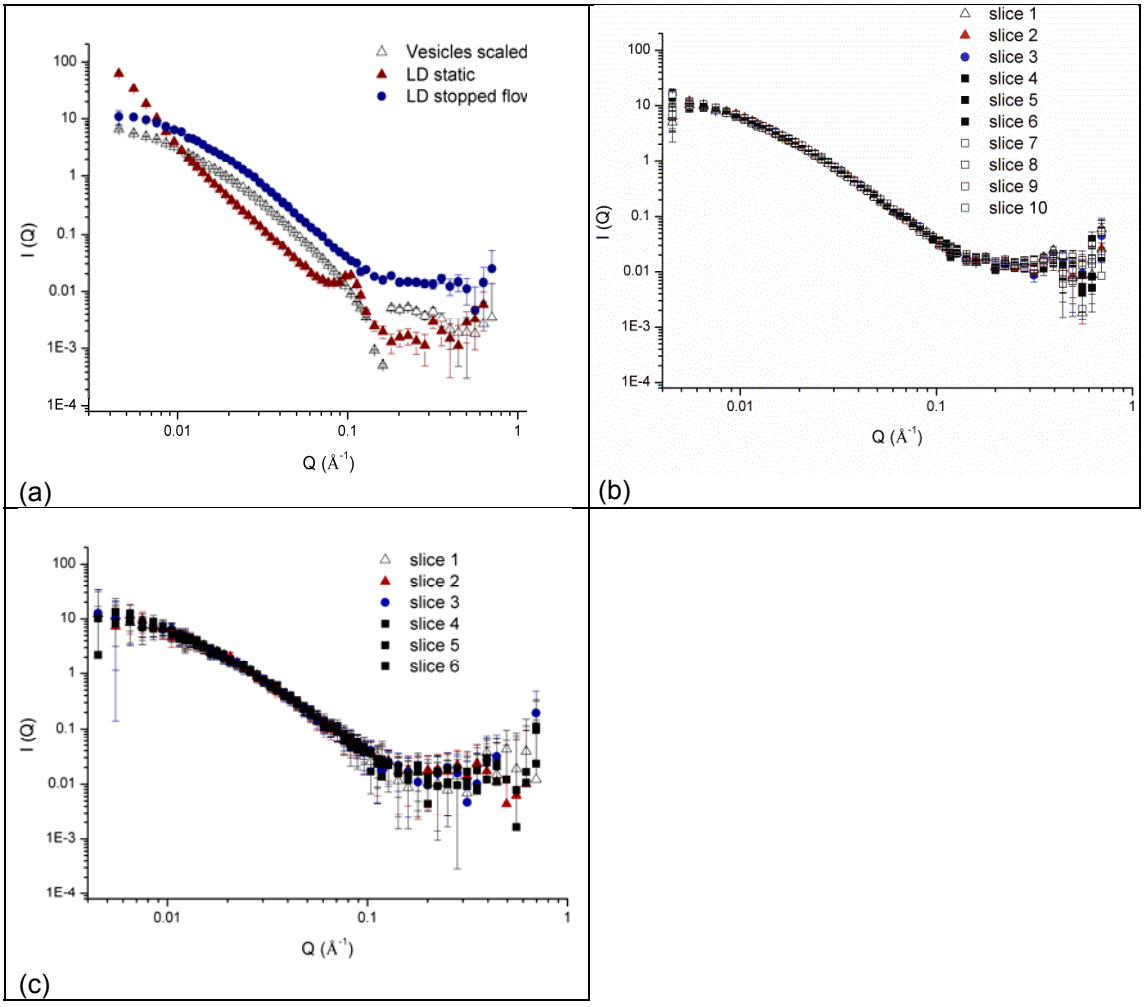

Figure 3.28 Small neutron scattering data for LDs prepared in D_2O. (a) static; (b) kinetic measurements (time-sliced every 60 seconds for 600 seconds, n = 14): slice 1 = 0-60 seconds; slice 2 = 61-120 seconds; slice 3 = 121-180 seconds; slice 4 = 181-240 seconds; slice 5 = 241-300 seconds; slice 6 = 301-360 seconds; slice 7 = 361-420; slice 8 = 421-480 seconds; slice 9 = 481-540 seconds; slice 10 = 541-600 seconds; (c) kinetic measurements (time-sliced every 10 seconds for 60 seconds, n = 14): slice 1 = 0-10 seconds; slice 2 = 11-20 seconds; slice 3 = 21-30 seconds; slice 4 = 31-40 seconds; slice 5 = 41-50 seconds; slice 6 = 51-60 seconds. LDs were made at lipid:DNA charge ratio of 2:1 (0.05 mg/mL ctDNA). Vesicles composed of DOTMA:DOPE at 1:1 molar ratio (1 mg/mL DOTMA) and were aged ~48 h. SANS measured at 25 ± 0.1°C on SANS2D.

3.2 Discussion

The bottle neck in the exploitation of gene therapy is the successful delivery of DNA to the nucleus of the target cells. The present study aim is to deliver DNA using a combination of cationic lipids and cationic peptides to form a complex known as a lipopolyplex (LPD). The ability of LPDs to deliver DNA has been assessed by measuring the level of luciferease transfection achieved *in vitro*. Significantly, the LPDs were shown to possess a far superior transfection efficiency *in vitro* when compared to their lipoplexes (LDs) and polyplexes (PDs) counterparts (Figure 3.1), suggesting that the presence of both lipid and peptide in a delivery system has a synergistic effect on the delivery of DNA. Furthermore, the synergistic effect of the combination of lipid and peptide on luciferase transfection was found to be correlated with the structure of the complexes regarding the protection it provided (Figure 3.2 and 3.4). Explaining the superiority of the LPDs over LDs and PDs form the point view of their structures has not been previously reported by others. The other factors that could contribute to the synergistic effect achieved using the LPDs could include their small size, their high ability to condense and therefore protect DNA, while at the same time being able to release from the complex (Gao et al, 1996).

Small angle neutron scattering (SANS) studies revealed the presence of a predominately single lipid bilayer in the LPDs while the LD counterparts possess a multilamellar structure and the PDs no structure (Figure 3.2 and 3.4). The LPDs were therefore proposed to contain a central core of DNA surrounded by a lipid bilayer. This proposed structure is in line with that suggested by Mustapa et al. (Mustapa et al, 2007) using fluorescence quenching studies of the LPDs containing DOTMA:DOPE 1:1 lipids and K16 targeting peptide (K16-GACRRETAWACG targeting to α5β1 Integrin receptors). These workers concluded that the lysine-rich portion of the K16 targeting peptide interacts with DNA, resulting in a tightly bound inner core of DNA and peptide. This inner core is surrounded by the lipid bilayer, from which the targeting portion of the peptides partially protruded, allowing it to interact with its target receptors. This core-shell structure is expected to afford the entrapped DNA protection against enzyme degradation. Indeed this DNA protection, presumably due to encapsulation inside the LPDs has been observed in agarose gel electrophoresis studies (Figure 3.10(b)), supporting the hypothesis that protection of DNA from enzymatic degradation leads to enhanced transfection.

In the present study, the preparation protocol has been found to be important in determining the ability of the LPD to transfect cells in vitro. For example, LPDs prepared by first mixing DNA solution and liposome suspension and then adding peptide solution (Protocols 2 and 5) were shown to exhibit much inferior transfection levels compared to the other protocols used (Figure 3.1). Small angle neutron scattering (SANS) studies of the structure of the LPDs has shown that the LPDs prepared using Protocols 2 and 5 possess a comparable structure to their multilamellar LD counterparts (Figure 3.2 and 3.4), no doubt accounting for their poor luciferase transfection. The structure of LPDs prepared by different protocols has not been previously reported before, though the multilamellar structure of the LDs has been reported in other studies (Kudsiova et al, 2011a and 2011b).

In view of the synergistic effect of combining peptides and lipids in the same DNA delivery system, the present study has focused on the preparation of LPDs. All the LPDs were prepared using Protocol 1 as this method (along with Protocols 3, 4, 6) gave the highest level of transfection and is the method used by other researchers in the field (Gao et al, 1996, Yu et al, 2004, Yan et al, 2012). The novelty of the current research is, in part, in the bifunctional peptides used to formulate LPDs.

The bifunctional peptides used in the current research contain a branched condensing portion and a cyclic targeting portion, connected via a degradable linker (Figure 2.1). The novelty of these peptides is a combination in a single molecule of regions that can condense DNA as well as being biodegradable and possessing a targeting moiety. To be specific, the branched condensing portion of the bifunctional peptides confers effective DNA condensation (Figure 3.10b), showing advantage over linear peptides used for DNA delivery (Chen et al, 2001). These peptides have been designed to have longer branches composing of either single or a mixture of amino acid residues than used previously (Welser et al, 2013). Moreover, the condensation branches are protonable in endosomes (due to the presence histidine residues) which has been shown to increase endosomal escape and therefore DNA transfection (Ou et al, 2009). The degradability of the peptides can also reduce the cytotoxicity of the formulation (Kim et al, 2009).

It is reassuring that the LPDs containing Series II peptides are superior in terms of transfection efficiency over those containing Series I (Figure 3.5) as the Series II peptides were specifically

designed to possess histidine residues on portion of the peptides intended to condense the DNA. Histidine is well-known for exerting a 'proton sponge' effect via the imidazole rings present and which can result in the destabilisation of endosomes (Benns et al, 2000, Putnam et al, 2001). The importance of the 'proton sponge' effect of histidine on endosomal escape and therefore DNA transfection has been seen in other studies. For example bafilomycin A1 is a specific inhibitor of vacuolar ATPase proton pump, which inhibits the protonation of histidine vector inside endosomes and thus prevents the endosomal escape of DNA payload. It has been shown that the transfection of a histidylated polylysine/DNA complex was drastically inhibited in the presence of bafilomycin A1 (Midoux et al, 1999). The contribution of the 'proton sponge' effect of histidine to endosomal escape and DNA transfection has also been reported for a histidylated polyarginine/DNA complex (Mann et al, 2014) while DNA transfection has been found to be proportional to the imidazole content of the imidazole conjugated polylysine (Putnam et al, 2001).

Besides transfection, the physicochemical properties of the LPDs prepared using the two series of peptides have been evaluated. It was clear from gel electrophoresis studies that the LPDs are effective at condensing, protecting and releasing the DNA they encapsulate. Picogreen fluorescence assay, however revealed a weaker condensation of DNA when using the LPDs containing Series II peptides. This result is consistent with the presence of histidine residues in the Series II peptides, which as a consequence of being weak bases would be expected to possess little ability to condense DNA. The dynamic light scattering and zeta-potential measurements revealed that the LPDs prepared in water were highly positively charged, small particles that exhibited a good stability over time (Figure 3.17 and 3.18). Interestingly, the LPDs containing Series II peptides appeared to be larger in size than those containing Series I peptides, which might be a consequence of the histidine residues in Series II peptides. In contrast to arginine and lysine, histidine is a weak base with a pka of ~6 (the pka of arginine and lysine are ~12 and 10, respectively). Therefore, the histidine-containing peptides in Series II possess a weaker binding ability than other peptides. The weaker binding of Series II peptides is also observed in the gel electrophoresis studies (Figure 3.10(a)).

One of the most exciting findings in the current study is that the LPDs prepared in 0.12 M aqueous NaCl solution demonstrated effective luciferase transfection in the presence of serum

(Figure 3.7(b)). This result is significant as to our knowledge the beneficial effect of NaCl on DNA transfection mediated by lipopolyplexes has not been previously reported.

It should be noted that serum contains DNA-degrading enzymes and therefore DNA needs to be protected to ensure effective transfection (Turek et al, 2000). Moreover, serum possesses a lot of proteins, the most abundant of which is albumin, which are characterised by a high content of charged amino acid residues. Gessner et al. have shown that positively charged particles predominantly adsorb negative albumin due to favourable electrostatic interactions [15, 16]. Therefore, the positively-charged LPDs in the present studies upon exposure to serum are expected to become covered by negatively charged albumin, leading to a charge neutralisation of the LPD.

It was clear from gel electrophoresis studies examining DNA protection by the LPDs that the LPDs prepared in 0.12 M aqueous NaCl solutions offered more effective DNA protection against DNAse I (Figure 3.11). Therefore, the effective protection afforded by the LPDs prepared in 0.12 M NaCl solutions could be related with its effective transfection. Interestingly, LPDs prepared in 0.12 M aqueous NaCl solution exhibit a weaker condensation of DNA as assessed by picogreen fluorescence assay. It might be anticipated that the weakly condensed DNA associated with the LPDs will be more readily released from the complex. Indeed, a study on the DNA condensation by cationic liposomes (DOTAP/DOPE and DOTAP/cholesterol) in the presence of NaCl has shown that 1.5 M NaCl, but not 0.15 M NaCl, prevented lipoplex formation and/or induced partial dissociation DNA from the complex (Even-Chen et al, 2012). The same study also found that the higher the salt concentration, DNA complexed in lipoplexes is more likely to behave like a free DNA as monitored by ethidium bromide intercalation. Overall, our study has shown that, although DNA condensation is important, it is important that a balance is obtained between DNA condensation (and the ability to protect DNA from degradation) and its release.

In view of the effective luciferase transfection observed using LPDs prepared in 0.12 M aqueous NaCl solutions, the transfection of the LPDs prepared in various strength aqueous NaCl solutions (i.e. 0.008, 0.04, 0.008 M) was subsequently determined (Figure 3.9). In line with the effect seen with the 0.12 M NaCl concentration result, luciferase transfection increased as the NaCl concentration increased, revealing a beneficial effect of salt. Indeed, the salt was also seen to increase the protection afforded to LPDs containing the (HHR)4BLY, with increasing

protection observed with increasing salt concentration (Figure 3.12). Once again a correlation seems between DNA protection and transfection efficiency. The protection afforded by the LPDs is consistent with our previous studies on the lipopolyplexes incorporating C14 glycerol-based lipids (Kudsiova et al, 2011b).

It is interesting that only when the parent vesicles were prepared in an aqueous NaCl solution were the resultant LPDs effective transfection agents in the presence of serum (VsLPDs > VwLPDs in Figure 3.9).

It is obvious that from dynamic light scattering and zeta-potential measurements that the size of the resultant LPDs increased as the final NaCl concentration of the solvent increased. As is well established, the condensation of DNA in the LPDs is driven by charge-charge interactions between the positively charged peptide/lipids and the negatively charged DNA. In the presence of NaCl, however, these charges can be reduced resulting in a reduction of the charge-charge interaction. As a consequence, therefore, DNA condensation in the LPD complex is reduced and the size of the resultant complex increased. Undoubtedly, the increase in size of the LPDs prepared with increasing strength aqueous NaCl solution is due to the charge-screening effect of NaCl. Indeed it has previously been reported, using an ethidium bromide fluorescence assay, that the binding of DNA with polylysine is inversely correlated with ionic strength up to 0.8 M NaCl (Tang et al, 1997).

Moreover, the increased size of the LPDs is paralleled by an increased transfection suggesting that, in the current study at least, the size of the LPDs can be correlated with the transfection. In the literature, however, the relationship between size of the DNA complex and transfection is variable. For example, in a study on LPDs formed using protamine, an increase in transfection was observed with a reduction in size of the LPDs (Gao et al, 1996). However, other workers have reported that larger lipopolyamine/DNA complex could form large intracellular endocytotic vesicles and these endocytotic vesicles could be more easily destabilized, thus facilitating DNA escape and transfection (Escriou et al, 1998). Unfortunately, while such correlations may be observed, DNA transfection is a complex process and can in fact be affected by many factors, often at the same time. These factors include the size/shape/surface charge/composition of the particles and the cell types/transfection solvents/protocols used for DNA transfection. As a

consequence therefore, any correlation of a single factor with transfection ability may in fact be coincidental.

Interestingly, the PDI of the apparent hydrodynamic size of the parent vesicles and the resultant LPD, both prepared in 0.12 M aqueous NaCl solution, was lower than the corresponding particles prepared in water (Figure 3.20(b)). The results suggest that, as the concentration of NaCl is increased, the formulation of the parent vesicles and the corresponding LPDs become more homogeneous, a property which is beneficial to the formulation of a drug delivery system. Moreover, the size of the LPDs prepared totally in an aqueous NaCl solution (VsLPDs) was larger than those partly prepared in an aqueous NaCl solution (VwLPDs). It is worth noting that the size of the parent vesicles prepared in NaCl solution (used for preparation of the VsLPDs) was also larger than that of the parent vesicles prepared in water (used for preparation of the VwLPDs). The increased size of the parent vesicles prepared in NaCl solutions is most likely a consequence of the charge screening effect. The cationic vesicles are composed of cationic DOTMA molecules and neutral DOPE molecules. There exists therefore charge-charge repulsion between head groups resulting in a lipid bilayer with a high curvature and a relatively small size (Figure 3.20(a)). However, in NaCl solutions, the repulsion between cationic DOTMA molecules is alleviated due to charge screening, leading to a lipid bilayer with a lower curvature and therefore larger size (Figure 3.20(a)). To note, as it has been observed that the size of the LPDs prepared in water was not influenced by the size of their parent vesicles (Kudsiova et al, 2011a), it is not expected that the size of the LPDs prepared in NaCl solution is influenced by that of their parent vesicles as well (Figure 3.20(a) and Figure 3.21(a)).

The concentration of 0.12 M NaCl was selected to be close to isotonic for the human body, 0.15 M NaCl being isotonic. As a consequence of its near isotonicity, the physicochemical properties of the LPDs prepared in 0.12 M aqueous NaCl solution were further investigated. The dynamic light scattering and zeta-potential measurements performed reveal that the LPDs prepared in 0.12 M aqueous NaCl solution were small, positively charged and stable over time (Figure 3.21 and 3.22 respectively). The LPDs containing Series II peptides appeared to be of approximately the same size and zeta-potential as those containing Series I peptides. It is interesting to note that the LPDs prepared in 0.12 M aqueous NaCl solution were larger, but more fairly monodisperse, than those in water when assessed by size and polydispersity. SANS studies

suggested that the LPDs prepared in 0.12 M aqueous NaCl solution were likely to have the same structure as those prepared in water and that there was no difference between the LPDs containing the two Series of peptides.

Overall, it is promising that the LPDs prepared in aqueous NaCl solutions exhibit effective *in vitro* transfection in the presence of serum. In particular, 0.12 M aqueous NaCl solution is close to saline which is commonly used for *in vivo* injection. Therefore, the LPDs prepared in 0.12 M NaCl solution should be further studied *in vivo*.

Chapter 4 Lipopolyplexes containing siRNA

4.1 Results

4.1.1 *In vitro* luciferase gene silencing activity of lipopolyplexes

The biological activity of the LPRs is evaluated by detecting *in vitro* luciferase silencing efficiency. The effect of siRNA amount is studied in the first place. The same as LPDs, the preparation (mixing protocols) and formulation (+/- charge ratio) of the LPRs is evaluated. Moreover, the preparation aqueous solutions for the LPR preparation and the silencing medium for cell incubation have also been thoroughly investigated, in view of the presence of electrolytes and serum in the body.

4.1.1.1 Effect of siRNA amount

Lipopolyplexes (LPRs) prepared using K4BLY and Lipofectamine 2000 (L2K) were selected to determine the effect of the amount of siRNA required to silence the production of luciferase by luciferase-transduced A549 cells. The cationic vesicles used to prepare the lipopolyplexes were composed of DOTMA/DOPE at a 1:1 molar ratio. The K4BLY-containing LPRs were made in OptiMEM (VwLPRo) at a L:P:R charge ratio of 0.5:12:1. The LPRs were diluted 1 to 4 in OptiMEM (VwLPRo/OptiMEM) and incubated with luciferase-transduced A549 cells for 24 h, after which time the cells were incubated in RPMI-1640 media containing 10% v/v FBS for 24 h. This incubation protocol was denoted the 24+24 h.

L2K/siRNA complexes were initially prepared in OptiMEM at a L2K:siRNA weight ratio of 4:1 (as per manufactures instructions) and then diluted a further 1 in 4 with OptiMEM before incubation with cells using the same protocol as described for the LPRs (LPRo/OptiMEM).

As seen in Figure 4.1(a) when naked siRNA was used at concentrations of 50 and 100 nM/well no luciferase gene silencing activity, and hence no knock down, was observed. In contrast when L2K, used as positive control, was examined over a similar concentration range it was clear that siRNA concentrations of 30 nM/well and above resulted in a least 80% knock down. When the LPRs prepared using K4BLY were examined they too exhibited a high level of known down with levels of at least 80% being achieved at siRNA concentrations of 50 and 100 nM/well. Excitingly the levels of knock down achieved with the K4BLY-containing LPRs were comparable to the positive control, L2K.

The corresponding protein assay for the cells treated with the negative control, L2K and the K4BLY-containing LPRs is shown in Figure 4.2(b). It is important to note that the amount of protein present at the end of the experiment is a good indicator of the toxicity of the formulation towards the transfected cells, with lower amounts of protein indicating a higher level of toxicity of the formulation. Encouragingly, the cells exposed to the K4BLY-containing LPR preparations exhibited comparable amounts of protein to the cells exposed to naked siRNA, with the exception of those cells exposed to the highest siRNA concentration of 100 nM/well. Significantly, the cells exposed to the positive control, L2K/siRNA complex exhibited the lowest level of protein, suggesting that this formulation is the most toxic.

Taking both the results of the knock down study and protein assay into account, a concentration of 50 nM/well of siRNA was chosen for all further luciferase gene silencing activity studies.

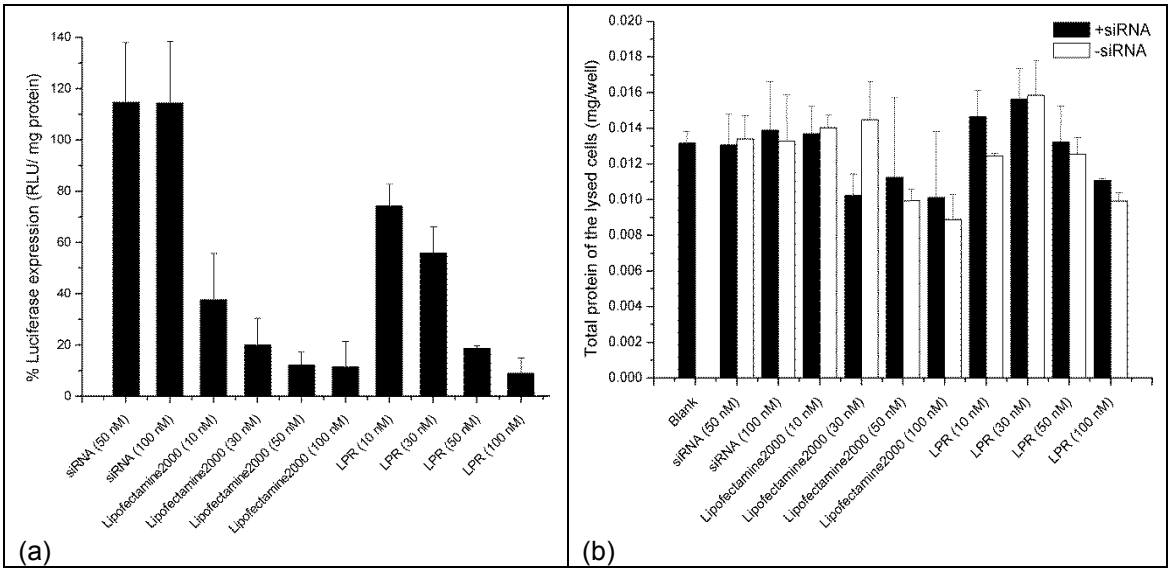

Figure 4.1 Luciferase gene silencing activity of naked siRNA, Lipofectamine 2000 (L2K), and lipopolyplexes (LPRs) containing K4BLY at different concentrations of siRNA, namely 10, 30, 50 and 100 nM/well. (a) Knock down of positive control (+siRNA, capable to express luciferase), L2K, and LPRs containing K4BLY as percentage of the negative control (-siRNA, scrambled and incapable to express luciferase) and (b) corresponding protein assay. LPRs were made fully in OptiMEM (VwLPRo/OptiMEM) at L:P:R charge ratio of 0.5:12:1. L2K-containing LRs prepared fully in OptiMEM (LRo/OptiMEM). 24+24h incubation with luciferase-transduced A549 cells. Error bars are the SD of three measurements of a single formulation (n = 3).

4.1.1.2 Order of mixing of lipopolyplexes

The mixing order of lipids, peptide and siRNA in the formulation of the lipopolyplexes was studied. The peptides H12BLY and (HR)6BLY from Series I and II, respectively, were selected to investigate the preparation of LPRs by different mixing protocols. In protocol 1 (denoted **LPR**),

peptide solution was added to an equal volume of vesicle suspension, followed by the addition of an equal volume of siRNA solution. Protocol 1 is the order of mixing commonly used by other researchers. In protocol 2 (**LRP**), siRNA solution was added to vesicle suspension followed by the addition of peptide solution (in equal volume). Similarly, in protocol 3 (**PLR**), vesicle suspension was added to peptide solution, followed by the addition of siRNA solution while in protocol 4 (**PRL**) siRNA solution was added to the peptide solution followed by the addition of vesicle suspension (in equal volume). Protocols 5 and 6 examined adding peptide and siRNA solution to the suspension of vesicles. In protocol 5 (**RLP**) and 6 (**RPL**), siRNA solution was first mixed with vesicle suspension and peptide solution respectively and then a third component was added to the resulting mixture (in equal volume).

For this experiment, the vesicle suspensions and the various lipopolyplexes were prepared in water and so were described using the nomenclature, VwLPRw. Furthermore, the LPRs were prepared at a lipid:peptide:RNA charge ratio of 0.5:12:1 while the knock down experiments were performed using VwLPRw diluted 1 in 4 in OptiMEM (VwLPRw/OptiMEM) and transfection studied using the 24h+24 h incubation protocol. Naked siRNA and L2K were used as negative and positive control, respectively. In addition, lipopolexes (LRs) and polyplexes (PRs), prepared using the same two peptides were also examined, prepared in water and diluted 1 in 4 with OptiMEM before use (LRw/OptiMEM and PRw/OptiMEM, respectively).

When compared to the binary complexes, namely the LRs and PRs, the ternary lipopolyplexes displayed a much greater level of knock down. Significantly, there was no difference in knock down achieved using the various protocols. Furthermore, regardless of the protocol used, lipopolypexes composed of the Series II peptide, (HR)6BLY, exhibited a greater level of knock down than the lipopolyplexes prepared using the Series I peptide, H12BLY. This observation is at variance with the corresponding results observed for the lipopolyplexes prepared using DNA (Chapter 3) as opposed to siRNA where the greatest level of transfection was achieved for lipopolyplexes in which the peptide was added before the vesicles. It is worth to note that the explanation could be due to the small molecular size of siRNA and the resulting ease of diffusion in solution. However, as protocol 1 is the most widely used method to prepare the LPRs it was decided to use protocol 1 in the following study, unless otherwise stated.

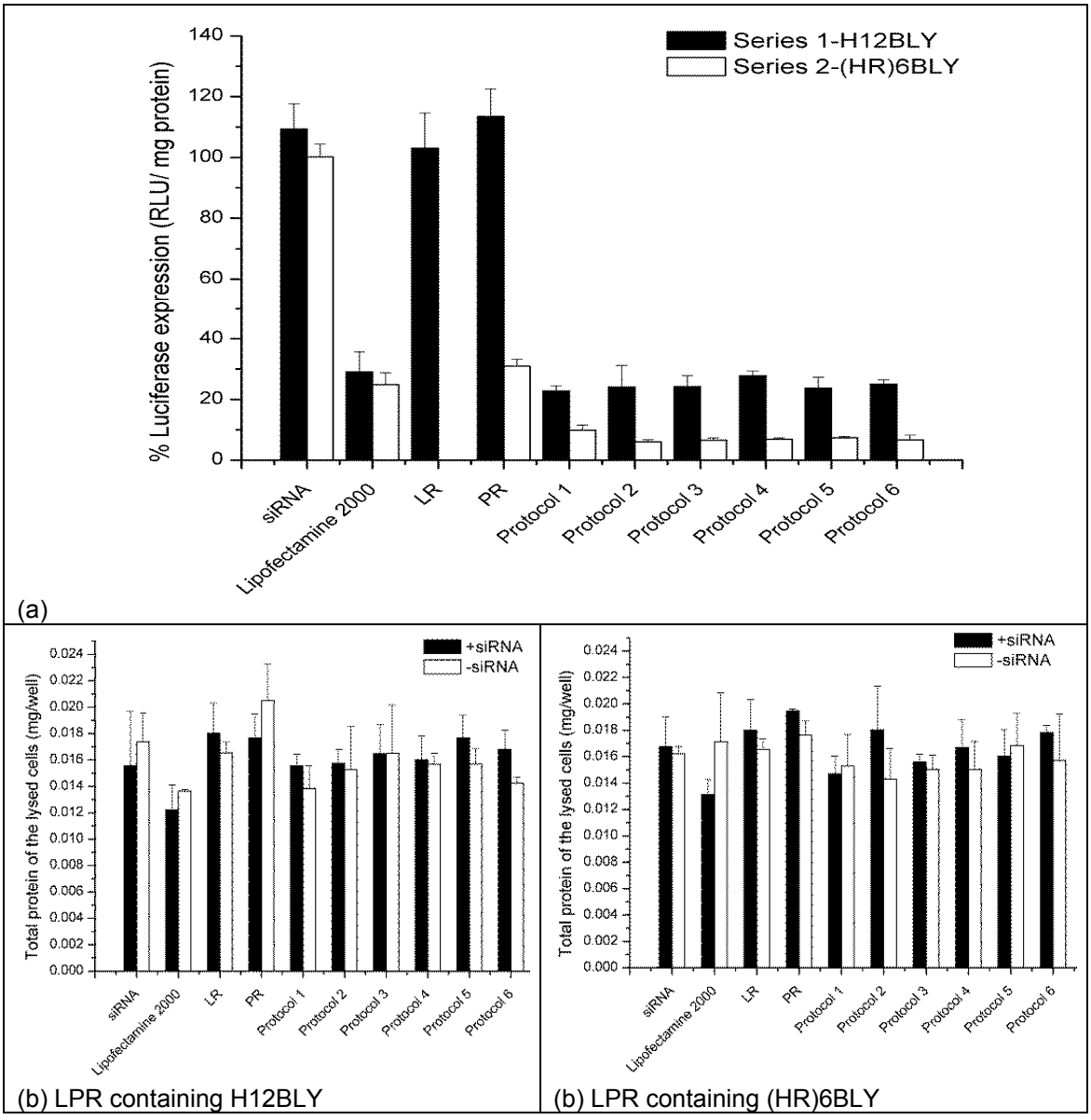

Figure 4.2 Effect of order of mixing of the lipopolyplexes (LPRs) on the knock down achieved in luciferase-transduced A549 cells after a 24+24h incubation: (a) knockdown and (b) corresponding protein assay. LPRs prepared using a Series I (H12BLY) and Series II (HR)6BLY peptide. 1 = LPR, 2 = LRP, 3 = PLR, 4 = PRL, 5 = RLP, 6 = RPL. Cationic vesicles composed of DOTMA/DOPE at 1:1 molar ratio. LPRs prepared at L:P:R charge ratio of 0.5:12:1, LRs made at a L:R charge ratio of 0.5:1 and PRs at a P:R charge ratio of 12:1. (+)siRNA, siRNA capable of expressing luciferase and (-)siRNA, scrambled siRNA, incapable of expressing luciferase. Knock down was performed after a 1 in 4 dilution of the LPRs, LRs and PRs in OptiMEM. Error bars are the SD of three measurements of a single formulation (n = 3).

4.1.1.3 Effect of charge ratio achieved using the lipopolyplexes

During preliminary studies, investigations using LPRs prepared at L:P:R charge ratios of 0.5:6:1 and 0.5:12:1 indicated that the optimal knock down in luciferase-induced A549 cells occurred within this range (Figure 4.3).

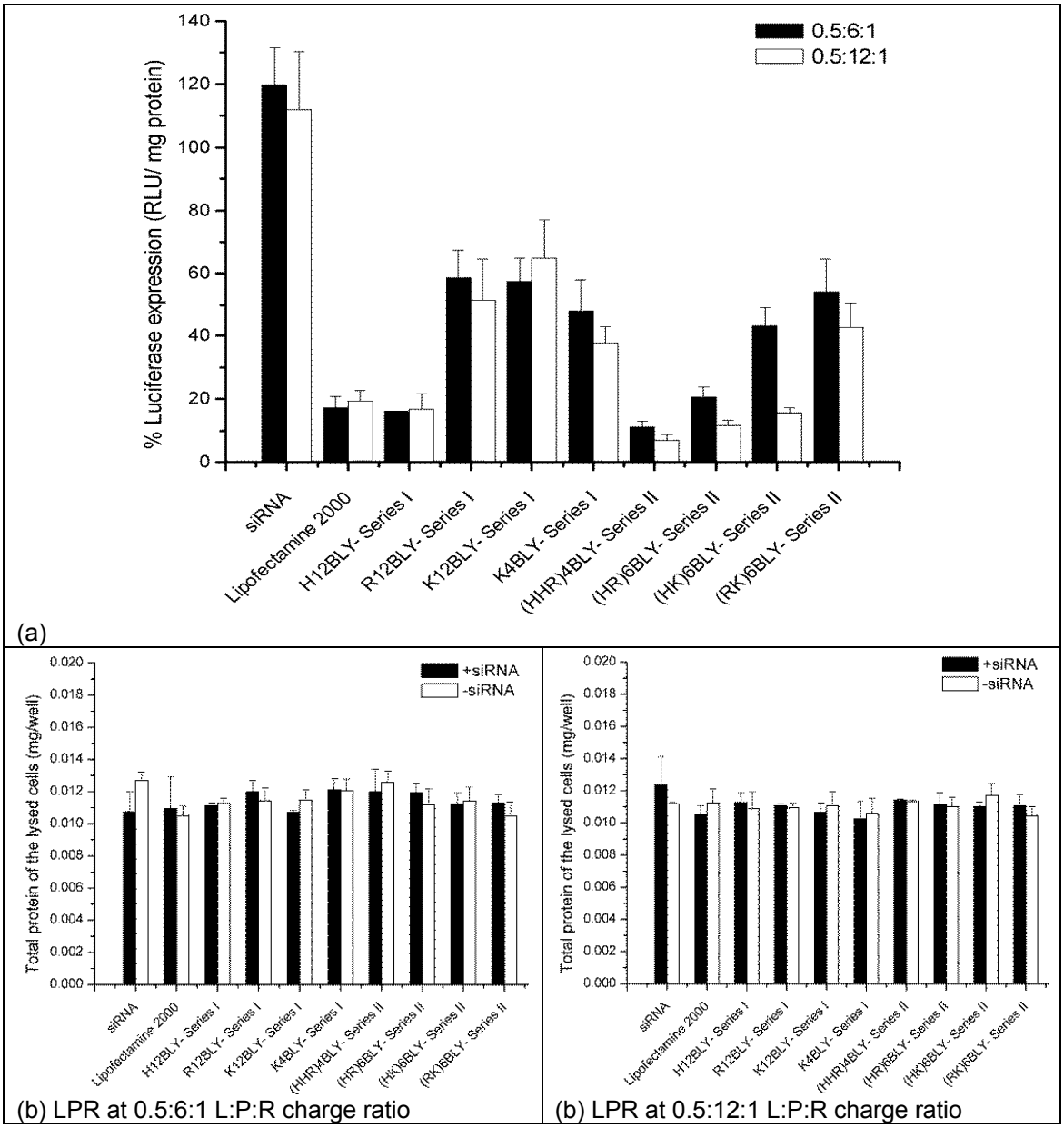

Figure 4.3 Luciferase gene silencing activity of lipopolyplexes (LPRs) prepared from Series I and Series II peptides. Knock down is of a positive control (+siRNA. capable of expression luciferase) expressed as a percentage of the negative control (-siRNA, scrambled, incapable of expression luciferase). Cationic vesicles composed of DOTMA/DOPE at a 1:1 molar ratio. LPRs prepared at L:P:R charge ratio of 0.5:6:1 and 0.5:12:1, respectively: (a) knock down and (b) corresponding protein assay. (+)siRNA, siRNA capable of expressing luciferase and (-)siRNA, scrambled siRNA, incapable of expressing luciferase. The knock down was performed after a 1 in 4 dilution of the LPRs in OptiMEM (VwLPRw/OptiMEM). 24+24h incubation with luciferase-transduced A549 cells. Error bars are the SD of three measurements of a single formulation (n = 3).

As can be seen LPRs tended to exhibit a higher level of knock down upon increasing peptide content, i.e. going from a L:P:R charge ratio of 0.5:6:1 to 0.5:12:1. As a consequence therefore, a L:P:R charge ratio of 0.5:12:1 charge ratio was used to prepare all LPRs in the following study,

unless otherwise stated. It is worth noting that in agreement with the results shown in Figure 4.2, the luciferase-induced A549 cells incubated with the LPRs prepared using Series II peptides, especially (HHR)4BLY, exhibited a higher level of knock down, than those incubated with the LPRs prepared using Series I peptides. The only exception being the LPRs prepared with the Series I peptide, H12BLY, which resulted in a high level of luciferase knock down. Interestingly, however, irrespective of the charge ratio used, the LPRs demonstrated a comparable, if not better, level of knock down than the commercially available, positive control L2K.

4.1.1.4 Effect of solvents used in preparation of the lipopolyplexes

In the above studies, both the vesicles used to prepare the LPRs and the LPRs themselves were prepared in water (VwLPRw). The ability of the VwLPRw to transfect luciferase-transduced A549 cells was then studied after a 4-fold dilution of the LPRs in OptiMEM (VwLPRw/OptiMEM). However, knock down achieved *in vitro* using OptiMEM cannot be correlated with knock down *in vivo* because of the serum present *in vivo* which is absent in the *in vivo* experiments As a consequence, it was necessary, therefore to examine the knock down of LPRs in presence of RPMI-1640 media containing 10% v/v of fetal bovine serum (FBS) and compare this with what is achieved in the presence of OptiMEM.

Preparing LPRs in water is not ideal for administration as the LPR suspension will not be isotonic with the body and therefore cannot be safely injected. As a consequence, therefore, the effect of varying the nature of the continuous phase used to prepare the LPRs has been investigated. The solvents used in this part of the study were water, OptiMEM, and an aqueous solution of 0.12 M NaCl (close to saline (0.154 M NaCl) which is isotonic with the body). In all cases the initial vesicles used to prepare the LPRs were made in an aqueous 0.12 M NaCl solution they were denoted as VsLPRs, when the LPRs were made in water they were denoted as VwLPRw, and in OptiMEM as VwLPRo. In this case all the LPRs were diluted 1 in 4 with OptiMEM before their incubation with the cells.

As can be seen in Figure 4.4, the trend obtained in the knock down trend of LPRs prepared in the various solvents were broadly the same, although the level of knock down was slightly greater when the LPRs were prepared in OptiMEM.

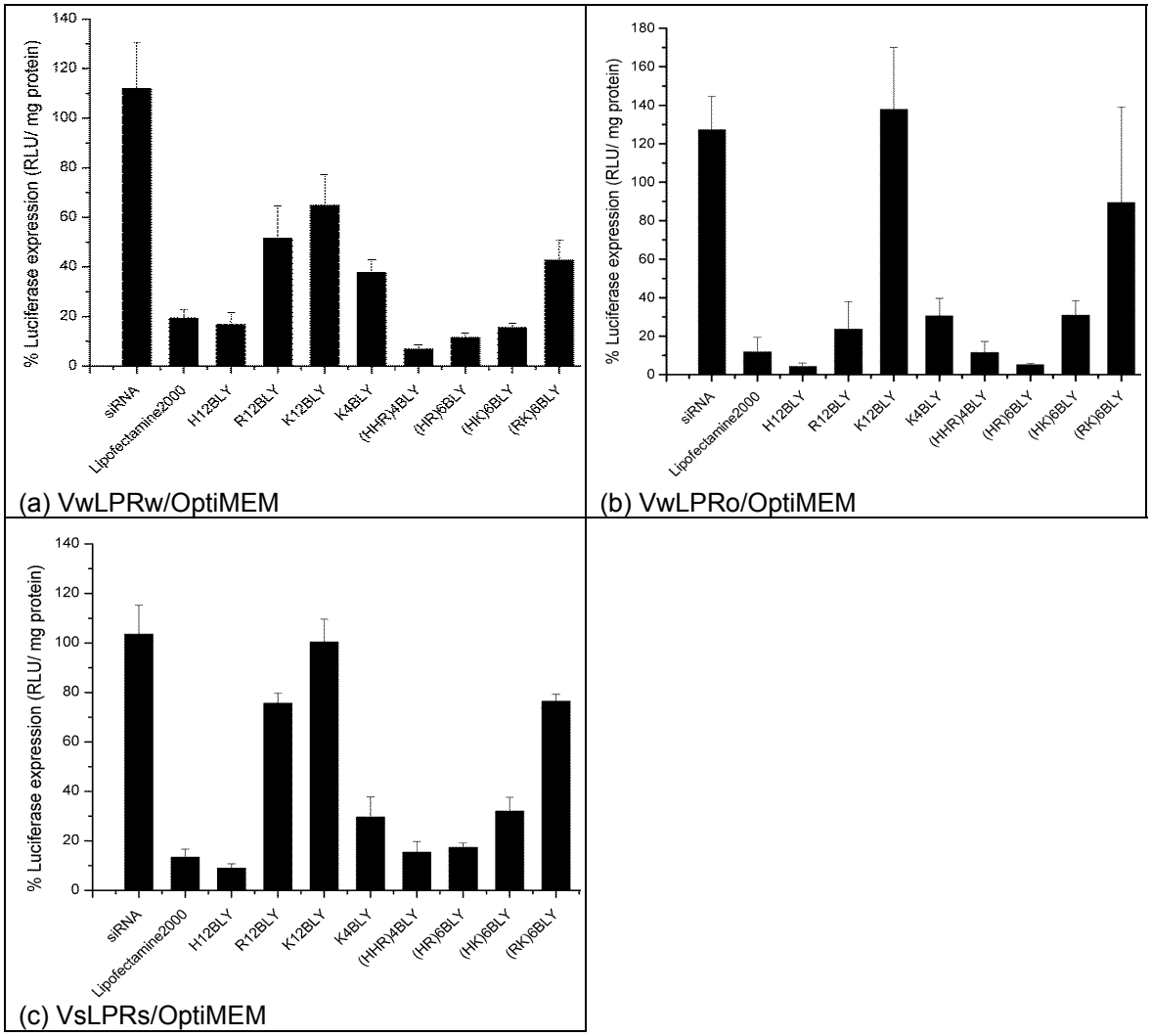

Figure 4.4 Knock down achieved in luciferase-transduced A549 cells after a 24+24h incubation with lipopolyplexes (LPRs) prepared from Series I and Series II peptides. LPRs prepared at L:P:R charge ratio of 0.5:12:1 in (a) water (VwLPRw), (b) OptiMEM (VwLPRo) and (c) 0.12 M NaCl solution (VsLPRs). Cationic vesicles composed of DOTMA/DOPE at 1:1 molar ratio. Knock down was performed after a 1 in 4 dilution of the LPRs in OptiMEM. Knock down is of a positive control (+siRNA. capable of expression luciferase) expressed as a percentage of the negative control (-siRNA, scrambled, incapable of expression luciferase). Error bars are the SD of three measurements of a single formulation (n = 3). Replicate experiments given in Appendix III.

In the previous study all the LPRs were diluted 1 in 4 with OptiMEM before their incubation with the cells. In this part of the study, the LPRs were diluted with RPMI-1640 media containing 10% v/v FBS (“media”) in the place of OptiMEM (Figure 4.5). It is noteworthy that no knock down is seen when the LPRs are prepared in water and diluted with media (Figure 4.5(a)). In contrast, knock down is observed for the LPRs prepared in OptiMEM (VwLPRo) and saline (VsLPRs) (Figures 4.5(b) and (c) respectively) with the greatest level of knock down being achieved for LPRs prepared in an aqueous solution of 0.12 M NaCl. Indeed when LPRs were prepared using

an aqueous solution of 0.12 M NaCl in the place of water, a high level of knock down was noted of greater than 80% was recorded for LPRs containing either H12BLY or (HR)6BLY. This is a particularly exciting result and suggests that the use of an aqueous solution of 0.12 M NaCl enhances the knock down achieved using the LPRs.

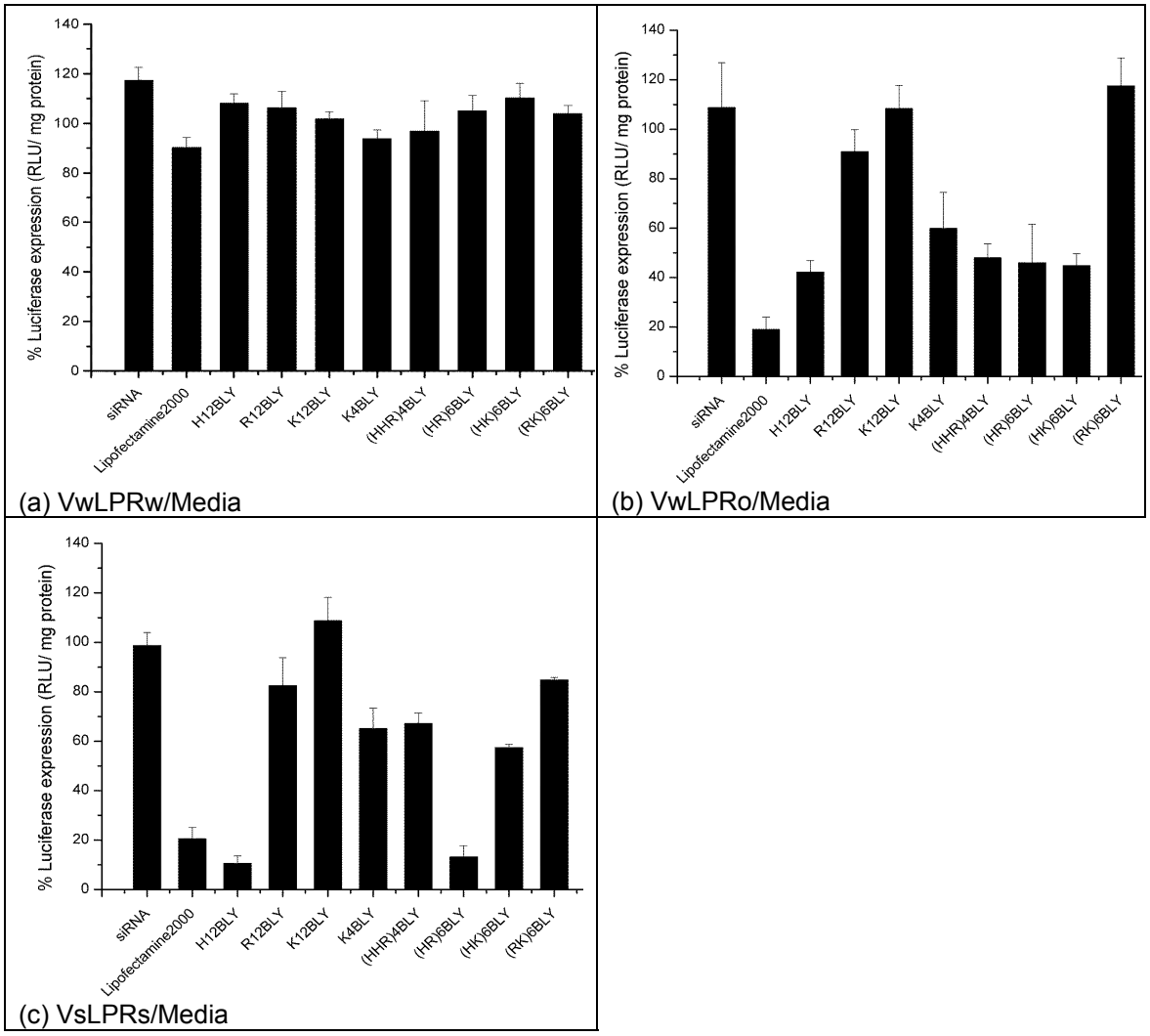

Figure 4.5 Knock down achieved in luciferase-transduced A549 cells after a 24+24h incubation with lipopolyplexes (LPRs) prepared from various peptides. LPRs prepared at L:P:R charge ratio of 0.5:12:1 in (a) water (VwLPRw), (b) OptiMEM (VwLPRo) and (c) 0.12 M NaCl solution (VsLPRs). Cationic vesicles composed of DOTMA/DOPE at 1:1 molar ratio. Knock down was performed after a 1 in 4 dilution of the LPRs in RPMI-1640 media containing 10% v/v of FBS. Knock down is of a positive control (+siRNA, capable of luciferase expression) expressed as a percentage of the negative control (-siRNA, scrambled, incapable of luciferase expression). Error bars are the SD of three measurements of a single formulation (n=3). Replicate experiment contained in Appendix III.

In the above studies, when the knock down was performed in the presence of the serum containing RPMI-1640 media in the place of OptiMEM, the luciferase-transduced A549 cells incubated with LPRs prepared in an aqueous solution of 0.12 M NaCl exhibited a high level of

knock down whereas those LPRs prepared in water showed no knock down. The major difference between the two types of media is the presence of 10% v/v of FBS in the RPMI-1640 media. It was therefore assumed that the FBS was responsible for the lack of knock down seen.

As it is known that RNAse is present in FBS, it was therefore decided to establish whether this is reason for the detrimental effect media has on the knock down achieved by LPRs diluted in RPMI-1640 media with FBS (Haupenthal et al, 2007). As a consequence, a gel electrophoresis study was performed to determine the effect of RNAase on naked (-)siRNA when dissolved in either water or RPMI-1640 media, without or with 10% v/v FBS alone or in the presence of varying concentrations of the enzyme inhibitor (RNAse A) (Figure 4.6).

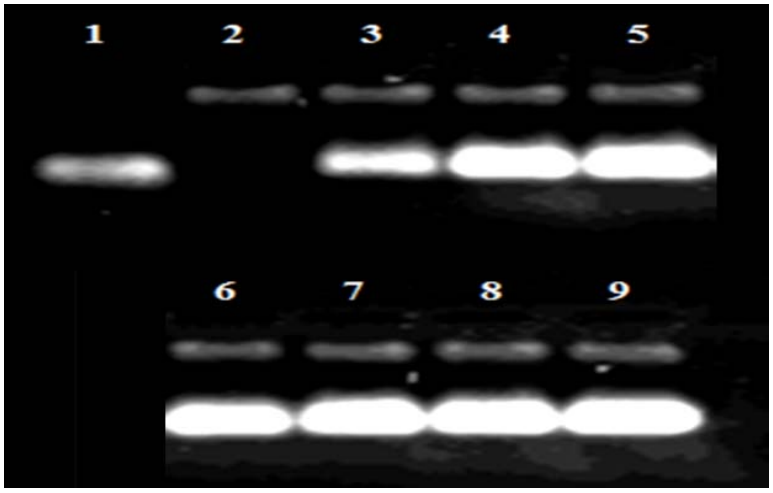

Figure 4.6 Agarose gel electrophoresis of naked (-)siRNA (0.01 mg/mL) dissolved in water, Lane (1); an aqueous solution of 10% v/v FBS, Lane (2); an aqueous solution of 10% v/v FBS and 2% v/v enzyme inhibitor (RNAse A), Lane (3); an aqueous solution of 10% v/v FBS and 4% v/v enzyme inhibitor (RNAse A), Lane (4); an aqueous solution of 10% v/v FBS and 10% v/v enzyme inhibitor (RNAse A), Lane (5); 10% v/v FBS in RPMI-1640 media, Lane (6); 10% v/v FBS and 2% v/v of enzyme inhibitor (RNAse A) in RPMI-1640 media, Lane (7); 10% v/v FBS and 4% v/v enzyme inhibitor (RNAse A) in RPMI-1640 media, Lane (8); 10% v/v FBS and 10% v/v enzyme inhibitor (RNAse A) in RPMI-1640 media, Lane (9).

siRNA was dissolved in either water, FBS solution and RPMI-1640 media containing FBS. It is seen from Lane 2 that naked siRNA was completely degraded by 10% v/v of FBS in water compared to the results obtained when the siRNA was dissolved in water (Lane 1). Addition of RNAse inhibitor at 2% v/v siRNA dissolved in FBS solution resulted in a greatly reduced level of degradation (Lane 3) while addition of 4 and 10% v/v RNAse inhibitor (Lanes 4 & 5) resulted in little or no degradation. Note that the extra band seen on the gel when FBS was present was confirmed to be due to FBS (data not shown).

Addition of 2% v/v RNAse inhibitor to the siRNA dissolved in FBS resulted in a greatly reduced level of degradation (Lane 3) whereas the presence of 4% and 10% v/v RNAse inhibitor (Lanes 4 & 5) resulted in little or no degradation of siRNA. Interestingly, when naked siRNA was dissolved in RPMI-1640 media with 10% v/v FBS, it was also not degraded (Lane 6), suggesting that any RNAse present was deactivated by the FBS contained in the RPMI-1640 media. In addition, the presence of up to 10% v/v RNAse inhibitor in the FBS containing RPMI-1640 media did not alter the observation that siRNA was not degraded (Lanes 7, 8 & 9, respectively).

As a consequence of these observations, it might quite reasonably be anticipated that siRNA present in LPRs prepared in water (VwLPRw) would not be degraded when the knock down was performed in RPMI-1640 media containing 10% v/v FBS. Any lack of any knock down in the luciferase-transduced A549 cells after incubation of VwLPRw/OptiMEM could therefore not explained by the degradation of siRNA due to RNAse.

FBS is a negatively charged protein, whereas the LPRs are positively charged. As a consequence of their opposing charges in may be that expected that FBS would bind to the exterior surface of the LPRs and either reducing uptake of the LPRs into the cells and/or releasing the siRNA before it can enter the cell.

4.1.2 Complexation, release and protection properties of lipopolyplexes

The ability of the LPRs containing the various peptides, prepared fully in water (VwLPRw) to complex, release and protect siRNA was determined using gel electrophoresis (Figure 4.7). The ability of the LPRs to complex siRNA is shown in Lane A, while the release and protection of siRNA within the LPRs is shown in Lanes B and C, respectively.

For the VwLPRw, with the exception of faint bands present in the LPRs prepared using the H12BLY and (HHR)4BLY peptides, there was no band attributable to intact siRNA present in Lane A. This observation suggests that, with the exception of H12BLY and (HHR)4BLY, siRNA was completely complexed within the VwLPRw prepared using both Series I and Series II peptides. In Lane B, strong bands attributable to siRNA were present, indicating that siRNA was completely released from various LPRs upon the addition of pAsp. When naked siRNA was treated with RNAse (Lane C), no band attributable to siRNA could be observed. In contrast, however, when the LPRs were treated with the same concentration of RNAse followed by pAsp

to release any siRNA, clear bands attributable to siRNA were observed suggesting that siRNA was protected when in the various VwLPRw.

Figure 4.7 Complexation, release and protection of lipopolyplexes (LPRs) using 0.01 mg/mL of (-)siRNA. LPRs prepared at a L:P:R charge ratio of 0.5:12:1. Cationic vesicles composed of DOTMA/DOPE at a 1:1 molar ratio. Upper panel shows VwLPRw, and the lower panel VsLPRs. Lane A: complexation, Lane B: release (treated with pAsp), Lane C: protection (treated with RNAse A at 37 ± 0.1°C and pAsp). C = 1x RNAse A (45 units μL^{-1}), C_1 = 2.5X RNAse A, C_2: 5.0X RNAse A. Replicate experiments contained in Appendix III.

LPRs prepared fully in an aqueous 0.12 M NaCl solution (VsLPRs) were also examined using gel electrophoresis and, as with the VwLPRw, the LPRs exhibited the ability to both fully complex (Labe A) and release siRNA (Lane B). Interestingly, however, when naked siRNA was treated with RNAse A (Lane C), there was clear band, attributable to siRNA, suggesting that either that the activity of RNAse was reduced in the presence of NaCl and/or else the NaCl in some way protects the siRNA from degradation. Indeed it has been reported that sodium salts activates RNAse A (Okuda et al, 2003).

In order to investigate the effect of NaCl on the ability of RNAse A to degrade siRNA, three levels of enzyme were investigated, namely with standard amount of RNAse A (Lane C), 2.5 times the standard amount (Lane C_1) and 5 times the standard amount (Lane C_2). As can be

seen, the greater the level of RNAse the greater the amount of naked siRNA was degraded. As a consequence of these observations which points to the reduction of RNAse activity in the presence of NaCl, it is not possible to unambiguously conclude that the siRNA was protected from RNAse A when entrapped inside the various VsLPRs.

4.1.3 Quantification of complexation efficiency of lipopolyplexes

The efficiency of complexation of siRNA in the various LPRs was quantified by a picogreen fluorescence assay which exploits the fact that picogreen, once bound to siRNA, exhibits greater than a 1000 times increase in fluorescence (Dragan et al, 2010). Picogreen competes with peptides to bind to siRNA and as a consequence, it is possible to determine the amount of unbound siRNA in LPR formulations by quantifying the fluorescence of picogreen.

In this part of the study, a series of LPRs were prepared at different P:R charge ratios whilst keeping the L:R charge ratio constant at 0.5:1. Two preparation protocols were investigated in an attempt to understand the structure of the complexes. In Protocol 1, pre-formed LPRs were mixed with picogreen while in Protocol 2, siRNA was first mixed with picogreen and then used to prepare LPRs.

The complexation efficiency of LPRs made in water and prepared by Protocol 1 is shown in Figure 4.8(a). For the VwLPRw prepared using the Series I peptides, ~20% of free siRNA was observed at a P:R charge ratio of 1:1, suggesting that ~80% of the siRNA was complexed. No major change in the amount of complexed siRNA was observed at higher P:R charge ratios. The only exception being the VwLPRw prepared with H12BLY where the extent of complexation gradually increased upon increasing the P:R charge ratio up to 18:1. Although LPRs prepared using Series II peptides demonstrated similar trend, they tended to exhibit a slightly lower level of complexation efficiency than the LPRs containing Series I peptides.

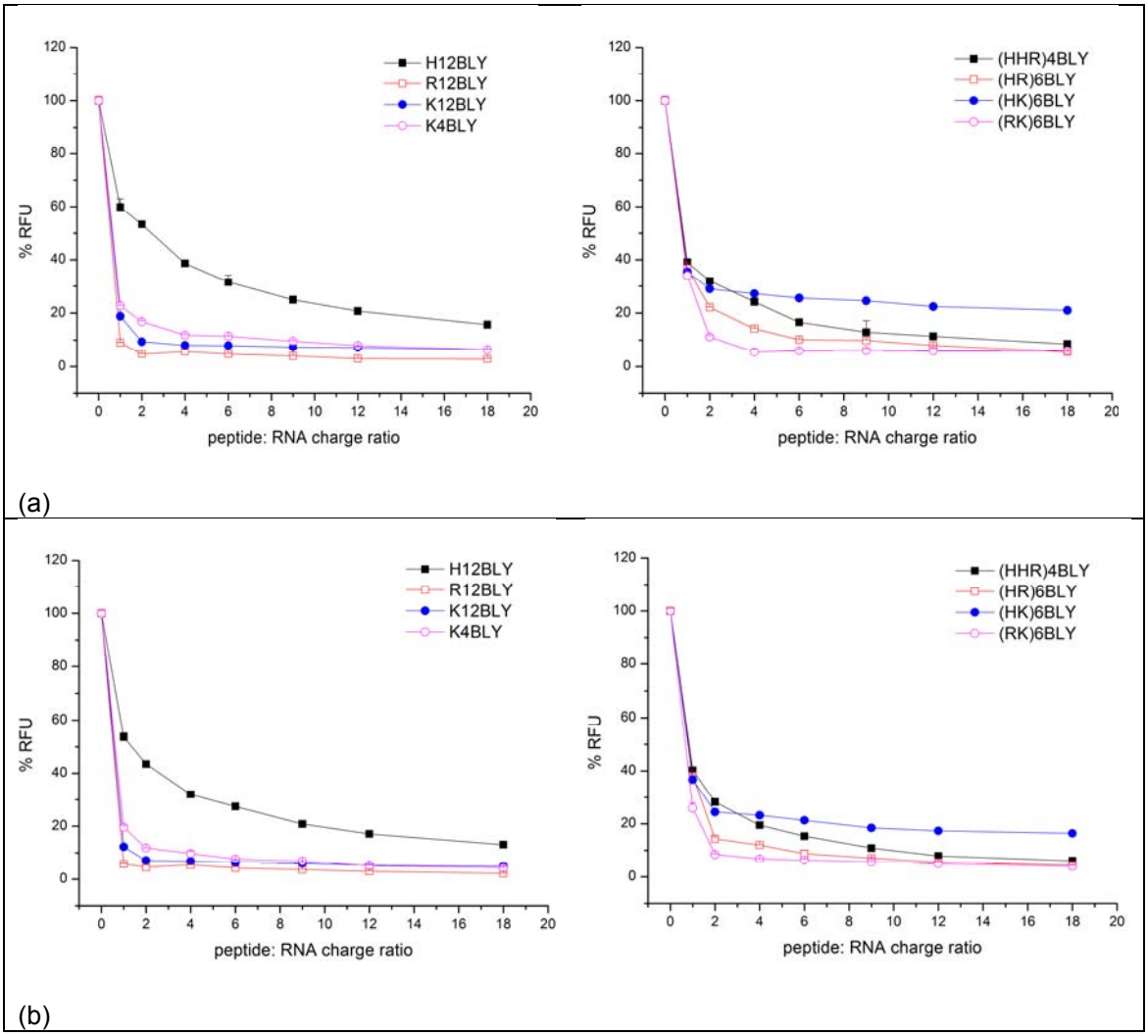

Figure 4.8 Quantification of siRNA complexed in lipopolyplexes (LPRs - VwLPRw) as determined as relative fluorescence units (RFU) using a picogreen fluorescence assay. LPRs containing 0.02 mg/mL of (-)siRNA and an LR ratio of 0.5:1 were prepared by (a) Protocol 1 and (b) Protocol 2. Protocol 1 = LPR + picogreen. Protocol 2 = LP + (R + picogreen). Error bars are the SD of three measurements of a single formulation (n = 3) at 25 ± 0.1°C. In most instances, the error bars are contained within the symbols.

The complexation of LPRs made in water and prepared by Protocol 2 is shown in Figure 4.8(b). Interestingly, the complexation efficiency of LPRs prepared by Protocol 2 was similar to that of LPRs prepared by Protocol 1, with the exception of a slightly higher level of complexation for the LPRs containing H12BLY and (HHR)4BLY.

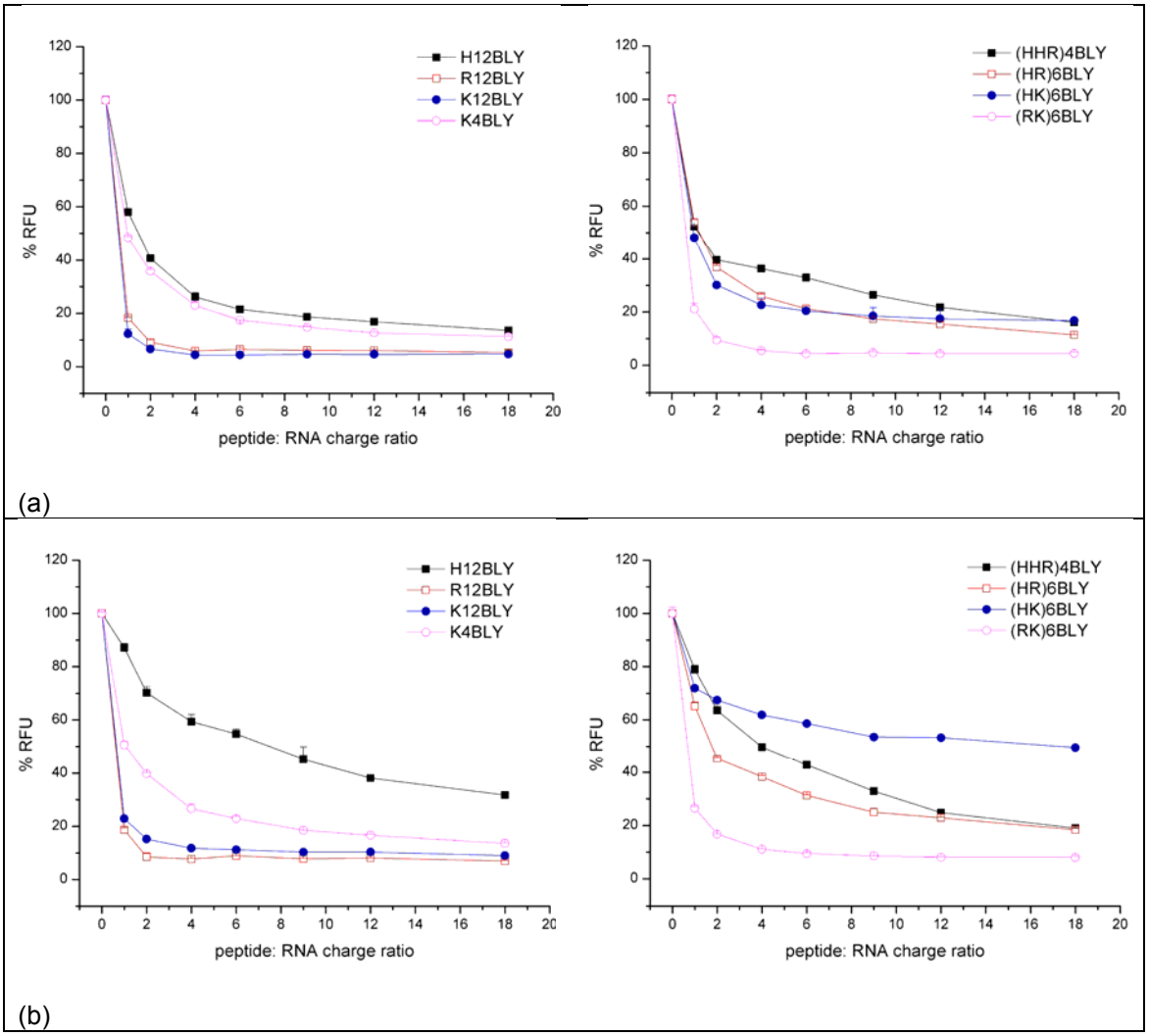

Figure 4.9 Quantification of siRNA complexed in lipopolyplexes (LPRs - VsLPRs) as determined as relative fluorescence units (RFU) using a picogreen fluorescence assay. LPRs containing 0.02 mg/mL of (-)siRNA and an LR ratio of 0.5:1 were prepared by (a) Protocol 1 and (b) Protocol 2. Protocol 1 = LPR + picogreen. Protocol 2 = LP + (R + picogreen). Error bars are the SD of three measurements of a single formulation (n = 3) at 25 ± 0.1°C. In most instances, the error bars are contained within the symbols.

4.1.4 Particle size and ζ- potential measurement of lipopolyplexes

The apparent hydrodynamic size of the vesicles and LPRs prepared in water (VwLPRw) is shown in Figure 4.10. When considered as a group, the LPRs prepared containing the various peptides, possessed apparent hydrodynamic sizes in the range of 40-55 nm (with the exception of the LPR containing K4BLY which exhibited a size of ~70 nm) and ζ-potential of the order of 25-40 mV. There was no significant difference in the apparent hydrodynamic size and the ζ-potential of the LPRs prepared at two charge ratios and with the two series of peptides. Generally the size of the LPRs was slightly smaller than the size of the parent vesicles.

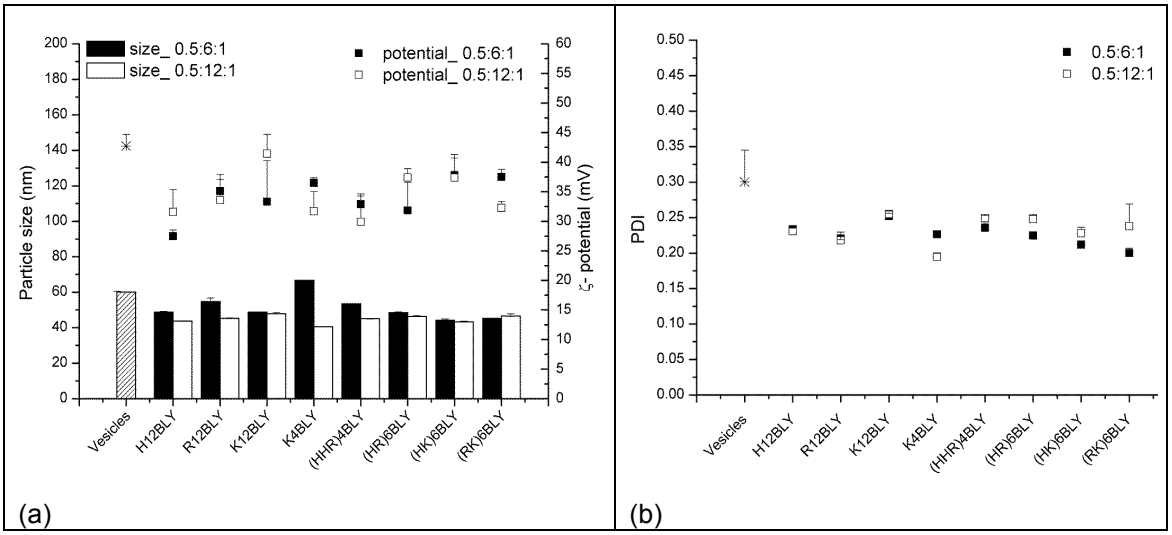

Figure 4.10 Mean apparent hydrodynamic size and ζ-potential (a) and polydispersity index (PDI) (b) of lipopolyplexes (LPRs) made in water (VwLPRw). LPRs prepared at L:P:R charge ratio of 0.5:6:1 and 0.5:12:1 using 0.025 mg/mL of (-)siRNA. Cationic vesicles composed of DOTMA/DOPE at 1:1 molar ratio. Error bars are SD of three measurements of a single formulation at 25 ± 0.1°C.

The PDI of the LPRs is another indicator of the quality of the preparation in that an LPR can be considered to be relatively homogeneous if the PDI less than 0.1 or 0.15 at most. Interestingly the parent vesicles were the most heterogeneous of the preparations, exhibiting a PDI of ~0.30. The LPRs were all heterogeneous as they exhibited PDIs in the approximate range 0.20 - 0.275.

In order to understand the effect of NaCl on the biophysical properties of the LPRs and hopefully on transfection, the above studies were repeated using a 0.12 M NaCl solution in replace of water. The apparent hydrodynamic size and ζ-potential of the vesicles and VsLPRs are shown in Figure 4.11. It is of particular note that the apparent hydrodynamic size of the cationic vesicles prepared in 0.12 M NaCl solution were ~3 times larger than those prepared in water, suggesting they were possibly multilamellar in nature. In this context, the larger the size of the particle, the more efficient knockdown, regardless of the presence or otherwise of serum (Turek et al, 2000). Furthermore, the cationic vesicles dispersed in 0.12 M NaCl possessed a lower ζ-potential at ~32 mV than the vesicles dispersed in water, namely as opposed to ~43 mV.

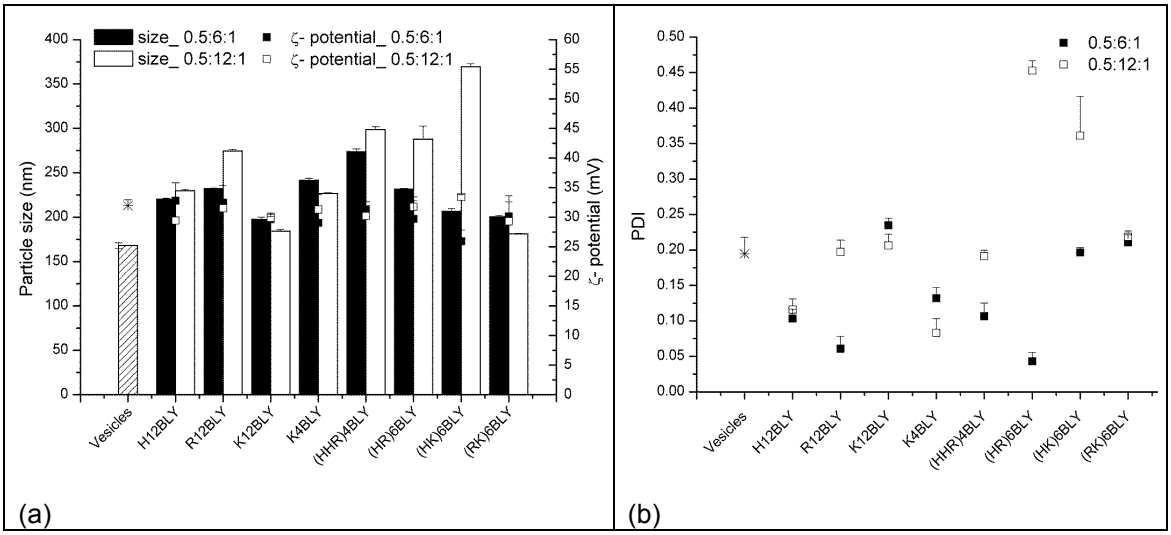

Figure 4.11 Apparent hydrodynamic size of lipopolyplexes (LPRs) made in 0.12 M NaCl solution (VsLPRs). LPRs prepared at L:P:R charge ratio of 0.5:6:1 and 0.5:12:1 using 0.025 mg/mL of (-)siRNA. Cationic vesicles composed of DOTMA/DOPE at 1:1 molar ratio (a) mean apparent hydrodynamic size and ζ-potential, (b) polydispersity index (PDI). Error bars are SD of three measurements of a single formulation (n = 3) at 25 ± 0.1°C.

Interestingly the apparent hydrodynamic size of the VsLPRs containing R12BLY, (HHR)4BLY, (HR)6BLY and (HK)6BLY at a L:P:R charge ratio of 0.5:12:1 were larger than those prepared at the lower charge ratio of 0.5:6:1. In contrast, there was no difference in the ζ-potential of the VsLPRs prepared at two charge ratios. It is also worth noting that the LPRs prepared in 0.12 M NaCl were bigger than the cationic vesicles from which they were prepared. The PDI of the majority of the VsLPRs prepared at a 0.5:12:1 charge ratio was ~0.20 whereas the PDI of the VsLPRs prepared at the lower charge ratio of 0.5:6:1 was smaller at ~0.10. It reveals that the VsLPRs made at the 0.5:12:1 charge ratio were polydisperse while those made at the 0.5:6:1 charge ratio were fairly monodisperse.

4.1.5 Size stability of lipopolyplexes prepared in water and saline solutions

The size of the LPRs prepared in water was constant at ~ 60 nm over the period of one week as seen in Figure 4.12(a). The PDI of the size of the LPRs prepared in water also remained stable at ~0.25 over the same period (Figure 4.12(b)). Both the size and the PDI results indicate that the LPRs prepared in water are stable over the time period studied. In comparison, the size of the LPRs prepared in 0.12 M NaCl solution (VsLPRs) increased from ~200 nm to several hundred nm over 1 week as shown in Figure 4.13. Correspondently, the PDI of the LPRs also increased over the same period. Therefore, the LPRs prepared in saline solution are less stable

than those prepared in water, which is probably a consequence of the reduced charge present on the surface of the LPRs in the presence of NaCl. Furthermore, the increased in size of the LPRs prepared in the presence of NaCl is due to a reduced charge-charge interaction.

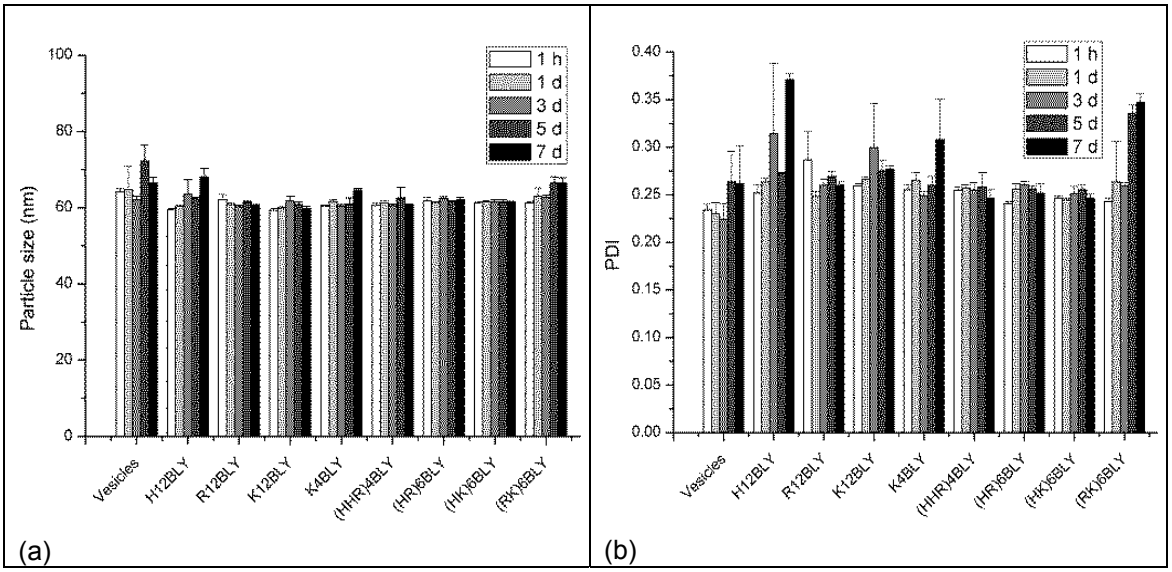

Figure 4.12 Variation in apparent hydrodynamic size over time of lipopolyplexes (LPRs) made in water (VwLPRw). LPRs prepared at L:P:R charge ratio of 0.5:12:1 using 0.025 mg/mL (-)siRNA. Cationic vesicle composed of DOTMA/DOPE at 1:1 molar ratio (a) mean apparent hydrodynamic size and ζ-potential, (b) polydispersity index (PDI). Error bars are the SD of three measurements of a single formulation (n = 3) at 25 ± 0.1°C.

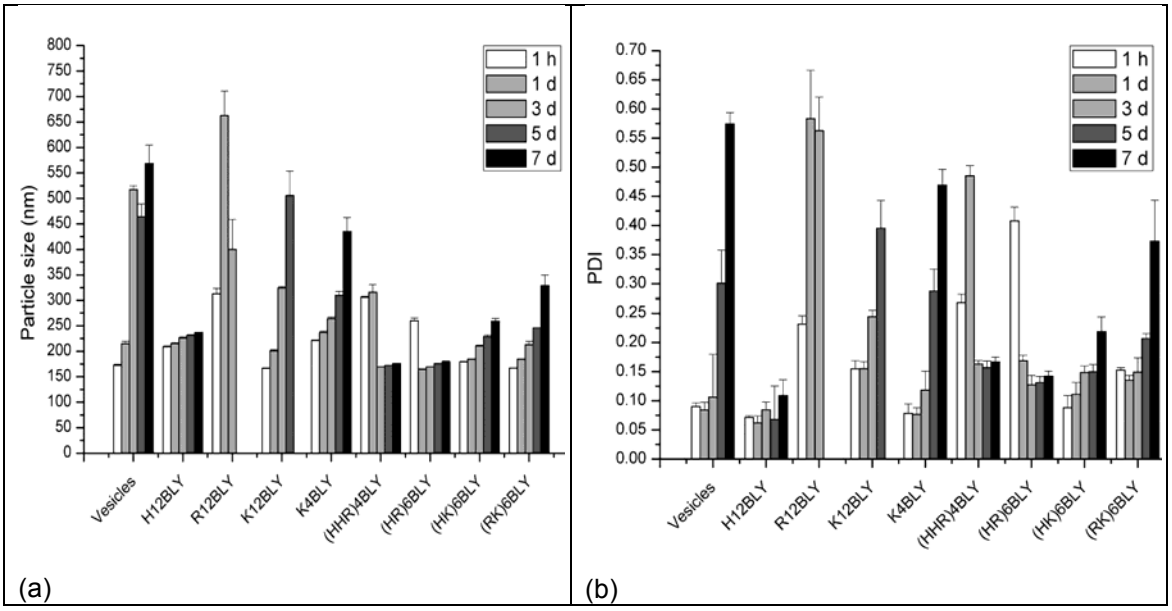

Figure 4.13 Variation in apparent hydrodynamic size over time of lipopolyplexes (LPRs) made in saline (VsLPRs). LPRs prepared at L:P:R charge ratio of 0.5:12:1 using 0.025 mg/mL (-)siRNA. Cationic vesicles composed of DOTMA/DOPE at 1:1 molar ratio (a) mean apparent hydrodynamic size and ζ-potential, (b) polydispersity index (PDI). Error bars are SD of three measurements from a single formulation (n = 3) at 25 ± 0.1°C.

4.1.6 Small angle neutron scattering study of lipopolyplexes

Small angle neutron scattering (SANS) studies were performed to detect any difference in the macromolecular structure of the lipopolyplexes (LPRs) prepared using either water or NaCl saline solutions. The SANS data of the LPRs, the neutron scattering intensity (I) as a function of momentum transfer, *Q*, was plotted against *Q*. In the present model of the single lipid bilayer sheets and stacks, the space between sheet repeats (*d*-spacing) is the sum of the thickness of the vesicle's lipid bilayer (*L*) and the thickness of the aqueous layer (d_w) as illustrated in Figure 3.3 (Chapter 3).

4.1.6.1 Lipopolyplexes prepared in D_2O

Figure 4.14 gives the variation in the intensity of the small angle neutron scattering (I) in cm^{-1} as a function of momentum transfer (q) in $Å^{-1}$ for DOPE:DOTMA vesicles, LRs and LPRs prepared from the vesicles - the LPRs containing the peptide (HR)6BLY - and the corresponding PRs. The LRs, LPRs and PRs were prepared at charge ratios of 2:1, 0.5:12:1 and 12:1, respectively. In all cases, all the samples were prepared in D_2O as opposed to H_2O in order to provide the contrast necessary for the SANS measurements. The much higher scattering of the parent vesicles is due to the higher concentration of the protonated material (here lipid) present compared to the other systems, for example the vesicles were measured at ~ a ninth of the lipid concentration of the LPRs, namely 1 mg/mL (in the parent vesicles) as opposed to 0.112 mg/mL of DOTMA (in the final LPRs). Furthermore, the mismatch in the backgrounds between the various samples is a result of the different levels of incoherent scattering due to the differences in the amounts of protonated material present.

The SANS data obtained for the LPRs containing the peptide (HR)6BLY (prepared at a lipid:peptide:siRNA charge ratio of 0.5:12:1) and the parent DOPE:DOTMA vesicles (Figure 4.14) were well fitted assuming the presence of single sheets of lamellae - the LPR and vesicles are being too large to be analysed as hollow spherical structures as may be expected for vesicular structures using the current SANS set-up. The parameters used to obtain the fits to the SANS data are given in Table 4.1.

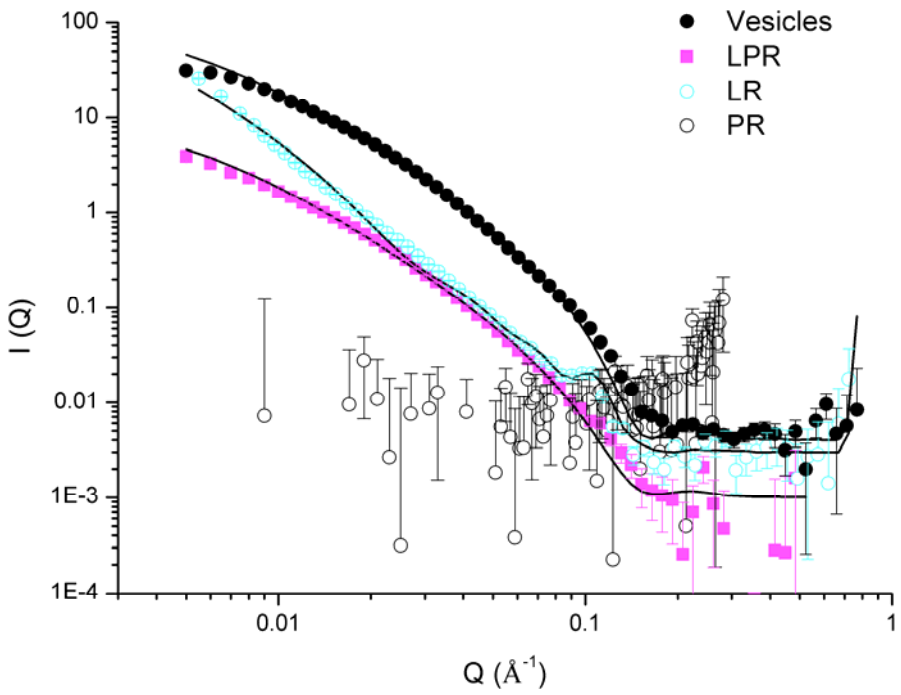

Figure 4.14 Small angle neutron scattering (SANS) data (dots) and the best fit to the data (solid line) for DOTMA/DOPE vesicles prepared at a DOTMA concentration of 1.0 mg/mL, lipopolyplexes (LPRs) containing (HR)6BLY, LR and PR containing (HHR)4BLY. LPRs were made at a lipid:peptide:siRNA charge ratio of 0.5:12:1. LR prepared at a L:R charge ratio of 2:1 and PR at a P:R charge ratio of 12:1. Sigma siRNA was at a concentration of 0.1 mg/mL. Vesicles used to prepare the LPRs composed of DOTMA:DOPE at 1:1 molar ratio and were aged ~48 h. SANS was measured at 25 ± 0.1°C on SANS2D.

In contrast, however, it was not possible to fit the SANS data obtained for the LRs (prepared at a 2:1 lipid:siRNA charge ratio) assuming the presence of only single sheets as was the case for the vesicles and LPRs, but rather it was necessary to add some multilamellar structure to the single sheet model to fit the Brag peak present in the data. Indeed, the ratio of multilamellar surface area to unilamellar surface area of the LRs was predicted to be 0.51 represented as the ratio of stack to sheet as shown in Table 4.1. This observation suggests that the LR possessed a quite different structure to the LPRs. In addition it was also necessary to increase the value of the R_{sigma} used to model the data from ~ 300 to ~ 800 suggesting that the bilayers present in the LRs are much more rigid in nature. This result is perhaps not unexpected due to the high rigidity of siRNA. In line with previous studies (Kudsiova et al, 2011), the scattering pattern obtained for the PR was very weak, probably a consequence of their large size and 'fluffy' (unstructured) nature.

Table 4.1 Structural parameters obtained for the vesicles, LPRs containing the peptide R12BLY, K12BLY, (HR)6BLY, and (HK)6BLY and LRs derived from FISH modelling of their SANS data. LPRs was prepared at a sigma siRNA concentration of 0.1 mg/mL and a lipid:peptide:siRNA charge ratio of 0.5:12:1 and 0.5:6:1 and LR prepared at a sigma siRNA concentration of 0.05 mg/mL and a L:R charge ratio of 2:1. Vesicles used to prepare the LPR composed of DOTMA:DOPE at 1:1 molar ratio (1.0 mg/mL DOTMA) and were aged ~48 h. SANS was measured at 25 ± 0.1°C on SANS2D.

Samples and mixing ratio	L (Å)	No. of layers	d-spacing (Å)	R_{sigma} (Å)	Ratio of stack: sheet	SWSE
Vesicles	38.7 (± 0.8)	-	-	300	-	727
LPR-R12BLY (0.5:12:1)	38.7 (± 1.2)	-	-	300	-	358
LPR-K12BLY (0.5:12:1)	38.7 (± 1.1)	-	-	300	-	453
LPR-(HR)6BLY (0.5:12:1)	38.7 (± 1.1)	-	-	300	-	426
LPR-(HK)6BLY (0.5:12:1)	38.7 (± 1.0)	-	-	300	-	322
LPR-R12BLY (0.5:6:1)	38.7 (± 1.1)	-	-	300	-	387
LPR-K12BLY (0.5:6:1)	38.7 (± 0.6)	-	-	300	-	147
LPR-(HR)6BLY (0.5:6:1)	38.7 (± 0.8)	-	-	300	-	210
LPR-(HK)6BLY (0.5:6:1)	38.7 (± 0.7)	-	-	300	-	194
LR (2:1)	32.7 (± 2.3)	4	56.6 (±2.0)	800	0.51	3552

Figures in brackets indicate the standard errors on the fitted parameter values. Ratio of stack to sheet represents the ratio of multilamellar surface area to unilamellar surface area. SWSE is sum of weighted square error.

Figure 4.15 and 4.16 shows the SANS data for the LPRs containing peptides, R12BLY, K12BLY, (HR)6BLY and (HK)6BLY prepared at 0.5:12:1 and 0.5:6:1 charge ratios. The scattering pattern recorded for the LPRs are very similar to one another and to the parent vesicles. The bilayer thickness of the various LPRs determined by modelling their SANS data assuming the presence of single sheets are given in Table 4.1. Significantly there was no difference in the bilayer thickness/structure for the LPRs containing various peptides at the same charge ratio and between charge ratios. This result suggests that the LPRs have the same bilayer structure as the vesicles. The similar observation was made for the LPDs.

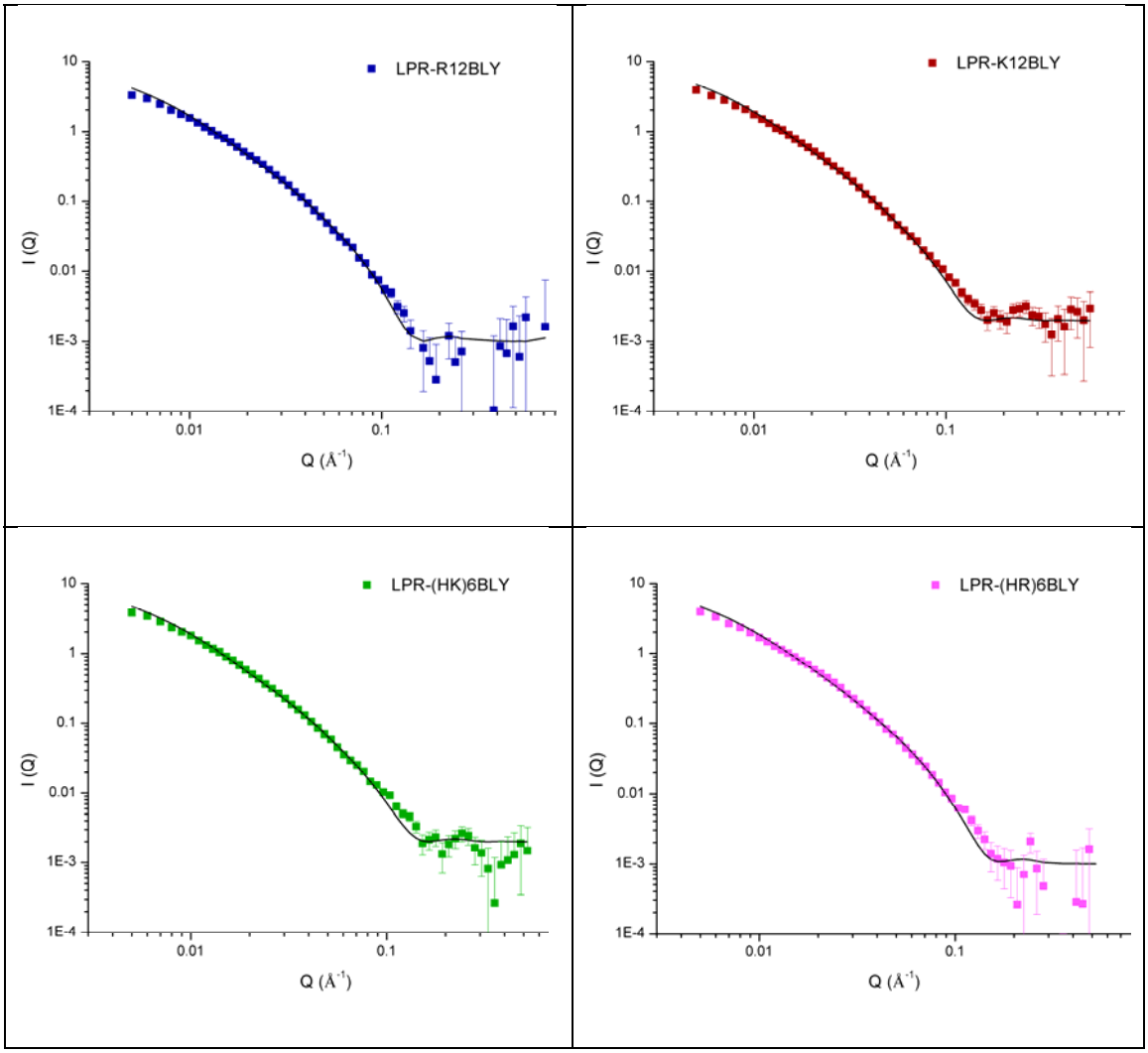

Figure 4.15 Small angle neutron scattering (SANS) data (dots) and the best fit to the data (solid line) for lipopolyplexes (LPRs) containing R12BLY, K12BLY, (HK)6BLY and (HR)6BLY. LPRs were made at lipid:peptide:siRNA charge ratio of 0.5:12:1 and contained 0.1 mg/mL sigma siRNA. Vesicles used to prepare the LPRs composed of DOTMA:DOPE at 1:1 molar ratio and were aged ~48 h. SANS was measured at 25 ± 0.1°C on SANS2D.

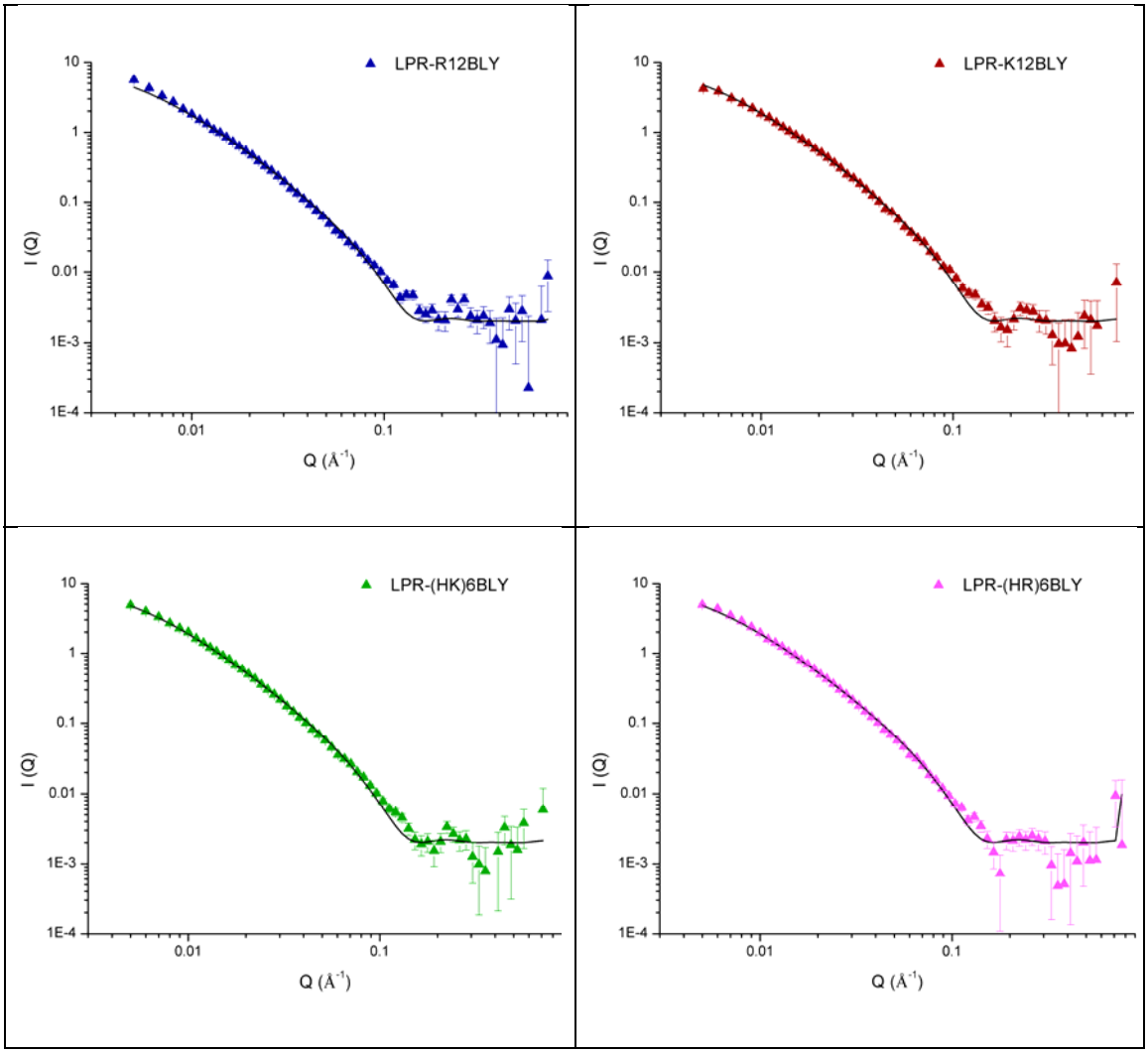

Figure 4.16 Small angle neutron scattering (SANS) data (dots) and the best fit to the data (solid line) for lipopolyplexes (LPRs) containing R12BLY, K12BLY, (HK)6BLY and (HR)6BLY. LPRs were made at lipid:peptide:siRNA charge ratio of 0.5:6:1 and contained 0.1 mg/mL sigma siRNA. Vesicles used to prepare the LPRs composed of DOTMA:DOPE at 1:1 molar ratio and were aged ~48 h. SANS was measured at 25 ± 0.1°C on SANS2D.

4.1.6.2 Lipopolyplexes prepared in D_2O and diluted in Optimem or Media

The LPRs containing (HR)6BLY and prepared in D_2O is diluted either in Optimem or Media containing 10% FBS (1:1 v:v). The SANS data of the LPR dilutions is shown in Figure 4.17. The fitting of the LPR dilutions assuming the presence of single sheets is given in Table 4.2. The scattering intensity of the LPR dilutions was much lower than that of the original LPRs. It suggests that the LPRs precipitate when diluted in Optimem or Media due to the coverage of serum proteins present in Optimem or Media which is the same as the LPDs. There was no

difference in the scattering pattern for the LPRs diluted either in Optimem or Media, revealing the same bilayer structure.

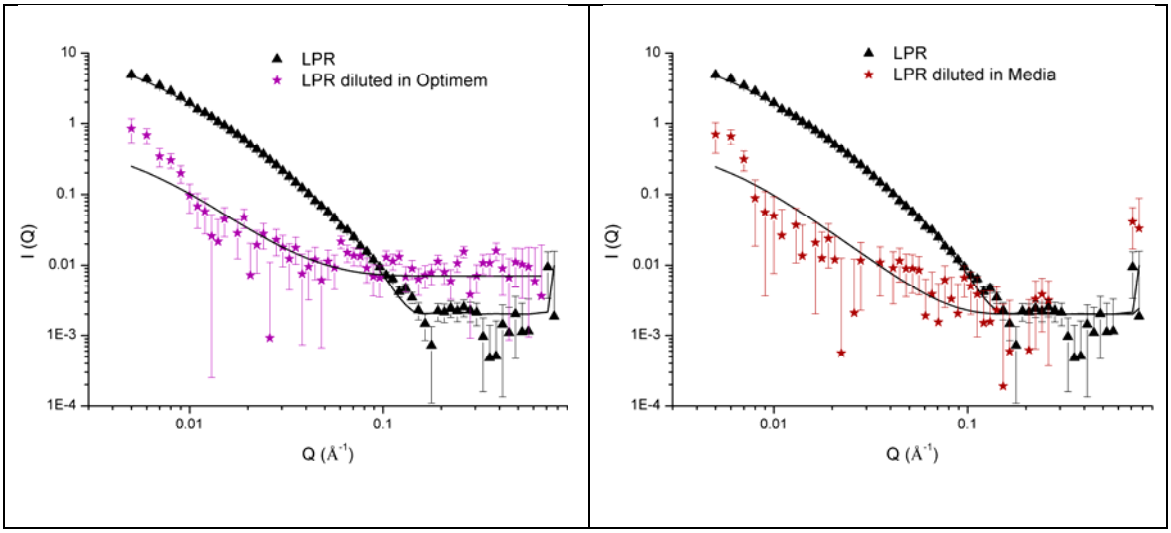

Figure 4.17 Small neutron scattering data (dots) and the best fit (solid line) to the data obtained for LPRs prepared using (HR)6BLY in D_2O and 1:1 diluted in Optimem and Media containing 10% v/v FBS. The LPRs were made at lipid:peptide:siRNA charge ratio of 0.5:6:1 (0.1 mg/mL sigma siRNA). Vesicles composed of DOTMA:DOPE at 1:1 molar ratio (1.0 mg/mL DOTMA) and were aged ~48 h. SANS measured at 25 ± 0.1°C on SANS2D.

Table 4.2 Structural parameters obtained from FISH modelling of the SANS data for LPRs containing (HR)6BLY in D_2O and 1:1 diluted in Optimem and Media containing 10% v/v FBS. LPRs were made at lipid:peptide:siRNA charge ratio of 0.5:6:1 (0.1 mg/mL sigma siRNA). Vesicles composed of DOTMA:DOPE at 1:1 molar ratio (1.0 mg/mL DOTMA) and were aged ~48 h. SANS was measured at 25 ± 0.1°C on SANS2D.

Samples	***L* (Å)**	**No. of layers**	***d*-spacing (Å)**	**R_{sigma} (Å)**	**Ratio of stack: sheet**	**Ratio of (I)**	**SWSE**
LPR	38.7 (±0.8)	-	-	300	-	-	219
LPR diluted in Optimem	38.7 (±39.5)	-	-	300	-	0.05	109
LPR diluted in Media	39.7 (±33.9)	-	-	300	-	0.03	60

Figures in brackets indicate the standard errors on the fitted parameter values. Ratio of stack to sheet represents the ratio of multilamellar surface area to unilamellar surface area. Ration of (I) reveals the ratio of diluted LPR's surface area to the original LPR's. SWSE is sum of weighted square error.

4.1.6.3 Lipopolyplexes prepared in NaCl solutions

In order to determine the effect of sodium chloride on the structure of the vesicles and the resulting LPRs, the SANS profile of the LPRs prepared in various strengths of NaCl solution, namely 0.04, 0.08 and 0.12 M prepared at a lipid:peptide:siRNA charge ratio of 0.5:6:1 and containing the peptide (HHR)4BLY is shown in Figure 4.18.

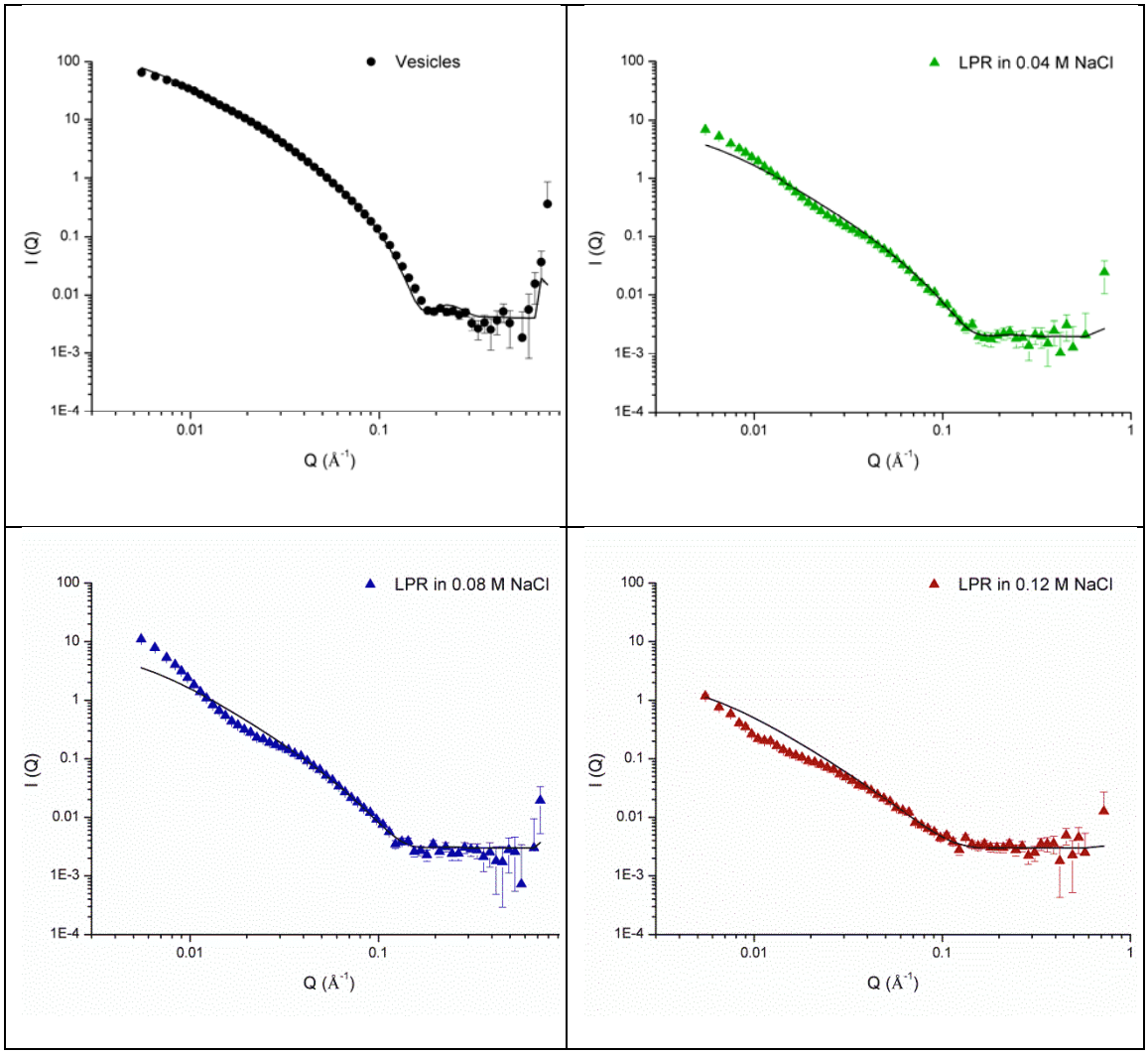

Figure 4.18 Small angle neutron scattering (SANS) data (dots) and the best fit to the data (solid line) for lipopolyplexes (LPRs) containing (HHR)4BLY. LPRs were made at lipid:peptide:siRNA charge ratio of 0.5:6:1 and contained 0.1 mg/mL sigma siRNA. Vesicles used to prepare the LPRs composed of DOTMA:DOPE at 1:1 molar ratio and were aged ~48 h. SANS was measured at 25 ± 0.1°C on SANS2D.

Unfortunately it did not prove possible to fit the SANS data over the whole Q range. It is interesting to see, however, that the LPRs prepared in NaCl solutions was well fitted in the high Q region (0.03 - 0.10 Å^{-1}) using sheet model. This observation suggests that perhaps more than

one structure of particle is present in the LPR preparation and that the main population within the LPR suspension has a structure of a single lipid bilayer. It should be noted that the increase in the SWSE is due to poor fit of the data at low Q. The thickness of the single bilayer obtained from the Fish modelling of this portion of the SANS curve is shown in Table 4.3. It was also possible to fit the SANS data for the LPRs prepared in the presence of NaCl well assuming the presence of hard spheres. The small size of these structures does not agree with the size of the LPRs obtained by dynamic light scattering which were much larger, once again suggesting the presence of more than one population of particle.

Table 4.3 Structural parameters obtained for the lipoolyplexes (LPRs) containing (HHR)4BLY prepared in NaCl solutions derived from FISH modelling of their SANS data. The LPRs was prepared at a sigma siRNA concentration of 0.1 mg/mL and a lipid:peptide:siRNA charge ratio of 0.5:12:1 and 0.5:6:1. Vesicles used to prepare the LPRs composed of DOTMA:DOPE at 1:1 molar ratio (1.0 mg/mL DOTMA) and were aged ~48 h. SANS was measured at 25 ± 0.1°C on SANS2D.

Samples	L (Å)	No. of layers	d-spacing (Å)	Rsigma (Å)	Ratio of stack: sheet	SWSE
Vesicles in D_2O	36.9 (±0.4)	-	-	300	-	6179
LPR in 0.04 M NaCl	36.9 (±3.9)	-	-	300	-	5880
LPR in 0.08 M NaCl	36.9 (±5.9)	-	-	300	-	14992
LPR in 0.12 M NaCl	36.9 (±9.0)	-	-	300	-	4050

Figures in brackets indicate the standard errors on the fitted parameter values. SWSE is sum of weighted square error. Ratio of stack to sheet represents the ratio of multilamellar surface area to unilamellar surface area.

4.1.7 Kinetic small angle neutron scattering

The formation of the lipopolyplexes (LPRs) and lipoplexes (LRs) was detected using a stopped flow SANS. The SANS curve obtained for the LPRs containing peptide K16 (0.5:6:1 lipid:peptide:siRNA charge ratio) using the usual 'static' measurement and the kinetic measurements (at equilibration state) is shown in Figure 4.19(a). The scattering curve for the parent DOTMA:DOPE vesicles is also displayed and scaled to the lipid concentration contained in the LPRs. When comparing the SANS data obtained for the LPRs prepared in two ways, the LPRs were overlapped well in the Q range of $0.01 < Q < 0.05$ $Å^{-1}$, but they did not overlap at the high and low Q area. Again, the origin of the high background for the SANS curve obtained using stopped flow is believed to be due to the gas detectors fitted at the time of the stopped

flow experiments. This data, however, suggests that at long time courses the various LPRs had the same structure.

Figure 4.19(b) depicts the evolution of the SANS curve for the LPRs using stopped flow measured every 60 sec for a total of 10 minutes. It can be seen that the neutron scattering does not change over this time period, suggesting that any structural change must occur more quickly than 60 seconds. The faster evolution (every 10 sec for a total of 1 minute) of the SANS curve for the LPRs is shown in Figure 4.19(c). There is no change in the neutron scattering over this time period, suggesting that any structural change occurs more quickly than 10 seconds.

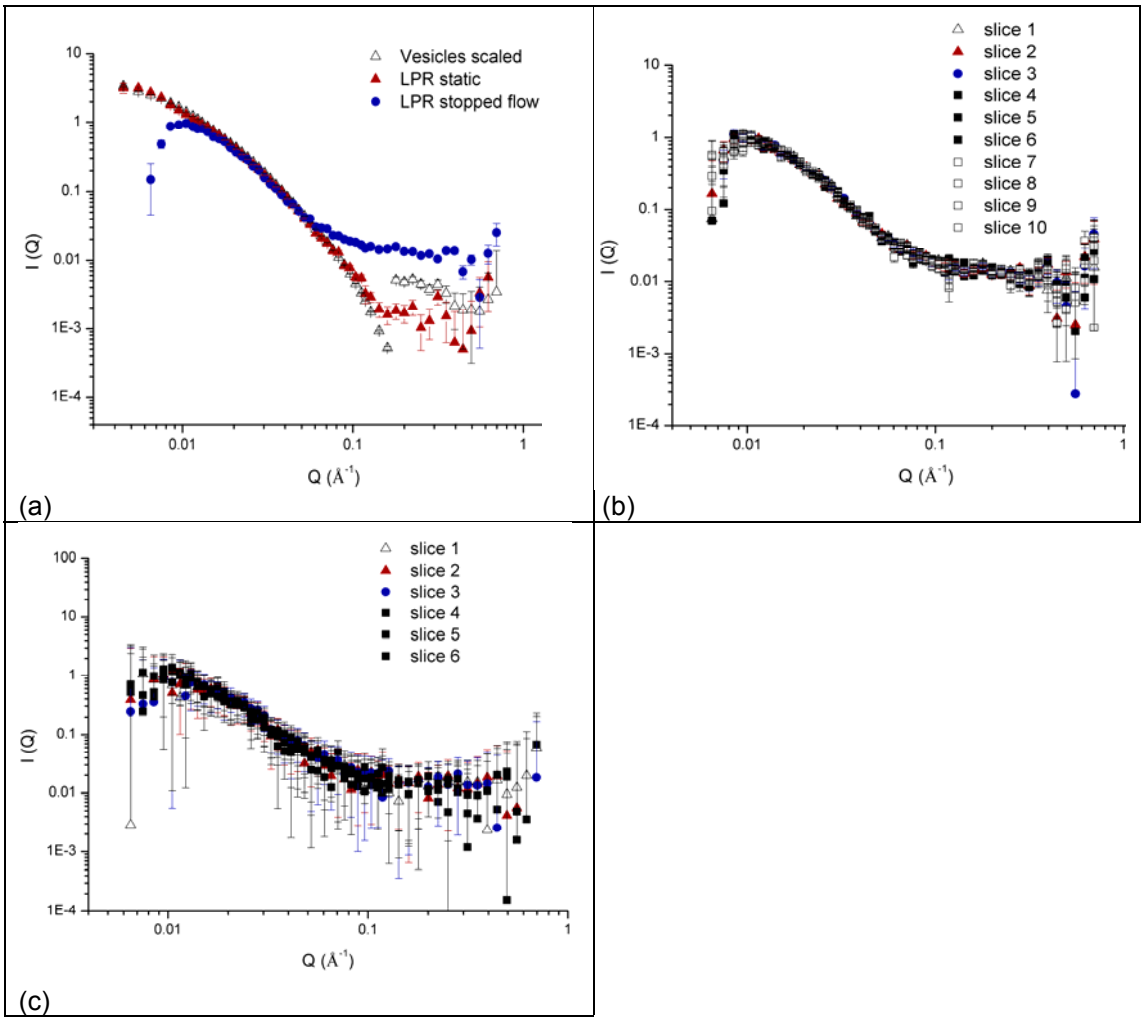

Figure 4.19 Small angle neutron scattering data for lipoplexes (LPRs) containing peptide K16 (a) static; (b) kinetic measurements time-sliced at 60 sec intervals over 600 sec (n = 14): slice 1 = 0 - 60 sec; Slice 2 = 61 - 120 sec; Slice 3 = 121-180 sec; Slice 4 = 181 - 240 sec; Slice 5 = 241 - 300 sec; Slice 6 = 301 - 360 sec; Slice 7 = 361 – 420; Slice 8 = 421-480 sec; Slice 9 = 481 - 540 sec; Slice 10 = 541 - 600 sec; (c) kinetic measurements time-sliced at 10 sec intervals over 60 sec: slice 1 = 0-10 seconds; slice 2 = 11-20 seconds; slice 3 = 21-30 seconds; slice 4 = 31-40 seconds; slice 5 = 41-50 seconds; slice 6 = 51-60 seconds. LPRs were made at a lipid:peptide:siRNA charge ratio of 0.5:6:1 and contained 0.1 mg/mL sigma siRNA. Vesicles composed of DOTMA:DOPE at 1:1 molar ratio and were aged ~48 h. SANS measured at 25 ± 0.1°C on SANS2D.

Figure 4.20(a) shows the SANS curve obtained for the LRs measured using the usual 'static' methodology and stopped flow at equilibration. While the SANS curve obtained using the normal static method exhibits a distinct Bragg peak, the corresponding data obtained from the stopped flow methodology did not. This lack of a Bragg peak is most likely due to the high background obtained for this sample masking the Bragg peak. The SANS curve obtained for the LR is clearly different to that seen for the parent vesicles.

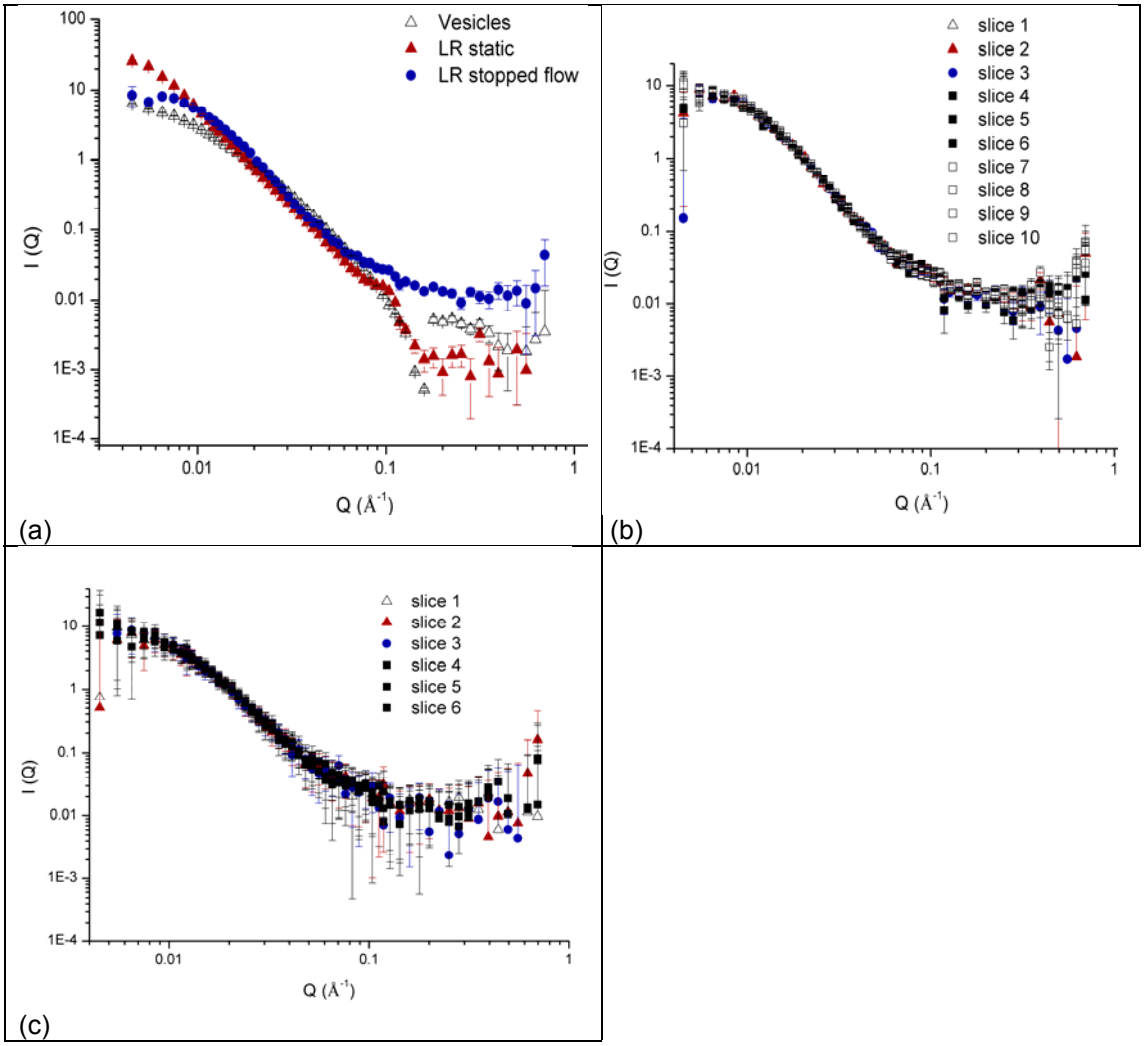

Figure 4.20 Small angle neutron scattering data for lipoplexes (LRs) (a) static; (b) kinetic measurements time-sliced at 60 sec intervals over 600 sec (n = 17): slice 1 = 0-60 sec; Slice 2 = 61-120 sec; Slice 3 = 121-180 sec; Slice 4 = 181-240 sec; Slice 5 = 241-300 sec; Slice 6 = 301-360 sec; Slice 7 = 361-420; Slice 8 = 421-480 sec; Slice 9 = 481-540 sec; Slice 10 = 541-600 sec; (c) kinetic measurements (time-sliced every 10 seconds for 60 seconds, n = 14): slice 1 = 0-10 seconds; slice 2 = 11-20 seconds; slice 3 = 21-30 seconds; slice 4 = 31-40 seconds; slice 5 = 41-50 seconds; slice 6 = 51-60 seconds. LRs were made at a lipid:siRNA charge ratio of 2:1 and contained 0.05 mg/mL (-)siRNA. Vesicles composed of DOTMA:DOPE at 1:1 molar ratio and were aged ~48 h. SANS measured at 25 ± 0.1°C on SANS2D.

Figure 4.20(b) depicts the evolution of the SANS curve for the LRs obtained using stopped flow measured every 60 sec for a total of 10 minutes. As can be seen the neutron scattering does not change over this time period, suggesting that any structural change must occur more quickly than 60 seconds. The 10 sec evolution for a total of 1 minute of the SANS curve for the LPRs is displayed in Figure 4.20(c). No change was observed over this time period, suggesting that any structural change must occur more quickly than 10 seconds.

4.2 Discussion

As reported in Chapter 3, DNA formulated as an LPD using the novel peptides developed in this study, exhibits effective transfection thereby influencing protein production. As DNA can only exert its effect in the nucleus of the cell, it can be concluded therefore that DNA has been translocated into nucleus by formulating it as a lipopolyplex. As with DNA, siRNA also plays an important role in the cellular regulation of proteins. Of particular interest in this part of the study is siRNA's ability to down regulate or 'silence' the production of a particular protein. The silencing effect of siRNA is achieved by its complimentarily binding to mRNA, resulting in the breakdown of mRNA (Montgomery et al, 1998) and a halting of protein production. Significantly in terms of gene delivery, as siRNA exerts its silencing effect in the cytosol rather than nucleus, it means it has to overcome fewer barriers to its site of action (Scholz et al, 2012).

In the present study, siRNA, as with DNA, has been complexed with a combination of lipid and bifunctional peptides to form a lipopolyplex (LPR). The ability of the LPRs to deliver successfully siRNA was assessed by measuring the level of luciferase expression *in vitro*. The negative control used in the study was a scrambled version of the siRNA, (-)siRNA, used such that the greater the difference in luciferase expression between siRNA and the negative control, the more effective the silencing.

It is interesting to note that, in the present study, the LPRs were far more effective at silencing protein production than their lipoplex (LR) and polyplex (PR) counterparts (Figure 4.2(a)). As was seen with DNA formulated as an LPD, the presence of both lipid and peptide in the siRNA containing LPR formulation exerted a beneficial effect on the delivery of siRNA. Again in agreement with the early studies on DNA, small angle neutron scattering (SANS) studies indicated that, while the counterpart LRs and PRs exhibited a multilamellar structure and no distinct structure, respectively the LPRs contained a lipid bilayer, predominantly in the form of a single bilayer (Figure 4.14). It was hypothesized in the present study that the differences in structure of the types of siRNA complex contributed to the synergistic effect on luciferase silencing observed in the presence of both lipid and peptide. By analogy with the LPD complexes studied, it is not unreasonable to assume that the LPRs contained a central core of siRNA and peptide surrounded by a bilayer of lipid. It is interesting that the structure of the lipid bilayer in the parent vesicles and the LPRs is the same and indeed the same as the bilayers

present in the LPDs, as evidenced by the SANS studies (Tables 3.1 and 4.1), suggesting that during the formation of the LPRs (and indeed LPDs) the vesicle bilayer must open and re-seal to allow entry of the peptide and siRNA (or DNA) which apparently forms the core of the nanoparticle. In support of the proposed structure of the lipopolyplexes in which siRNA is encapsulated inside lipid bilayer, it is of note that siRNA was protected from enzymatic degradation as seen by the gel electrophoresis studies (Figure 4.7).

In contrast to the situation observed for the LPDs, the preparation protocol of the LPRs had no effect on the ability of the LPRs to silence protein *in vitro* as the same level of silencing observed irrespective of preparation method (Figure 4.2(a)). It reveals that siRNA can be successfully delivered into cytosol no matter what preparation protocols. As the siRNA exerts its effect in cytosol of the cell, effective silencing can only be achieved if siRNA is released intact from the endosomes. It is worth noting that both the lipid, DOPE (Xu et al, 1996) and the histidine containing peptides (Tang et al, 1997, Midoux et al, 1999, Putnam et al, 2001) are potentially capable of facilitating the endosomal escape of the complex containing siRNA or of siRNA itself.

Regarding the effect of the bifunctional peptides, it is interesting to note that once again, the LPRs containing Series II peptides exhibited a superior silencing power over those containing Series I, presumably due to the presence of histidine residues in the Series II peptides (Figure 4.2(a) and 4.3(a)). In the Series II peptides, because of the presence of the histidine residues, it is expected that they behave like ‘proton sponges’ facilitating the endosomal escape of siRNA (Tang 1997, Midoux 1999, Putnam 2001). Additionally, the LPRs containing H12BLY peptides also exhibited a strong silencing activity (Figure 4.2(a), 4.3(a), 4.4, 4.5). Interestingly the LPDs containing H12BLY were not effective at delivering DNA (Figure 3.5(a), 3.7(a), 3.7(b), 3.8(a)). This difference might be a consequence of the different sites of intracellular action of siRNA and DNA. A major barrier for both the delivery of siRNA and DNA is their escape of the endosome. DNA in addition, has the additional barrier of nuclear translocation to overcome. An explanation as to different effects seen in the siRNA and DNA lipopolyplexes containing H12BLY is that while the H12BLY is able to facilitate the endosomal escape of siRNA and DNA due to its ability to act as a proton sponge, it does not promote the entry of DNA into the nucleus.

It is interesting, however, that the Series II peptides which contain a mixture of amino acids (HR or HK) are able to deliver DNA to nucleus of the cell as evidenced by the effective transfection of LPDs containing these peptides (Figure 3.5(a), 3.7(a), 3.7(b), 3.8(a)). In this context, it is of note that the effectiveness of these peptides in delivering DNA to the nucleus could be a consequence of the presence of the R/K sequence which is also present in nuclear translocation signal (NLS) peptides such as large T antigen NLS ($_{126}$PKKKRRV$_{132}$) and nucleoplasmin NLS ($_{155}$KRPAATKKAGQAKKKK$_{170}$) (Kalderon et al, 1984, Dingwall et al, 1991, Vives et al, 1997). Moreover, it was found that only a single NLS peptide is sufficient to carry DNA to cell nucleus, revealing an efficient NLS-mediated nuclear delivery (Zanta et al, 1999).

As was seen with the LPDs, the LPRs containing K4BLY exhibited a better activity than those containing K12BLY. The reason for this difference is not obvious. However, as was observed with the LPDs, the formation of a strong complex between the DNA and the rest of the lipopolyplexes was not beneficial for its subsequent release, leading to poor transfection. In may be therefore that the shorter length branches present in K4BLY in comparison to K12BLY might result in the easier release of siRNA leading to a better silencing. Indeed, it has been reported that LPRs containing linear peptides were more condensed and stable than branched peptide formulations, although in this case their silencing activity was lower (Tagalakis et al, 2013).

Moreover, it is interesting to note that LPRs prepared at a higher charge ratio tended to show more effective silencing (Figure 4.3(a)) while the LPDs prepared at a lower charge ratio were superior (Figure 3.5(a)). The difference in charge ratio requirement could be because DNA molecules are large and supercoiled while siRNA molecules are smaller and more rigid (Figure 1.1 and Table 1.1). Therefore, siRNA are expected to require more cationic materials to associate with and to facilitate their delivery, supported and evidenced by other studies (Byrne et al, 2013, Gu et al, 2014).

Regarding physicochemical properties of the LPRs, gel electrophoresis studies showed that the LPRs are effective at associating with, protecting and releasing the siRNA they encapsulate, as similar observation was made for the LPDs. The picogreen fluorescence assay, however, revealed a weaker condensation of siRNA with the lipopolyplexes when using the LPRs containing Series II peptides. This result is probably a consequence of the presence of histidine

residues in the Series II peptides, which due to it being a weak base would be expected to possess little ability to associate with siRNA.

Dynamic light scattering and ζ-potential measurements revealed that the LPRs prepared in water were very small particles with a positive charge (Figure 4.10(a)). In contrast to what was seen with the LPDs, the LPRs containing Series II peptides are the same size as those containing Series I peptides. The same size resulting from different peptides might be due to the same state that siRNA is complexed in the LPRs. It is reasonable to speculate that siRNA is associated with cationic materials rather than condensed due to the small size and rigid molecular structure of siRNA. Indeed, no conformational change was observed for the siRNA complexed in the LPRs as suggested by others' studies (Kudsiova et al, 2014). It is worth noting that unlike LPRs, LPDs containing Series II peptides possessed a larger size than those containing Series I (Figure 3.17). It is likely that DNA underwent a conformational change from the B-form to the more tightly packed C-form when condensed in the LPDs, an effect reported by others (Welser et al, 2013), supporting the hypothesis that the size of the LPD/LPR particles is related with the condensation/association state of DNA/siRNA. In addition, the size of the LPRs was larger and less stable than that of the LPDs when prepared in 0.12 M NaCl solution (Figure 4. 11(a), Figure 3.22(a)). It is consistent with the above assumption as well.

It is encouraging that the beneficial effect of NaCl on siRNA silencing mediated by lipopolyplexes in the presence of serum has also been observed for the LPRs (Figure 4.5(c)). To note, the intrinsic RNA-degrading enzyme activity of serum has been displayed in gel electrophoresis experiments (Figure 4.6). However, in the present study, it is not possible to correlate the siRNA silencing observed with the protection against enzyme degradation afforded by the LPRs prepared in 0.12 M NaCl, because naked siRNA was not completely degraded by RNAase A at the concentration investigated (Figure 4.7).

Moreover, the LPRs prepared in 0.12 M NaCl solution exhibit a weaker association of siRNA as assessed by the picogreen fluorescence assay (Figure 4.8 and 4.9). As with the LPDs, the weaker association is thought to be due to the charge screening effect of the salt. Furthermore, the LPRs containing peptides with histidine residues exhibit the weakest association, supporting the hypothesis that release from the complex is important for good silencing, an observation consistent with the results obtained for the LPDs.

Last but not least, the effective silencing seen with LPRs prepared in 0.12 M NaCl solution may be also the result of enhanced endosomal escape initiated by lipids. The lipids used in the LPR formulation include DOPE. DOPE typically forms non-bilayer structures, which are able to destabilise membranes and thereby facilitate the endosomal escape of DNA/siRNA complex (Figure 1.10) (Xu et al, 1996). The other lipid present in the LPRs/LPDs formulations is DOTMA. DOTMA is a bilayer lipid that has head and tails of similar volume. As the head of DOTMA molecule is positive, the repulsion of the charged heads of the adjacent DOTMA molecules can be reduced in the presence of NaCl due to a charge screening effect, resulting in a smaller effective head group volume. As a consequence, in the presence of NaCl, the DOTMA molecule could also adopt a cone-like structure favouring the formation of a reversed hexagonal structure, possibly facilitating endosomal escape and DNA/siRNA transfection/silencing.

Chapter 5 Conclusion

The aim of the present study is to establish a vector to deliver DNA/siRNA to targeted cancer cells. The vector established contains a ternary combination of cationic DOTMA:DOPE **L**ipids, a cationic novel **P**eptide, and a **D**NA/si**R**NA payload, denoted **LPD**s/**LPR**s. These LPDs/LPRs have shown far superior *in vitro* transfection/silencing over their binary LD/LR or PD/PR counterparts, which is found to be related with their structures. The special design of the novel peptides with a DNA/siRNA binding portion and a receptor targeting portion has contributed to the effective transfection/silencing of the LPDs/LPRs. In particular, Series II peptides are characteristic of histidine residues on their DNA/siRNA binding portion, conferring 'buffering effect' to facilitate endosomal escape and therefore its transfection/silencing.

Further *in vitro* transfection/silencing studies have shown that the LPDs/LPRs, irrespective prepared in water or NaCl solution (0.12 M), possessed the effective transfection/silencing when performed in Optimem (75% v/v). However, only the LPDs/LPRs prepared in NaCl solution (0.12 M) exhibited the effective transfection/silencing when performed in RPMI-1640 media containing 10% v/v FBS (75% v/v), revealing the importance of NaCl present in the formulation. Moreover, the transfection of the LPDs prepared in NaCl solutions has been found to be proportional to NaCl concentration (up to 0.12 M).

A comprehensive study on the physicochemical properties of the LPDs/LPRs prepared in NaCl solution (0.12 M) has been performed. In the complexation, release and protection studies performed by gel electrophoresis, all the LPDs/LPRs irrespective of in water or NaCl solutions have shown effective complexation and release properties. However, the LPDs/LPRs prepared in NaCl solutions (0.12 M) afforded better protection than those in water. Moreover, the protection capability of the LPDs increased with the NaCl concentration (up to 0.12 M). The protection of DNA/siRNA afforded by the LPDs/LPRs is found to be due to its encapsulation in a lipid bilayer as suggested by small angle neutron scattering experiments. Therefore, the transfection/silencing efficiency of the LPDs/LPRs can be correlated with their protection capability.

Furthermore, picogreen fluorescence assay has revealed a weaker DNA/siRNA condensation in the LPDs/LPRs when prepared in NaCl solution due to the charge screening effect of salt. The

weak DNA/siRNA condensation has been seen to be more obvious for the LPDs/LPRs containing Series II peptides due to the presence of histidine residues. In addition, the LPDs/LPRs prepared in NaCl solution are larger in apparent hydrodynamic size than those in water, consistent with looser condensation in the presence of NaCl. The loose DNA/siRNA condensation is beneficial to the release of the DNA/siRNA encapsulated in the LPDs/LPRs, which might contribute to their effective transfection/silencing.

Overall, the results of this study have suggested that the LPDs/LPRs containing the bifunctional peptides are effective DNA/siRNA delivery vector *in vitro*. However, there are still some issues to be solved. Firstly, the cellular fate of the resultant LPDs/LPRs needs to be illustrated, which may provide an insight into the related mechanism of effective DNA/siRNA delivery afforded by functionalised peptides and lipids, such as endosomal escape and nuclear translocation of DNA. On the other hand, the morphology and more detailed internal structure of the effective LPDs/LPRs should be studied which relates to their physicochemical properties and biological activities, providing useful information to the design of novel DNA/siRNA delivery vector. To be specific, the morphology of the LPD/LPR particles can be visualised using cryo-electron microscopy while the complexing state of the DNA/siRNA might be detected by small angle X-ray scattering. Besides, the stoichiometry of components of LPDs/LPRs can be detected using fluorescence correlation spectroscopy. Secondly, the effect of preparation and serum on the structure and physicochemical property of the LPDs/LPRs should be further clarified. Last but not least, the candidate LPDs/LPRs should be tested for safety and transfection/silencing efficiency in animals studies.

References

Aied A., Greiser U., Pandit A., Wang W.X. (2013). Polymer gene delivery: overcoming the obstacles. Drug Discovery Today **18**(21-22): 1090-1098.

Akinc A., Langer R. (2002). Measuring the pH environment of DNA delivered using nonviral vectors: Implications for lysosomal trafficking. Biotechnology and Bioengineering **78**(5): 503-508.

Akinc A., Thomas M., Klibanov A.M.Langer R. (2005). Exploring polyethylenimine-mediated DNA transfection and the proton sponge hypothesis. Journal of Gene Medicine **7**(5): 657-663.

Aleku M., Schulz P., Keil O., Santel A., Schaeper U., Dieckhoff B., Janke O., Endruschat J., Durieux B., Roder N., Loffler K., Lange C., Fechtner M., Mopert K., Fisch G., Dames S., Arnold W., Jochims K., Giese K., Wiedenmann B., Scholz A.Kaufmann J. (2008). Atu027, a liposomal small interfering RNA formulation targeting protein kinase N3, inhibits cancer progression. Cancer Research **68**(23): 9788-9798.

Alton E.W.F.W., Stern M., Farley R., Jaffe A., Chadwick S.L., Phillips J., Davies J., Smith S.N., Browning J., Davies M.G., Hodson M.E., Durham S.R., Li D., Jeffery P.K., Scallan M., Balfour R., Eastman S.J., Cheng S.H., Smith A.E., Meeker D.Geddes D.M. (1999). Cationic lipid-mediated CFTR gene transfer to the lungs and nose of patients with cystic fibrosis: a double-blind placebo-controlled trial. Lancet **353**(9157): 947-954.

Balazs DA G.W. (2011). Liposomes for use in gene delivery. Journal of Drug Delivery. Article ID 326497.

Behr J.P. (1997). The proton sponge: A trick to enter cells the viruses did not exploit. Chimia **51**(1-2): 34-36.

Benns J.M., Choi J.S., Mahato R.I., Park J.S.Kim S.W. (2000). pH-sensitive cationic polymer gene delivery vehicle: N-Ac-poly(L-histidine)-graft-poly(L-lysine) comb shaped polymer. Bioconjugate Chemistry **11**(5): 637-645.

Bernstein E., Caudy A.A., Hammond S.M., Hannon G.J. (2001). Role for a bidentate ribonuclease in the initiation step of RNA interference. Nature **409**(6818): 363-366.

Blaese R.M., Culver K.W., Miller A.D., Carter C.S., Fleisher T., Clerici M., Shearer G., Chang L., Chiang Y.W., Tolstoshev P., Greenblatt J.J., Rosenberg S.A., Klein H., Berger M., Mullen C.A., Ramsey W.J., Muul L., Morgan R.A., Anderson W.F. (1995). T-lymphocyte-directed gene-therapy for Ada(-) Scid - initial trial results after 4 years. Science **270**(5235): 475-480.

Boussif O., Lezoualch F., Zanta M.A., Mergny M.D., Scherman D., Demeneix B., Behr J.P. (1995). A versatile vector for gene and oligonucleotidetransfer into cells in culture and in-vivo - polyethylenimine. Proceedings of the National Academy of Sciences of the United States of America **92**(16): 7297-7301.

Bryant L.M., Christopher D.M., Giles A.R., Hinderer C., Rodriguez J.L., Smith J.B., Traxler E.A., Tycko J., Wojno A.P., Wilson J.M. (2013). Lessons learned from the clinical development and market authorization of Glybera. Human Gene Therapy Clinical Development **24**(2): 55-64.

Byrne M., Victory D., Hibbitts A., Lanigan M., Heise A., Cryan S.A. (2013). Molecular weight and architectural dependence of well-defined star-shaped poly(lysine) as a gene delivery vector. Biomaterials Science **1**(12): 1223-1234.

Caplen N.J., Parrish S., Imani F., Fire A., Morgan R.A. (2001). Specific inhibition of gene expression by small double-stranded RNAs in invertebrate and vertebrate systems. Proceedings of the National Acadamy of Science of the United States of America **98**(17): 9742-9747.

Cesana D., Ranzani M., Volpin M., Bartholomae C., Duros C., Artus A., Merella S., Benedicenti F., Sergi L.S., Sanvito F., Brombin C., Nonis A., Di Serio C., Doglioni C., von Kalle C., Schmidt M., Cohen-Haguenauer O., Naldini L., Montini E. (2014). Uncovering and dissecting the genotoxicity of self-inactivating lentiviral vectors in vivo. Molecular Therapy 22(4): 774-785.

Chen Q.R., Zhang L., Stass S.A., Mixson A.J. (2001). Branched copolymers of histidine and lysine are efficient carriers of plasmid. European Journal of Pharmaceutics and Biopharmaceutics 54(2): 165–170.

Chen C.W., Yeh M.K., Shiau C.Y., Chiang C.H., Lu D.W. (2013). Efficient downregulation of VEGF in retinal pigment epithelial cells by integrin ligand-labeled liposome-mediated siRNA delivery. International Journal of Nanomedicine **8**: 2613-2627.

Chen G., Kronenberger P., Teugels E., Umelo I.A., De Greve J. (2012). Targeting the epidermal growth factor receptor in non-small cell lung cancer cells: the effect of combining RNA interference with tyrosine kinase inhibitors or cetuximab. Biomedicalcentral Medicine **10**:28.

Chen J., Sun X., Yu Z., Gao J., Liang W. (2012). Influence of lipid components on gene delivery by polycation liposomes: transfection efficiency, intracellular kinetics and in vivo tumor inhibition. International Journal of Pharmaceutics **422**(1-2): 510-515.

Chen Y., Bathula S.R., Yang Q., Huang L. (2010). Targeted nanoparticles deliver siRNA to melanoma. Journal of Investigative Dermatology **130**(12): 2790-2798.

Cherng J.Y., Talsma H., Crommelin D.J.A., Hennink W.E. (1999). Long term stability of poly((2-dimethylamino)ethyl methacrylate)-based gene delivery systems. Pharmaceutical Research **16**(9): 1417-1423.

Chono S., Li S.D., Conwell C.C., Huang L. (2008). An efficient and low immunostimulatory nanoparticle formulation for systemic siRNA delivery to the tumor. Journal of Controlled Release **131**(1): 64-69.

Chou S.T., Leng Q., Scaria P., Woodle M., Mixson A.J. (2011). Selective modification of HK peptides enhances siRNA silencing of tumor targets in vivo. Cancer Gene Therapy **18**(10): 707-716.

Chou S.T., Leng Q.X., Scaria P., Kahn J.D., Tricoli L.J., Woodle M., Mixson A.J. (2013). Surface-modified HK:siRNA nanoplexes with enhanced pharmacokinetics and tumour growth inhibition. Biomacromolecules **14**(3): 752-760.

Davis M.E., Zuckerman J.E., Choi C.H.J., Seligson D., Tolcher A., Alabi C.A., Yen Y., Heidel J.D., Ribas A. (2010). Evidence of RNAi in humans from systemically administered siRNA via targeted nanoparticles. Nature **464**(7291): 1067-U1140.

De Souza A.T., Dai X.D., Spencer A.G., Reppen T., Menzie A., Roesch P.L., He Y.D., Caguyong M.J., Bloomer S., Herweijer H., Wolff J.A., Hagstrom J.E., Lewis D.L., Linsley P.S., Ulrich R.G. (2006). Transcriptional and phenotypic comparisons of Ppara knockout and siRNA knockdown mice. Nucleic Acids Research **34**(16): 4486-4494.

Desgrosellier J.S., Cheresh D.A. (2010). Integrins in cancer: biological implications and therapeutic opportunities. Nature Reviews Cancer **10**(1): 9-22.

Devi G.R. (2006). siRNA-based approaches in cancer therapy. Cancer Gene Therapy **13**(9): 819-829.

Dingwall C., Laskey R.A. (1991). Nuclear targeting sequences - a consensus. Trends in Biochemical Sciences **16**(12): 478-481.

Donsante A., Vogler C., Muzyczka N., Crawford J.M., Barker J., Flotte T., Campbell-Thompson M., Daly T., Sands M.S. (2001). Observed incidence of tumorigenesis in long-term rodent studies of rAAV vectors. Gene Therapy **8**(17): 1343-1346.

Dragan A.I., Casas-Finet J.R., Bishop E.S., Strouse R.J., Schenerman M.A., Geddes C.D. (2010). Characterization of picogreen interaction with dsDNA and the origin of its fluorescence enhancement upon binding. Biophysical Journal **99**(9): 3010-3019.

Dunlap D.D., Maggi A., Soria M.R., Monaco L. (1997). Nanoscopic structure of DNA condensed for gene delivery. Nucleic Acids Research **25**(15): 3095-3101.

Escriou V., Ciolina C., Lacroix F., Byk G., Scherman D., Wils P. (1998). Cationic lipid-mediated gene transfer: effect of serum on cellular uptake and intracellular fate of lipopolyamine/DNA complexes. Biochimica Et Biophysica Acta-Biomembranes **1368**(2): 276-288.

Even-Chen S., Cohen R., Barenholz Y. (2012). Factors affecting DNA binding and stability of association to cationic liposomes. Chemistry and Physics of Lipids **165**(4): 414-423.

Fang B.L., Roth J.A. (2003). Tumour-suppressing gene therapy. Cancer Biology & Therapy **2**(4): S115-S121.

Felgner P.L., Gadek T.R., Holm M., Roman R., Chan H.W., Wenz M., Northrop J.P., Ringold G.M., Danielsen M. (1987). Lipofection - a highly efficient lipid-mediated DNA-transfection procedure. Proceedings of the National Academy of Sciences of the United States of America **84**(21): 7413-7417.

Fire A., Xu S.Q., Montgomery M.K., Kostas S.A., Driver S.E., Mello C.C. (1998). Potent and specific genetic interference by double-stranded RNA in Caenorhabditis elegans. Nature **391**(6669): 806-811.

Fitzgerald K., Frank-Kamenetsky M., Shulga-Morskaya S., Liebow A., Bettencourt B.R., Sutherland J.E., Hutabarat R.M., Clausen V.A., Karsten V., Cehelsky J., Nochur S.V., Kotelianski V., Horton J., Mant T., Chiesa J., Ritter J., Munisamy M., Vaishnaw A.K., Gollob J.A., Simon A. (2014). Effect of an RNA interference drug on the synthesis of proprotein convertase subtilisin/kexin type 9 and the concentration of serum LDL cholesterol in healthy volunteers: a randomised, single-blind, placebo-controlled, phase 1 trial. Lancet **383**(9911): 60-68.

Freitas C., Muller R.H. (1998). Effect of light and temperature on zeta potential and physical stability in solid lipid nanoparticle (SLN (TM)) dispersions. International Journal of Pharmaceutics **168**(2): 221-229.

Gao X., Huang L. (1996). Potentiation of cationic liposome-mediated gene delivery by polycations. Biochemistry **35**(3): 1027-1036.

Garcia L., Bunuales M., Duzgunes N., Tros de Ilarduya C. (2007). Serum-resistant lipopolyplexes for gene delivery to liver tumour cells. European Journal of Pharmaceutics and Biopharmaceutics **67**(1): 58-66.

Georgiou C.D., Papapostolou I. (2006). Assay for the quantification of intact/fragmented genomic DNA. Analytical Biochemistry 358(2): 247-256.

Gesser A., Lieke A., Paulke B.R., Muller R.H. (2002). Influence of surface charge density on protein adsorption on polymeric nanoparticles: analysis by two-dimensional electrophoresis. European Journal of Pharmaceutics and Biopharmaceutics 54(2):165–170.

Godbey W.T., Wu K.K., Mikos A.G. (1999). Size matters: molecular weight affects the efficiency of poly(ethylenimine) as a gene delivery vehicle. Journal of Biomedical Materials Research **45**(3): 268-275.

Goldring W.P.D., Jubeli E., Downs R.A., Johnston A.J.S., Khalique N.A., Raju L., Wafadari D., Pungente M.D. (2012). Novel macrocyclic and acyclic cationic lipids for gene transfer: synthesis and in vitro evaluation. Bioorganic & Medicinal Chemistry Letters **22**(14): 4686-4692.

Gu L., Nusblat L.M., Tishbi N., Noble S.C., Pinson C.M., Mintzer E., Roth C.M., Uhrich K.E. (2014). Cationic amphiphilic macromolecule (CAM)-lipid complexes for efficient siRNA gene silencing. Journal of Controlled Release **184**: 28-35.

Hama S., Akita H., Ito R., Mizuguchi H., Hayakawa T., Harashima H. (2006). Quantitative comparison of intracellular trafficking and nuclear transcription between adenoviral and lipoplex systems. Molecular Therapy **13**(4): 786-794.

Hammond S.M., Bernstein E., Beach D., Hannon G.J. (2000). An RNA-directed nuclease mediates post-transcriptional gene silencing in Drosophila cells. Nature **404**(6775): 293-296.

Hart S.L., Arancibia-Carcamo C.V., Wolfert M.A., Mailhos C., O'Reilly N.J., Ali R.R., Coutelle C., George A.J., Harbottle R.P., Knight A.M., Larkin D.F., Levinsky R.J., Seymour L.W., Thrasher A.J., Kinnon C. (1998). Lipid-mediated enhancement of transfection by a nonviral integrin-targeting vector. Human Gene Therapy **9**(4): 575-585.

Hartikka J., Bozoukova V., Jones D., Mahajan R., Wloch M.K., Sawdey M., Buchner C., Sukhu L., Barnhart K.M., Abai A.M., Meek J., Shen N., Manthorpe M. (2000). Sodium phosphate enhances plasmid DNA expression in vivo. Gene Therapy **7**(14): 1171-1182.

Harvie P., Dutzar B., Galbraith T., Cudmore S., O'Mahony D., Anklesaria P., Paul R. (2003). Targeting of lipid-protamine-DNA (LPD) lipopolyplexes using RGD motifs. Journal of Liposome Research **13**(3-4): 231-247.

Hatakeyama H., Ito E., Akita H., Oishi M., Nagasaki Y., Futaki S., Harashima H. (2009). A pH-sensitive fusogenic peptide facilitates endosomal escape and greatly enhances the gene silencing of siRNA-containing nanoparticles in vitro and in vivo. Journal of Controlled Release **139**(2): 127-132.

Haupenthal J., Baehr C., Zeuzem S., Piiper A. (2007). RNAse A-like enzymes in serum inhibit the anti-neoplastic activity of siRNA targeting Polo-like kinase 1. International Journal of Cancer **121**(1): 206-210.

Hirsch-Lerner D., Zhang M., Eliyahu H., Ferrari M.E., Wheeler C.J., Barenholz Y. (2005). Effect of "helper lipid" on lipoplex electrostatics. Biochimica et Biophysica Acta-Biomembranes **1714**(2): 71-84.

Hofland H.E.J., Shephard L., Sullivan S.M. (1996). Formation of stable cationic lipid/DNA complexes for gene transfer. Proceedings of the National Academy of Sciences of the United States of America **93**(14): 7305-7309.

Huynh N.T., Passirani C., Saulnier P., Benoit J.P. (2009). Lipid nanocapsules: A new platform for nanomedicine. International Journal of Pharmaceutics **379**(2): 201-209.

Hyndman L., Lemoine J.L., Huang L., Porteous D.J., Boyd A.C., Nan X. (2004). HIV-1 Tat protein transduction domain peptide facilitates gene transfer in combination with cationic liposomes. Journal of Controlled Release **99**(3): 435-444.

Hyndman L., Lemoine J.L., Huang L., Porteous D.J., Boyd A.C., Nan X.S. (2004). HIV-1 Tat protein transduction domain peptide facilitates gene transfer in combination with cationic liposomes. Journal of Controlled Release **99**(3): 435-444.

Hynes N.E., Lane H.A. (2005). ERBB receptors and cancer: The complexity of targeted inhibitors. Nature Reviews Cancer **5**(5): 341-354.

Immordino M.L., Dosio F., Cattel L. (2006). Stealth liposomes: review of the basic science, rationale, and clinical applications, existing and potential. International Journal of Nanomedicine **1**(3): 297-315.

Inoue Y., Kurihara R., Tsuchida A., Hasegawa M., Nagashima T., Mori T., Niidome T., Katayama Y., Okitsu O. (2008). Efficient delivery of siRNA using dendritic poly(L-lysine) for loss-of-function analysis. Journal of Controlled Release **126**(1): 59-66.

Ishida O., Maruyama K., Tanahashi H., Iwatsuru M., Sasaki K., Eriguchi M., Yanagie H. (2001). Liposomes bearing polyethyleneglycol-coupled transferrin with intracellular targeting property to the solid tumors in vivo. Pharmaceutical Research **18**(7): 1042-1048.

Kalderon D., Richardson W.D., Markham A.F., Smith A.E. (1984). Sequence requirements for nuclear location of Simian Virus-40 Large-T-Antigen. Nature **311**(5981): 33-38.

Kanai Y., Ushijima S., Nakanishi Y., Sakamoto M., Hirohashi S. (2003). Mutation of the DNA methyltransferase (DNMT) 1 gene in human colorectal cancers. Cancer Letters **192**(1): 75-82.

Kazunori K.T., Ryouji K., Yasuya K., Shota K., Yoichi T., Kazuo S. (2005). Transition from a normal to inverted cylinder for an amidine-bearing lipid/pDNA complex and its excellent transfection. Bioconjugate Chemistry **16** (6):1349–1351.

Khalil I.A., Kogure K., Futaki S., Hama S., Akita H., Ueno M., Kishida H., Kudoh M., Mishina Y., Kataoka K., Yamada M., Harashima H. (2007). Octaarginine-modified multifunctional envelope-type nanoparticles for gene delivery. Gene Therapy **14**(8): 682-689.

Kim J.K., Choi S.H., Kim C.O., Park J.S., Ahn W.S., Kim C.K. (2003). Enhancement of polyethylene glycol (PEG)-modified cationic liposome-mediated gene deliveries: effects on serum stability and transfection efficiency. Journal of Pharmacy and Pharmacology **55**(4): 453-460.

Kim S.S., Peer D., Kumar P., Shimaoka M., Shankar P. (2009). siRNA Delivery with Integrin LFA-1-targeted nanoparticles prevents HIV infection in humanized mice. Clinical Immunology **131**: S75-S76.

Kim T.I., Ou M., Lee M., Kim S.W. (2009). Arginine-grafted bioreducible poly(disulfide amine) for gene delivery systems. Biomaterials **30**(4): 658-664.

Knop K., Hoogenboom R., Fischer D., Schubert U.S. (2010). Poly(ethylene glycol) in drug delivery: pros and cons as well as potential alternatives. Angewandte Chemie-International Edition **49**(36): 6288-6308.

Kogure K., Moriguchi R., Sasaki K., Ueno M., Futaki S., Harashima H. (2004). Development of a non-viral multifunctional envelope-type nano device by a novel lipid film hydration method. Journal of Controlled Release **98**(2): 317-323.

Koichiro Kishia T.Y., Haruo Takeshitaa (2001). DNase I: structure, function, and use in medicine and forensic science. Legal Medicine **3**: 69-83.

Kudsiova L., Welser K., Campbell F., Mohammadi A., Dawson N., Cui L., Hailes H.C., Lawrence M.J., Tabor A.B. (2014). Targeted delivery of siRNA using ternary complexes containing branched cationic peptides: the role of peptide sequence and branching. Submitted to Biomaterials.

Kudsiova L., Fridrich B., Ho J., Mustapa M.F., Campbell F., Welser K., Keppler M., Ng T., Barlow D.J., Tabor A.B., Hailes H.C., Lawrence M.J. (2011a). Lipopolyplex ternary delivery systems incorporating C14 glycerol-based lipids. Mollecular Pharmaceutics **8**(5): 1831-1847.

Kudsiova L., Ho J., Fridrich B., Harvey R., Keppler M., Ng T., Hart S.L., Tabor A.B., Hailes H.C., Lawrence M.J. (2011b). Lipid chain geometry of C14 glycerol-based lipids: effect on lipoplex structure and transfection. Mollecular Biosystem **7**(2): 422-436.

Kwak E.L., Bang Y.J., Camidge D.R., Shaw A.T., Solomon B., Maki R.G., Ou S.H.I., Dezube B.J., Janne P.A., Costa D.B., Varella-Garcia M., Kim W.H., Lynch T.J., Fidias P., Stubbs H., Engelman J.A., Sequist L.V., Tan W.W., Gandhi L., Mino-Kenudson M., Wei G.C., Shreeve S.M., Ratain M.J., Settleman J., Christensen J.G., Haber D.A., Wilner K., Salgia R., Shapiro G.I., Clark J.W., Iafrate A.J. (2010). Anaplastic lymphoma kinase inhibition in non-small-cell lung cancer. New England Journal of Medicine **363**(18): 1693-1703.

Laemmli U.K. (1975). Characterization of DNA condensates induced by poly(ethylene oxide) and polylysine. Proceedings of the National Academy of Sciences of the United States of America **72**(11): 4288-4292.

Lechardeur D., Verkman A.S., Lukacs G.L. (2005). Intracellular routing of plasmid DNA during non-viral gene transfer. Advanced Drug Delivery Reviews **57**(5): 755-767.

Lechardeur D., Verkman A.S., Lukacs G.L. (2005). Intracellular routing of plasmid DNA during non-viral gene transfer. Advanced Drug Delivery Review **57**(5): 755-767.

Leenders F., Mopert K., Schmiedeknecht A., Santel A., Czauderna F., Aleku M., Penschuck S., Dames S., Sternberger M., Rohl T., Wellmann A., Arnold W., Giese K., Kaufmann J., Klippel A. (2004). PKN3 is required for malignant prostate cell growth downstream of activated PI 3-kinase. The EMBO Journal **23**(16): 3303-3313.

Leng Q., Scaria P., Lu P., Woodle M.C., Mixson A.J. (2008). Systemic delivery of HK Raf-1 siRNA polyplexes inhibits MDA-MB-435 xenografts. Cancer Gene Therapy **15**(8): 485-495.

Leng Q., Scaria P., Zhu J., Ambulos N., Campbell P., Mixson A.J. (2005). Highly branched HK peptides are effective carriers of siRNA. Journal of Gene Medicine **7**(7): 977-986.

Leng Q.X., Chou S.T., Scaria P.V., Woodle M.C., Mixson A.J. (2012). Buffering capacity and size of siRNA polyplexes influence cytokine levels. Molecular Therapy **20**(12): 2282-2290.

Leng Q.X., Mixson A.J. (2005). Modified branched peptides with a histidine-rich tail enhance in vitro gene transfection. Nucleic Acids Research **33**(4): e40.

Li J., Chen Y.C., Tseng Y.C., Mozumdar S., Huang L. (2010). Biodegradable calcium phosphate nanoparticle with lipid coating for systemic siRNA delivery. Journal of Controlled Release **142**(3): 416-421.

Li S., Huang L. (1997). In vivo gene transfer via intravenous administration of cationic lipid-protamine-DNA (LPD) complexes. Gene Therapy **4**(9): 891-900.

Li S., Rizzo M.A., Bhattacharya S., Huang L. (1998). Characterization of cationic lipid-protamine-DNA (LPD) complexes for intravenous gene delivery. Gene Therapy **5**(7): 930-937.

Li S.D., Chen Y.C., Hackett M.J., Huang L. (2008). Tumor-targeted delivery of siRNA by self-assembled nanoparticles. Molecular Therapy **16**(1): 163-169.

Liu F., Qi H., Huang L., Liu D. (1997). Factors controlling the efficiency of cationic lipid-mediated transfection in vivo via intravenous administration. Gene Therapy **4**(6): 517-523.

Liu F., Shollenberger L.M., Conwell C.C., Yuan X., Huang L. (2007). Mechanism of naked DNA clearance after intravenous injection. Journal of Gene Medicine **9**(7): 613-619.

Liu F., Yang J.P., Huang L., Liu D.X. (1996). Effect of non-ionic surfactants on the formation of DNA/emulsion complexes and emulsion-mediated gene transfer. Pharmaceutical Research **13**(11): 1642-1646.

Liu J.L., Ma Q.P., Huang Q.D., Yang W.H., Zhang J., Wang J.Y., Zhu W., Yu X.Q. (2011). Cationic lipids containing protonated cyclen and different hydrophobic groups linked by uracil-PNA monomer: Synthesis and application for gene delivery. European Journal of Medicinal Chemistry **46**(9): 4133-4141.

Lo S.L., Wang S. (2008). An endosomolytic Tat peptide produced by incorporation of histidine and cysteine residues as a nonviral vector for DNA transfection. Biomaterials **29**(15): 2408-2414.

Lundqvist M., Stigler J., Elia G., Lynch I., Cedervall T., Dawson K.A. (2008). Nanoparticle size and surface properties determine the protein corona with possible implications for biological impacts. Proceedings of the National Academy of Sciences of the United States of America **105**(38): 14265-14270.

Mack G.S. (2007). MicroRNA gets down to business. Nature Biotechnology **25**(6): 631-638.

Mann A., Shukla V., Khanduri R., Dabral S., Singh H., Ganguli M. (2014). Linear short histidine and cysteine modified arginine peptides constitute a potential class of DNA delivery agents. Molecular Pharmaceutics **11**(3): 683-696.

Mannisto M., Vanderkerken S., Toncheva V., Elomaa M., Ruponen M., Schacht E., Urtti A. (2002). Structure-activity relationships of poly(L-lysines): effects of pegylation and molecular shape on physicochemical and biological properties in gene delivery. Journal of Controlled Release **83**(1): 169-182.

Masuda T., Akita H., Nishio T., Niikura K., Kogure K., Ijiro K., Harashima H. (2008). Development of lipid particles targeted via sugar-lipid conjugates as novel nuclear gene delivery system. Biomaterials **29**(6): 709-723.

Midoux P., Monsigny M. (1999). Efficient gene transfer by histidylated polylysine pDNA complexes. Bioconjugate Chemistry **10**(3): 406-411.

Miyagishi M., Hayashi M., Taira K. (2003). Comparison of the suppressive effects of antisense oligonucleotides and siRNAs directed against the same targets in mammalian cells. Antisense & Nucleic Acid Drug Development **13**(1): 1-7.

Moghimi S.M., Symonds P., Murray J.C., Hunter A.C., Debska G., Szewczyk A. (2005). A two-stage poly(ethylenimine)-mediated cytotoxicity: Implications for gene transfer/therapy. Molecular Therapy **11**(6): 990-995.

Montgomery M.K., Xu S.Q., Fire A. (1998). RNA as a target of double-stranded RNA-mediated genetic interference in Caenorhabditis elegans. Proceedings of the National Academy of Sciences of the United States of America **95**(26): 15502-15507.

Mounkes L.C., Zhong W., Cipres-Palacin G., Heath T.D., Debs R.J. (1998). Proteoglycans mediate cationic liposome-DNA complex-based gene delivery in vitro and in vivo. Journal of Biological Chemistry **273**(40): 26164-26170.

Mukherjee A., Prasad T.K., Rao N.M., Banerjee R. (2005). Haloperidol-associated stealth liposomes - A potent carrier for delivering genes to human breast cancer cells. Journal of Biological Chemistry **280**(16): 15619-15627.

Murray K.D., Etheridge C.J., Shah S.I., Matthews D.A., Russell W., Gurling H.M., Miller A.D. (2001). Enhanced cationic liposome-mediated transfection using the DNA-binding peptide mu from the adenovirus core. Gene Therapy **8**(6): 453-460.

Mustapa M.F., Grosse S.M., Kudsiova L., Elbs M., Raiber E.A., Wong J.B., Brain A.P., Armer H.E., Warley A., Keppler M., Ng T., Lawrence M.J., Hart S.L., Hailes H.C., Tabor A.B. (2009). Stabilized integrin-targeting ternary LPD (lipopolyplex) vectors for gene delivery designed to disassemble within the target cell. Bioconjugate Chemistry **20**(3): 518-532.

Mustapa M.F., Bell P.C., Hurley C.A., Nicol A., Guenin E., Sarkar S., Writer M.J., Barker S.E., Wong J.B., Pilkington-Miksa M.A., Papahadjopoulos-Sternberg B., Shamlou P.A., Hailes H.C., Hart S.L., Zicha D., Tabor A.B. (2007). Biophysical characterization of an integrin-targeted lipopolyplex gene delivery vector. Biochemistry **46**(45): 12930-12944.

Nakamura Y., Kogure K., Futaki S., Harashima H. (2007). Octaarginine-modified multifunctional envelope-type nano device for siRNA. Journal of Controlled Release **119**(3): 360-367.

Nel A.E., Madler L., Velegol D., Xia T., Hoek E.M.V., Somasundaran P., Klaessig F., Castranova V., Thompson M. (2009). Understanding biophysicochemical interactions at the nano-bio interface. Nature Materials **8**(7): 543-557.

Nguyen H.D., Nguyen Q.A., Ferreira R.C., Ferreira L.C.S., Tran L.T., Schumann W. (2005). Construction of plasmid-based expression vectors for Bacillus subtilis exhibiting full structural stability. Plasmid **54**(3): 241-248.

Nicholson R.I., Gee J.M.W., Harper M.E. (2001). EGFR and cancer prognosis. European Journal of Cancer **37**: S9-S15.

Niven R., Pearlman R., Wedeking T., Mackeigan J., Noker P., Simpson-Herren L.Smith J.G. (1998). Biodistribution of radiolabeled lipid - DNA complexes and DNA in mice. Journal of Pharmaceutical Sciences **87**(11): 1292-1299.

Ohsaki M., Okuda T., Wada A., Hirayama T., Niidome T., Aoyagi H. (2002). In vitro gene transfection using dendritic poly(L-lysine). Bioconjugate Chemistry **13**(3): 510-517.

Okuda T., Sugiyama A., Niidome T., Aoyagi H. (2004). Characters of dendritic poly((L)-lysine) analogues with the terminal lysines replaced with arginines and histidines as gene carriers in vitro. Biomaterials **25**(3): 537-544.

Okuda T., Kidoaki S., Ohsaki M., Koyama Y., Yoshikawa K., Niidome T., Aoyagi H. (2003). Time-dependent complex formation of dendritic poly(L-lysine) with plasmid DNA and correlation with in vitro transfection efficiencies. Organic & Biomolecular Chemistry **1**(8): 1270-1273.

Opstad C.L., Sliwka H.R., Partali V., Elgsaeter A., Leopold P., Jubeli E., Khalique N.A., Raju L., Pungente M.D. (2013). Synthesis, self-assembling and gene delivery potential of a novel highly unsaturated, conjugated cationic phospholipid. Chemistry and Physics of Lipids **170**: 65-73.

Ou M., Xu R.Z., Kim S.H., Bull D.A., Kim S.W. (2009). A family of bioreducible poly(disulfide amine)s for gene delivery. Biomaterials **30**(29): 5804-5814.

Patnaik S., Gupta K.C. (2013). Novel polyethylenimine-derived nanoparticles for in vivo gene delivery. Expert Opinion on Drug Delivery **10**(2): 215-228.

Pearson S., Jia H.P., Kandachi K. (2004). China approves first gene therapy. Nature Biotechnology **22**(1): 3-4.

Pilkington-Miksa M.A., Sarkar S., Writer M.J., Barker S.E., Shamlou P.A., Hart S.L., Hailes H.C., Tabor A.B. (2008). Synthesis of bifunctional integrin-binding peptides containing PEG spacers of defined length for non-viral gene delivery. European Journal of Organic Chemistry **2008**(17): 2900-2914.

Pushparaj P.N., Aarthi J.J., Manikandan J., Kumar S.D. (2008). siRNA, miRNA, and shRNA: in vivo Applications. Journal of Dental Research **87**(11): 992-1003.

Putnam D., Gentry C.A., Pack D.W., Langer R. (2001). Polymer-based gene delivery with low cytotoxicity by a unique balance of side-chain termini. Proceedings of the National Academy of Sciences of the United States of America **98**(3): 1200-1205.

Quaye L., Gayther S.A., Ramus S.J., Di Cioccio R.A., McGuire V., Hogdall E., Hogdall C., Blaakr J., Easton D.F., Ponder B.A.J., Jacobs I., Kjaer S.K., Whittemore A.S., Pearce C.L., Pharoah P.D.P., Song H. (2008). The effects of common genetic variants in oncogenes on ovarian cancer survival. Clinical Cancer Research **14**(18): 5833-5839.

Rana T.M. (2007). Illuminating the silence: understanding the structure and function of small RNAs. Nature Reviews Molecular Cell Biology **8**(1): 23-36.

Ratcliff F., Harrison B.D., Baulcombe D.C. (1997). A similarity between viral defense and gene silencing in plants. Science **276**(5318): 1558-1560.

Ren T., Song Y.K., Zhang G., Liu D. (2000). Structural basis of DOTMA for its high intravenous transfection activity in mouse. Gene Therapy **7**(9): 764-768.

Ribbeck K., Gorlich D. (2001). Kinetic analysis of translocation through nuclear pore complexes. Embo Journal **20**(6): 1320-1330.

Sakurai F., Nishioka T., Saito H., Baba T., Okuda A., Matsumoto O., Taga T., Yamashita F., Takakura Y., Hashida M. (2001a). Interaction between DNA-cationic liposome complexes and erythrocytes is an important factor in systemic gene transfer via the intravenous route in mice: the role of the neutral helper lipid. Gene Therapy **8**(9): 677-686.

Sakurai F., Nishioka T., Yamashita F., Takakura Y., Hashida M. (2001b). Effects of erythrocytes and serum proteins on lung accumulation of lipoplexes containing cholesterol or DOPE as a helper lipid in the single-pass rat lung perfusion system. European Journal of Pharmaceutics and Biopharmaceutics **52**(2): 165-172.

Schaffer D.V., Fidelman N.A., Dan N., Lauffenburger D.A. (2000). Vector unpacking as a potential barrier for receptor-mediated polyplex gene delivery. Biotechnology and Bioengineering **67**(5): 598-606.

Scheule R.K., StGeorge J.A., Bagley R.G., Marshall J., Kaplan J.M., Akita G.Y., Wang K.X., Lee E.R., Harris D.J., Jiang C.W., Yew N.S., Smith A.E., Cheng S.H. (1997). Basis of pulmonary

toxicity associated with cationic lipid-mediated Gene transfer to the mammalian lung. Human Gene Therapy **8**(6): 689-707.

Scholz C., Wagner E. (2012). Therapeutic plasmid DNA versus siRNA delivery: common and different tasks for synthetic carriers. Journal of Controlled Release **161**(2): 554-565.

Scott E.S., Wiseman J.W., Evans M.J., Colledge W.H. (2001). Enhanced gene delivery to human airway epithelial cells using an integrin-targeting lipoplex. Journal of Gene Medicine **3**(2): 125-134.

Sharma S.V., Bell D.W., Settleman J., Haber D.A. (2007). Epidermal growth factor receptor mutations in lung cancer. Nature Reviews Cancer **7**(3): 169-181.

Sheridan C. (2011). Gene therapy finds its niche. Nature Biotechnology **29**(2): 121-128.

Shulga N., Mosammaparast N., Wozniak R., Goldfarb D.S. (2000). Yeast nucleoporins involved in passive nuclear envelope permeability. Journal of Cell Biology **149**(5): 1027-1038.

Sibbald B. (2001). Death but one unintended consequence of gene-therapy trial. Canadian Medical Association Journal **164**(11): 1612-1612.

Sonawane N.D., Szoka F.C., Verkman A.S. (2003). Chloride accumulation and swelling in endosomes enhances DNA transfer by polyamine-DNA polyplexes. Journal of Biological Chemistry **278**(45): 44826-44831.

Song H., Wang G., He B., Li L., Li C., Lai Y., Xu X., Gu Z. (2012). Cationic lipid-coated PEI/DNA polyplexes with improved efficiency and reduced cytotoxicity for gene delivery into mesenchymal stem cells. International Journal of Nanomedicine **7**: 4637-4648.

Strasser C., Grote P., Schauble K., Ganz M., Ferrando-May E. (2012). Regulation of nuclear envelope permeability in cell death and survival. Nucleus **3**(6): 540-551.

Subbarao N.K., Parente R.A., Szoka F.C., Nadasdi L., Pongracz K. (1987). Ph-dependent bilayer destabilization by an amphipathic peptide. Biochemistry **26**(11): 2964-2972.

Suh J., Paik H.J., Hwang B.K. (1994). Ionization of poly(ethylenimine) and poly(allylamine) at various pH's. Bioorganic Chemistry **22**: 318-327.

Sugano M., Negishi Y., Endo-Takahashi Y., Suzuki R., Maruyama K., Yamamoto M., Aramaki Y. (2012). Gene delivery system involving bubble liposomes and ultrasound for the efficient in vivo delivery of genes into mouse tongue tissue. International Journal of Pharmaceutics **422**(1-2): 332-337.

Summerton J.E. (2006). Endo-Porter: a novel reagent for safe, effective delivery of substances into cells. Annals of the New York Academy of Sciences **1058**(1): 62-75.

Tabernero J., Shapiro G.I., LoRusso P.M., Cervantes A., Schwartz G.K., Weiss G.J., Paz-Ares L., Cho D.C., Infante J.R., Alsina M., Gounder M.M., Falzone R., Harrop J., White A.C.S., Toudjarska I., Bumcrot D., Meyers R.E., Hinkle G., Svrzikapa N., Hutabarat R.M., Clausen V.A., Cehelsky J., Nochur S.V., Gamba-Vitalo C., Vaishnaw A.K., Sah D.W.Y., Gollob J.A., Burris H.A. (2013). First-in-humans trial of an RNA interference therapeutic targeting VEGF and KSP in cancer patients with liver involvement. Cancer Discovery **3**(4): 406-417.

Tagalakis A.D., He L., Saraiva L., Gustafsson K.T., Hart S.L. (2011). Receptor-targeted liposome-peptide nanocomplexes for siRNA delivery. Biomaterials **32**(26): 6302-6315.

Tagalakis A.D., Saraiva L., McCarthy D., Gustafsson K.T., Hart S.L. (2013). Comparison of nanocomplexes with branched and linear peptides for siRNA delivery. Biomacromolecules **14**(3): 761-770.

Takahashi Y., Nishikawa M., Takakura Y. (2009). Nonviral vector-mediated RNA interference: its gene silencing characteristics and important factors to achieve RNAi-based gene therapy. Advanced Drug Delivery Review **61**(9): 760-766.

Tang M.X., Szoka F.C. (1997). The influence of polymer structure on the interactions of cationic polymers with DNA and morphology of the resulting complexes. Gene Therapy **4**(8): 823-832.

Timmons L., Fire A. (1998). Specific interference by ingested dsRNA. Nature **395**(6705): 854.

Toriyabe N., Hayashi Y., Harashima H. (2013). The transfection activity of R8-modified nanoparticles and siRNA condensation using pH sensitive stearylated-octahistidine. Biomaterials **34**(4): 1337-1343.

Tros de Ilarduya C., Sun Y., Duzgunes N. (2010). Gene delivery by lipoplexes and polyplexes. European Journal of Pharmaceutical Science **40**(3): 159-170.

Turek J., Dubertret C., Jaslin G., Antonakis K., Scherman D., Pitard B. (2000). Formulations which increase the size of lipoplexes prevent serum-associated inhibition of transfection. Journal of Gene Medicine **2**(1): 32-40.

Van de Water F.M., Boerman O.C., Wouterse A.C., Peters J.G., Russel F.G., Masereeuw R. (2006). Intravenously administered short interfering RNA accumulates in the kidney and selectively suppresses gene function in renal proximal tubules. Drug Metabolism and Disposition **34**(8): 1393-1397.

Varkouhi A.K., Foillard S., Lammers T., Schiffelers R.M., Doris E., Hennink W.E., Storm G. (2011). SiRNA delivery with functionalized carbon nanotubes. International Journal of Pharmaceutics **416**(2): 419-425.

Vercauteren D., Rejman J., Martens T.F., Demeester J., De Smedt S.C., Braeckmans K. (2012). On the cellular processing of non-viral nanomedicines for nucleic acid delivery: mechanisms and methods. Journal of Controlled Release **161**(2): 566-581.

Vives E., Brodin P., Lebleu B. (1997). A truncated HIV-1 Tat protein basic domain rapidly translocates through the plasma membrane and accumulates in the cell nucleus. Journal of Biological Chemistry **272**(25): 16010-16017.

Watanabe K., Harada-Shiba M., Suzuki A., Gokuden R., Kurihara R., Sugao Y., Mori T., Katayama Y., Niidome T. (2009). In vivo siRNA delivery with dendritic poly(L-lysine) for the treatment of hypercholesterolemia. Molecular Biosystems **5**(11): 1306-1310.

Watson J. D.,.Crick F. (1953). Molecular structure of nucleic acids. Nature **171**: 737-738.

Welser K., Campbell F., Kudsiova L., Mohammadi A., Dawson N., Hart S.L., Barlow D.J., Hailes H.C., Lawrence M.J., Tabor A.B. (2013). Gene delivery using ternary lipopolyplexes incorporating branched cationic peptides: the role of peptide sequence and branching. Molecular Pharmaceutics **10**(1): 127-141.

Weintraub H., Cheng P.F., Conrad K. (1986). Expression of transfected DNA depends on DNA topology. Cell **46**(1): 115-122.

Wilson J.M. (2005). Gendicine: the first commercial gene therapy product. Hum Gene Ther **16**(9): 1014-1015.

Wirth T., Parker N., Yla-Herttuala S. (2013). History of gene therapy. Gene **525**(2): 162-169.

Wiseman J.W., Scott E.S., Shaw P.A., Colledge W.H. (2005). Enhancement of gene delivery to human airway epithetial cells in vitro using a peptide from the polyoma virus protein VP1. Journal of Gene Medicine **7**(6): 759-770.

Wolfert M.A., Schacht E.H., Toncheva V., Ulbrich K., Nazarova O., Seymour L.W. (1996). Characterization of vectors for gene therapy formed by self-assembly of DNA with synthetic block co-polymers. Human Gene Therapy **7**(17): 2123-2133.

Writer M.J., Marshall B., Pilkington-Miksa M.A., Barker S.E., Jacobsen M., Kritz A., Bell P.C., Lester D.H., Tabor A.B., Hailes H.C., Klein N., Hart S.L. (2004). Targeted gene delivery to human airway epithelial cells with synthetic vectors incorporating novel targeting peptides selected by phage display. Journal of Drug Target **12**(4): 185-193.

Xiong F., Mi Z., Gu N. (2011). Cationic liposomes as gene delivery system: transfection efficiency and new application. Pharmazie **66**(3): 158-164.

Xie T.D., Tsong T.Y. (1993). Study of mechanisms of electric-field-induced DNA transfection: Effects of DNA topology on surface binding, cell uptake, expression, and integration into host chromosomes of DNA in the mammalian-cell. Biophysical Journal **65**(4): 1684-1689.

Xu G.Y., Xu X.J., Li Z.L., He Q.G., Wu B., Sun S.F., Chen H.C. (2004). Construction of recombinant pseudorabies virus expressing NS1 protein of Japanese encephalitis (SA14-14-2) virus and its safety and immunogenicity. Vaccine **22**(15-16): 1846-1853.

Xu Y., Szoka F.C. Jr. (1996). Mechanism of DNA release from cationic liposome/DNA complexes used in cell transfection. Biochemistry **35**(18): 5616-5623.

Yamagata M., Kawano T., Shiba K., Mori T., Katayama Y., Niidome T. (2007). Structural advantage of dendritic poly(L-lysine) for gene delivery into cells. Bioorganic & Medicinal Chemistry **15**(1): 526-532.

Yamauchi J., Hayashi Y., Kajimoto K., Akita H., Harashima H. (2010). Comparison between a multifunctional envelope-type nano device and lipoplex for delivery to the liver. Biological & Pharmaceutical Bulletin **33**(5): 926-929.

Yan J., Berezhnoy N.V., Korolev N., Su C.J., Nordenskiold L. (2012). Structure and internal organization of overcharged cationic-lipid/peptide/DNA self-assembly complexes. Biochimica Et Biophysica Acta-Biomembranes **1818**(7): 1794-1800.

Yoshioka T., Yoshida S., Kurosaki T., Teshima M., Nishida K., Nakamura J., Nakashima M., To H., Kitahara T., Sasaki H. (2009). Cationic liposomes-mediated plasmid DNA delivery in murine hepatitis induced by carbon tetrachloride. Journal of Liposome Research **19**(2): 141-147.

Yu W., Pirollo K.F., Yu B., Rait A., Xiang L.M., Huang W.Q., Zhou Q., Ertem G., Chang E.H. (2004). Enhanced transfection efficiency of a systemically delivered tumor-targeting immunolipoplex by inclusion of a pH-sensitive histidylated oligolysine peptide. Nucleic Acids Research **32**(5): e48.

Zamore P.D., Tuschl T., Sharp P.A., Bartel D.P. (2000). RNAi: Double-stranded RNA directs the ATP-dependent cleavage of mRNA at 21 to 23 nucleotide intervals. Cell **101**(1): 25-33.

Zanta M.A., Belguise-Valladier P., Behr J.P. (1999). Gene delivery: A single nuclear localization signal peptide is sufficient to carry DNA to the cell nucleus. Proceedings of the National Academy of Sciences of the United States of America **96**(1): 91-96.

Zeng J., Wang X., Wang S. (2007). Self-assembled ternary complexes of plasmid DNA, low molecular weight polyethylenimine and targeting peptide for nonviral gene delivery into neurons. Biomaterials **28**(7): 1443-1451.

Zeng J.M., Wang S. (2005). Enhanced gene delivery to PC12 cells by a cationic polypeptide. Biomaterials **26**(6): 679-686.

Zhang C., Liu H.M., Li Q.W., Chen G.W., Liang X., Meng C.Y. (2014). Construction of recombinant adenovirus vector containing hBMP2 and hVEGF165 genes and its expression in rabbit Bone marrow mesenchymal stem cells. Tissue & Cell **46**(5): 311-317.

Zhang S.B., Xu Y.M., Wang B., Qiao W.H., Liu D.L., Li Z.S. (2004). Cationic compounds used in lipoplexes and polyplexes for gene delivery. Journal of Controlled Release **100**(2): 165-180.

Zhu H., Dong, H., Ren T., Wen X., Su J., Li Y. (2014). Cleavable PEGylation and hydrophobic histidylation of polylysine for siRNA delivery and tumour gene therapy. Applied materials and interfaces **6**(13): 10393-10407.

Appendix I HPLC analysis and mass spectra of peptides

1. H_{12}BLY, Mw. 5238

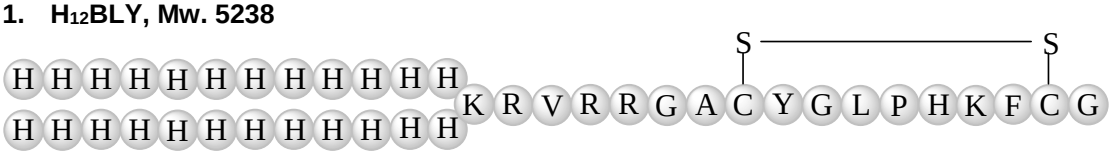

Purification was carried out as described in Chapter 2 Methods (**Method B**). Analysis (**Method C**: R_T = 5.715min) *m/z* (ES+) 1048.18($[M+5H]^{5+}$), 873.76($[M+6H]^{6+}$), 749.06($[M+7H]^{7+}$), 655.66($[M+8H]^{8+}$).

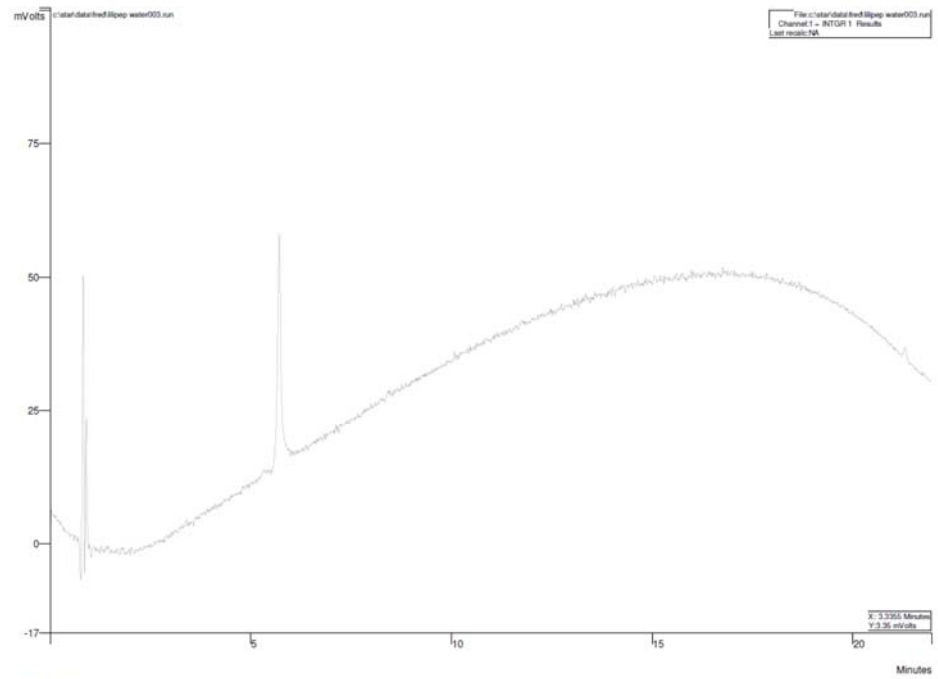

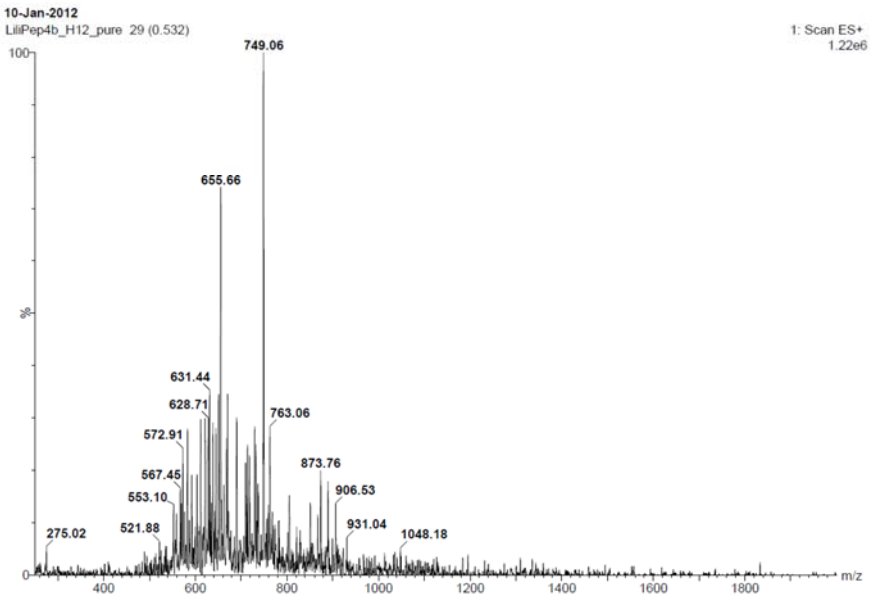

2. R_{12}BLY, Mw. 5695

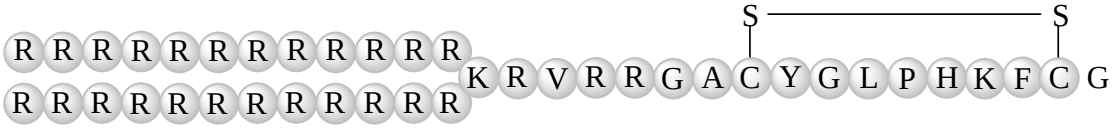

Purification was carried out as described in Chapter 2 Methods (**Method B**). Analysis (**Method C**: R_T = 5.71 min, *m/z* (ES+) 950.29([M+6H]$^{6+}$), 814.46([M+7H]$^{7+}$), 712.72([M+8H]$^{8+}$).

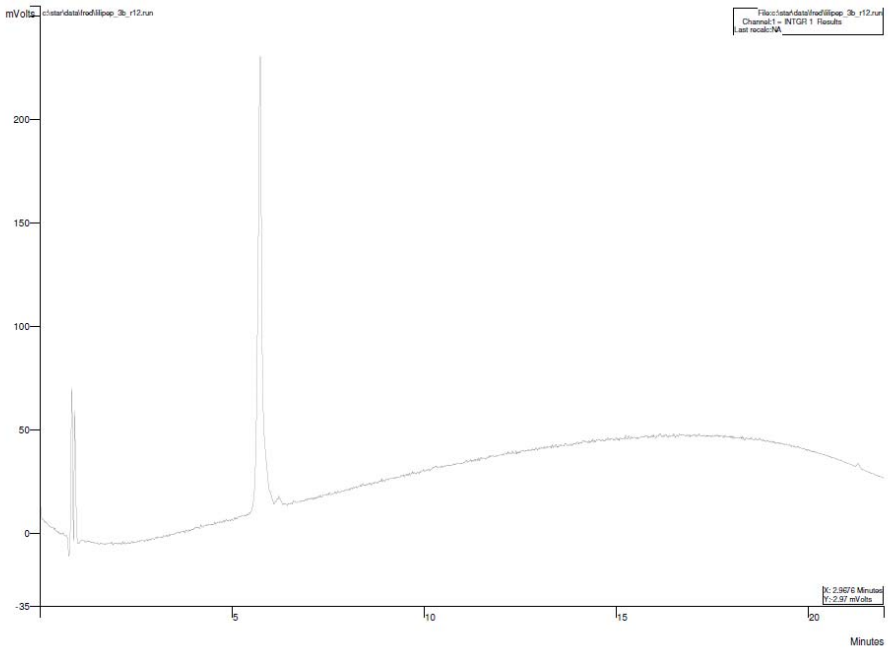

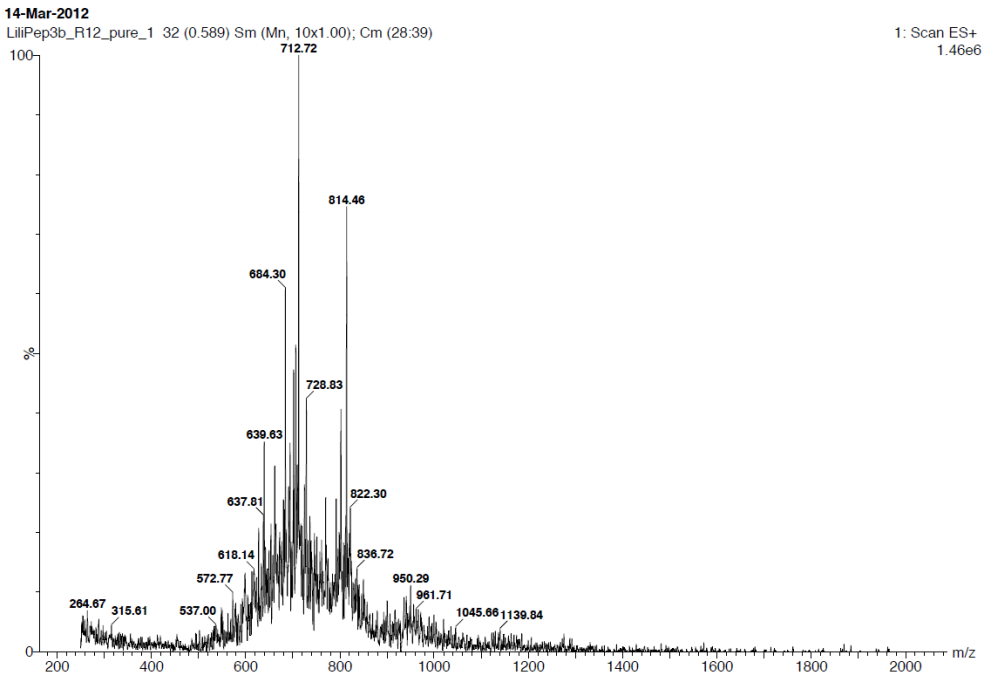

3. K_{12}BLY, Mw. 5022

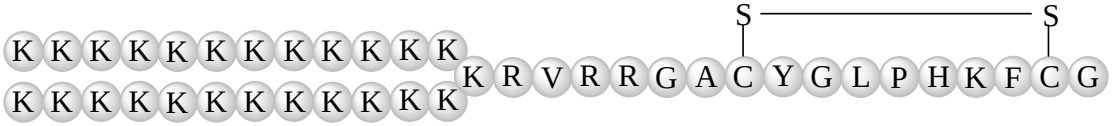

Purification was carried out as described in Chapter 2 Methods (**Method B**). Analysis (**Method C**): R_T = 5.147min, *m/z* (ES+) 1005.40([M+5H]$^{5+}$),837.98([M+6H]$^{6+}$), 718.39([M+7H]$^{7+}$), 628.71([M+8H]$^{8+}$), 558.91([M+9H]$^{9+}$).

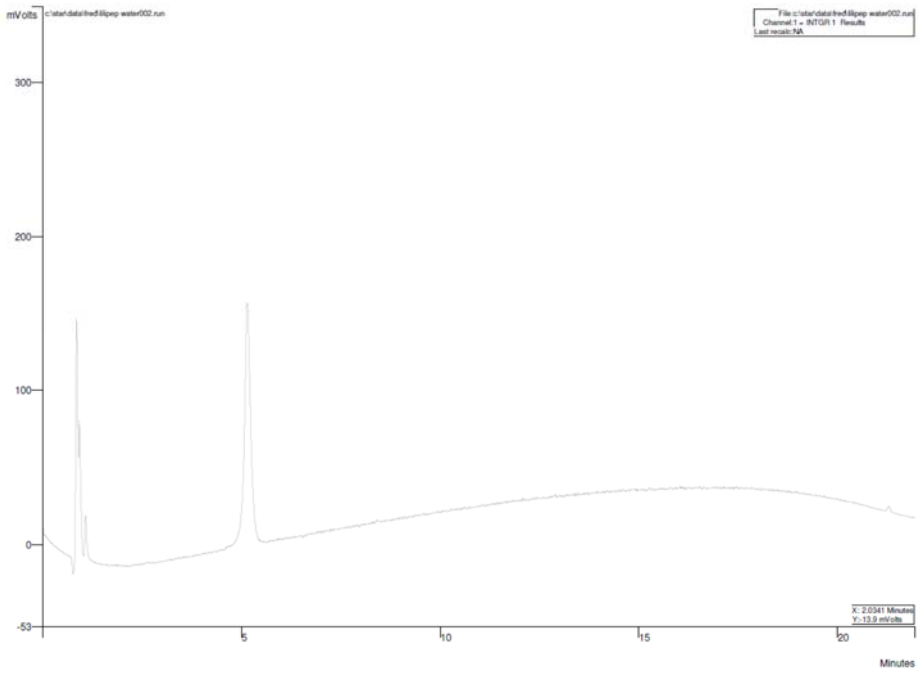

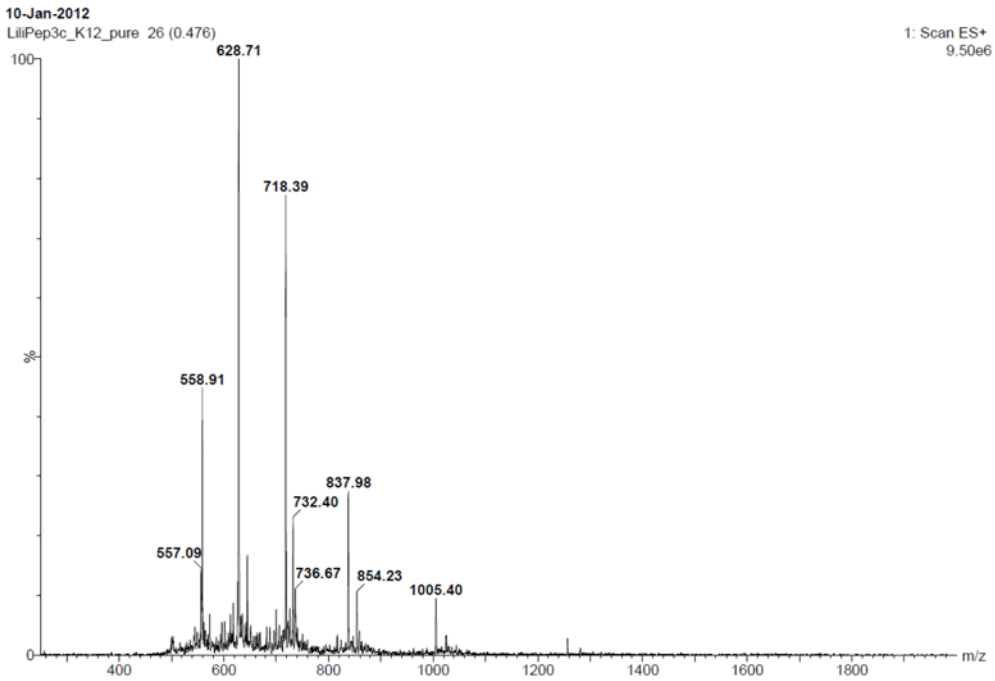

4. **K_4BLY**, **Mw. 2972**

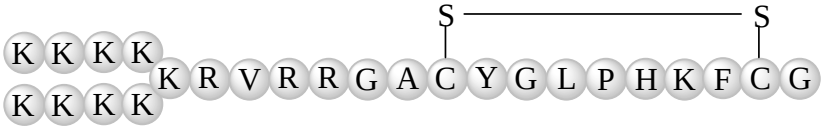

Purification was carried out as described in Chapter 2 Methods (**Method A**). Analysis (**Method C**): R_T = 7.3086min, *m/z* (ES+) 743.74 ($[M+4H]^{4+}$), 595.17($[M+5H]^{5+}$), 496.05($[M+6H]^{6+}$).

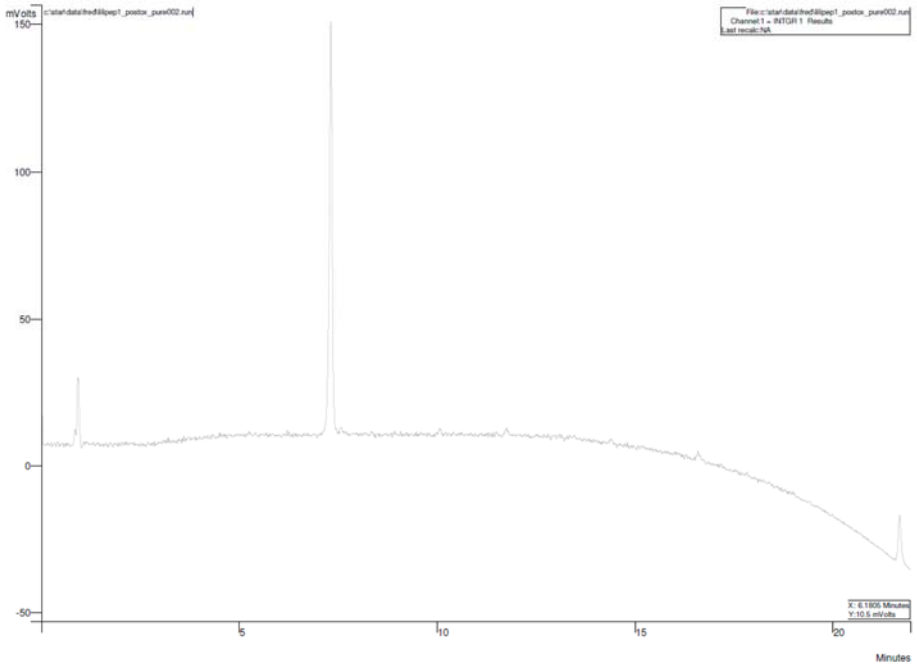

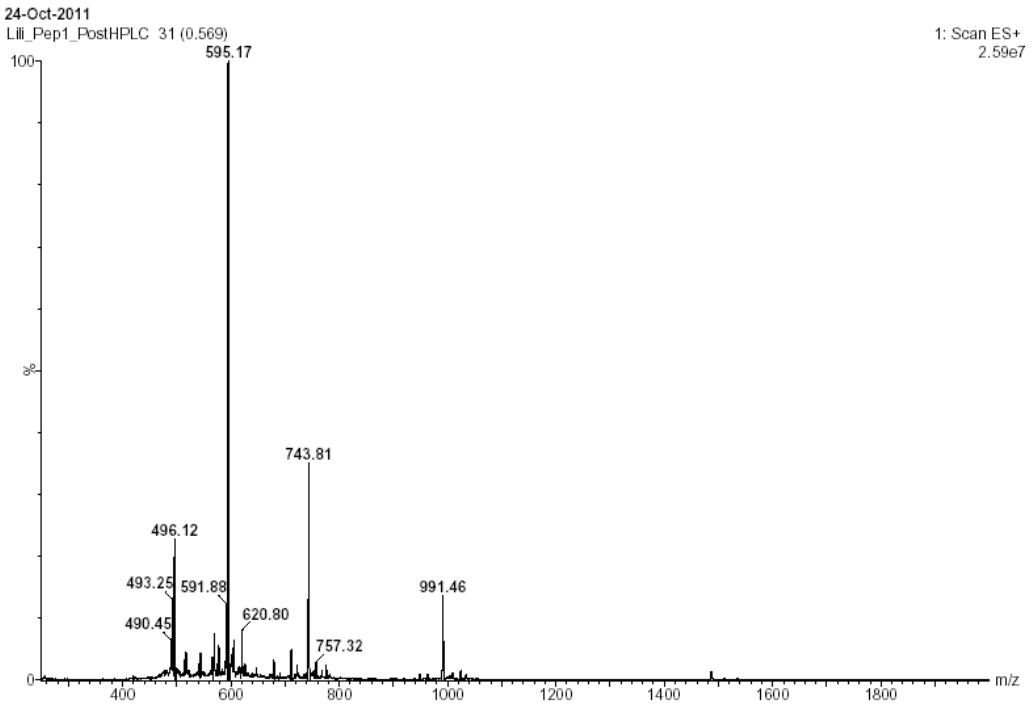

5. $(HHR)_4$BLY, Mw. 5390

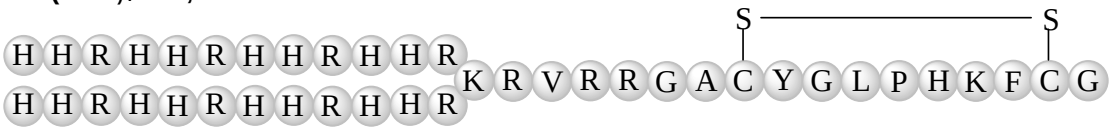

Purification was carried out as described in Chapter 2 Methods (**Method A**). Analysis (**Method C**): R_T = 10.129min, *m/z* (ES+) 899.60($[M+6H]^{6+}$), 771.11($[M+7H]^{7+}$), 674.84($[M+8H]^{8+}$), 599.86($[M+9H]^{9+}$).

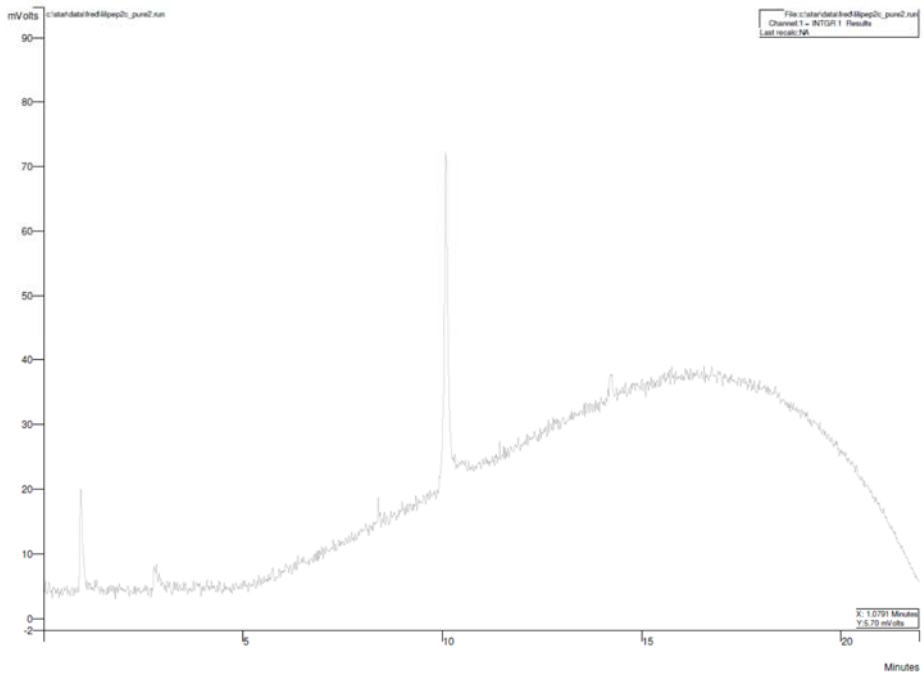

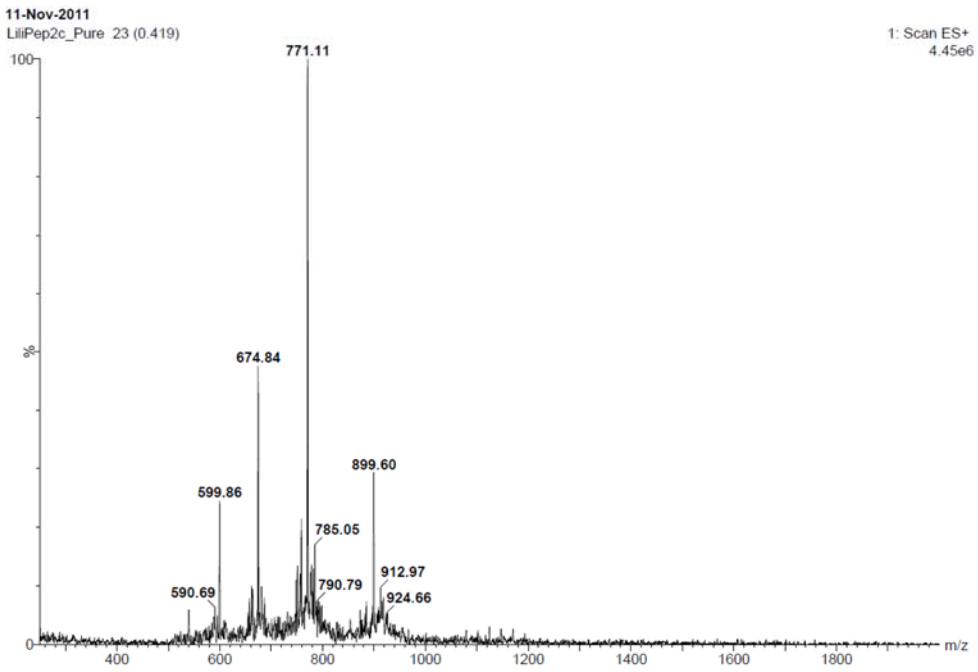

6. $(HR)_6$BLY, Mw. 5466

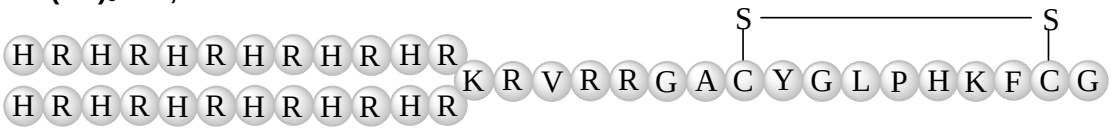

Purification was carried out as described in Chapter 2 Methods (**Method A**). Analysis (**Method C**): R_T =10.195min, *m/z* (ES+) 912.13 ($[M+6H]^{6+}$), 781.97 ($[M+7H]^{7+}$), 684.44($[M+8H]^{8+}$), 608.40($[M+9H]^{9+}$).

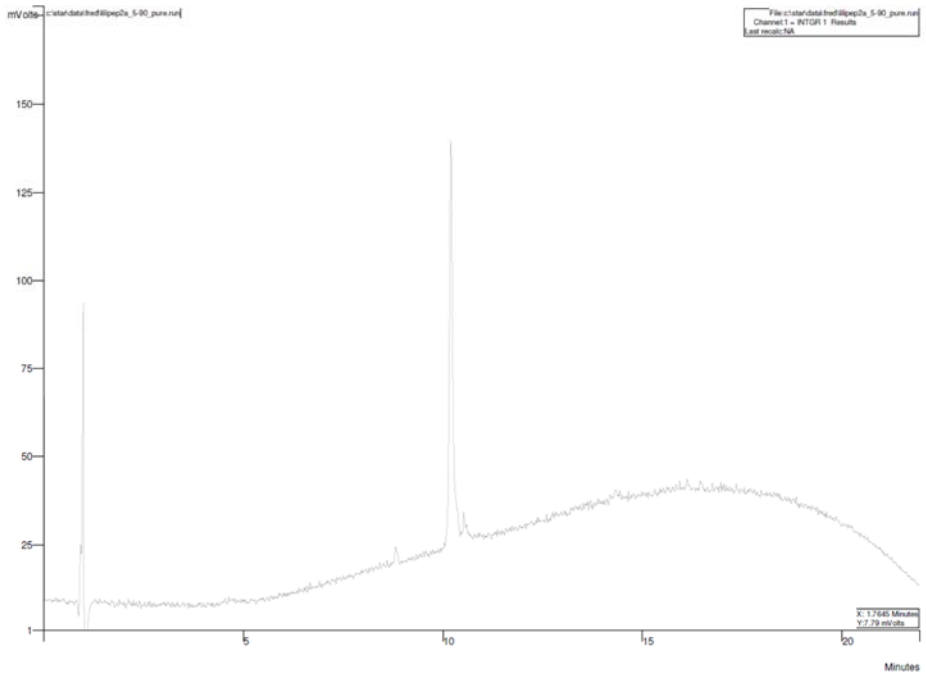

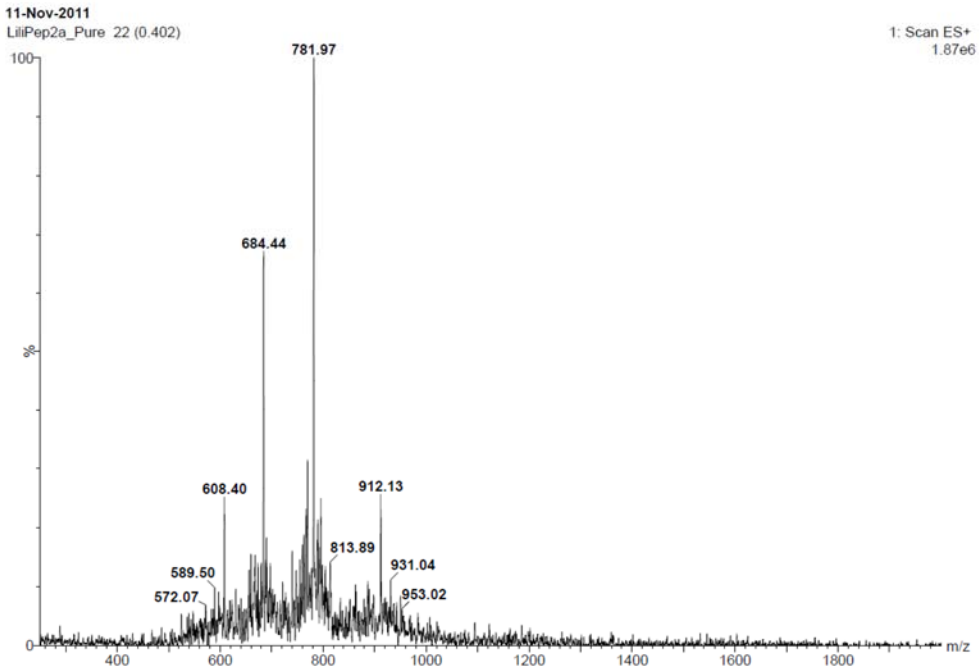

7. **(HK)$_6$BLY, Mw. 5130**

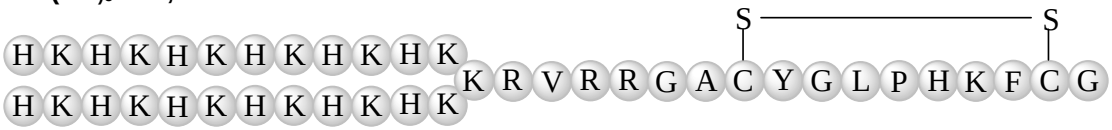

Purification was carried out as described in Chapter 2 Methods (**Method B**). Analysis (**Method D**): R_T = 6.630min, *m/z* (ES+) 1026.96([M+5H]$^{5+}$),855.98([M+6H]$^{6+}$), 733.73([M+7H]$^{7+}$), 642.15([M+8H]$^{8+}$), 570.88([M+9H]$^{9+}$).

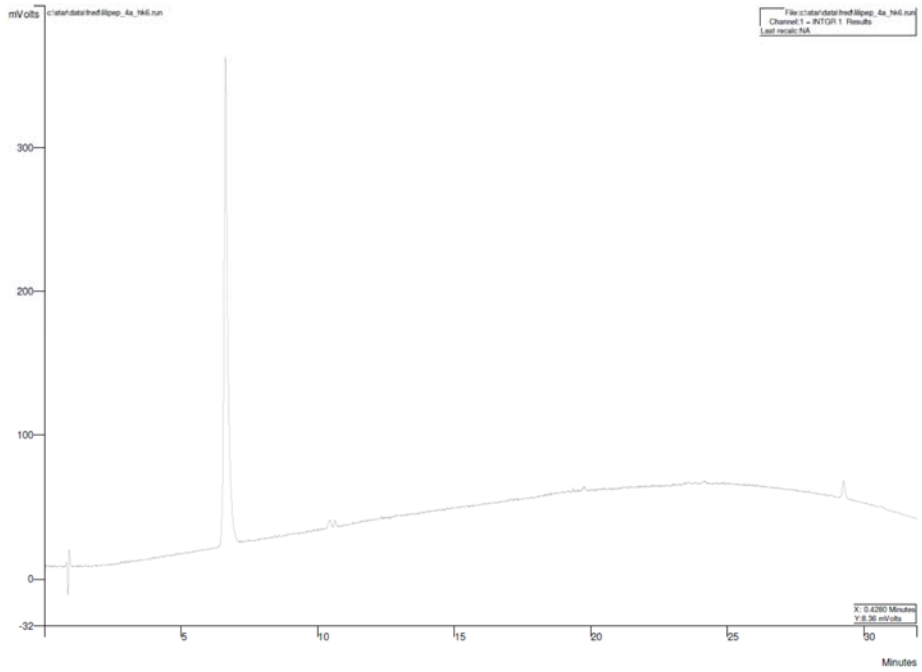

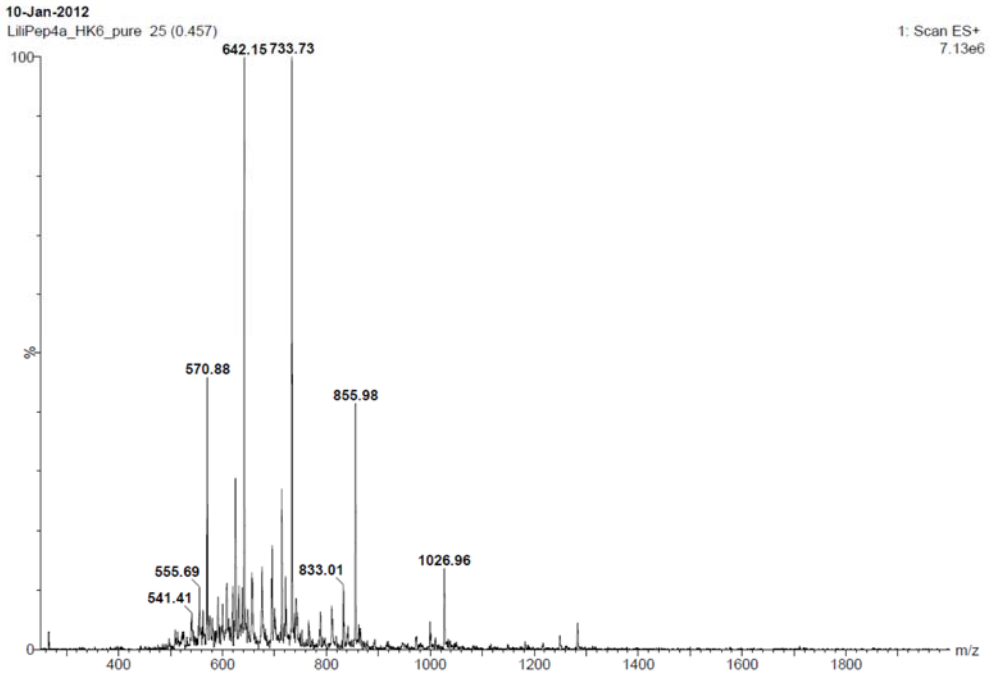

8. $(RK)_6$BLY, Mw. 5359

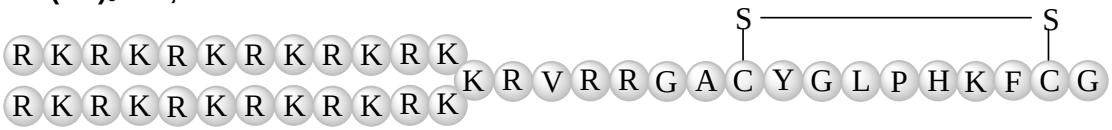

Purification was carried out as described in Chapter 2 Methods (**Method B**). Analysis (**Method D**): R_T = 6.690min, *m/z* (ES+) 910.66($[M+6H]^{6+}$), 766.42($[M+7H]^{7+}$), 670.71($[M+8H]^{8+}$), 596.29($[M+9H]^{9+}$), 536.86($[M+10H]^{10+}$).

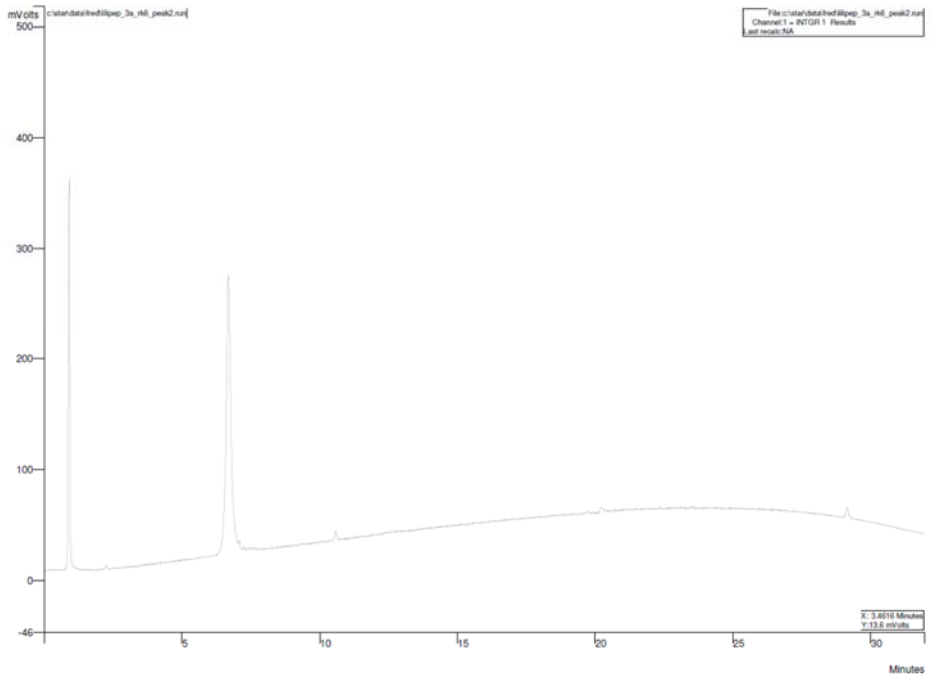

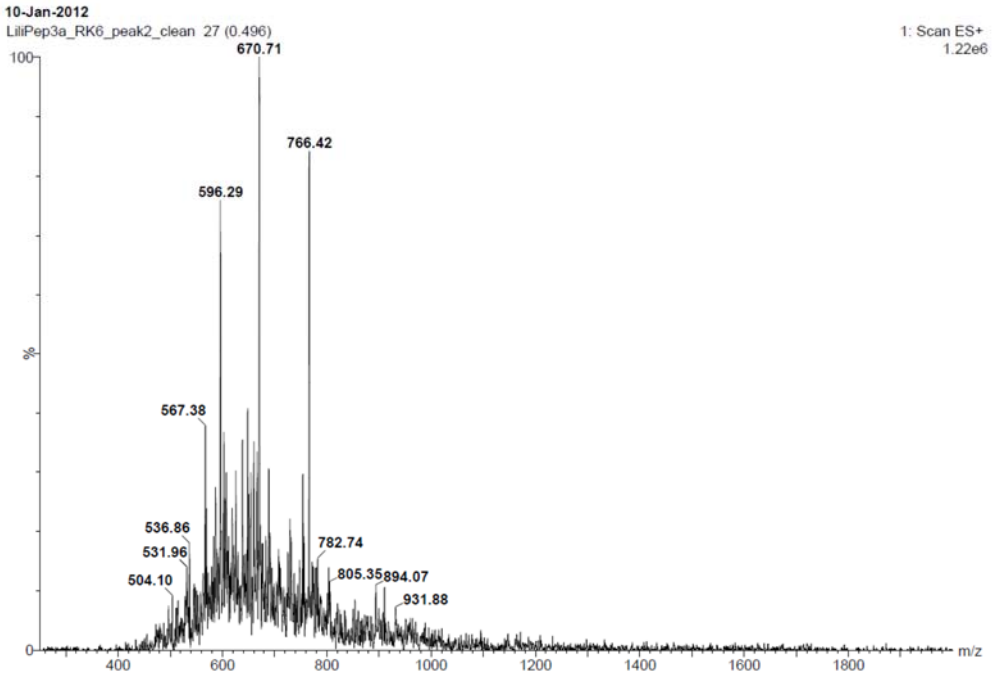

Appendix II Repeats of LPD results

1. Transfection

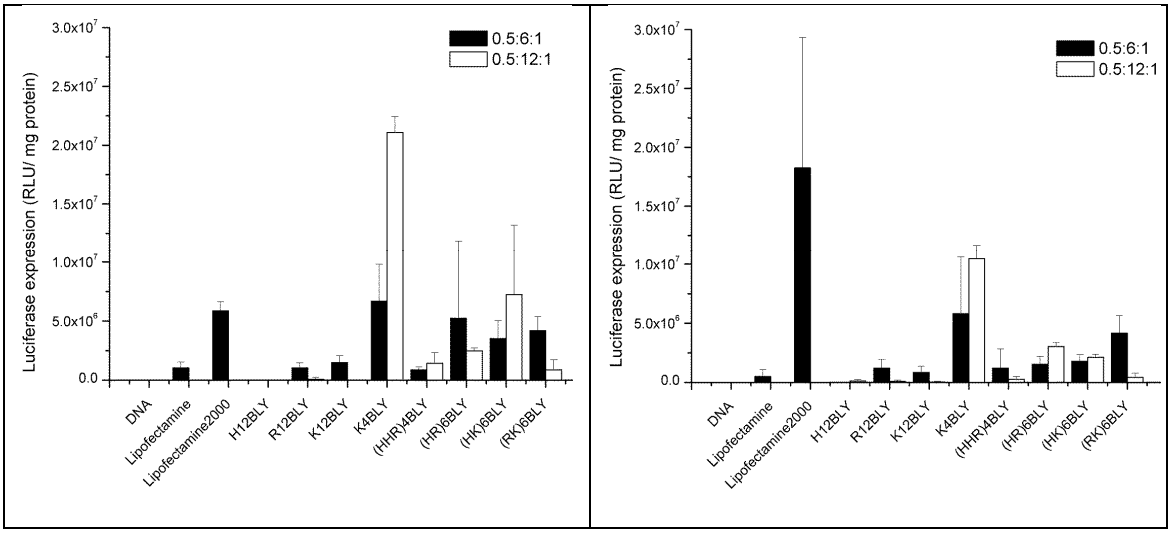

(a) transfection (24+24h) (a) transfection (4+44h)

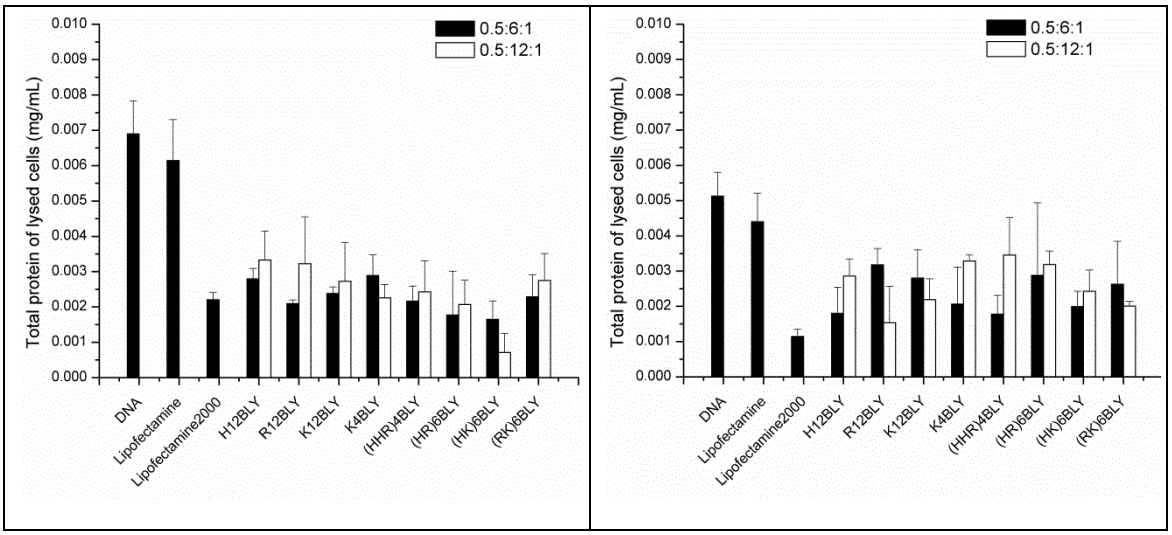

(b) protein assay (24+24h) (b) protein assay (4+44h)

Figure 1 (a) levels of luciferase transfection and (b) protein assay after 24+24h (left panel) and 4+44h (right panel) incubation of A549 cells with LPDs. LPDs were prepared fully in water at a L:P:D charge ratio of 0.5:6:1, and mixed in a 1:3 volume ratio of LPDs in water and OptiMEM (VwLPDw/OptiMEM). The final DNA concentration was 0.0025 mg/mL. Vesicles used to prepare the LPDs composed of DOTMA:DOPE at 1:1 molar ratio. Error bars are the SD of triplicate measurements of a single (n=3).

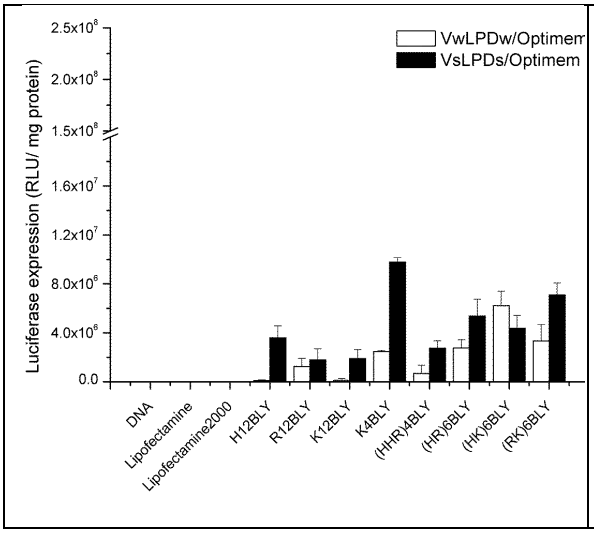

(a) transfection (repeat 1)

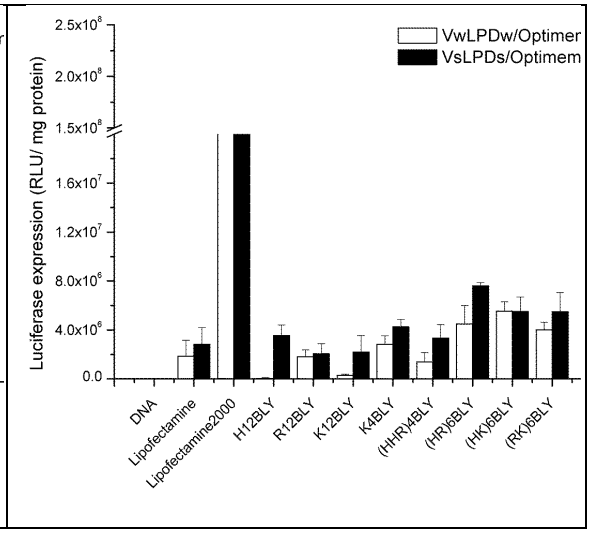

(a) transfection (repeat 2)

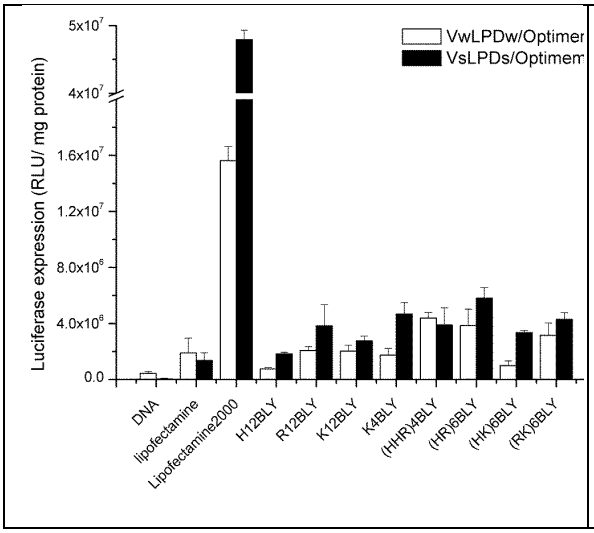

(a) transfection (repeat 3)

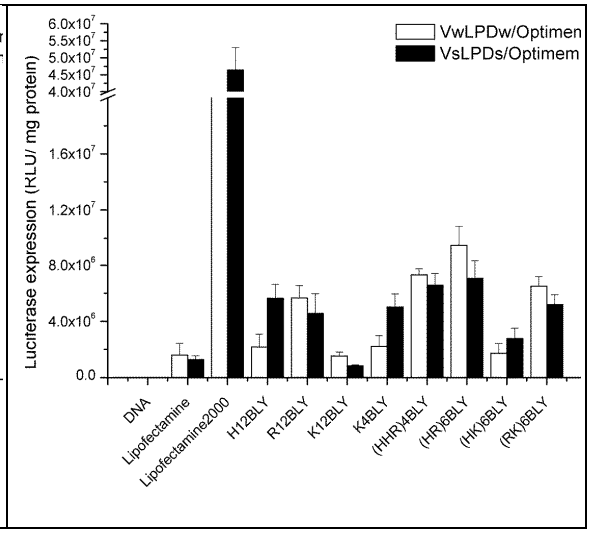

(a) transfection (repeat 4)

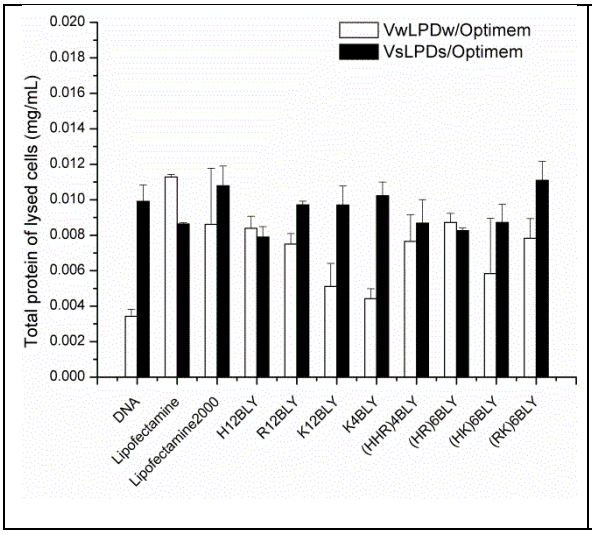

(b) protein assay (repeat 1)

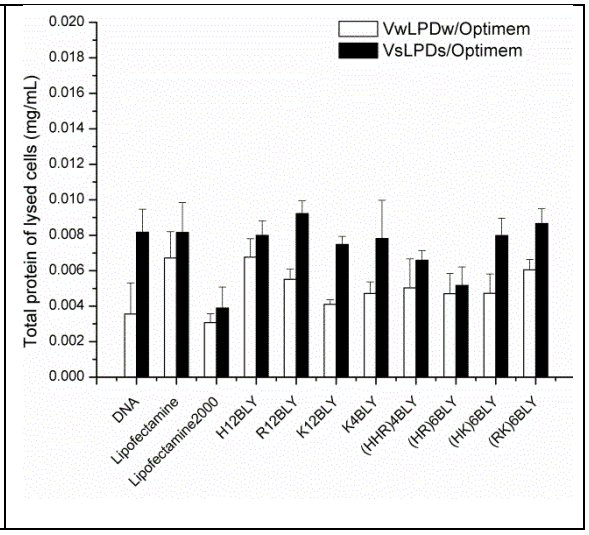

(b) protein assay (repeat 2)

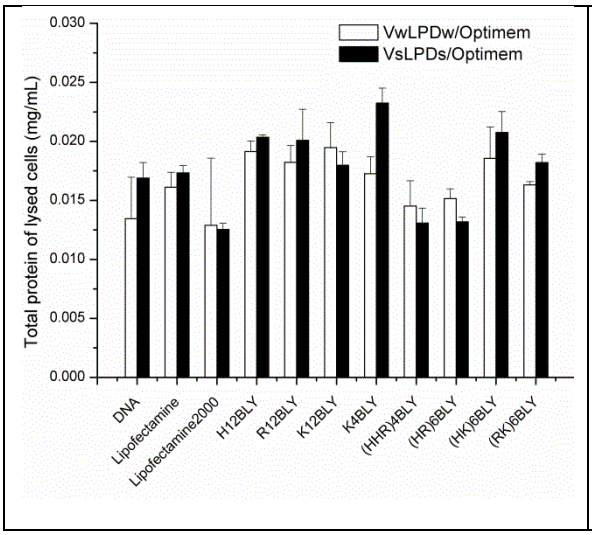

(b) protein assay (repeat 3)

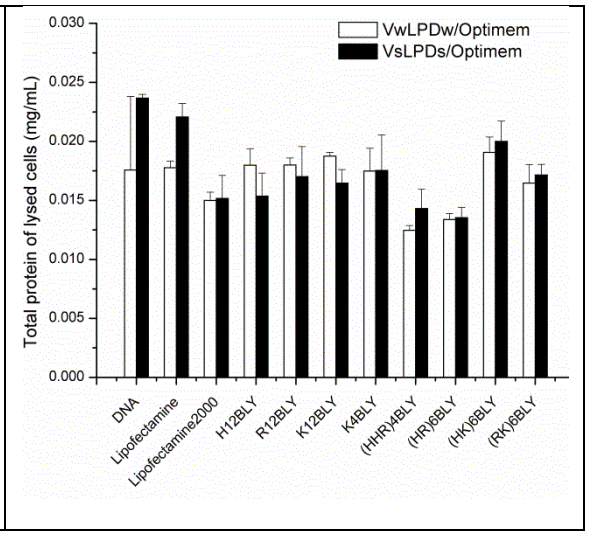

(b) protein assay (repeat 4)

Figure 2 (a) levels of luciferase transfection and (b) protein assay in A549 cells after exposure to LPDs using a 4+44 h incubation protocol. LPDs were prepared fully in water or 0.15 M NaCl solution and diluted with 75% v/v OptiMEM (VwLPDw/OptiMEM and VsLPDs/OptiMEM). LPDs were prepared at a L:P:D charge ratio of 0.5:6:1. Cationic vesicles used to prepare the LPDs were composed of DOTMA/DOPE lipids at 1:1 molar ratio. Error bars are the SD of 3 measurements of a single formulation (n=3).

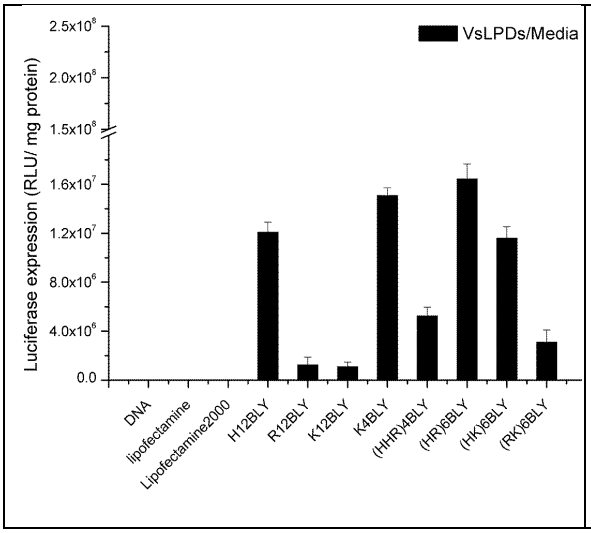

(a) transfection (repeat 1)

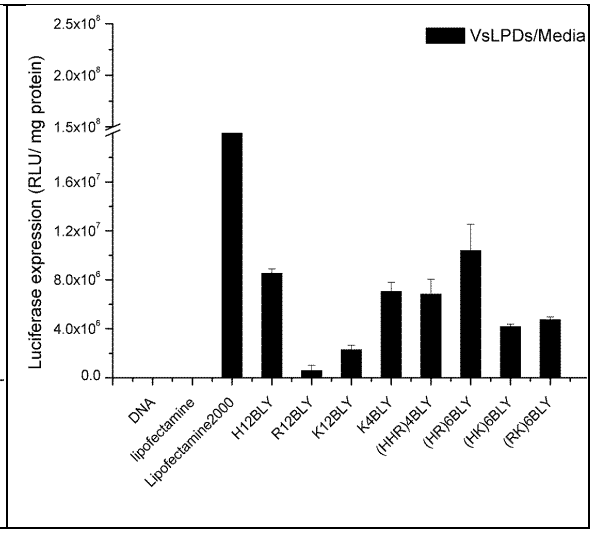

(a) transfection (repeat 2)

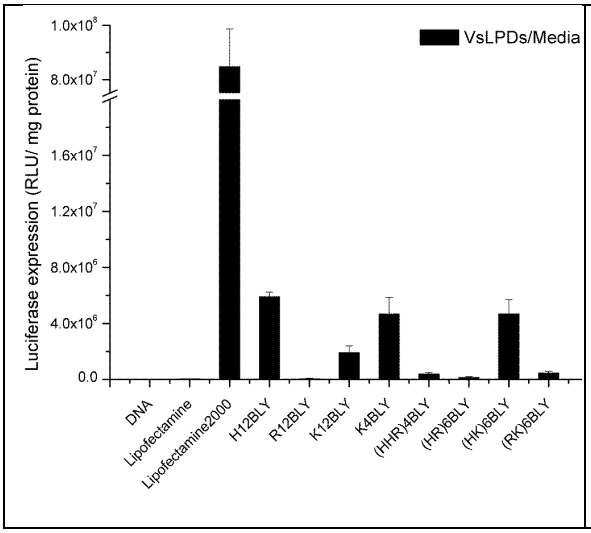

(a) transfection (repeat 3)

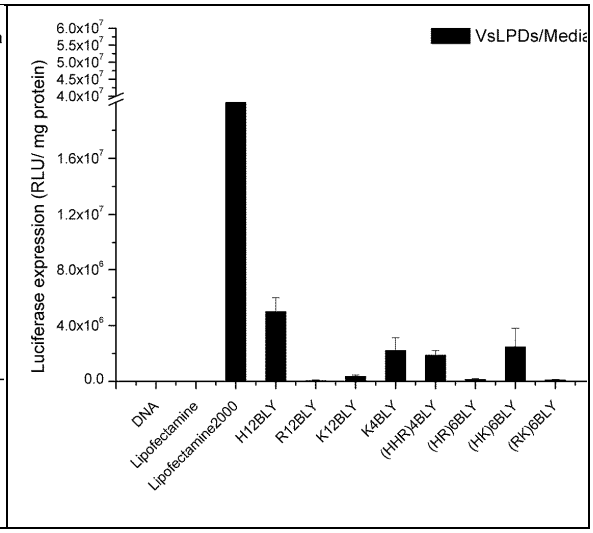

(a) transfection (repeat 4)

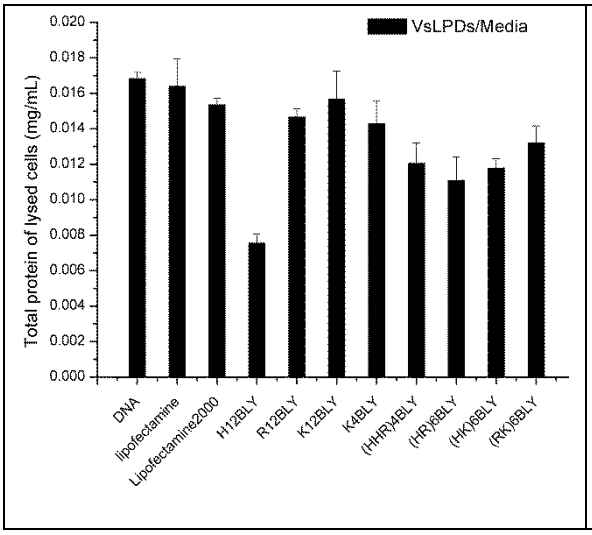

(b) protein assay (repeat 1)

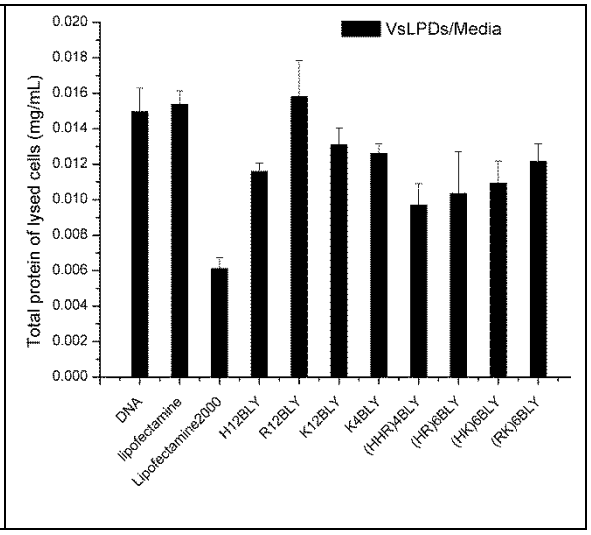

(b) protein assay (repeat 2)

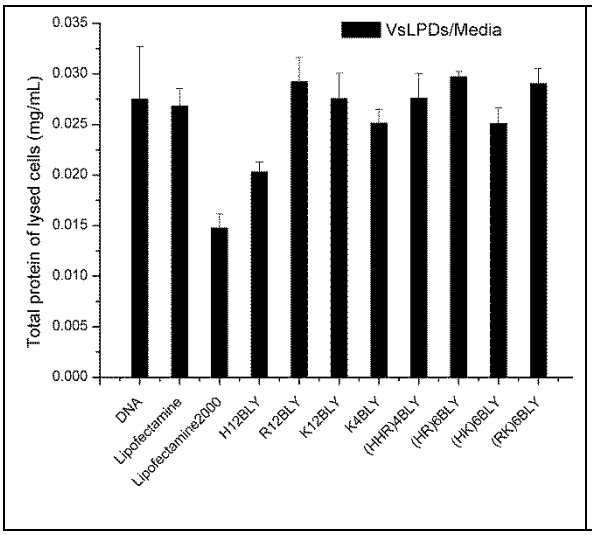

(b) protein assay (repeat 3)

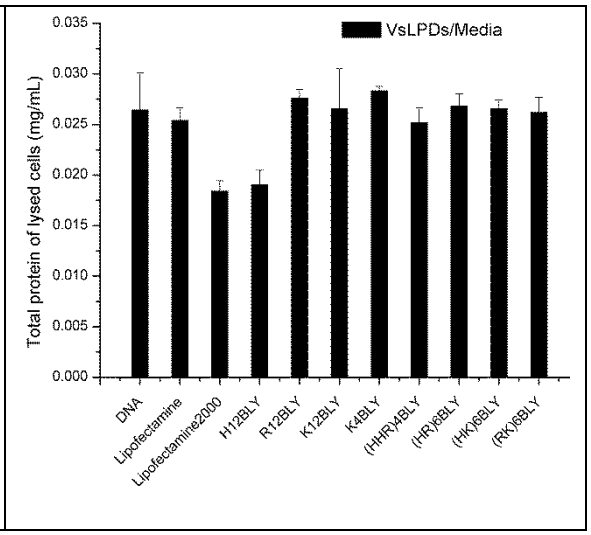

(b) protein assay (repeat 4)

Figure 3 (a) levels of luciferase transfection and (b) protein assay in A549 cells after exposure to LPDs using a 4+44 h incubation protocol. LPDs were prepared fully in 0.15 M NaCl solution and diluted with 75% v/v Media containing 10% FBS (VsLPDs/Media). LPDs were prepared at a L:P:D charge ratio of 0.5:6:1. Cationic vesicles used to prepare the LPDs were composed of DOTMA/DOPE lipids at 1:1 molar ratio. Error bars are the SD of 3 measurements of a single formulation (n=3).

2. Agarose gel electrophoresis

Repeat 1 Repeat 2

Figure 4 condensation, release and protection properties of LPDs (VwLPDw and VsLPDs) using agarose gel electrophoresis (0.025 mg/mL of pDNA). LPDs were prepared at lipid:peptide:DNA charge ratio of 0.5:6:1. The effect of the peptide component on DNA condensation (Lane A), DNA release (Lane B), and protection from DNAse I (Lane C) was studied. Lane A: DNA or LPD. Lane B: DNA and LPDs treated with pAsp. Lane C: LPDs treated with DNAse I at 37°C followed by pAsp.

3. Dynamic light scattering

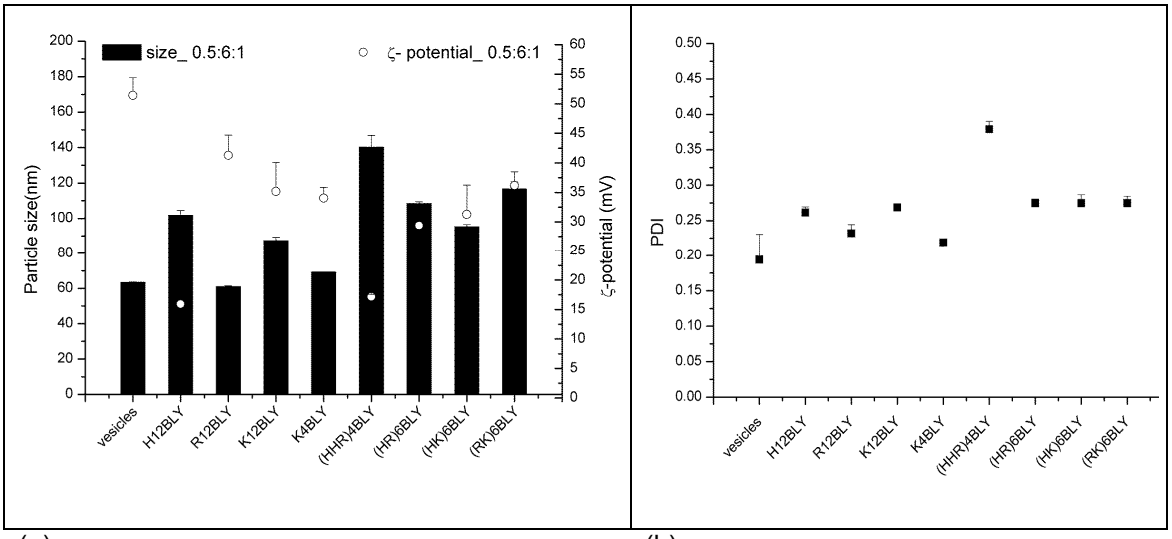

(a) (b)

Figure 5 Mean apparent hydrodynamic particle size and ζ-potential of LPDs made in water (VwLPDw). Samples prepared at a lipid:peptide:DNA charge ratios of 0.5:6:1 (final DNA concentration of 0.01 mg/mL). Vesicle suspension composed of DOTMA/DOPE at 1:1 molar ratio. (a) mean apparent hydrodynamic size and ζ-potential, (b) polydispersity index (PDI) of mean apparent hydrodynamic size (n=3). Error from SD of three measurements of a single formulation at 25°C.

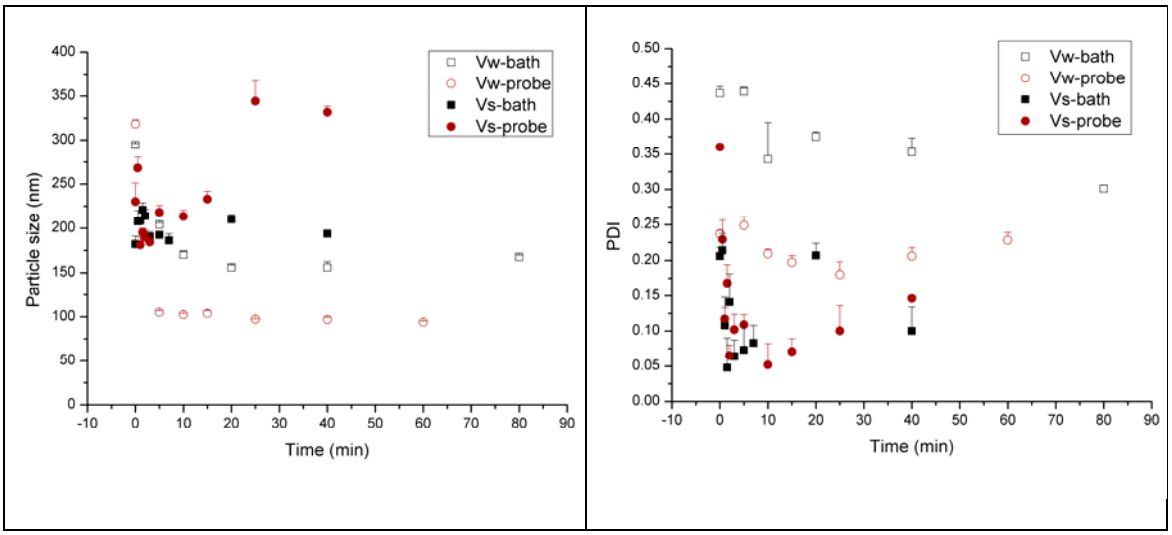

(a) (b)

Figure 6 Mean apparent hydrodynamic particle size of vesicles made in water (Vw) and 0.15 M NaCl solution (Vs). The size of the vesicles was reduced by bath and probe sonication respectively over 80 min. Vesicle suspension composed of DOTMA/DOPE at 1:1 molar ratio (1.0 mg/mL DOTMA). Error from SD of three measurements of a single formulation (n=3) at 25°C.

4. Small angle neutron scattering

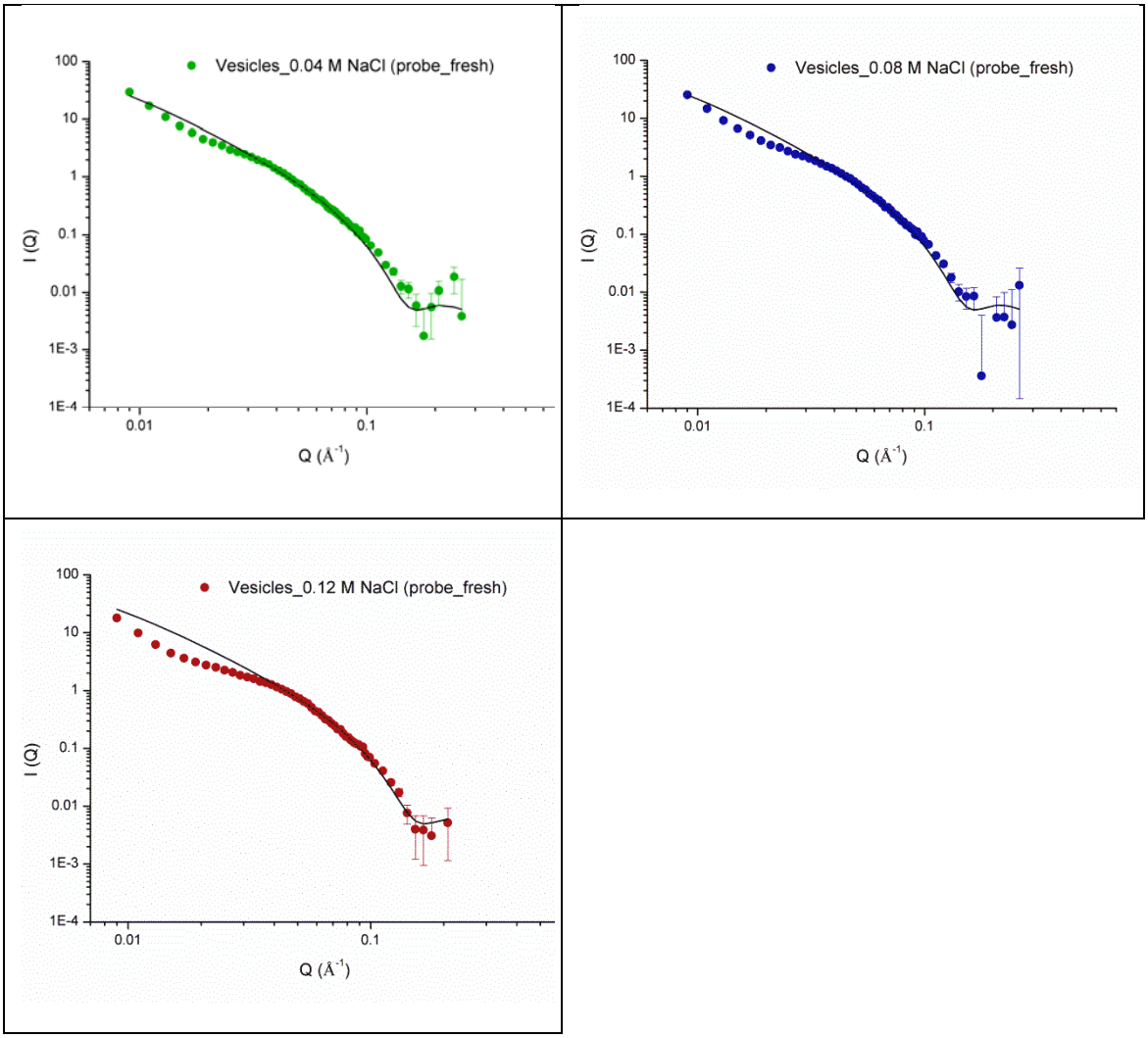

Figure 7 Small neutron scattering data obtained for DOTMA:DOPE vesicles (1:1 molar ratio) prepared in various strengths of aqueous NaCl solution at 1 mg/mL of DOTMA. The vesicles were freshly prepared using probe sonication. SANS measured at 25 ± 0.1°C on LoQ.

Table 1 Structural parameters obtained from FISH modelling of the SANS data for probe-sonicated vesicles in various NaCl solutions (fresh) in Figure 7. Vesicles composed of DOTMA:DOPE at 1:1 molar ratio (1.0 mg/mL DOTMA). SANS was measured at 25 ± 0.1°C on LoQ.

Samples_D2O	***L* (Å)**	**No. of layers**	***d*-spacing (Å)**	**R sigma (Å)**	**Ratio of stack:sheet**	**SWSE**
Vesicles_0.04 M NaCl	39.7 (±2.5)	-	-	300	0	7478
Vesicles_0.08 M NaCl	39.7 (±3.5)	-	-	300	0	15333
Vesicles_0.12 M NaCl	39.7 (±6.3)	-	-	300	0	75351

Figures in brackets indicate the standard errors on the fitted parameter values. SWSE is sum of weighted square error. Ratio of stack to sheet represents the ratio of multilamellar surface area to unilamellar surface area.

Appendix III Repeats of LPR results

1. Knock down

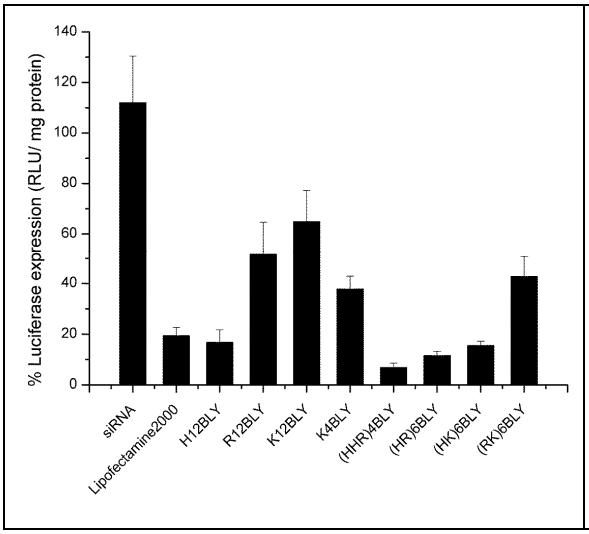

(a) knock down (repeat 1)

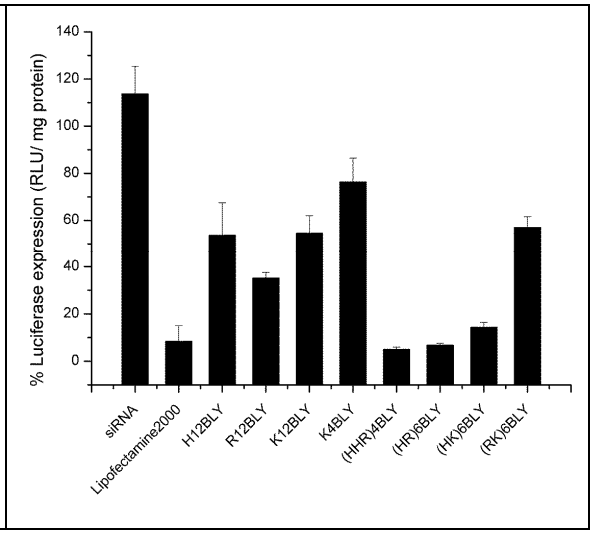

(a) knock down (repeat 2)

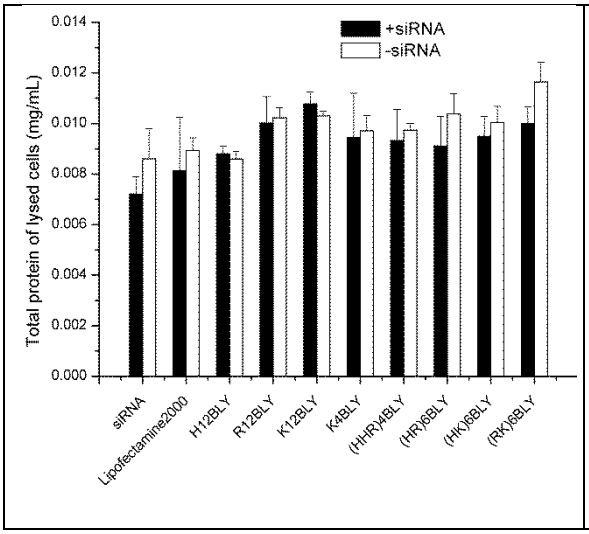

(b) protein assay (repeat 1)

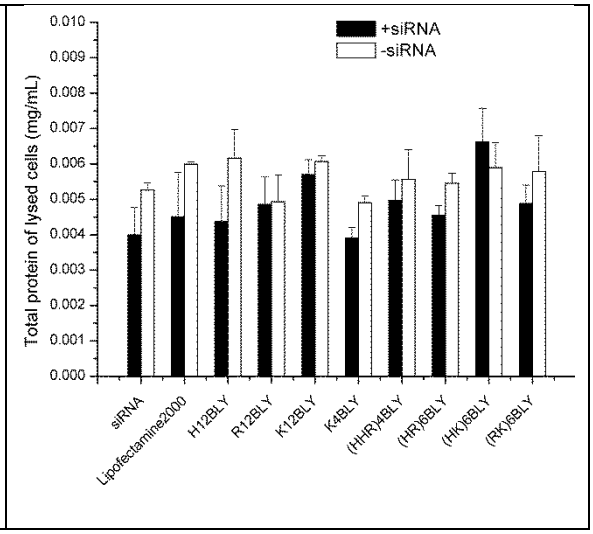

(b) protein assay (repeat 2)

Figure 1 (a) knock down and (b) protein assay in luciferase-transduced A549 cells after a 24+24h incubation with LPRs at L:P:R charge ratio of 0.5:12:1 in water and 1 in 4 dilution in OptiMEM (VwLPRw/OptiMEM). Cationic vesicles composed of DOTMA/DOPE at 1:1 molar ratio. Error bars are the SD of three measurements of a single formulation (n = 3).

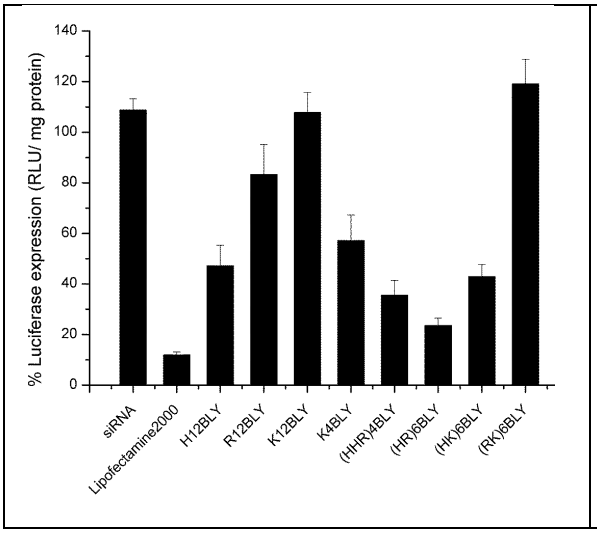

(a) knock down (repeat 1)

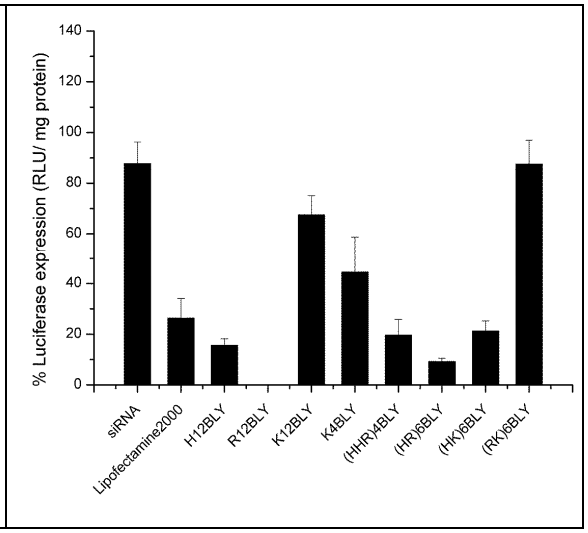

(a) knock down (repeat 2)

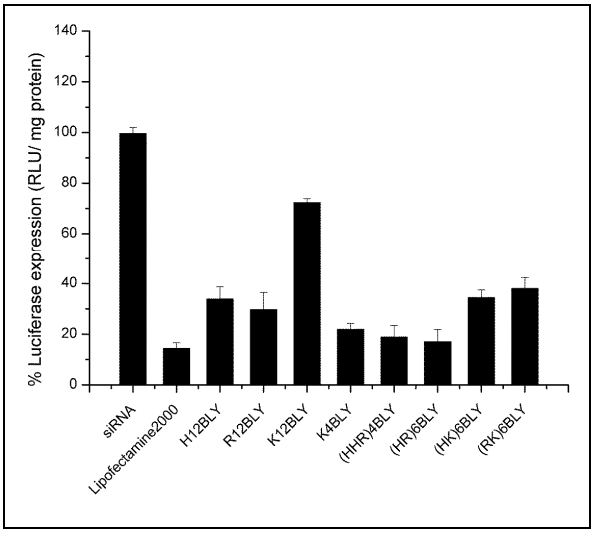

(a) knock down (repeat 3)

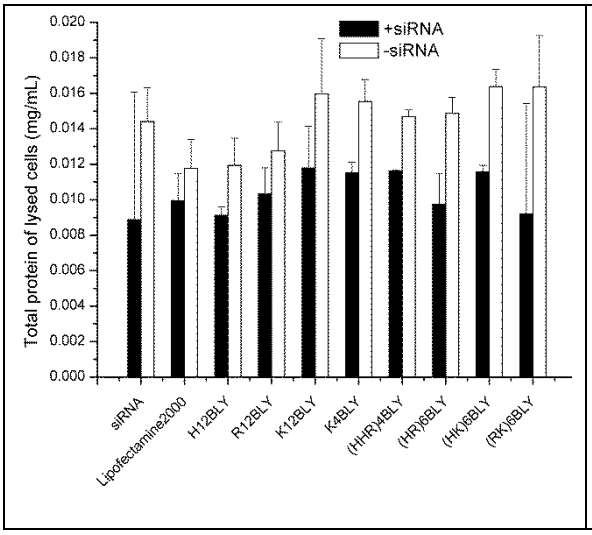

(b) protein assay (repeat 1)

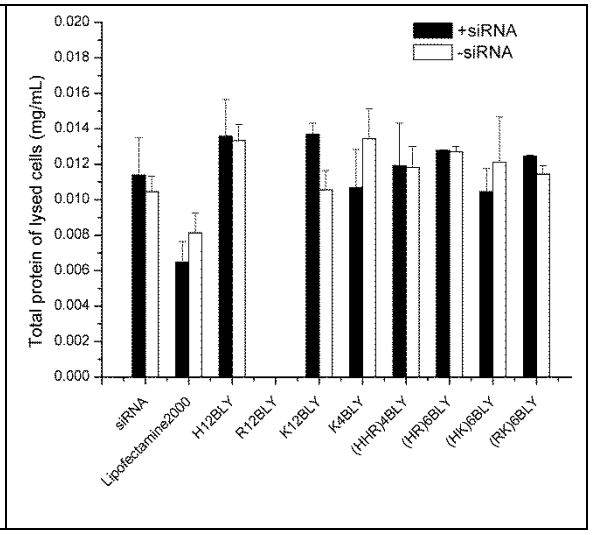

(b) protein assay (repeat 2)

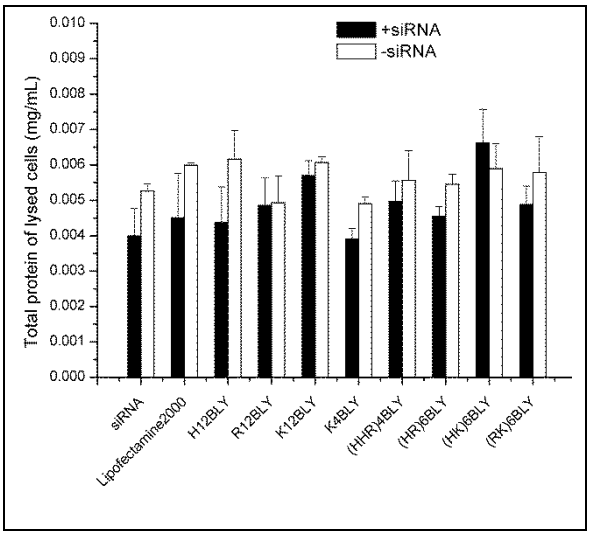

(b) protein assay (repeat 3)

Figure 2 (a) knock down and (b) protein assay in luciferase-transduced A549 cells after a 24+24h incubation with LPRs at L:P:R charge ratio of 0.5:12:1 in OptiMEM and 1 in 4 dilution in OptiMEM (VwLPRo/OptiMEM). Cationic vesicles composed of DOTMA/DOPE at 1:1 molar ratio. Error bars are the SD of three measurements of a single formulation (n = 3).

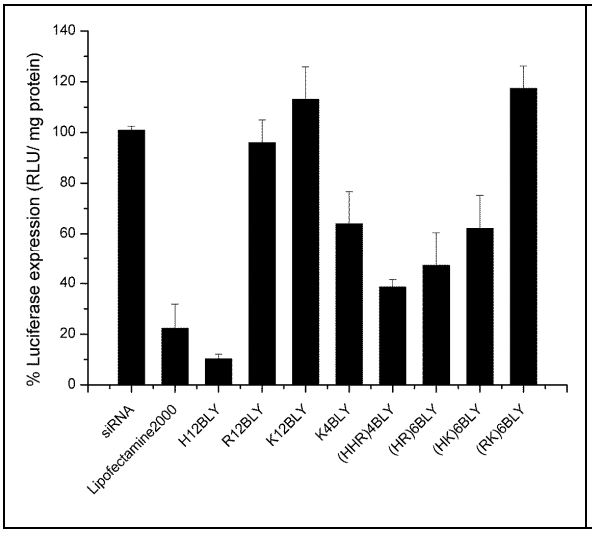

(a) knock down (repeat 1)

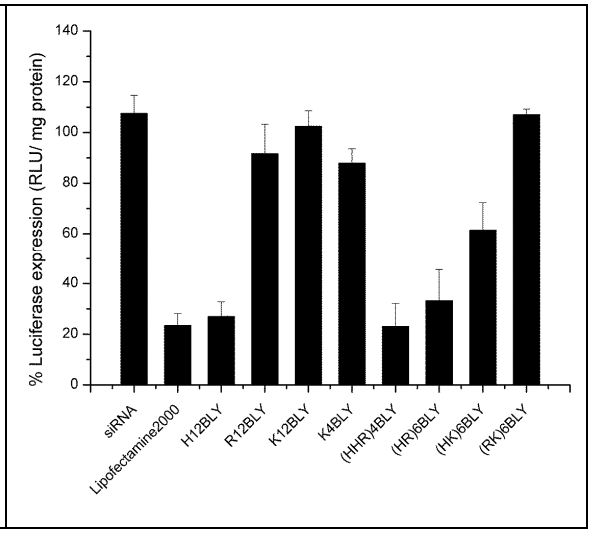

(a) knockdown (repeat 2)

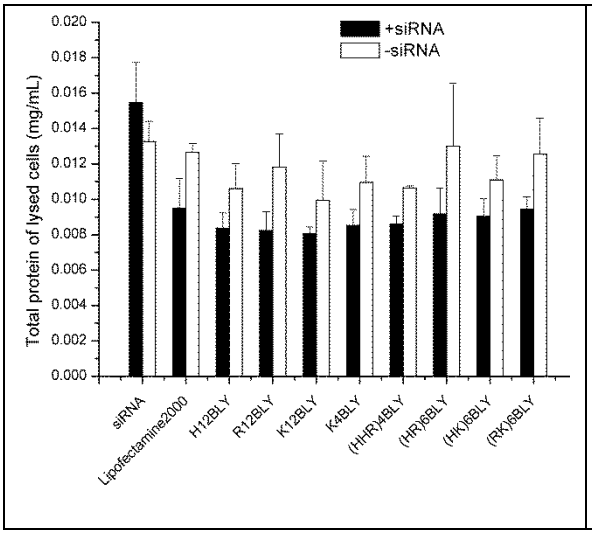

(b) protein assay (repeat 1)

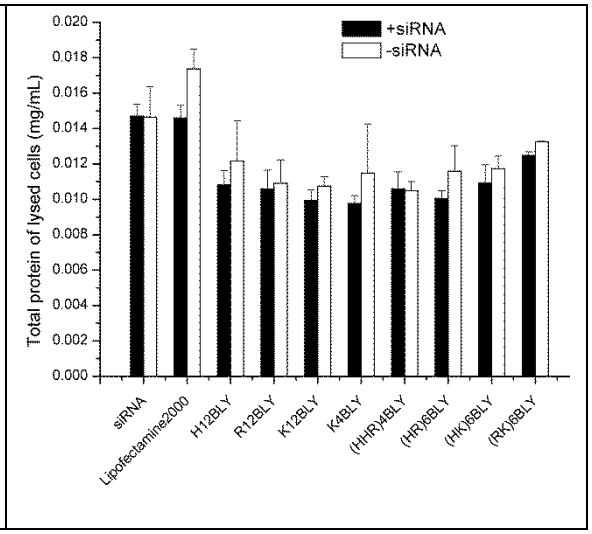

(a) knockdown (repeat 2)

Figure 3 (a) knock down and (b) protein assay in luciferase-transduced A549 cells after a 24+24h incubation with LPRs at L:P:R charge ratio of 0.5:12:1 in saline and 1 in 4 dilution in OptiMEM (VsLPRs/OptiMEM). Cationic vesicles composed of DOTMA/DOPE at 1:1 molar ratio. Knock down was performed after a. Error bars are the SD of three measurements of a single formulation (n = 3).

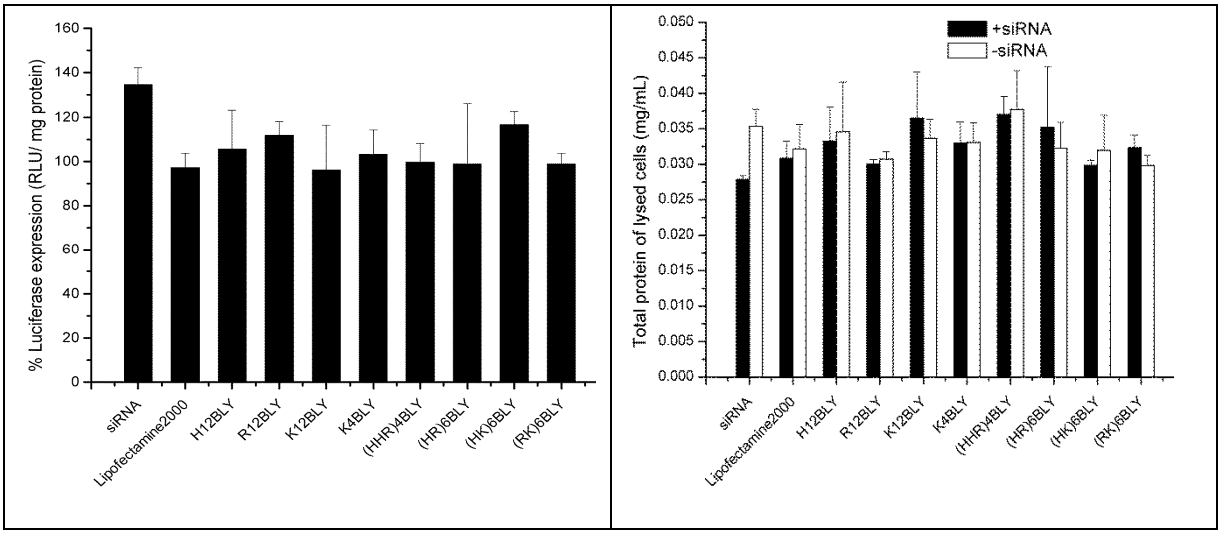

(a) knock down (b) protein assay

Figure 4 (a) knock down and (b) protein assay in luciferase-transduced A549 cells after a 24+24h incubation with LPRs at L:P:R charge ratio of 0.5:12:1 in water and 1 in 4 dilution in Media (VwLPRw/Media). Cationic vesicles composed of DOTMA/DOPE at 1:1 molar ratio. Error bars are the SD of three measurements of a single formulation (n = 3).

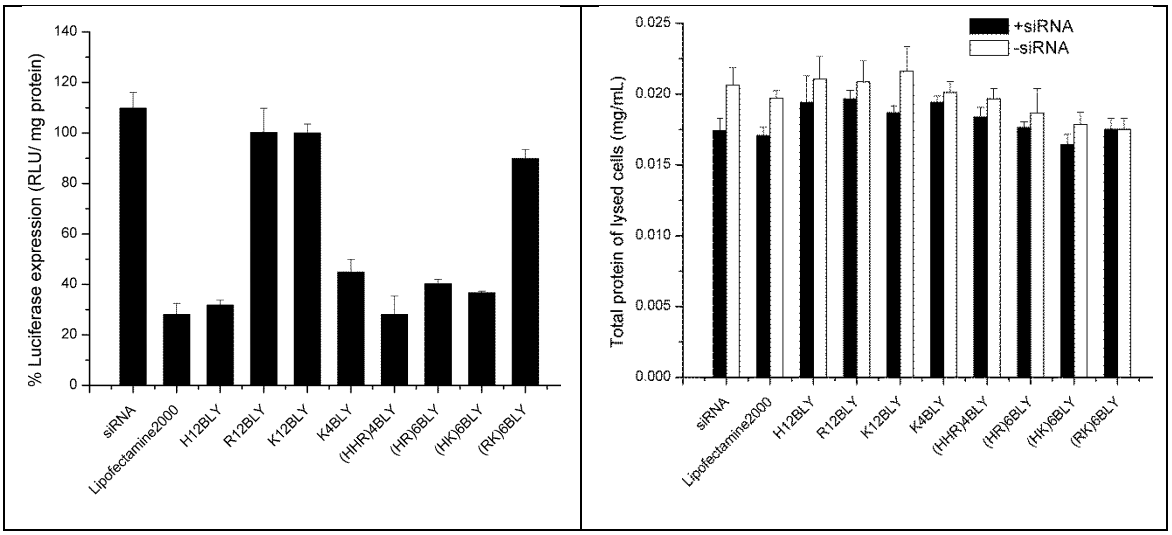

(a) knock down (b) protein assay

Figure 5 (a) knock down and (b) protein assay in luciferase-transduced A549 cells after a 24+24h incubation with LPRs at L:P:R charge ratio of 0.5:12:1 in OptiMEM and 1 in 4 dilution in Media (VwLPRo/Media). Cationic vesicles composed of DOTMA/DOPE at 1:1 molar ratio. Error bars are the SD of three measurements of a single formulation (n = 3).

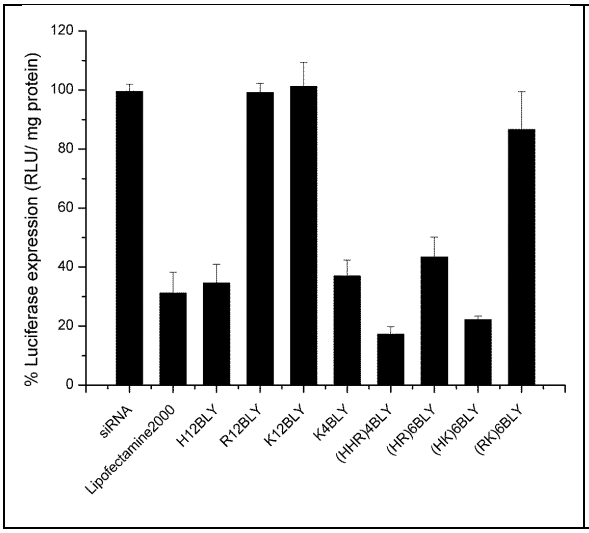

(a) knock down (repeat 1)

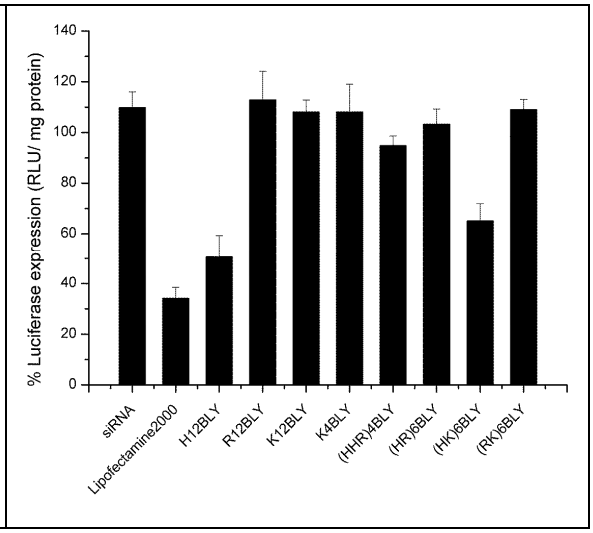

(a) knock down (repeat 2)

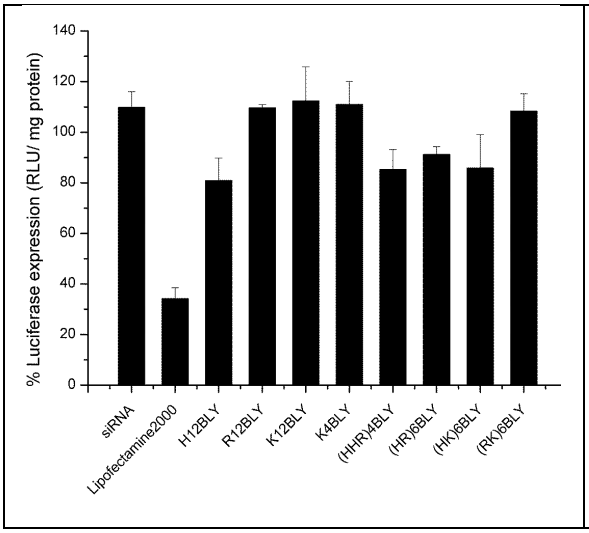

(a) knock down (repeat 3)

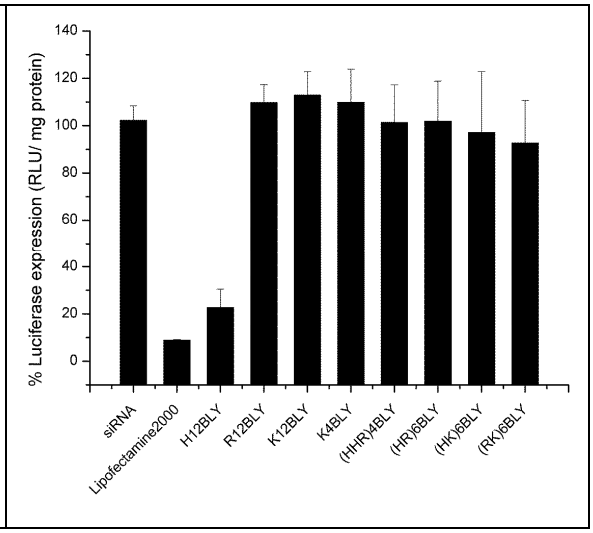

(a) knock down (repeat 4)

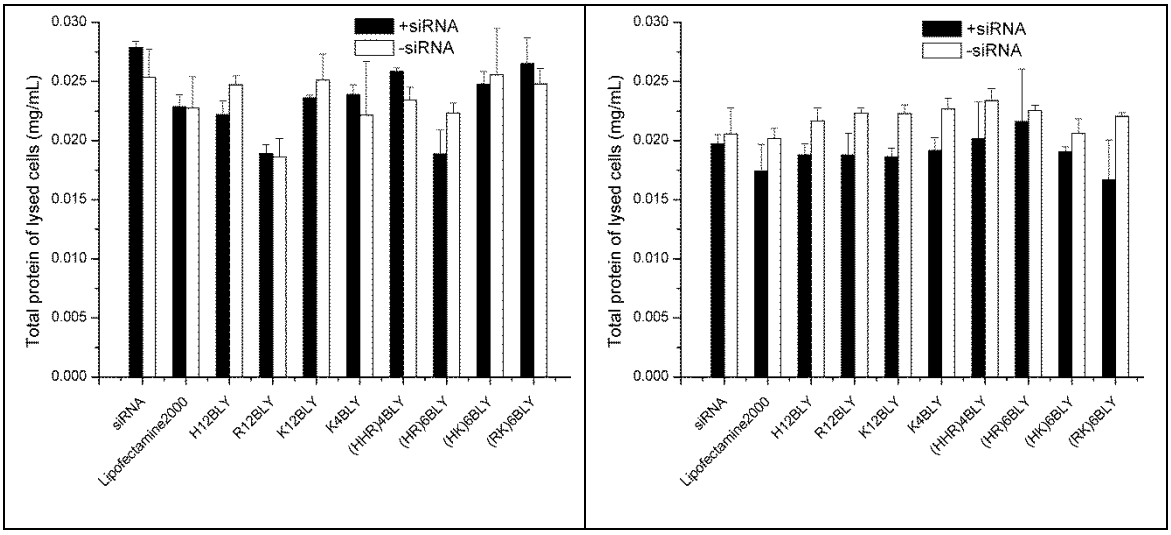

(b) protein assay (repeat 1) (b) protein assay (repeat 2)

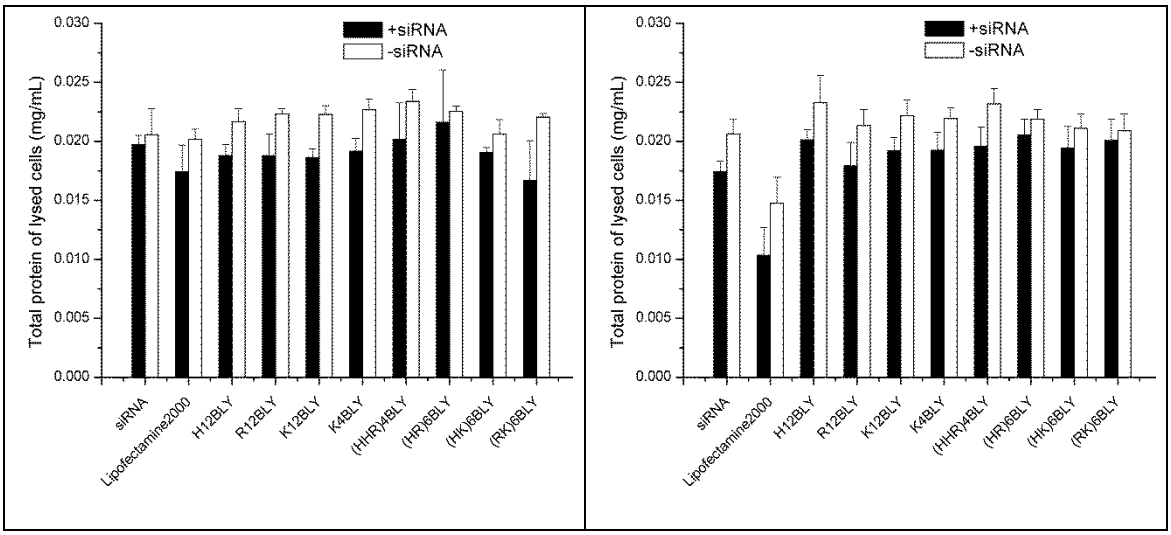

(b) protein assay (repeat 3) (b) protein assay (repeat 4)

Figure 6 (a) knock down and (b) protein assay in luciferase-transduced A549 cells after a 24+24h incubation with LPRs at L:P:R charge ratio of 0.5:12:1 in saline and 1 in 4 dilution in Media (VsLPRs/Media). Cationic vesicles composed of DOTMA/DOPE at 1:1 molar ratio. Error bars are the SD of three measurements of a single formulation (n = 3).

2. Agarose gel electrophoresis

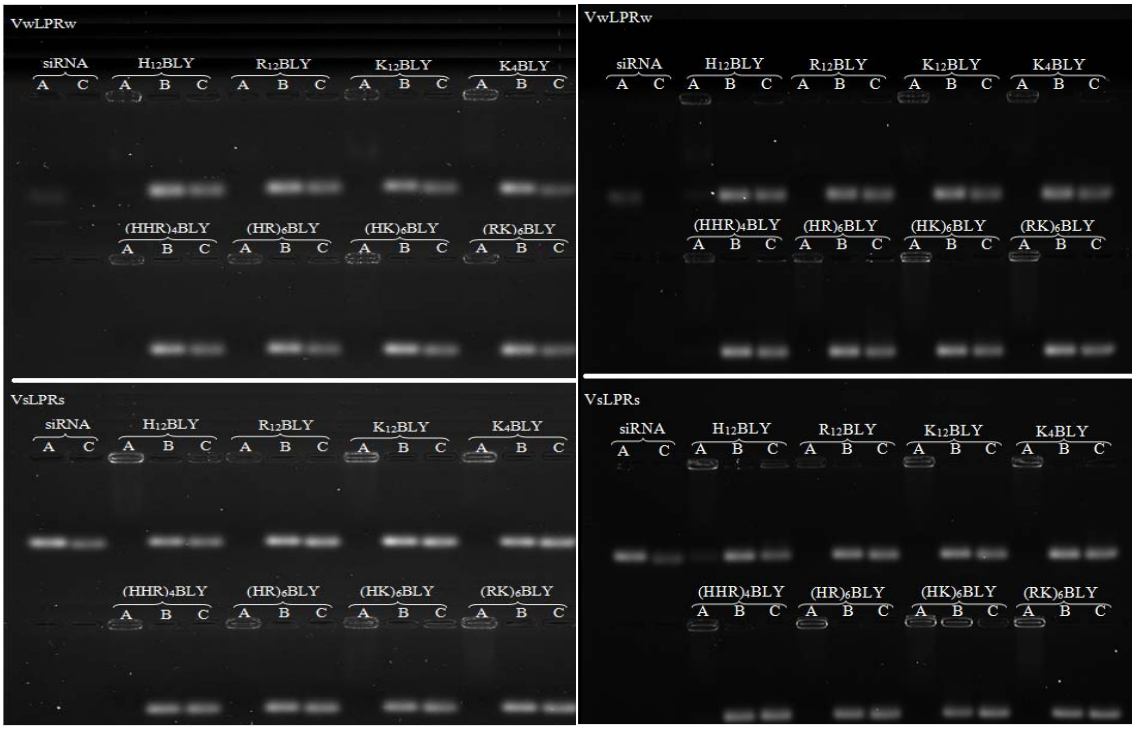

repeat 1 **repeat 2**

Figure 7 Complexation, release and protection of LPRs using luciferase (-)siRNA (0.01 mg/mL). LPRs prepared at L:P:R charge ratio of 0.5:12:1. Cationic vesicles composed of DOTMA/DOPE at 1:1 molar ratio. Upper panel shows VwLPRw, and the lower panel VsLPRs. Lane A: Complexation. Lane B: Release (treated with pAsp). Lane C: Protection (treated with RNAse A and pAsp).